UAB
Universitat Autònoma
de Barcelona

litoclean
INVESTIGACIÓN
& REMEDIACIÓN DE SUELOS

UNIVERSITAT DE
BARCELONA

N. Blázquez Pallí

Assessing the feasibility of bioremediation strategies in aquifers polluted by chlorinated solvents

Assessing the feasibility of bioremediation strategies in aquifers polluted by chlorinated solvents

Natàlia Blázquez Pallí

PhD thesis
November 2019

DOCTORATS
INDUSTRIALS
Aliança de talent!

UAB

Universitat Autònoma
de Barcelona

Assessing the feasibility of bioremediation strategies in aquifers polluted by chlorinated solvents

Natàlia Blázquez Pallí

UAB

Universitat Autònoma
de Barcelona

Escola d'Enginyeria

Departament d'Enginyeria Química, Biològica i Ambiental

Assessing the feasibility of bioremediation strategies in aquifers polluted by chlorinated solvents

PhD Thesis

Natàlia Blázquez Pallí

Doctorat en Ciència i Tecnologia Ambientals

PhD in Environmental Science and Technology

Supervised by

Dr. Ernest Marco Urrea

Dra. M. Teresa Vicent Huguet

Dra. Mònica Rosell Linares

Bellaterra, Cerdanyola del Vallès, Barcelona

November 2019

Title: Assessing the feasibility of bioremediation strategies in aquifers polluted by chlorinated solvents

PhD candidate: Natàlia Blázquez Pallí

Supervisors: Ernest Marco Urrea, M. Teresa Vicent Huguet, and Mònica Rosell Linares.

Tutor: M. Teresa Vicent Huguet

PhD program in Environmental Science and Technology

Departament d'Enginyeria Química, Biològica i Ambiental

Escola d'Enginyeria

Universitat Autònoma de Barcelona

Departament d'Enginyeria Química, Biològica i Ambiental

Escola d'Enginyeria

UAB
Universitat Autònoma
de Barcelona

ERNEST MARCO URREA, Professor Agregat del Departament d'Enginyeria Química, Biològica i Ambiental de la Universitat Autònoma de Barcelona; M. TERESA VICENT HUGUET, Professora Titular del Departament d'Enginyeria Química, Biològica i Ambiental de la Universitat Autònoma de Barcelona, i MÒNICA ROSELL LINARES, Professora Agregada del Departament de Mineralogia, Petrologia i Geologia Aplicada de la Universitat de Barcelona,

CERTIFIQUEM

que l'Enginyera Química Natàlia Blázquez Pallí ha realitzat, sota la nostra direcció, i als laboratoris del Departament d'Enginyeria Química, Biològica i Ambiental de la Universitat Autònoma de Barcelona, el treball amb el títol *"Assessing the feasibility of bioremediation strategies in aquifers polluted by chlorinated solvents"*, que es presenta en aquesta memòria, i el qual constitueix la seva tesi per optar al Grau de Doctor per la Universitat Autònoma de Barcelona.

I perquè en prengueu coneixement i consti als efectes oportuns, presentem a l'Escola de Postgrau de la Universitat Autònoma de Barcelona l'esmentada tesi, amb el present certificat signat a Bellaterra, novembre de l'any 2019,
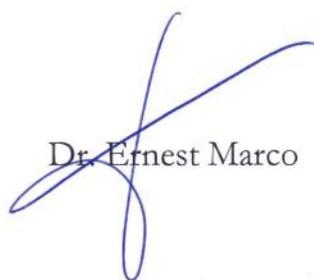
Dr. Ernest Marco

Dra. M. Teresa Vicent

Dra. Mònica Rosell

Als meus pares,
Ramon i Rosa Maria,
per donar-me la vida.

A l'avi Ramón i a l'àvia Sion,
que mai no deixin de fluir els records.

A l'avi Josep, la tita Antonia i en Pere,
la vostra empremta mai no quedarà enrere.

A l'àvia Maria i l'àvia Isabel,
us estimo amb bogeria,
sou més grans que el cel.

I a la Gal·la,
la meva arrel.

Mó

Summary

The worldwide contamination of soils and groundwater by organochlorides has become a pressing concern due to the human health risks that derive from it. Moreover, this pollution endangers several aspects of the environment and, thus, the ecosystem services, which are very relevant in light of climate change (for example, in the water scarcity scenario).

Bioremediation is a sustainable technology that has recently emerged as a cost-effective alternative to clean up aquifers polluted by chlorinated solvents compared to the conventional physicochemical techniques that have been used for a long time. This biological approach uses the metabolism of bacteria to transform the contaminants and detoxify groundwater. However, even though a lot of research in the last years has focused on understanding the physiology and biochemistry of such degrading mechanisms, its successful implementation in the field is, nowadays, still limited.

For this reason, this thesis aimed at deepening the knowledge on *in-situ* anaerobic biodegradation processes (natural and enhanced) of chlorinated solvents in order to improve future bioremediation strategies applied at contaminated sites. To do so, three different sites contaminated by different families of chlorinated solvents, representing increasing complexity scenarios, were investigated.

At Site 1, which had been polluted by tetrachloroethene (PCE) in the past, the feasibility of bioremediation was assessed by combining hydrogeochemical data of the site, microcosm studies, concentrations of metabolites, compound-specific stable carbon isotope analysis (CSIA) and the identification of selected reductive dechlorination biomarker genes. The laboratory investigation evidenced that PCE was naturally transformed to trichloroethene (TCE) and *cis*-1,2-

dichloroethene (*cis*-DCE), and the detection of the required biomarkers confirmed the presence of native bacteria capable of detoxification. However, a *cis*-DCE stall was confirmed in the microcosms and could only be prevented by adding organic substrates as electron donors, which promoted the dechlorination of *cis*-DCE up to ethene (ETH), unlike the natural attenuation observed at the field. The complementary lines of evidence that were gathered suggested that a biologic enhanced reductive dechlorination (ERD) using lactate as electron donor was the best strategy to successfully detoxify this site.

Afterwards, at this same site, an *in-situ* ERD pilot test consisting of a single injection of electron donor (lactate) in a monitoring well was performed and monitored for 190 days. The methodology used to follow the performance of the pilot test was more complete than the integrative approach described above, and included the analysis of i) hydrochemistry, including redox potential (Eh) and the concentrations of redox sensitive species, chlorinated ethenes (CEs), lactate, and acetate; ii) stable isotope composition of carbon of CEs, and sulphur and oxygen of sulphate; and iii) 16S rRNA gene sequencing from groundwater samples. It was demonstrated that the injection of lactate promoted a decrease in the Eh, which allowed for the full reductive dechlorination of CEs to ETH in the injection well. Moreover, the addition of lactate induced a shift towards the predominance of native fermentative bacteria. Given the success of the *in-situ* pilot test, a full-scale ERD with lactate was implemented at the site and, through carbon isotopic mass balances, it was confirmed that PCE dechlorination to ETH was occurring across the site, after one year of treatment, without a significant accumulation of toxic intermediates.

Lastly, two complex sites (Site 2 and Site 3, with no active and active source at the time of the study, respectively) that were contaminated by multiple families of volatile organic compounds (VOCs) were investigated to find lines of evidence

of biodegradation and reveal any potential setbacks that could occur in the event of a future bioremediation application. In this case, the carbon and chlorine (C–Cl) isotopic characterization of several commercial pure phase chlorinated compounds and, specifically, of the dichloromethane (DCM) fermentation reaction by a *Dehalobacterium*-containing culture, were performed to obtain valuable information to support the interpretation of stable isotope analyses derived from polluted sites. Afterwards, the bioremediation potential of Sites 2 and 3, which were mainly contaminated by DCM, its potential parental chloroform (CF), TCE, and monochlorobenzene (MCB)) was evaluated through the study of hydrochemistry, C–Cl CSIA, laboratory microcosms testing for biostimulation as well as bioaugmentation, and microbiological data. At Site 2, carbon and chlorine compositions from field samples were consistent with laboratory microcosms, which showed complete degradation of CF, DCM and TCE, while MCB remained accumulated. Moreover, the identification of *Dehalobacter* sp. in CF-enriched microcosms further supported the biodegradation capability of the aquifer to remediate chlorinated methanes (CMs). At Site 3, however, hydrochemistry and C–Cl CSIA from field samples suggested little DCM, CF and TCE transformation, while microcosms evidenced that their degradation was slow, inefficient and severely inhibited, even for the two commercial inocula reported to degrade the target contaminants. In addition, a dual C–Cl isotopic assessment using results from both sites and reference values from the literature allowed elucidation of the origin and fate of both CF and DCM. Given the recalcitrance of MCB and the inhibition observed at Sites 2 and 3, respectively, a combination of remediation treatments seems the best approach for the detoxification of the sites.

Resumen

La extensa contaminación por organoclorados en suelos y en aguas subterráneas se ha convertido en una urgente preocupación a nivel mundial debido a los riesgos que conllevan para la salud. Además, esta contaminación pone en peligro diversos aspectos del medio ambiente y, por tanto, los servicios ecosistémicos, que serán muy relevantes con el cambio climático (por ejemplo, en un escenario de escasez de agua).

La biorremediación es una tecnología sostenible que ha emergido en las últimas décadas como alternativa rentable para la descontaminación de acuíferos con disolventes clorados, en comparación con las técnicas fisicoquímicas más convencionales y que se han utilizado durante mucho tiempo. Este tratamiento biológico de la contaminación utiliza el metabolismo de las bacterias para degradar los contaminantes y detoxificar las aguas subterráneas. Pero, aunque mucha investigación se ha centrado en el estudio de la fisiología y bioquímica de estos procesos bacterianos, la exitosa implementación en campo es todavía un reto hoy en día.

Por este motivo, esta tesis ha tenido como objetivo profundizar el conocimiento sobre los procesos de biodegradación anaerobia *in-situ* (naturales y estimulados) de disolventes clorados en aguas subterráneas, para mejorar futuras estrategias de biorremediación aplicadas a emplazamientos contaminados. Para ello, se han investigado tres lugares diferentes, contaminados por familias de disolventes clorados diferentes, y que representan escenarios de complejidad creciente.

Para el primer emplazamiento (*Site 1*), que en el pasado había sido contaminado por tetracloroetileno (PCE), se evaluó la viabilidad de un tratamiento de biorremediación mediante el estudio de la hidrogeoquímica del

acuífero, ensayos de microcosmos, concentraciones de los metabolitos de interés, análisis de los isótopos estables del carbono de los contaminantes de interés (CSIA), y la identificación de genes seleccionados como biomarcadores de la reacción de decloración reductiva. Esta investigación en el laboratorio evidenció que el PCE se podía transformar de forma natural en tricloroetileno (TCE) y *cis*-1,2-dicloroetileno (*cis*-DCE), y la detección de los biomarcadores correspondientes confirmó la presencia de bacterias nativas capaces de la detoxificación de las aguas subterráneas. Sin embargo, los microcosmos demostraron que la acumulación de *cis*-DCE que se producía en condiciones naturales (también en el acuífero) sólo se podía evitar con la adición de sustratos orgánicos fermentables. Con la ayuda de estos estimulantes, que actúan como donadores de electrones, se promovía la decloración del *cis*-DCE hasta el eteno (ETH), un compuesto inocuo. Así pues, las líneas de evidencia complementarias obtenidas en el laboratorio sugirieron que la mejor estrategia para detoxificar el emplazamiento de forma exitosa era la decloración reductiva biológica estimulada (ERD) con la utilización de lactato como donador de electrones.

A continuación, en este mismo emplazamiento y a partir de los resultados obtenidos en el laboratorio, se llevó a cabo una prueba piloto ERD *in-situ* que consistió en una sola inyección de donador de electrones (lactato) en un solo pozo de seguimiento. La prueba piloto se monitorizó durante 190 días mediante una metodología más completa que la utilizada en el laboratorio, y a través de los siguientes parámetros: 1) hidroquímica, incluyendo el potencial redox (Eh) y la concentración de especies sensibles al redox, etenos clorados (CEs), lactato y acetato; 2) composición de los isótopos estables del carbono de los CEs y del azufre y el oxígeno de los sulfatos; y 3) la secuenciación del gen 16S rRNA de las muestras de agua subterránea. Los resultados demostraron que la inyección de lactato promovió una disminución del Eh, que permitió la completa decloración reductiva de los CEs a ETH en el pozo de inyección. Además, la adición de

lactato indujo un cambio en la comunidad microbiana hacia el predominio de bacterias fermentadoras. Dado el éxito de la prueba piloto *in-situ*, se implementó una ERD con lactato a escala emplazamiento y, mediante el cálculo del balance de masa isotópico del carbono, se confirmó que la decloración del PCE a ETH estaba ocurriendo en todos los pozos estudiados, después de un año de tratamiento, sin una acumulación significativa de compuestos intermediarios tóxicos.

Por último, dos emplazamientos complejos (*Site 2* y *Site 3*, sin y con fuente de contaminación activa en el momento del estudio, respectivamente), y que estaban contaminados por múltiples familias de compuestos orgánicos volátiles (VOCs), fueron investigados con el objetivo de encontrar líneas de evidencia de biodegradación y detectar posibles contratiempos que podrían surgir en un futuro tratamiento de biorremediación. En primer lugar, se llevó a cabo la caracterización isotópica del carbono y del cloro (C–Cl) de varios solventes clorados comerciales puros, y de la reacción de fermentación del diclorometano (DCM) por un cultivo con *Dehalobacterium*, para obtener información valiosa que apoye la interpretación de los resultados obtenidos en análisis de isótopos estables derivados de emplazamientos contaminados. Seguidamente, se evaluó el potencial de biorremediación de los *Sites 2* y *3*, que estaban principalmente contaminados por DCM, su potencial compuesto parental cloroformo (CF), TCE y monoclorobenceno (MCB)), a través del estudio de la hidroquímica, C–Cl CSIA, microcosmos de laboratorio que ensayaban tratamientos tanto de bioestimulación como de bioaumentación, y datos microbiológicos de las muestras de agua subterránea. Al *Site 2*, las composiciones isotópicas del carbono y del cloro provenientes de las muestras de campo resultaron ser consistentes con los microcosmos preparados en el laboratorio, que mostraron la degradación completa del CF, DCM y del TCE, y la acumulación del MCB. Además, la identificación de *Dehalobacter* sp. en cultivos enriquecidos con CF aún dio más

fuerza a la capacidad biodegradadora del acuífero para remediar los metanos clorados (CMs). Sin embargo, para el *Site 3*, los resultados del análisis de la hidroquímica y de C–Cl CSIA de las muestras de campo indicaron muy poca transformación del DCM, CF y TCE, mientras que los microcosmos evidenciaron que la degradación de todos ellos era lenta, ineficiente y estaba fuertemente inhibida, incluso en los dos inóculos comerciales destinados a degradar los contaminantes de interés. Además, una evaluación isotópica dual (C–Cl) a partir de los resultados obtenidos en los dos emplazamientos y de los valores de referencia de la literatura, permitieron la elucidación del origen de ambos CF y DCM. Dada la resistencia a la degradación del MCB y la inhibición general observada en los *Sites 2* y *3*, respectivamente, una combinación de diferentes tratamientos de descontaminación parece la mejor estrategia para la detoxificación de los dos emplazamientos.

Resum

L'extensa contaminació per organoclorats en sòls i en aigües subterrànies s'ha convertit en una urgent preocupació a nivell mundial degut als riscos per a la salut que se'n deriven. A més, aquesta contaminació posa en perill diversos aspectes del medi ambient i, per tant, els serveis ecosistèmics, que esdevindran molt rellevants amb el canvi climàtic (per exemple, en un escenari d'escassetat d'aigua).

La bioremediació és una tecnologia sostenible que ha emergit en les últimes dècades com a alternativa rendible per a la descontaminació d'aqüífers amb dissolvents clorats, en comparació amb les tècniques fisicoquímiques més convencionals i que s'han utilitzat durant molt de temps. Aquest tractament biològic de la contaminació utilitza el metabolisme dels bacteris per degradar els contaminants i detoxificar les aigües subterrànies. Però, tot i que molta recerca s'ha centrat en l'estudi de la fisiologia i bioquímica d'aquests processos bacterians, l'exitosa implementació al camp és encara un repte avui en dia.

Per aquest motiu, aquesta tesi ha tingut com a objectiu aprofundir el coneixement sobre els processos de biodegradació anaeròbia *in-situ* (naturals i estimulats) de dissolvents clorats en aigües subterrànies, per tal de millorar futures estratègies de bioremediació aplicades a emplaçaments contaminats. Per fer-ho, s'han investigat tres llocs diferents, contaminats per famílies de dissolvents clorats diferents, i que representen escenaris de complexitat creixent.

Pel primer emplaçament (*Site 1*), que en el passat havia estat contaminat per tetracloroetilè (PCE), es va avaluar la viabilitat d'un tractament de bioremediació per mitjà de l'estudi de la hidrogeoquímica de l'aqüífer, assajos de microcosmos, concentracions dels metabòlits d'interès, anàlisi dels isòtops estables del carboni dels contaminants d'interès (CSIA), i la identificació de gens seleccionats com a biomarcadors de la reacció de decloració reductiva. Aquesta investigació al

laboratori va evidenciar que el PCE es podia transformar de forma natural a tricloroetilè (TCE) i a *cis*-1,2-dicloroetilè (*cis*-DCE), i la detecció dels biomarcadors corresponents va confirmar la presència de bacteris natius capaços de la detoxificació de les aigües subterrànies. Tot i això, els microcosmos van demostrar que l'acumulació de *cis*-DCE que es produïa en condicions naturals (també a l'aqüífer) només es podia evitar amb l'addició de substrats orgànics fermentables. Amb l'ajuda d'aquests estimulants, que actuen com a donadors d'electrons, es promovia la decloració del *cis*-DCE fins a l'etè (ETH), un compost innocu. Així doncs, les línies d'evidència complementàries obtingudes al laboratori van suggerir que la millor estratègia per detoxificar l'emplaçament de forma exitosa era la decloració reductiva biològica estimulada (ERD) amb l'ús del lactat com a donador d'electrons.

A continuació, en aquest mateix emplaçament i a partir dels resultats obtinguts al laboratori, es va dur a terme una prova pilot ERD *in-situ* que va consistir en una sola injecció de donador d'electrons (lactat) en un sol pou de seguiment. La prova pilot es va monitoritzar durant 190 dies mitjançant una metodologia més completa que la utilitzada al laboratori, i a través dels següents paràmetres: 1) hidroquímica, incloent el potencial redox (Eh) i la concentració d'espècies sensibles al redox, etens clorats (CEs), lactat i acetat; 2) composició dels isòtops estables del carboni dels CEs i del sofre i l'oxigen dels sulfats; i 3) la seqüenciació del gen 16S rRNA de les mostres d'aigua subterrània. Els resultats van demostrar que la injecció de lactat va promoure una disminució del Eh, que va permetre la completa decloració reductiva dels CEs a ETH al pou d'injecció. A més, l'addició de lactat va induir un canvi en la comunitat microbiana cap a la predominança de bacteris fermentadors. Donat l'èxit de la prova pilot *in-situ*, es va implementar una ERD amb lactat a escala emplaçament i, mitjançant el càlcul del balanç de massa isotòpic del carboni, es va confirmar que la decloració del PCE a ETH estava

ocorrent a tots els pous estudiats, després d'un any de tractament, sense una acumulació significativa de compostos intermediaris tòxics.

Per acabar, dos emplaçaments complexos (*Site 2* i *Site 3*, sense i amb font de contaminació activa en el moment de l'estudi, respectivament), i que estaven contaminats per múltiples famílies de compostos orgànics volàtils (VOCs), van ser investigats amb l'objectiu de trobar línies d'evidència de biodegradació i detectar possibles contratemps que podrien sorgir en un futur tractament de bioremediació. Primer de tot, es va dur a terme la caracterització isotòpica del carboni i del clor (C–Cl) de diversos solvents clorats comercials purs, i de la reacció de fermentació del diclormetà (DCM) per un cultiu amb *Dehalobacterium*, per obtenir informació valuosa que recolzi la interpretació dels resultats obtinguts en anàlisis d'isòtops estables derivats d'emplaçaments contaminats. Seguidament, es va avaluar el potencial de bioremediació dels *Sites 2* i *3*, que estaven principalment contaminats per DCM, el seu potencial compost parental cloroform (CF), TCE i monoclorobenzè (MCB)), a través de l'estudi de la hidroquímica, C–Cl CSIA, microcosmos de laboratori que assajaven tractaments tant de bioestimulació com de bioaugmentació, i dades microbiològiques de les mostres d'aigua subterrània. Al *Site 2*, les composicions isotòpiques del carboni i del clor provinents de les mostres de camp van resultar ser consistents amb els microcosmos preparats al laboratori, que van mostrar la degradació completa del CF, DCM i del TCE, i la acumulació del MCB. A més, la identificació del *Dehalobacter* sp. en cultius enriquits amb CF encara va donar més força a la capacitat biodegradadora de l'aqüífer per remeiar els metans clorats (CMs). Al *Site 3*, però, els resultats de l'anàlisi de la hidroquímica i de C–Cl CSIA de les mostres de camp van indicar molt poca transformació del DCM, CF i TCE, mentre que els microcosmos van evidenciar que la degradació de tots ells era lenta, ineficient i estava fortament inhibida, fins i tot als dos inòculs comercials destinats a degradar els contaminants d'interès. A més, una avaluació isotòpica dual (C–Cl)

a partir dels resultats obtinguts en els dos emplaçaments i dels valors de referència de la literatura, van permetre l'elucidació de l'origen d'ambdós CF i DCM. Donada la resistència a la degradació del MCB i la inhibició general observada als *Sites 2* i *3*, respectivament, una combinació de diferents tractaments de descontaminació sembla la millor estratègia per la detoxificació dels dos emplaçaments.

List of contents

List of abbreviations

1,1-DCE	1,1-dichloroethene
16S rRNA	16S ribosomal ribonucleic acid
ACA	Agència Catalana de l'Aigua
ARC	Agència de Residus de Catalunya
ATP	Adenosine triphosphate
ATSDR	U.S. Agency for Toxic Substances and Disease Registry
BTEX	Benzene, toluene, ethylbenzene and the xylene isomers
BvcA	Vinyl chloride reductive dehalogenase strain BAV1
CAH	Chlorinated aliphatic hydrocarbons
CCiT-UB	*Centres Científics i Tecnològics* of *Universitat de Barcelona*
C–Cl	Carbon–chlorine
CEs	Chlorinated ethenes
CF	Chloroform or trichloromethane
CI	Confidence interval
cis-DCE	*cis*-1,2-dichloroethene
CM	Chloromethane
CMs	Chlorinated methanes
CSIA	Compound-specific stable isotope analysis
CT	Carbon tetrachloride
CVOCs	Chlorinated volatile organic compounds
D%	Extent of degradation
D. elyunquensis	*Candidatus* Dichloromethanomonas elyunquensis
D. mccartyi	*Dehalococcoides mccartyi*
DCE	Dichloroethene
DCM	Dichloromethane
Dhb	*Dehalobacterium*
Dhb f.	*Dehalobacterium formicoaceticum*

Dhc	*Dehalococcoides*
Dhg	*Dehalogenimonas*
DI	Dual inlet
DNA	Deoxyribonucleic acid
DNAPL	Dense non-aqueous phase liquid
DO	Dissolved oxygen
DOC	Dissolved organic carbon
DPE	Dual-phase extraction
EA	Elemental analyser
EC	Electrical conductivity
EDTA	Ethylenediaminetetraacetic acid
Eh	Corrected redox potential
ERD	Enhanced reductive dechlorination
ETBE	Ethyl tert-butyl ether
ETH	Ethene
E.U.	European Union
FID	Flame ionization detector
G. lovleyi	*Geobacter lovleyi*
GC	Gas chromatography
HPLC	High pressure liquid chromatography
HS-SPME	Headspace solid-phase microextraction
IARC	International Agency for Research on Cancer
IRMS	Isotope ratio mass spectrometry
ISCO	*In-situ* chemical oxidation
ISCR	*In-situ* chemical reduction
ISTD	*In-situ* thermal desorption
LNAPL	Light non-aqueous phase liquid
MBT	Molecular biological tools
MCB	Monochlorobenzene
MNA	Monitored natural attenuation

MTBE	Methyl tert-butyl ether
NSZ	Non-saturated zone
OHRB	Organohalide-respiring bacteria
ORP	Oxidation-reduction potential (measured *in-situ*)
P&T	Pump and treat
PCE	Tetrachloroethene or perchloroethene
PceA	Tetrachloroethylene reductive dehalogenase
PCR	Polymerase chain reaction
PRB	Permeable reactive barriers
PTFE	Polytetrafluoroethylene
qPCR	Quantitative polymerase chain reaction
rdh	Reductive dehalogenases
RdhA	Reductive dehalogenase subunit A
RdhB	Reductive dehalogenase subunit B
SMOC	Standard Mean Ocean Chloride
SPME	Solid phase micro-extraction
SVE	Soil vapor extraction
SZ	Saturated zone
T	Temperature
TCE	Trichloroethene
TceA	Trichloroethylene reductive dehalogenase subunit A
TOC	Total organic carbon
TPH	Total petroleum hydrocarbons
trans-DCE	*trans*-1,2-dichloroethene
U.S.	United States
U.S. EPA or USEPA	U.S. Environmental Protection Agency
UV	Ultraviolet
VC	Vinyl chloride
VCDT	Vienna Canyon Diablo Troillite
VcrA	Vinyl chloride reductive dehalogenase subunit A

VFAs	Volatile fatty acids
VOCs	Volatile organic compounds
VPDB	Vienna Pee Dee Belemnite
VSMOW	Vienna Standard Mean Ocean Water
ZVI	Zero-valent iron
$\delta^{13}C$	Delta carbon thirteen
$\delta^{13}C_{sum}$	Carbon thirteen isotopic mass balance
$\delta^{37}Cl$	Delta chlorine thirty-seven
$\delta^{18}O$	Delta oxygen eighteen
$\delta^{34}S$	Delta sulphur thirty-four
$\varepsilon^{13}C$	Carbon thirteen isotopic fractionation
$\varepsilon^{37}Cl$	Chlorine thirty-seven isotopic fractionation
$\Lambda^{C/Cl}$	Dual C–Cl isotope correlation

Chapter 1

General introduction

List of contents

1.1. Organochlorides: natural and anthropogenic sources

Organohalides (or halogenated compounds) are chemical structures that contain one or more halogens (i.e. fluorine, chlorine, bromine, iodine) in combination with carbon and other elements. Organohalides are produced naturally as a result of halogen biogeochemical cycles. These substances derive from living organisms (e.g. microalgae, bacteria, higher plants, insects or animals) and from abiotic processes (e.g. volcanoes, forest fires, or oxidation of soil organic matter) (Gribble, 2010). In terrestrial environments, the abundance of the chloride ion results in the widespread existence of organochloride substances, both biogenic and from abiotic processes (Gribble, 2010). For instance, organochlorides are linked to the mineralisation of organic matter and soil humus formation. After the initial transformation of inorganic chloride from plant leaves to aliphatic and aromatic organochloride substances, the former group are stable but the latter fraction keeps increasing during the advanced stages of humification (Leri et al., 2007; Leri and Myneni, 2010; Myneni, 2002). Such a role in very common processes results in the wide occurrence of organochlorides in the environment (Field, 2016; Öberg, 2003; Öberg and Bastviken, 2012; Redon et al., 2013). Of the natural organohalides described to date, half of them contain chlorine, the other half contain bromine, and hundreds contain both halogens. Iodine- and fluorine-containing compounds are also produced naturally but they are less common (Field, 2016; Gribble, 2004a, 2004b).

Besides their natural release, organohalides, and organochlorides in particular, are also produced anthropogenically. These compounds have often been used as solvents and degreasing agents; herbicides, insecticides and fungicides; hydraulic and heat transfer fluids; flame retardants; pharmaceuticals, and intermediates for chemical synthesis. In addition, they also are by-products of industrial processes (Zanaroli et al., 2015). Chlorinated aliphatic hydrocarbons (CAH) are typically

manufactured from hydrocarbons such as methane, ethane, ethene, and chlorine. In their production, the hydrogen atom is replaced by a chlorine one. Otherwise, they can also be obtained from the selective dechlorination of a higher chlorinated compound to a lesser chlorinated one (USEPA, 2000). Among the chlorinated hydrocarbons family, the most commonly produced due to their industrial importance are the chlorinated derivatives from methane, ethane, propane, butane and benzene (Marshall and Pottenger, 2016) (Table 1.1). Organochlorides of industrial and commercial use can also be referred to as chlorinated solvents.

Table 1.1. Chlorinated solvents of industrial importance. Their physicochemical properties can be found in Table 1.2. Table adapted from Marshall and Pottenger (2016).

IUPAC name	Common name	Formula	Acronym
Chloromethane	Methyl chloride	CH_3Cl	CM
Dichloromethane	Methylene chloride	CH_2Cl_2	DCM
Trichloromethane	Chloroform	$CHCl_3$	CF
Tetrachloromethane	Carbon tetrachloride	CCl_4	CT
Chloroethene	Vinyl chloride	$CHCl=CH_2$	VC
1,1-dichloroethene	Vinylidene chloride	$CCl_2=CH_2$	1,1-DCE
cis-1,2-dichloroethene	*cis*-1,2-dichloroethylene	$CHCl=CHCl$	*cis*-DCE
trans-1,2-dichloroethene	*trans*-1,2-dichloroethylene	$CHCl=CHCl$	*trans*-DCE
Trichloroethene	Trichloroethylene	$CCl_2=CHCl$	TCE
Tetrachloroethene	Perchloroethylene	$CCl_2=CCl_2$	PCE
Chlorobenzene	Monochlorobenzene	C_6H_5Cl	MCB

1.2. Environmental pollution by organochlorides

The physical properties of organochlorides are tightly linked to the number of chlorines in the molecule (Table 1.2). In general, progressive chlorination increases density, viscosity and solubility in organic and inorganic materials, but decreases flammability, specific heat, water solubility and vapour pressure (Marshall and Pottenger, 2016; USEPA, 2000). In regards to the latter, most organochlorides have an initial boiling point less than or equal to 250 °C

measured at a standard atmospheric pressure of 101.3 kPa, so they are classified as volatile organic compounds (VOCs) (USEPA, 2015). Chemically, these substances are very stable and resistant to degradation, which makes them very versatile and useful for chemical synthesis as they participate in many chemical reactions (Marshall and Pottenger, 2016). Such characteristics have been very useful in industry; however, they are also the reason why organochlorides are dangerous to the environment and human health.

Given the industrial origin of chlorinated solvents, these compounds are frequently detected in aquifers of industrial and urban areas as a result of improper management and disposal, as well as accidental spills. Because of their very long half-lives, chlorinated solvents are very persistent. Consequently, their fate and transport in the environment is governed by their physical and chemical properties (USEPA, 2000).

A chlorinated compound released into the aquifer as a pure liquid solvent is commonly referred to as LNAPL or DNAPL (Light Non-Aqueous Phase Liquid or Dense Non-Aqueous Phase Liquid), depending on whether their density is lower or higher than water, respectively. Most of the chlorinated solvents discussed in the present work are DNAPLs, except for vinyl chloride (VC) and chloromethane (CM), which are gaseous under typical environmental conditions. When a DNAPL reaches the aquifer, it sinks through the unsaturated and saturated zones until it reaches the lowest point possible, usually a confining layer of the aquifer, where eventually forms "pools" (USEPA, 2000). There, depending on its properties, it can remain as a DNAPL, adsorb to soil, dissolve in groundwater, or volatilize, to reach equilibrium (Figure 1.1A) (Huling and Weaver, 1991; USEPA, 2000). Besides the transfer between phases, chlorinated solvents can also migrate within phases to other parts of the aquifer by advection, dispersion and diffusion (Figure 1.1B) (Sims et al., 1992; USEPA, 2000).

Table 1.2. Main physicochemical properties of some of the chlorinated VOCs (CVOCs). Table adapted from Marshall and Pottenger (2016) *and* Cwiertny and Scherer (2010).

VOC	CAS registry number	Molecular weight (g/mol)	Melting Point (°C)	Boiling Point (°C)	Density at 25 °C (g/mL)	Solubility in water (mg/L)	Vapour pressure (torr)	Log K_{ow}	Henry's Law constant ($\cdot 10^{-3} \cdot atm \cdot m^3/mol$)	Log K_{oc}
CM	74-87-3	50.5	-97.7	-24.1	0.92	5235	4275.0	0.91	9.6	-
DCM	75-09-2	84.9	-97.2	40.0	1.33	13200	415.0	1.25	1.7	-
CF	67-66-3	119.4	-63.4	61.2	1.49	8200	196.8	1.97	3.8	1.52
CT	56-23-5	153.8	-22.6	76.8	1.59	800	153.8	2.64	28.9	1.90
VC	75-01-4	62.5	-153.8	-13.3	0.91	2763	2660.0	1.38	79.2	-
1,1-DCE	75-35-4	96.9	-122.6	31.6	1.22	3344	604.0	2.13	23.0	-
cis-DCE	156-59-2	96.9	-80.0	60.0	1.28	3500	203.0	1.86	7.4	-
trans-DCE	156-60-5	96.9	-50.0	48.0	1.26	6260	333.0	1.93	6.8	-
TCE	79-01-6	131.4	-84.7	87.2	1.46	1100	74.2	2.53	11.7	1.53
PCE	127-18-4	165.8	-22.3	121.3	1.63	150	18.1	2.88	26.3	2.29
MCB	108-90-7	112.6	-45.3	131.7	1.11	500	11.9	2.84	3.11	-

"-" *means that no value was reported in the reference source.*
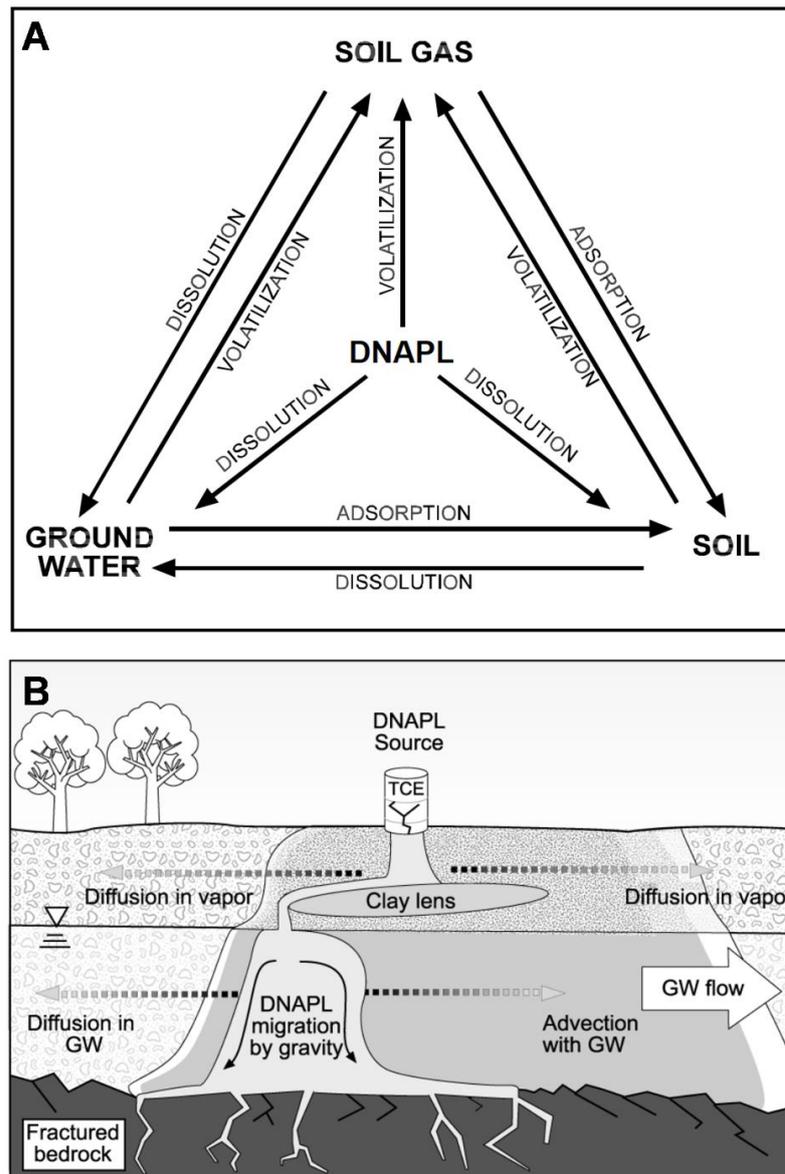
Figure 1.1. (A) Phase-equilibrium mechanisms of CAH. (B) CAH subsurface transport processes from a DNAPL source. DNAPL: dense non-aqueous phase liquid, TCE: trichloroethene. Source: USEPA (2000).

As a result of the beforementioned physicochemical processes, chlorinated solvents released into groundwater tend to form a contamination plume, in which the DNAPL is the source. In contrast, the most soluble solvents are the easiest and, thus, furthest to be transported and are typically detected in the distal areas of the plume due to advection, as it is one of the key processes affecting migration of contaminants in groundwater (Figure 1.1B) (Sims et al., 1992; USEPA, 2000).

The rise of modern industrial processes around the world has resulted in the increasing release of organic chemicals to the environment, leading to an unprecedented pollution of terrestrial systems by chlorinated solvents (Loganathan, 2011). Contamination of soil and groundwater by organochlorides can either derive from point sources (e.g. industrial spills) or non-point sources (e.g. widespread application in agriculture). Typically, point sources are more common and exhibit higher concentrations compared to non-point sources (Meckenstock et al., 2015). Several studies have reported the widespread groundwater contamination by chlorinated solvents in the United States (Moran, 2006; Moran et al., 2007; Zogorski et al., 2006). In Europe, it has been estimated from 16 countries (representing 40% of the study population) that chlorinated solvents represent the 8.3% and 10.0% of contaminants affecting soil and groundwater, respectively (Panagos et al., 2013). Lastly, a similar distribution has been assessed for the autonomous community of Catalonia (Spain) for the period 2012–2016 by *Agència de Residus de Catalunya* (ARC, authority responsible for the waste generated in Catalonia), in which chlorinated solvents represented around 8-9% of pollutants in soils (ARC, 2016, 2015, 2014, 2013, 2012). Here, about 80% of the impacted soil and groundwater is the result of industrial and commercial practices (Fernàndez-Garcia et al., 2014).

Even though some of these industrially produced organochlorides can also be found naturally in the environment, many of them can become a problem when natural systems can neither adapt to their presence nor degrade them rapidly (Lyon and Vogel, 2013). Their recalcitrance under oxic conditions is boosted by their toxicity to microbes; the lack of complete catabolic pathways for their degradation by microorganisms; and, related to the latter, the accumulation of intermediates which usually are highly reactive and toxic as well (Nikel et al., 2013). In the recent years, the awareness of the consequences of environmental pollution have promoted efforts to prevent further spills to soil and groundwater.

However, in many cases, the damage to the ecosystem was already done and pollution caused by the historical accumulation of organochlorides in aquifers has become one of the major challenges for scientists and engineers.

1.3. Toxicological risks and contaminant levels in groundwater

In general, organochlorides have been known to be toxic for a long time (Freitag et al., 1994). However, studies are showing that their effects to the environment and human health (Diamanti-Kandarakis et al., 2009; Ruder, 2006) are even broader and more severe than previously expected.

Organochloride pesticides in soils and water bioaccumulate in living organisms and are biomagnified along the food chain. Hence, these pollutants can affect a wide range of non-target species, such as zooplankton, mussels, earthworms, birds, and mammals (Carson, 1962; Jayaraj et al., 2016; Muller et al., 2004; Naidoo et al., 2009; Sparling, 2016). Specific mixtures of organochloride pesticides can cause health adverse effects such as reproductive defects, neurobehavioral abnormalities, endocrine and immunological toxicity, and fatty acid metabolism disorders (Liu et al., 2017; Mrema et al., 2013), as well as increased risk of breast cancer and diabetes (Boada et al., 2012; Daniels et al., 2018).

Exposure to chlorinated VOCs (CVOCs) represents a risk factor for several kinds of cancer (Barul et al., 2017; Cogliano et al., 2011; Wartenberg et al., 2000). For instance, both trichloroethene (TCE) and VC are classified in Group 1 as carcinogenic; dichloromethane (DCM) and tetrachloroethene (PCE) in Group 2A as probably carcinogenic; and carbon tetrachloride (CT) and chloroform (CF) in Group 2B as possibly carcinogenic to humans (IARC, 2019). In addition, CT, CM and DCM can also potentially harm the global environment by threatening stratospheric ozone (Harper, 2000; Hossaini et al., 2017; Penny et al., 2010).

Consequently, many of the chlorinated solvents detected in groundwater and investigated here are included in the list of priority pollutants of both the U.S. Agency for Toxic Substances and Disease Registry (ATSDR) as well as the European Commission (2012). The ATSDR list is revised and published on a 2-year basis with the U.S. Environmental Protection Agency (U.S. EPA) and is based on detection frequency of these substances at facilities on the National Priorities List and their potential threats to human health due to toxicity and exposure (ATSDR, 2017). To date, the ranking for some of these solvents, out of 274 substances, is: VC (4th), CF (11th), TCE (16th), PCE (33rd), CT (50th), DCM (88th), monochlorobenzene (MCB, 128th), *trans*-1,2-dichloroethene (*trans*-DCE, 180th), CM (192nd), 1,2-dichloroethene (DCE, 220th, mixture of *cis*- and *trans*-), and *cis*-1,2-dichloroethene (*cis*-DCE, 274th) (ATSDR, 2017).

Given the risks posed by chlorinated solvents, maximum contaminant levels in soils, water and groundwater have been set by several authorities to ensure the safety of both the environment and human population. Table 1.3 compares the thresholds for concentration of chlorinated solvents in groundwater proposed by U.S. EPA (USEPA, 2019), the European Union (E.U.) (European Commission, 2008) and *Agència Catalana de l'Aigua*, the public authority executing the Catalan government's policy on water (ACA, 2010, 2009). On its side, the Spanish Government set a maximum level of 100 μg/L for the sum of the three trihalomethanes (bromodichloromethane, bromoform and CF); of 10 μg/L for the sum of TCE and PCE; and of 0.5 μg/L for VC (Real Decreto 140/2003).

The quality standards for groundwater established by the abovementioned authorities are intended to enforce public and private parties to act on their polluted sites. Consequently, remediation efforts worldwide focus on developing new technologies and improving the traditional ones to achieve such environmental regulations.

Table 1.3. Maximum contaminant levels in groundwater expressed in µg/L proposed by several authorities (U.S. EPA, EU and ACA). MCLG: maximum contaminant level goal. MCL: maximum contaminant level allowed. VGNR: no-risk generic value. VGI: intervention generic value. "-" means that no levels were set for that contaminant by the entity.

	U.S. EPA		E.U. [a]		ACA	
	MCLG (µg/L)	**MCL** (µg/L)	**MCLG** (µg/L)	**MCL** (µg/L)	**VGNR** (µg/L)	**VGI** (µg/L)
CM	-	-	-	-	-	-
DCM	0	5	-	20	250	750
CF	70	-	-	2.5	70	210
CT	0	5	-	12	8	30
VC	0	2	-	-	0.25	5
1,1-DCE	7	7	-	-	<10 [b]	60
trans-DCE	100	100	-	-	80	240
cis-DCE	70	70	-	-	-	-
TCE	0	5	-	10	<10 [b]	50
PCE	0	5	-	10	<10 [b]	75
MCB	100	100	-	-	80	240

[a] *The Directive applies to water and does not specify on groundwater.*
[b] *The sum of these three pollutants cannot be greater than 10 µg/L.*

1.4. Groundwater remediation technologies

As the migration of a DNAPL depends on its physicochemical properties but also the hydrogeochemical properties of the aquifer in which it has been released, it often ends up at the bottom of aquifers, where accessibility is relatively low (Majone et al., 2015). Therefore, an in-depth understanding of the site (i.e. lithology, heterogeneity, permeability, hydraulic conductivity, existence of preferential flow paths, etc.) is required before being able to characterize the contamination plume and design a remediation strategy.

The clean-up of soils and groundwater polluted by chlorinated solvents can be approached in different ways, depending on the characteristics of the site and the contamination plume. The decision of which treatment to use will be affected by whether the contaminants are in the non-saturated (NSZ) or the saturated zone

(SZ) of the aquifer, and whether they can be treated on-site (*in-situ* or *ex-situ*) or they must be removed and treated off-site (*ex-situ*). In this regard, *in-situ* and *ex-situ* refer to the exact location of the contaminants, i.e. if they can be treated exactly where they were detected in the aquifer. Thus, the extraction of groundwater and subsequent treatment by e.g. air stripping (Majone et al., 2015), is considered an *ex-situ* approach, even though it is performed at the same location.

A summary of the remediation techniques that are typically used in DNAPL contaminated sites is presented below (based on Fernàndez-Garcia et al. (2014)).

Excavation

Consists in the excavation and extraction of the DNAPL contaminated soil volume from the NSZ. It generates large volumes of polluted soils, requiring further treatment *ex-situ*.

Soil vapor extraction (SVE)

SVE is the application of vacuum at the NSZ to induce an air-vapor flow that is later recovered and treated. It is effective to remove VOCs and promote aeration and aerobic biodegradation processes, but it may lose efficiency in low permeability or stratified heterogeneous media (Kirtland and Aelion, 2000).

Surfactants

Surfactants improve DNAPL dilution into groundwater and increase their mobility and availability in the SZ, allowing their treatment via other strategies such as biodegradation, groundwater pumping or soil washing (Wang et al., 2019). The cost-effectiveness of this strategy depends on the characteristics of the injections, heterogeneity of the media and surfactant distribution, and the risks of uncontrolled DNAPL mobility.

Pump and treat (P&T)

Consists in the groundwater pumping and extraction from the DNAPL source zone in the SZ. Pumped groundwater must be treated later at another treatment facility (Figure 1.2) (Rivett et al., 2006). The flow of groundwater through the source zone eases DNAPL dilution and its recovery from the aqueous phase. It is not very cost-effective for DNAPL polluted sites due to the dilution process, which can be very slow (Mackay and Cherry, 1989; Voudrias, 2001), and the risks of DNAPL displacement and contamination of previously clean zones.
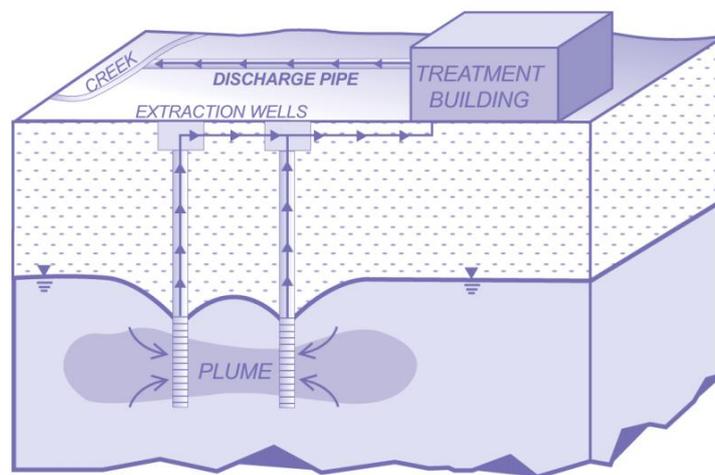
Figure 1.2. Scheme for a P&T remediation system. Source: USEPA (2002).

Dual-phase extraction (DPE) or bioslurping

It is used to pump and remove DNAPL and vapours near the water table while promoting air circulation and aerobic bioremediation, if applicable (Figure 1.3) (Alvarez and Illman, 2005a).

In-situ thermal desorption (ISTD)

This technique is based on the use of heat to increase volatility of VOCs and remove them from the soil. VOCs can be collected later via SVE (Heron et al., 1998) or destroyed by the effect of temperature (Friis et al., 2007). In many cases,

it is combined with bioremediation, as temperature induces aquifer changes that may be favourable to microorganisms (Badin et al., 2016).
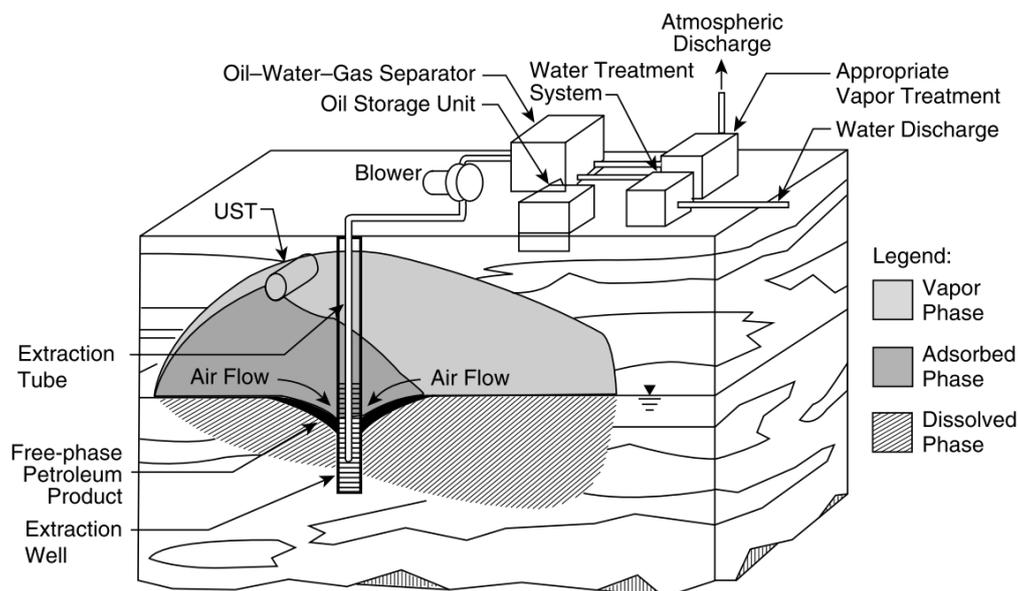
Figure 1.3. Scheme for a DPE remediation system. Source: USEPA (1995).

Physical barriers

Physical barriers are used to contain DNAPL transport both in the NSZ and SZ, but do not eliminate the contaminant. Thus, there is always the risk of leakage. They are usually applied together with other remediation techniques.

Permeable reactive barriers (PRB)

These barriers create an *in-situ* treatment zone both in the NSZ and the SZ that passively captures and removes pollutants from groundwater either via chemical or biological reactions, or adsorption and precipitation (Higgins and Olson, 2009). However, there is risk of leakage and formation of harmful metabolites.

In-situ chemical oxidation (ISCO)

ISCO is the injection of chemical oxidants (e.g. potassium permanganate) to the subsoil to treat pollutants in the SZ (Krembs et al., 2010). Chemical oxidation

should transform them to innocuous substances (e.g. PCE and TCE oxidation to CO_2 and Cl^-). It is not clear, however, what are the ISCO effects when DNAPL is still present. In addition, efficiency depends on the media heterogeneity and the distribution of the injected oxidant.

In-situ chemical reduction (ISCR)

ISCR is the use of chemical reductants (e.g. reduced iron solids or minerals such as zero-valent iron, ZVI) to degrade contaminants in the SZ. This approach involves a broader and more complex spectrum of reductive pathways, is strongly surface dependent, and can be enhanced trough the use of chemical and/or biological reduction (Brown, 2010; Brown et al., 2009). These reductants can be injected into the subsoil or installed as a PRB (Audí-Miró et al., 2015).

Bioremediation

This *in-situ* and/or *ex-situ* strategy is based on the exploitation of the metabolism of living organisms to degrade pollutants. It can be low-cost and does not generate a final residue, but it can entail relatively long treatment times. In *in-situ* approaches, it is limited by aquifer conditions from both the NSZ and the SZ. Bioremediation is usually combined with other strategies (Soares et al., 2010; Vidali, 2001).

Monitored natural attenuation (MNA)

MNA is the comprehensive monitoring of natural or induced degradation of DNAPLs from both the NSZ and the SZ, either by dilution, volatilization, biodegradation, etc. It is one of the most used techniques to reduce mass of pollutants from the source zone. However, it is typically accompanied by other remediation techniques such as P&T, ISCO, ISCR or bioremediation, as natural degradation is oftentimes limited.

Even though there seems to be a wide spectrum of technologies to clean-up groundwater, the field of groundwater remediation has reached an interesting crossroads in the recent years (Majone et al., 2015; Spira et al., 2006). The growth of technological knowledge and the establishment of stricter environmental regulations, in terms of subsoil investigation and quality, has allowed for the discovery of many point-source pollution incidents (Figure 1.4) (ACA, 2017).
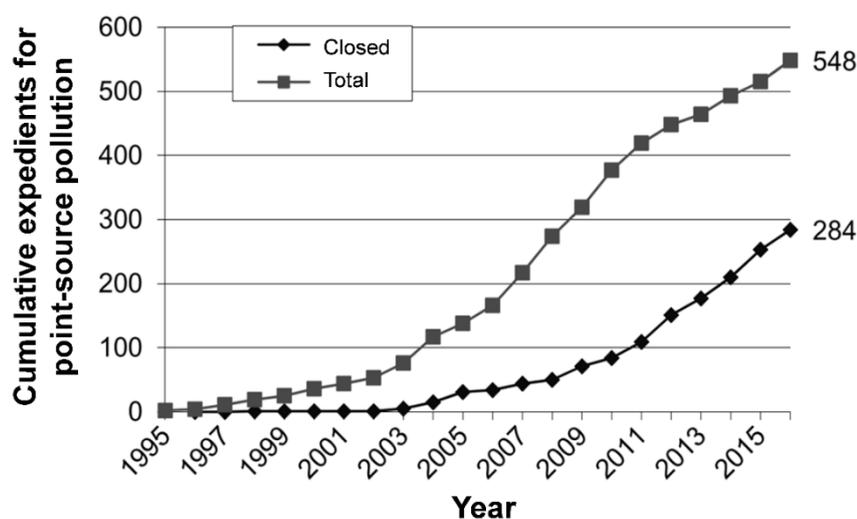
Figure 1.4. Evolution of point-source pollution incidents in Catalunya and comparison between total expedients registered and those that have been closed. Source: adapted from ACA (2017).

Moreover, innovation has improved the characterization and understanding of polluted sites, increasing their complexity in terms of contamination and remediation approach (Leeson et al., 2013). For instance, remediation in the U.S. has rapidly developed since the late 1970s. Originally, planned treatment times for groundwater remediation were relatively short and P&T was the most used technology (USEPA, 1989, 1983). However, this led to the non-compliance of short-term remediation goals and motivated the choice of MNA and other *in-situ* remediation treatments, at least, as often as P&T (Leeson et al., 2013; USEPA, 2010). Consequently, research efforts in the recent years have focused on the development and improvement of *in-situ* treatment approaches (Leeson et al., 2013).

To this end, many reports have provided a guideline or toolkit for practitioners to consult when considering *in-situ* remediation technologies such as ISTD, ISCO, ISCR and bioremediation (Kueper et al., 2014; Leeson et al., 2013; Stroo and Ward, 2010). Nevertheless, even though the cost and performance of such approaches is relatively well understood, remediation companies are usually hesitant regarding which treatment to use, as it depends on the characteristics of the site and contamination plume (Leeson et al., 2013).

Within the realm of remediation possibilities, *in-situ* bioremediation rises as a very competitive contender due to its cost-effectiveness, implementation ease, lack of final residue, and reduced life-cycle and local toxic impacts (Lemming et al., 2010). For this reason, it has emerged as one of the preferred alternatives for soil and groundwater remediation (Pandey et al., 2009).

1.5. Bioremediation: using biology to clean up groundwater

According to Crawford and Crawford (2005), bioremediation is "*the process whereby organic wastes are biologically degraded under controlled conditions to an innocuous state, or to levels below concentration limits established by regulatory authorities*". As it exploits the metabolic processes of living organisms, the degradation of contaminants can occur naturally as long as they are present and environmental conditions are appropriate for their survival and performance. Such approach already represents an improvement over some of the conventional remediation strategies as it detoxifies the contaminants, rather than contain and/or relocate them, which involves long-term maintenance, high costs and potential liabilities (Spira et al., 2006; Vidali, 2001).

Within the biological remediation field, two branches can be distinguished: the vegetation-based remediation, referred to as phytoremediation, and the

remediation by microorganisms such as bacteria, algae, and fungi. The term bioremediation is commonly associated to the latter.

In phytoremediation, plants are used to remove pollutants from soil and water via uptake, absorption, stabilization, degradation, or extraction and volatilization (Lee, 2013). These techniques have been investigated and tested over the years and, even though such remediation approaches seem promising (Peuke and Rennenberg, 2005), experts have expressed some concerns on their remediation capability and efficiency (Conesa et al., 2012).

Microbe-based bioremediation treatments can either be *ex-situ* or *in-situ*. The former include techniques such as biopiles, windrow and in-vessel composting, landfarming, and bioreactors; while the latter can include permeable reactive barriers, bioventing, biosparging, or bioslurping (Atlas and Philp, 2005; Stroo and Ward, 2010). The present thesis is focused on MNA, biostimulation and bioaugmentation, three *in-situ* strategies that, in this study, use the metabolism of anaerobic bacteria to transform chlorinated solvents to innocuous end-products.

In this framework, MNA, also named intrinsic biodegradation, is defined as "*the natural occurring processes in soil and groundwater environments that act without human intervention to reduce the mass, toxicity, mobility, volume, or concentration of contaminants in those media*" (Odencrantz et al., 2003) and, hence, is the less invasive *in-situ* biodegradation alternative. However, the greatest demand of this approach is to provide lines of evidence of the occurrence and extent of biodegradation, to avoid the suspicions of not acting on the pollution incident, and guarantee the detoxification within an acceptable time period (Atlas and Philp, 2005; Smets and Pritchard, 2003).

Biostimulation, also known as enhanced reductive dechlorination (ERD) or enhanced anaerobic biodegradation, aims at promoting the activity of native or

indigenous bacteria that can transform and detoxify pollutants. Such approach is typically selected when MNA is not feasible (Leeson et al., 2004). The stimulation of bacterial activity can be achieved either by the addition of substrates than can take up the role of carbon source, electron donor/acceptor, etc.; or by the control of temperature, redox potential, pH, etc. (Atlas and Philp, 2005; Majone et al., 2015). Through these actions, the aquifer system can be modified so that bacteria have everything they need to thrive. Thus, once the amendment is added in groundwater through the injection wells (Figure 1.5A), the degradation of contaminants can occur naturally (as if it were an MNA), and the only remaining task is the monitoring of the remediation process.

Lastly, bioaugmentation is chosen when neither MNA nor ERD are feasible, which occurs when the required degrading bacteria are not active or even present in the ecosystem. This technology consists in the inoculation of specific bacterial strains or consortia to improve the biodegradation capacity of the aquifer for a target contaminant. In such cases, it is customary to add a substrate as well, like in a biostimulation approach, to make sure that aquifer conditions are adequate for the inoculated bacteria. For this reason, this is the most costly, intrusive and complex of the three alternatives, as the design and successful implementation of the remediation treatment is delicate and depends on many factors (Atlas and Philp, 2005; Stroo et al., 2013).

Commonly, organic fermentable substrates are the amendments that are used for the conditioning of the subsoil towards anoxic conditions, as they can serve as both carbon source (e.g. acetate) and electron donor (e.g. hydrogen) for the degrading anaerobic bacteria. Once they are added to groundwater, they are fermented by indigenous fermentative bacteria, leading to the release of hydrogen and depletion of the dissolved oxygen via aerobic respiration. Afterwards, other terminal electron acceptors from the aquifer are reduced, lowering the oxidation-

reduction potential (i.e. redox potential, Eh) of groundwater. Microorganisms typically use the alternative electron acceptors (if possible) in the following order of preference: nitrate > manganese and ferric iron hydroxides or oxyhydroxides > sulphate > carbon dioxide (Figure 1.5B) (Henry, 2010). The consecutive occurrence of these reduction reactions converts aquifer zones that were naturally oxic to anoxic. Under the new reduced conditions achieved via the organic substrate addition (Figure 1.5B), anaerobic degraders can outcompete the other microorganisms present in the aquifer ecosystem for hydrogen and perform the anaerobic biodegradation of the pollutants (Lovley, 2001).

Several aerobic and anaerobic mechanisms have been described to degrade chlorinated solvents in groundwater, but anaerobic biodegradation may be the most efficient in the detoxification of chlorinated ethenes, ethanes and methanes (Bouwer, 1994; Henry, 2010). For instance, anaerobic biodegradation of PCE and TCE can occur under nitrate-reducing to methanogenic conditions (Bouwer, 1994; Bradley, 2003; Van Der Zaan et al., 2010), especially if an excess of electron donor is present (Aulenta et al., 2007). But this transformation process can be inhibited through the competition for electron donors between anaerobic degraders of CVOCs and other indigenous anaerobic microorganisms that use hydrogen (Wei and Finneran, 2011). For this reason, one of the key decisions in the implementation of bioremediation is the type and concentration of amendment (i.e. electron donor) to use, which may vary depending on the site.

In-situ biodegradation via bacterial metabolism has several advantages over the other most used remediation approaches (Alvarez and Illman, 2005b; Majone et al., 2015). For instance, treating and detoxifying the contamination plume *in-situ* reduces the risk of pollutant exposure to workers and the environmental impact, while also avoids the production of waste products. In addition, one of the major advantages when compared to the other technologies is its cost-effectiveness.
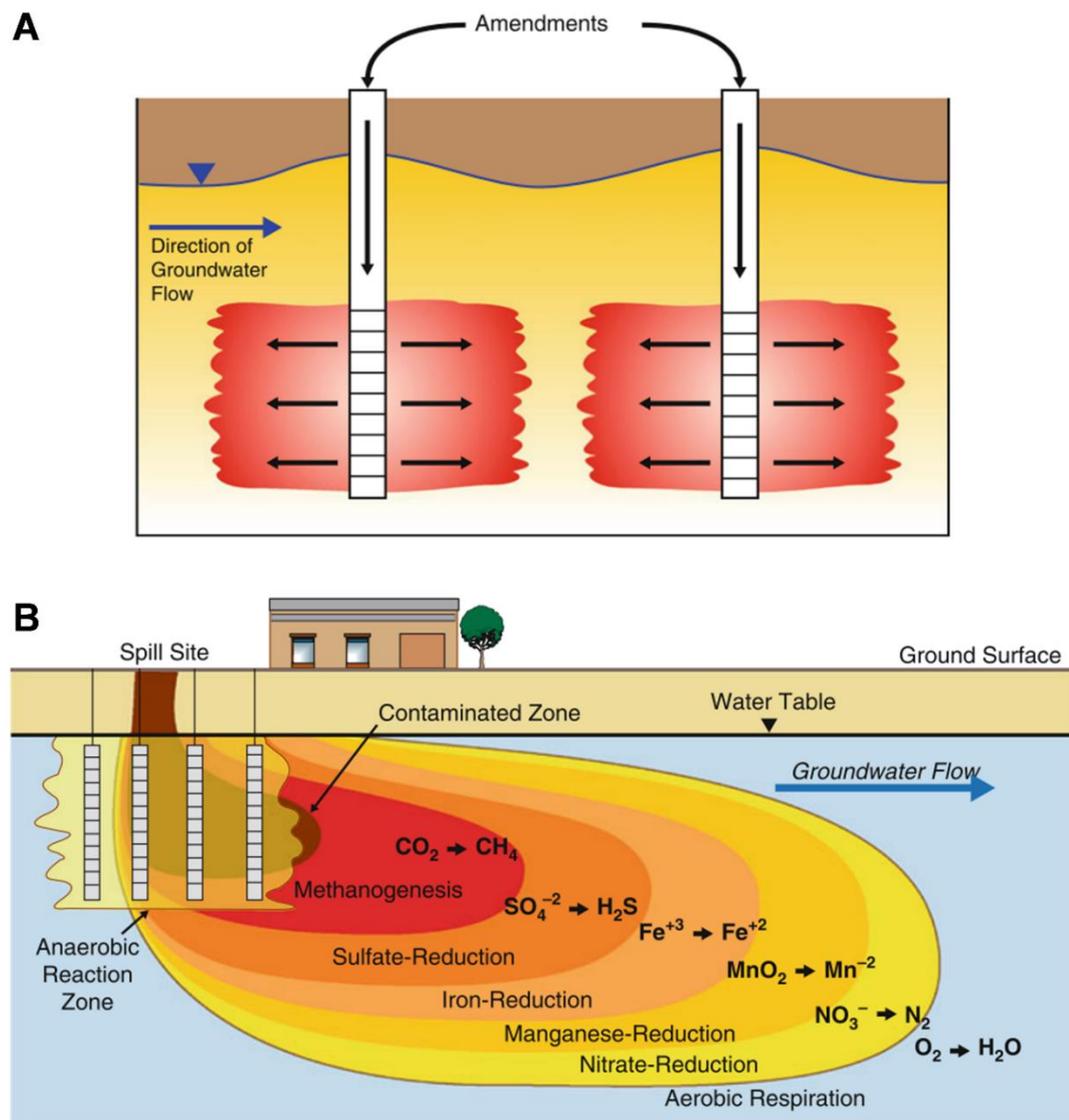
Figure 1.5. (A) Schematics of a direct substrate injection for an ERD of chlorinated solvents. (B) Changes in the reducing zones downgradient of an ideal substrate injection for an ERD of chlorinated solvents. Source: Henry (2010).

Many of the physicochemical strategies, e.g. P&T or SVE, require a heavy infrastructure (i.e. pumps, compressors, pipelines) and energy to run it for a long period of time. Moreover, they also require an external treatment system for the extracted vapours or groundwater. In contrast, the only extra cost in an *in-situ* biodegradation treatment comes from the purchase of the amendments, if required, as it can use the boreholes from the site investigation as the monitoring and/or injection wells. Therefore, such bioremediation approach is potentially

ideal for the decontamination of chlorinated solvents from soils and groundwater (USEPA, 2000).

1.6. Organohalide-degrading bacteria

In the same manner that organohalides are produced naturally, ecosystems can also harbour microorganisms with the potential to degrade them. Since polluted aquifers are often anoxic, or present anoxic microenvironments, and chlorinated solvents are recalcitrant under oxic conditions, biodegradation by strict anaerobic bacteria has revealed itself as one of the most efficient remediation alternatives of groundwater to date (Adrian and Löffler, 2016a). Nevertheless, these pollutants can also be degraded by other bacteria that are not strictly anaerobes. For example, facultative methylotrophic bacteria can degrade DCM (Muller et al., 2011) and facultative anaerobes such as *Pseudomonas* or *Xanthobacter* can degrade several chlorinated solvents through co-metabolic processes (Bhatt et al., 2007).

The capability of anaerobic bacteria to degrade organohalides depends on the chemical bond between both the halogen and the carbon atoms. In particular, the carbon–chlorine (C–Cl) bond is the second strongest and shortest (in length) of all the halogens (Reineke, 1984). Those aspects, together with the reactivity of the C–Cl bond, are influenced by the type of carbon attached to the halogen (e.g. aromatic or aliphatic). Moreover, as halogens are strongly electronegative, they form stable bonds with carbon. This electronegativity gives organohalides an oxidizing character, making them susceptible to degradation under anoxic conditions (Dolfing, 2016).

The biodegradation of organochlorides by anaerobic bacteria under reducing conditions usually occurs through a reaction that is referred to as reductive

dechlorination (i.e. reductive dehalogenation for halogens in general). In this reaction, the C–Cl bond gets broken and the chloride atom is released, and this can occur via two mechanisms: hydrogenolysis or β-elimination (i.e. dihaloelimination or dichloroelimination for chloride). In the former, a mole of HCl is produced per two electrons ($2H^+$); in the latter, two moles of HCl are produced per two electrons ($2H^+$) during the removal of two chloride atoms from vicinal carbon atoms (Figure 1.6) (Dolfing, 2016). For instance, PCE is sequentially dechlorinated to ethene (ETH) through several consecutive hydrogenolysis steps, with the formation of the lesser chlorinated ethenes (CEs) as intermediates (i.e. TCE, DCE and VC) (McCarty, 2016).
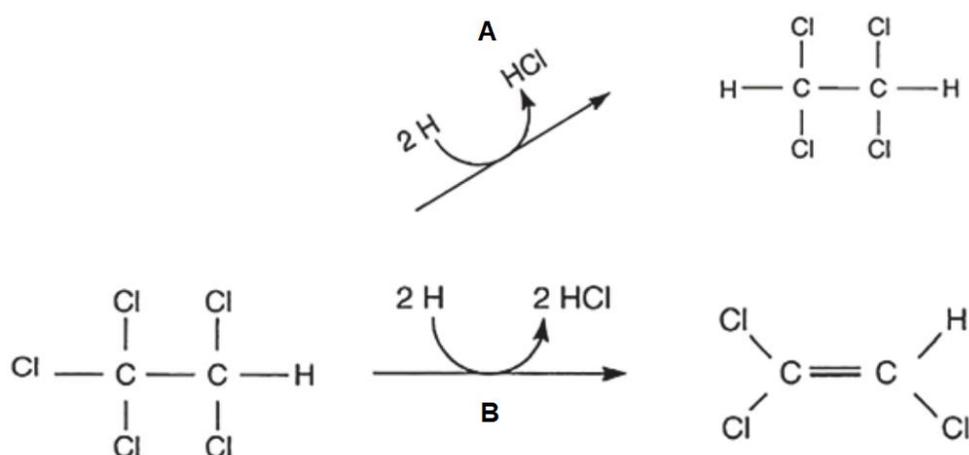
Figure 1.6. Examples of the reductive dechlorination reactions of pentachloroethane to tetrachloroethane by hydrogenolysis (A) and β-elimination (B). Source: Dolfing (2016).

Even though reductive dechlorination is a common mechanism to degrade chlorinated solvents under anoxic conditions, it is not the only one described. To date, strict anaerobes that are capable of degrading organohalides to less chlorinated compounds can be divided into two groups depending on their metabolism and the mechanism used in that transformation. These two bacterial groups are known as organohalide-respiring bacteria (OHRB) and organohalide-fermenting bacteria, and their main characteristics are presented in the below sections.

1.6.1. Organohalide-respiring bacteria

OHRB use organohalides during microbial respiration for energy conservation and growth, thus, they couple the reductive dechlorination of the pollutants under anoxic conditions to survival. In detail, organohalides are used as terminal electron acceptors in the respiratory chain, while the necessary electrons can be provided by external electron donors (e.g. hydrogen) or other oxidizable compounds. This process is coupled to a proton movement across the cell membrane and energy conservation (Adrian and Löffler, 2016a). Figure 1.7A presents a much simplified scheme of a microbe cell performing organohalide respiration and the principal components involved, as recent publications have reported that this reaction may involve much more complex mechanisms (Jugder et al., 2016; Kublik et al., 2016; Seidel et al., 2018).

The cleavage of the carbon–chlorine (C–Cl) bond in organochlorides is driven by dehalogenase enzymes. There are three different mechanisms for which this process can occur. The chloride substituent can either be replaced with i) an hydroxyl group from water by hydrolytic dehalogenases; ii) an hydroxyl group from oxygen by oxygenolytic dehalogenases; or iii) an hydrogen atom by reductive dehalogenases (rdh) (Figure 1.7A) (Adrian and Löffler, 2016a).

Rdh are a diverse protein family from which there are still a lot of unanswered questions in regards to sequence diversity, substrate specificities, global distribution, and modes of inheritance (Hug, 2016). Nevertheless, the rdh that have been characterized and proved to be functional in microbial respiration are encoded by rdh operons mainly composed by the genes *rdhA* and *rdhB*. The former encodes the catalytic unit, while the latter putatively encodes a small membrane-anchoring protein and other accessory genes (Hug et al., 2013) (Figure 1.7B). Other *rdhA* homologs have been described to function in a non-respiratory manner. This means that they can act in the cleavage of the

C–Cl bond of organohalides, so that the less- or non-halogenated daughter products are available to microorganisms for subsequent catabolism, but this process is not coupled to growth. So far, it seems that these rdh are not encoded with associated *rdhB* genes (Chen et al., 2013; Payne et al., 2015).
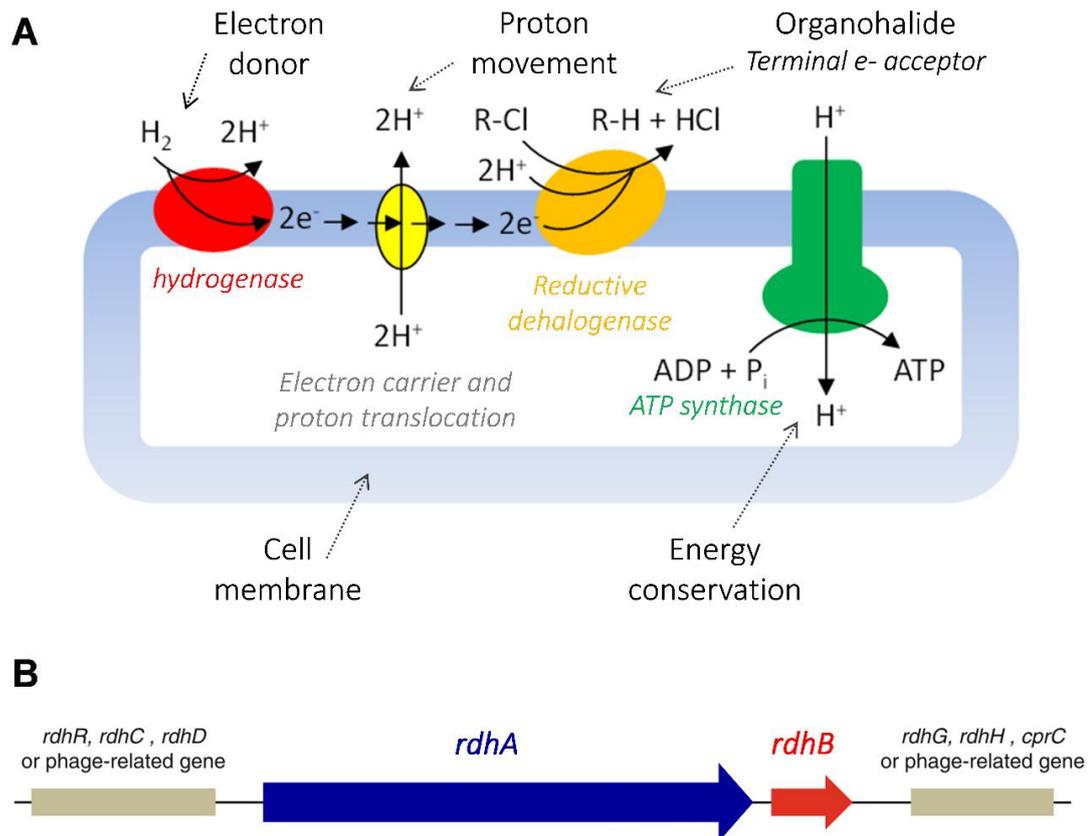
Figure 1.7. (A) Simplified scheme of a microbe cell performing organohalide respiration and the principal components involved. Source: Enviro Wiki contributors (2018). *(B) Scheme of a generic Dehalococcoides (Dhc) rdh operon. All Dhc rdh gene clusters consist of rdhA and rdhB, which is located downstream of rdhA. Most putative Dhc rdh gene clusters lack one or all of the accessory genes rdhC, rdhD and rdhG, which can be located on the forward or reverse strands and their functions are unclear. Arrows indicate the direction of the open reading frames in a typical rdh operon. Source: adapted from* Löffler et al. (2012).

The reductive dechlorination reaction during organohalide respiration is a very exergonic process, thus, microbes can obtain a considerable amount of energy from this reaction (Dolfing, 2016). The harnessed energy does not come

directly from the participating compounds but from the electric potential difference between the redox couples (Figure 1.7A) (Adrian and Löffler, 2016a). In theory, it yields enough energy for ATP generation (Figure 1.7A), but biomass yields are highly variable and depend on the organism and substrate used. However, OHRB produce about 4-fold more biomass per mole of hydrogen consumed than other microorganisms in other processes (e.g. hydrogenotrophic methanogens). Hence, OHRB are really efficient at harnessing the energy released during degradation of organohalides (Dolfing, 2016).

Even though the breakage of the C–Cl bond is thermodynamically favourable (Dolfing, 2016), growth yields for OHRB are low and that is possibly the reason why they are a minor representation of natural microbial populations. But, even if that were the case, it has been proved that a modest OHRB population can degrade organochlorides at high concentrations (Adrian and Löffler, 2016a).

There are several OHRB genera that can degrade different families of pollutants. On the one hand, those that belong to the genus *Dehalogenimonas* are obligate OHRB and, generally, degrade halogenated alkanes with halogens in adjacent carbons (e.g. 1,2-dichloropropane, 1,2-dichloroethane, or ethylene dibromide) (Moe et al., 2016), but have been reported to degrade CEs as well (Molenda et al., 2016; Yang et al., 2017b). On the other hand, there are the facultative OHRB from the genera *Desulfitobacterium*, which can use both chlorinated aliphatic and aromatic compounds (e.g. CEs, chlorophenols) as electron acceptors, among others (Futagami and Furukawa, 2016), or *Sulfurospirillum*, which can grow with many substrates but only a few organisms use organohalides (mainly CEs) as electron acceptors (Goris and Diekert, 2016). Among all the OHRB genera described to date (Atashgahi et al., 2016),

three of them will be thoroughly discussed in this thesis as they can degrade a wide range of chlorinated solvents that are usually detected in groundwater at industrial areas: *Geobacter*, *Dehalococcoides* and *Dehalobacter*.

Geobacter

Geobacter genus belongs to the *Proteobacteria* (Phylum), *Deltaproteobacteria* (Class), *Desulfuromonadales* (Order) and *Geobacteraceae* (Family) and was first identified by Lovley et al. (1993). This genus is a facultative OHRB since organohalide respiration is not their only mechanism to harness energy and their metabolism is more versatile, i.e. they can grow on a wide spectrum of electron acceptors (Maphosa et al., 2010). The species *Geobacter lovleyi* (*G. lovleyi*) strain SZ was isolated from a non-impacted freshwater sediment and couples the oxidation of acetate to the dechlorination of PCE to *cis*-DCE for growth (Figure 1.8) (Sung et al., 2006a). This strain can use both pyruvate and molecular hydrogen as electron donors, and PCE, TCE, Fe(III), Mn(IV), U(VI), malate, nitrate, fumarate and elemental sulphur as electron acceptors (Sung et al., 2006a). Other isolates sharing 99-100% nucleotide identity with strain SZ and also performing the PCE to *cis*-DCE dechlorination have been described elsewhere (Wagner et al., 2012). Similarly, *G. lovleyi* strain KB-1 was described to dechlorinate PCE to *cis*-DCE as well (Duhamel and Edwards, 2006). Recently, the functional expression and characterisation of the PCE dehalogenase *PceA* from *Geobacter* sp. was described by Nakamura et al. (2018).

Dehalococcoides

Dehalococcoides (*Dhc*) belongs to the *Chloroflexi* (Phylum), *Dehalococcoidia* (Class), *Dehalococcoidales* (Order) and *Dehalococcoidaceae* (Family) (Löffler et al., 2013). Several strains have been isolated to date (*Dehalococcoides ethenogenes* 195, CBDB1, BAV1, VS, FL2, GT, JNA, CG1, CG4, CG5, SG1, AD14-1, and

AD14-2) and have been classified as the genus and species *Dehalococcoides mccartyi* (*D. mccartyi*) (Atashgahi et al., 2016; Löffler et al., 2013). *Dhc* are obligate anaerobes and are metabolically restricted to organohalide respiration, molecular hydrogen as electron donor, and acetate as a carbon source (Löffler et al., 2013). To date, it has been reported that different strains can use different chlorinated ethenes as electron acceptors but, in general, *Dhc* can sequentially transform PCE or TCE to *cis*-DCE, which is the most common metabolite in TCE biodegradation (Bouwer, 1994), to VC to ETH (Figure 1.8). Other electron acceptors used by *Dhc* include chlorobenzenes, polychlorinated biphenyls, dioxins, pentachlorophenol or bromophenol (Zinder, 2016).
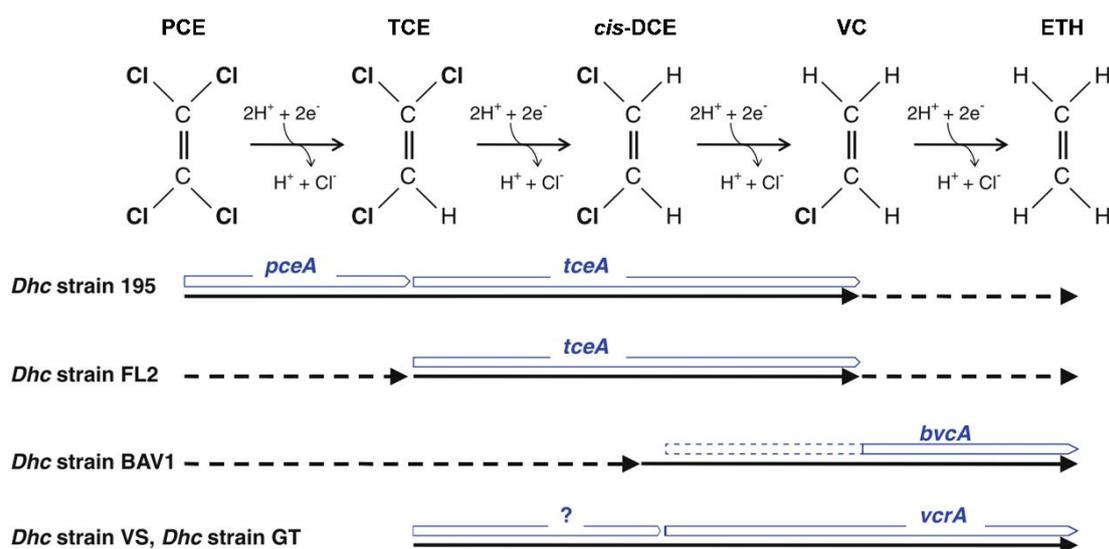
Figure 1.8. Dhc rdh genes implicated in the reductive dechlorination of CEs. Strains GT and VS dechlorinate TCE but do not possess tceA. VcrA dechlorinates all DCE isomers and VC (Muller et al., 2004). *BvcA is implicated in VC dechlorination* (Krajmalnik-Brown et al., 2004) *but its involvement in DCE dechlorination has yet to be demonstrated. Source: adapted from* Löffler et al. (2012).

Several rdh have been characterized (they have a known function) for *Dhc*, including *PceA*, *TceA*, *BvcA*, *VcrA*, *CbrA* and *DcpA*, but these only represent a subset of the total rdh genes that are implicated in the organohalide respiration of chlorinated solvents (Löffler et al., 2012; Zinder, 2016). In particular, the

former four are implicated in the sequential reductive dechlorination of PCE to ETH (Figure 1.8) (Löffler et al., 2012).

Dehalobacter

Dehalobacter bacteria belong to the *Firmicutes* (Phylum), *Clostridia* (Class), *Clostridiales* (Order) and *Peptococcaceae* (Family) (Holliger et al., 1998). *Dehalobacter* spp. are obligate OHRB and require acetate as a carbon source and molecular hydrogen as electron donor, except for a couple of cases that were reported to grow fermentatively on CM and DCM, where the latter was transformed to acetate (Justicia-Leon et al., 2012; Lee et al., 2012). These findings suggest that growth of *Dehalobacter* is not limited to organohalide respiration. To date, *Dehalobacter* spp. has been described to use PCE, TCE, CF, chlorinated ethanes, 2,4,6-trichlorophenol, 2,4,6-tribromophenol, chlorinated benzenes, β-hexachlorocyclohexane, and phthalide as electron acceptors during reductive dechlorination (Atashgahi et al., 2016). According to this, several rdh have been characterized to date, including *PceA* (Maillard et al., 2003), *CfrA* and *DcrA* (Tang and Edwards, 2013), *TmrA* (Jugder et al., 2017) and *TcbA* (Alfán-Guzmán et al., 2017).

1.6.2. Organohalide-fermenting bacteria

Even though a broad spectrum of organochlorides commonly detected in groundwater can be degraded by OHRB, no evidence of the hydrogenolysis of DCM, another frequent pollutant in aquifers, has been reported to date.

One alternative for the degradation of organohalides is fermentation, which is a type of anaerobic catabolism, a redox reaction in which organohalides both donate and accept electrons without any involvement of an external electron acceptor (Madigan et al., 2018). Fermentation is a reaction that is disproportionate, which means that the part of the compound of intermediate

oxidation is oxidized, while the other part is reduced (Madsen, 2015). This type of metabolism harnesses energy at the expense of other reactions (Madigan et al., 2018). From a thermodynamic point of view, many organohalides could be transformed through fermentation due to their chemical structure (i.e. being good electron acceptors). For instance, both trichloroethane and chlorophenol could be fermentable, but these reactions have only been predicted theoretically and, to date, not reported to occur naturally. Until now, the only organohalide that has been described as fermentable, and it can occur in nature, is DCM (Dolfing, 2016).

Within strict anaerobes, biodegradation of DCM has been solely reported for three genera affiliated with the *Peptococcaceae* family: *Dehalobacterium* (*Dhb*), *Dehalobacter*, and *Candidatus* Dichloromethanomonas elyunquensis (D. elyunquensis) and all of them metabolize DCM through a fermentation reaction.

Dehalobacterium

Dehalobacterium formicoaceticum (*Dhb f.*) was the first, and only one to date, to be isolated and characterized, and it ferments DCM to formate and acetate (Mägli et al., 1998). However, the mechanism for which the chloride substituents are removed is still unclear (Dolfing, 2016). Furthermore, it seems that organohalide respiration is not involved, as no rdh are encoded in the genome (Chen et al., 2017). Recently, a stable enriched DCM-degrading culture containing *Dhb* was obtained by our research group (Trueba-Santiso et al., 2017).

Dehalobacter

As briefly mentioned in section 1.6.1, cultures that contained *Dehalobacter*, among other taxa, have also been reported to ferment DCM. In the non-

methanogenic culture obtained by Justicia-Leon et al. (2012), the fermentation of DCM yielded acetate and biomass, whereas acetate, methane, traces of formate and biomass were produced after the consumption of DCM by the culture described in Lee et al. (2012).

Candidatus Dichloromethanomonas elyunquensis

Recently, the novel species *Candidatus* Dichloromethanomonas elyunquensis has been identified and reported to ferment DCM to acetate as well. Moreover, production of hydrogen was observed prior to the formation of acetate and methane. This could suggest that the formation of hydrogen during DCM fermentation could further support microorganisms that consume or require it. Interestingly, rdh were found to be encoded in the sequence of the genome (Kleindienst et al., 2017).

Even though significant research advances are being made, there is still a lot to discover about these DCM fermenters. A deeper understanding of their degradation mechanisms, genomics and the enrichment of cultures and isolation of these bacteria would allow the development of tools to distinguish, assess, monitor and implement DCM biodegradation *in-situ*.

1.7. Monitoring of the bioremediation process

Whether the bioremediation of organohalides is investigated at the laboratory or the field scale, it needs to be closely monitored to understand the main mechanisms that govern it, assess the extent and success of the process, and identify any potential setbacks. An overview of the lines of evidence that have been investigated in this thesis to assess and monitor biodegradation both at the laboratory and the field scale are presented below.

1.7.1. Hydrogeochemistry

Given that bioremediation depends on the survival and growth of bacteria, it is necessary that aquifer conditions are appropriate for them. In the case of chlorinated solvents, it has been already mentioned in the previous sections that anaerobic bacteria are highly specialized for their degradation. Therefore, it is mandatory that the aquifer stays anoxic through the remediation process to guarantee its success (whether it was naturally anoxic or conditioned by means of substrate addition).

The first line of evidence of the potential for biodegradation and, thus, that the aquifer is in the appropriate conditions to harbour OHRB, is obtained from the evolution of the concentrations of the compounds of interest. Target substances include major anions and cations in groundwater, which can be used as redox sensitive species to monitor Eh; the pollutants (in this thesis, chlorinated solvents), which are the electron acceptors; and the electron donor, either natural or amended (i.e. organic fermentable substrate of choice).

The determination of the anions and cations in groundwater such as nitrate, ferrous iron, and sulphate gives information on the availability of alternate electron acceptors. Their consumption and, hence, chemical reduction can provide evidence of the achievement of anoxic conditions (Figure 1.9) (Leeson et al., 2004). These redox sensitive species can qualitatively indicate that aquifer conditions are favourable to reductive dechlorination reactions when their concentrations are <1 mg/L for nitrate, <20 mg/L for sulphate, >1 mg/L for iron (II) and >0.5 mg/L for methane (Wiedemeier et al., 1998)). Dissolved oxygen (DO) in groundwater is another parameter that gives information regarding the oxic or anoxic conditions of the aquifer is the. According to Carter et al. (2008), DO concentrations that are ≥0.5 mg/L are considered oxic, whereas they are considered anoxic if they are <0.5 mg/L. However, in

the latter scenario, not all occurring degradation is necessary linked to anaerobic bacteria (Rosell et al., 2010).

Additionally, Eh monitoring also keeps track of the redox conditions. As depicted in Figure 1.5B, the anaerobic reaction zone, where bacteria will be able to degrade chlorinated solvents, will be created when iron-reducing to methanogenic conditions are achieved. The optimal Eh range for the anaerobic dechlorination of chlorinated solvents is from -100 to -250 mV, approximately (Figure 1.9) (Bouwer, 1994; Leeson et al., 2004). However, it is possible that anaerobic dechlorination starts even before than that, as the one-electron reduction potentials for CT, CF and some chlorinated ethanes range, approximately, from +200 to -100 mV (Elsner and Hofstetter, 2011). Thus, as long as Eh values are adequate for anaerobic dechlorination, the aquifer can be considered conditioned for biodegradation (i.e. anoxic).

Some of the other parameters that must be controlled, as they are also relevant for the success of the bioremediation process, are pH and temperature (T). For instance, the acidity generated from both the fermentation of the amended electron donor in a biostimulation, and the dechlorination of the pollutants, can affect the degrading activity, hence, it is important that pH is maintained within the neutral range of 6-8, which has been reported as optimal for OHRB (Adrian and Löffler, 2016b; Yang et al., 2017a). Regarding T, optimal growth of OHRB occurs when it ranges between 25–30 ºC, although some bacteria can grow with T up to 40 ºC (Adrian and Löffler, 2016b). Bacteria can also grow at T as low as 10 ºC, for example, but the process is a lot slower in such conditions.

The monitoring of the electron donor can be achieved by measuring either its concentrations and the concentrations of its fermentation products (e.g. added lactate, and pyruvate, acetate, and formate), or the dissolved or total organic

carbon present in the aquifer (DOC or TOC, respectively). The information obtained from these analyses provides evidence on the presence of an electron donor and carbon source, the usage of such electron donor by fermentative bacteria, and can even shed light on the active reaction pathways.

Redox Potential (E_h°)
in millivolts @ pH = 7
and 25 degrees Celsius

Aerobic

Anaerobic

Decreasing Amount of Energy Released During Election Transfer

Possible Range for Anaerobic Dechlorination

Optimal Range for Anaerobic Dechlorination

$$O_2 + 4H^+ + 4e^- \longrightarrow 2H_2O \ (E_h^{\circ} = +820)$$

$$2NO_2^- + 12H^+ + 10e^- \longrightarrow N_2 + 6H_2O$$
$$(E_h^{\circ} = +740)$$

$$MnO_2(s) + HCO_3^- + 3H^+ + 2e^- \longrightarrow MnCO_2(s) + 2H_2O$$
$$(E_h^{\circ} = +520)$$

$$FeOOH(s) + HCO_3^- + 2H^+ + e^- \longrightarrow FeCO_3 + 2H_2O$$
$$(E_h^{\circ} = -50)$$

$$SO_4^{2-} + 9H^+ + 8e^- \longrightarrow HS^- + 4H_2O \ (E_h^{\circ} = -220)$$

$$CO_2 + 8H^+ + 8e^- \longrightarrow CH_4 + 2H_2O \ (E_h^{\circ} = -240)$$

Figure 1.9. Redox potentials (Eh) for several electron-accepting processes and optimal ranges for anaerobic dechlorination. Source: Leeson et al. (2004).

Lastly, the analysis of the concentrations of the pollutants and dechlorination products can reveal information on the biochemical processes that are taking place either in the laboratory or in the field. The decrease and elimination of the parent compound and increase of the dechlorination product will typically suggest that biodegradation is occurring. But if the monitored bioremediation process is at the field scale, in an open system (i.e. aquifer), these results should be taken with caution. In these situations, a decrease in concentration can also be caused by other processes besides biodegradation (e.g. dilution, sorption, volatilization). Therefore, variations in the concentration of the target compounds can be a line of evidence of occurring biodegradation, can hint at it, but cannot confirm it on its own.

1.7.2. Compound specific isotope analysis (CSIA)

As explained above, assessing the biodegradation process in groundwater is tricky due to the openness of the system. Mass balances based on concentrations of the pollutants have traditionally been used to monitor remediation, but they can show remarkable variations and not always be linked to their remediation. For instance, concentration of pollutants in groundwater can decrease due to dilution after a rainfall, or adsorption to soil, or advection to other parts of the aquifer. Thus, it is not a standalone parameter that can confirm that degradation and elimination of contaminants is occurring.

An alternative to this problem is the compound-specific stable isotope analysis (CSIA). Stable isotope approaches are based on the existence, in nature, of two or more stable isotopes of the same element that have different natural abundances. For example, 98.93% of carbon in nature is in the form of ^{12}C, while only 1.07% of carbon is in the form of ^{13}C. For chlorine, 75.76% occurs as ^{35}Cl, while the remaining 24.24% occurs as ^{37}Cl. For hydrogen, 99.9885% is ^{1}H and 0.0115% is ^{2}H (i.e. deuterium). Similarly, 94.99% is ^{32}S and 0.75% is ^{33}S, and for oxygen, 99.757% is ^{16}O, while 0.038% is ^{17}O, and 0.205% is ^{18}O (Laeter et al., 2003).

Isotopes of the same element exhibit nearly the same chemical behaviour, as it is largely dependent on its electrons and not on its neutrons. However, due to the mass differences, heavier isotopes form shorter and more stable chemical bonds, and diffuse more slowly, than the lighter ones. And this is reflected in environmental processes like biochemical transformations, where different rates can be obtained for the same mechanism/reaction by the different isotopes. Typically, chemical bonds with the lighter isotope are degraded faster by bacteria, leading to the enrichment of the lighter isotope in the daughter product, and the enrichment of the heavier isotope in the residual

parent compound. These rate differences and isotopic preferences that occur during biochemical transformations cause a shift in the isotopic composition of the pollutants, which can be measured through the abundance ratio of those stable isotopes (Aelion et al., 2009).

In contrast to concentrations, this isotopic shift is linked to the transformation of the pollutants present in groundwater, thereby, the conclusions obtained from its measurement are more conclusive. Furthermore, the change in the isotopic compositions caused by biodegradation is considered significant compared to that of physical processes such as dilution or adsorption, which is commonly regarded as negligible (Figure 1.10) (Aelion et al., 2009; Hunkeler et al., 1999). Therefore, the monitoring of the transformation process via isotopes is more reliable than via concentrations as the shift in isotopic compositions is an evidence that can be associated to biodegradation and nothing else. In particular, this is of great interest for the site investigation and remediation field, as legislation requires a direct line of evidence of biodegradation (Aelion et al., 2009; Elsner, 2010).

CSIA is a useful tool that allows practitioners to assess the effectiveness of remediation treatments, either biotic or abiotic. The measurement of the isotopic composition can be used for source apportionment (i.e. identify which are the sources of pollution and how much of each contributes to total pollution), as well as the monitoring of transformation processes in the field (Elsner, 2010; Hunkeler et al., 2008). In addition, a quantitative estimation of the biodegradation extent in the field is possible as well (Aelion et al., 2009).

Dual isotope analysis (i.e. the study of more than one element) improves the identification of the source and fate of pollutants in the field. The latter is based on that the relationship between the isotopic shifts in both elements reflect ongoing degradation mechanisms (Elsner, 2010). Thus, information

gathered from laboratory studies can be compared with that obtained from groundwater samples to investigate degradation processes in the field (Aelion et al., 2009). All relevant isotopic parameters (e.g. $\delta^h E$, ε, and Λ) are defined in Chapter 3, section 3.2.7.

For chlorinated solvents, the isotopes of interest typically are $^{13}C/^{12}C$, $^{37}Cl/^{35}Cl$ and $^{2}H/^{1}H$, but nitrogen, sulphate or oxygen stable isotope analysis of redox sensitive species can also be useful to understand the reduction reactions of alternative electron acceptors that are occurring on site.
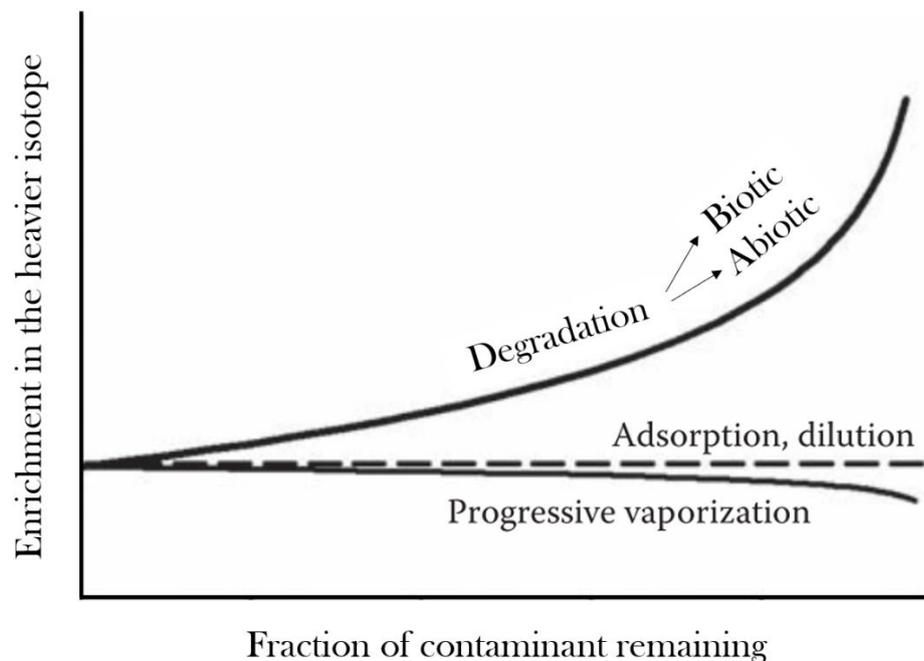
*Figure 1.10. Illustration of the potential of CSIA to distinguish between physical processes and degradation (both biotic and abiotic) in the field. Source: adapted from* Aelion et al. (2009).

1.7.3. Molecular biological tools (MBT)

Another line of evidence that could indicate the feasibility of a bioremediation strategy, or monitor and confirm its success, is the presence and identification

of the required bacteria in the aquifer. This can be achieved by investigating the bacterial population and identifying either the genera or species of bacteria that are present and, more importantly, active, or the genes that catabolise the reaction of interest. The use of molecular biological tools (MBT) for this purpose, both from a qualitative or quantitative perspective, is becoming very common. MBT include techniques such as the polymerase chain reaction (PCR), the quantitative polymerase chain reaction (qPCR), and the DNA high-throughput sequencing (e.g. Illumina) (Bombach et al., 2010; Jugder et al., 2016; Löffler et al., 2012).

The qualitative (presence and/or expression) or quantitative assessment of specific genes, such as rdh and/or 16S rRNA, can be applied as biomarkers to evaluate the intrinsic bioremediation potential or activity of OHRB at polluted sites. For instance, MBT targeting *tceA*, *bvcA*, *vcrA*, and/or 16S rRNA genes from *Dhc* can be used to predict and/or monitor *in-situ* reductive dechlorination of CEs (Muller et al., 2004; Tarnawski et al., 2016).

1.8. Present challenges of bioremediation

As outlined in the above sections, the discovery of the metabolism of OHRB has created a feasible solution for sites that have been impacted with organohalides. Their ability of transforming those pollutants into less toxic or even innocuous compounds represents one of the best approaches for site remediation to date. Thus, bioremediation has emerged as one of the most favoured and sustainable means of soils and groundwater clean-up.

However, there are still a lot of unanswered questions regarding these microbial-mediated processes (Meckenstock et al., 2015). Among those, the identification of the rdh genes that catabolise the dehalogenation reactions, in an

effort to expand the catalog for biomarkers, but also allow the prediction of fate of organohalides in aquifer systems (Adrian and Löffler, 2016c). Furthermore, some of these pollutants have not been sufficiently investigated (e.g. chlorinated methanes (CMs) and emerging contaminants). This is also important because the presence of complex mixtures of contaminants in groundwater is very common and co-contamination can compromise the success of bioremediation due to inhibition issues (Duhamel et al., 2002; Mayer-Blackwell et al., 2016).

In all, even though recent efforts have managed to improve substantially the understanding of OHRB, more research is still necessary to better define their roles in natural microbial communities, and fully exploit their capacity for remediation (Adrian and Löffler, 2016c).

Chapter 2

Objectives of the thesis

The present thesis aims at deepening the knowledge on anaerobic biodegradation processes (natural and enhanced) of chlorinated solvents at field groundwater conditions in order to improve future bioremediation strategies applied at contaminated sites. This general purpose is sought, primarily, by means of an integrative approach that combines hydrogeochemical data, microcosm experiments, and molecular and isotopic techniques at the:

- Laboratory scale, on a diagnosis level, to assess the intrinsic bioremediation potential of three sites contaminated with different chlorinated solvents and representing different case scenarios.

- Field scale, to monitor the implementation of an *in-situ* enhanced biological reductive dechlorination, aiming to detoxify an aquifer contaminated with chlorinated ethenes and based on the previous diagnosis for a successful bioremediation strategy.

In order to achieve these main objectives, the present study has the following specific objectives:

1) To determine whether the hydrogeochemical conditions of the polluted aquifers are appropriate for the growth and survival of organohalide-respiring bacteria.

2) To investigate whether *in-situ* biodegradation processes are occurring through the analysis of stable isotopic compositions of the detected chlorinated solvents.

3) To identify biomarkers that confirm the presence of the required bacteria for the complete detoxification of the aquifer.

4) To confirm the above-mentioned lines of evidence with the establishment of field-derived microcosms, which would demonstrate the real capability of the ecosystems to transform chlorinated solvents to innocuous end-

products and help elucidate the active transformation reactions and degradation pathways.

5) To investigate the effect of different case scenarios (single parent compound, co-contamination in complex multi-contaminated sites, and active sources) on the intrinsic biodegradation potential of these sites.

6) To gather and/or determine the stable isotopic compositions of commercial pure phase chlorinated solvents and the fractionation associated to their anaerobic biodegradation to improve the interpretation of field data and degradation pathways.

7) To combine the previous results to assess the intrinsic bioremediation potential of these aquifers and recommend a bioremediation strategy, at least, for one of the sites.

8) To implement an *in-situ* pilot test and monitor the biodegradation process with a selection of the techniques described above.

9) On the basis of the results obtained in the *in-situ* pilot test, to implement a full-scale biological treatment and monitor the success of the bioremediation.

Chapter 3

General materials and methods

List of contents

3.1. Materials

All chemicals and reagents used in the present work were of analytical grade and purchased at the highest purity available. Purities, suppliers, state (solid (S), liquid (L) or gas (G)) and abbreviations (used along the text) of the compounds used are indicated in Table 3.1.

Table 3.1. List of chemicals and reagents used in this thesis.

Chemicals (abbreviation)	Purity	Supplier	State
4-Aminobenzoic acid		Sigma Aldrich	S
Acetic acid		Sigma Aldrich	L
Acetone		Sigma Aldrich	L
Agarose		Biorad	S
Ammonium chloride		Panreac	L
Biotin		Sigma Aldrich	S
Boric acid		Panreac	S
Calcium chloride		Panreac	S
Calcium pantothenate		Sigma Aldrich	S
Hydrochloric acid	37%	Honeywell	L
Chloroform (CF)	>99%	Sigma Aldrich	L
Chloroform (CF)	>99%	Alfa Aesar	L
Chloroform (CF)	>99%	Merck	L
Chloromethane (CM)		Sigma Aldrich	L
cis-1,2-dichloroethene (*cis*-DCE)	>99%	Chem Service	L
Cobalt chloride 6-hydrate		VWR	S
Copper (II) chloride dihydrate		Sigma Aldrich	S
Dichloromethane (DCM)	>99%	Sigma Aldrich	L
Dichloromethane (DCM)	>99%	Fisher	L
Dichloromethane (DCM)	>99%	SDS	L
Dichloromethane (DCM)	>99%	Merck	L
DNA gel loading dye		Thermofisher	L
DNA safe gel stain		Thermofisher	L
Ethanol	>99%	Scharlau	L
Ethene (ETH)	>99%	Sigma Aldrich	G
Formic acid		Merck	L
Gas mix CO2/N2		Carburos Metálicos	G
Hydrogen		Carburos Metálicos	G
Iron (II) chloride tetrahydrate		Sigma Aldrich	S
L-Cysteine	97%	Sigma Aldrich	S
Magnesium chloride hexahydrate		Sigma Aldrich	S
Manganese (II) chloride 4- hydrate		Panreac	S

Chemicals (abbreviation)	Purity	Supplier	State
Mastermix (iQ Supermix)		Biorad	L
Methanol		Sigma Aldrich	L
Molecular ruler		Biorad	L
Monochlorobenzene (MCB)	>99%	Sigma Aldrich	L
Nickel (II) chloride		Sigma Aldrich	S
Nicotinic acid		Sigma Aldrich	S
Nitric acid	70%	Sigma Aldrich	L
Nitrilotriacetic acid	>99%	Sigma Aldrich	S
Nitrogen		Carburos metálicos	G
Perchloroethene (PCE)	>99%	Panreac	L
Perchloroethene (PCE)	>99%	Sigma Aldrich	L
Potassium chloride		Panreac	S
Potassium dihydrogen phosphate		VWR	S
Propionic acid	>99%	Sigma Aldrich	L
Pyridoxine hydrochloride		Sigma Aldrich	S
Pyruvic acid	>98%	Panreac	L
Resazurin sodium salt		Sigma Aldrich	S
Sodium 2-bromoethanesulfonate	>99%	Sigma Aldrich	S
Sodium acetate		Panreac	S
Sodium bicarbonate		Sigma Aldrich	S
Sodium chloride		Panreac	S
Sodium DL-lactate (Lactate-1)	>99%	Sigma Aldrich	S
Sodium formate		Alfa Aesar	S
Sodium hydroxide		Panreac	S
Sodium L-lactate (60% w/w, Lactate-2)	97%	Purac (Corbion)	L
Sodium molybdenum oxide dihydrate	98%	VWR	S
Sodium pyruvate		VWR	S
Sodium selenite pentahydrate	98%	Sigma Aldrich	S
Sodium sulphide nonahydrate	98%	Sigma Aldrich	S
Sodium tungstate dihydrate	99%	Acros	S
Sulphuric acid	96%	Sigma Aldrich	L
Thiamine chloride hydrochloride		Merck	S
trans-1,2-dichloroethene (*trans*-DCE)		Sigma Aldrich	L
Trichloroethene (TCE)	>98%	Panreac	L
Tris-acetate-EDTA buffer		Thermofisher	L
Vancomycin hydrochloride hydrate		Sigma Aldrich	S
Vinyl chloride (VC)	>99%	Chem Service	L
Vitamin B12	>99%	Sigma Aldrich	S
Water for molecular biology		Sigma Aldrich	L
Yeast extract		Scharlau	S
Zinc chloride		VWR	S

3.2. Methods

The general analytical methods that have been used in this work are presented below. The particularities of each experiment will be described in the corresponding result chapters.

3.2.1. Groundwater sampling and *in-situ* parameters

Groundwater samples from selected monitoring wells were generally collected with a peristaltic pump, although bailers were used when the water table was too low. In the three study sites, the monitoring wells were conventional fully screened wells and the obtained values are an average of the whole screen length, which might be heterogeneous. The first step in the collection of groundwater samples was the measurement of the *in-situ* field parameters, in this order: (1) the piezometric level; (2) the worker short-term exposure to volatile organic compounds (VOCs) and other gases, with a MiniRAE Lite direct-reading photoionization detector (RAE Systems, Spain); and (3) the hydrogeochemical parameters of groundwater, once they were steady, using a flow-through cell to avoid contact with the atmosphere. The monitored parameters were temperature, pH, electric conductivity (EC), and the oxidation-reduction potential (ORP), and they were measured with a multiparameter probe 3430 WTW (Weilheim). For ORP, the redox sensor was a SenTix ORP 900. To obtain the redox potential (Eh), the *in-situ* ORP measurements were corrected to the standard hydrogen electrode system (UH) by adding the reference electrode potential at the temperature of groundwater to the measured potential (ORP). The description of the equipment used for the *in-situ* measurements is depicted in Figure 3.1.

Once all parameters were annotated, samples from the aquifer were obtained. Groundwater for stable isotope analyses (CSIA) and chemical characterization

(i.e. hydrochemistry) was collected at 1 m above the bottom of the monitoring wells, to avoid sediments. The ones for CSIA were chemically preserved (with acid or base, depending on the VOCs present) to prevent further biodegradation reactions.
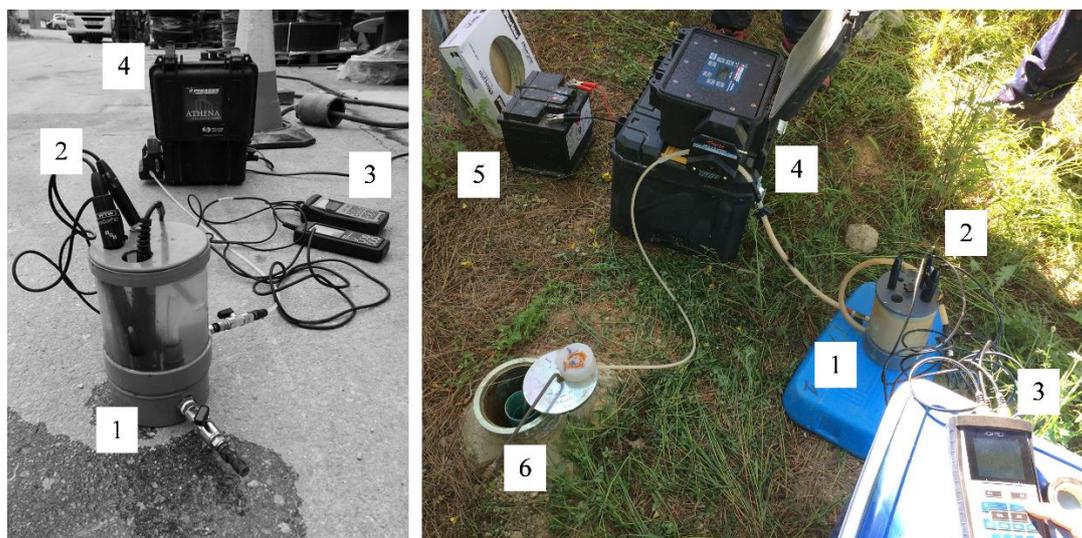
Figure 3.1. Equipment used for the measurement of the in-situ field parameters and the collection of groundwater. 1. Flow-through cell. 2. Sensors (pH, EC, T, ORP). 3. Multiparameter probe. 4. Peristaltic pump. 5. Battery. 6. Monitoring well. The photoionization detector and the sensor to measure the piezometric level are not in the pictures.

For the establishment of field-derived microcosms, groundwater with fine sediments was collected from the bottom of the monitoring wells. Samples were put with caution into transparent or amber autoclaved glass bottles to minimise bacterial contact with oxygen (e.g. through bubbling). The glass bottles had been previously filled with nitrogen gas. Afterwards, they were sealed with polytetrafluoroethylene (PTFE) caps to minimise adsorption of VOCs. All groundwater samples were kept in the dark at 4ºC until analysis.

3.2.2. Establishment of field-derived microcosms

Field-derived microcosms were prepared in an anaerobic glovebox. Glass serum sterile bottles of 100 mL were filled with 70 mL of sampled

groundwater and were sealed with Teflon-coated butyl rubber septa and aluminium crimp caps (Figure 3.2A). Afterwards, if applicable, the amendments were added according to the experimental design. Microcosms were incubated at 25 °C in the dark under static conditions. In order to reach the equilibrium between the water and the gas phase, the initial concentration of VOCs was analysed from the head space the day after the microcosms were set up (see section 3.2.4).

3.2.3. Cultivation and enrichment of field-derived cultures

When required, specific active field-derived microcosms that showed dechlorinating activity were selected for cultivation to maintain or enrich the degrading microbial population.

Cultivation was performed in the form of microcosms as well. However, in this case, a modified anoxic synthetic media was used instead of groundwater, and it was prepared as reported elsewhere (Adrian et al., 1998). The media contained (per litre): 0.2 g of KH_2PO_4, 0.27 g of NH_4Cl, 1 g of $NaCl$, 0.41 g of $MgCl_2 \cdot 6H_2O$, 0.52 g of KCl, 0.15 g of $CaCl_2 \cdot 2H_2O$, 0.7 mg of $ZnCl_2$, 0.8 mg of $MnCl_2 \cdot 4H_2O$, 0.06 mg of H_3BO_3, 0.19 mg of $CoCl_2 \cdot 6H_2O$, 0.02 mg of $CuCl_2 \cdot 2H_2O$, 0.24 mg of $NiCl_2 \cdot 6H_2O$, 0.36 mg of $Na_2MoO_4 \cdot 2H_2O$, 20 mg of $FeCl_2 \cdot 4H_2O$, and 128 mg of nitriloacetic acid. Once the media was prepared, it was vacuumed for 45 min and later bubbled with nitrogen, to remove oxygen, for 20 min. The media was then placed inside the anaerobic glovebox and aliquots of 65 mL were prepared in 100 mL glass serum bottles. After sealing the bottles with Teflon-coated butyl rubber septa and aluminium crimp caps, they were all autoclaved at 121 °C for 40 min. Once they were cooled down, the following components were added aseptically and anoxically from the sterile and anoxic stock solutions: buffer solution (1 g/L $NaHCO_3$), reducing agent solution (25 mg/L $Na_2S \cdot 9H_2O$ + L-cysteine), and filter

sterilized vitamin solution (containing 40 mg/L 4-aminobenzoic acid, 10 mg/L D(+)-biotin, 100 mg/L nicotinic acid, 50 mg/L calcium pantothenate, 150 mg/L pyridoxine hydrochloride, 0.1 mL thiamine chloride hydrochloride). Afterwards, the field-derived inoculum, the gas mixture of N_2/CO_2 (4:1 v/v, 0.2 bar overpressure), H_2 (added to an overpressure of 0.4 bar), the electron acceptor of choice, and other amendments if applicable, were added according to the experimental design (Figure 3.2B). Microcosms were sealed and incubated at 25 °C in the dark under static conditions. As described before, initial VOCs concentration was analysed the following day.
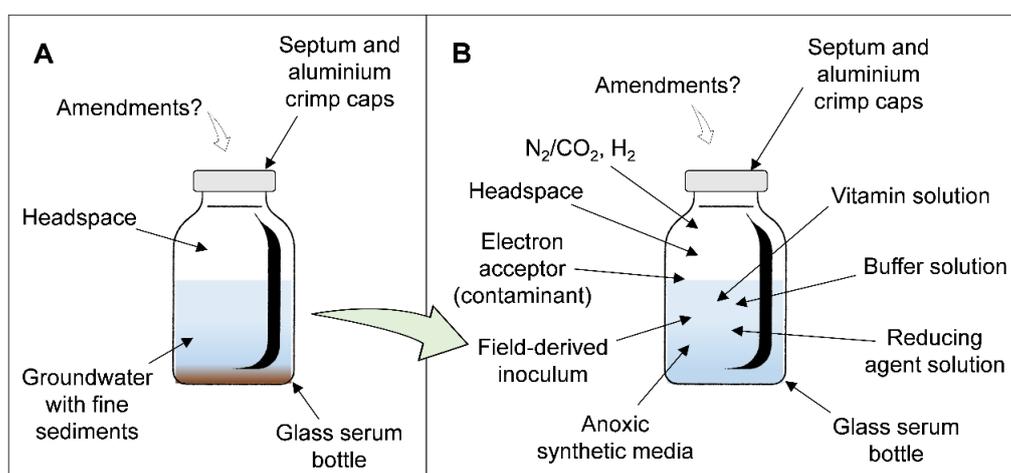
Figure 3.2. (A) Components of the field-derived microcosms. (B) Components for the cultivation (maintenance and/or enrichment) of the degrading microbial population from selected active field-derived cultures.

In order to enrich de microbial population responsible for the degradation of VOCs, active cultivated cultures that depleted the initial dose of electron acceptor, which were all chlorinated solvents in this thesis, were reamended with the same dose of contaminant. During the exponential degradation phase of, at least, the second dose of contaminant (i.e. 80% of contaminant was degraded, approximately), 10% v/v of the culture was transferred (i.e. inoculated) to fresh synthetic media as described above. Such transfers were carried out, at least, in duplicate. Along the serial transferences, the

contaminant dose that was amended was increased progressively, so that the organohalide-degrading bacteria (OHRB) were favoured in front of the other microorganisms present, as explained elsewhere (Löffler et al., 2005).

To enrich the cultures even further and achieve a greater predominance of the OHRB, the dilution-to-extinction method in liquid media was used (Löffler et al., 2005). This method was conducted similarly to the set-up used for the cultivation of field-derived cultures (section 3.2.3) but using 20 mL glass vials containing 12 mL of the synthetic media instead of the 100 mL glass serum bottles with 65 mL of media. In this case, however, a sequential dilution series was generated instead of replicates, with serial 1:10 dilutions that started from an active culture in the exponential degradation phase of the contaminant and ended with a 10^{10} dilution (Figure 3.3).
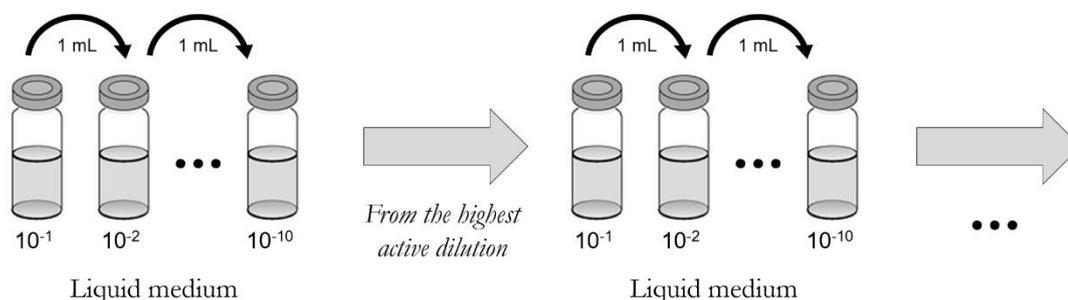
Figure 3.3. Dilution-to-extinction method to enrich the organohalide-degrading cultures.

3.2.4. Concentration of CVOCs and gases

Direct field groundwater or microcosm samples were analysed in the same manner by placing 70 mL into glass serum sterile bottles of 100 mL. To reach the equilibrium between the water and the gas phase, the initial VOCs concentration was analysed from the headspace the day after the bottles were set up. In the case of microcosms, they were later monitored periodically. Prior to sampling, the surface of the septa was flame sterilised. Afterwards, 500 μL

of gaseous headspace sample was obtained with a 1 mL gas tight pressure-lock precision analytical syringe and injected into the injector of a gas chromatograph (GC) model 6890N (Agilent Technologies) coupled to a flame ionization detector (FID). Identification of compounds was by comparison with the retention times of standards analysed in the same manner.

Chlorinated volatile organic compounds (CVOCs)

In the case of CVOCs, the GC-FID was equipped with a DB-624 column (30 m × 0.32 mm, 0.25 µm film thickness, Agilent Technologies). Helium was used as the carrier gas (0.9 mL/min). The injector and detector temperatures were set at 250 and 300 °C, respectively. After the injection of the sample (split ratio 1:2), the initial oven temperature (35 °C) was held for 3 min and then ramped up at 10 °C/min to 240 °C, which was held for 4 min. Run time lasted 27 min and peak areas were quantified with the Millennium/Empower software (Waters).

Ethene and methane

In the case of ethene and methane, the same GC-FID was equipped with a HP Plot Q column (30 m × 0.53 mm, 40 µm film thickness, Agilent Technologies). The oven temperature was fixed at 150 °C, the injector temperature at 250 °C and the detector temperature at 260 °C. Run time lasted 7 min and the peak areas were quantified with the Chromeleon software 6.8 (Thermofisher).

Calibration curves

Calibration curves were obtained from aqueous standards that were prepared in the same manner (liquid/headspace volume ratio) as the microcosms. Glass serum bottles were filled with 70 mL of Mili-Q water and sealed with Teflon-

coated butyl rubber septa and aluminium crimp caps, and chemical standards were added later. The ethene and methane gas stocks were prepared by diluting 1 mL of the pure gas in 1 L nitrogen Tedlar gas sampling bags. From this, different gas volumes were injected into each one of the prepared glass serum bottles with water according to the selected concentrations. The liquid standards were prepared by diluting selected volumes of pure CVOCs, or acetone stock solutions prepared beforehand, into each one of the prepared glass serum bottles with water. Both gas and liquid standards were left to reach equilibrium overnight and were later analysed by GC-FID as outlined above. Lastly, calibration curves were calculated by plotting the obtained peak area versus the selected concentrations. Results are presented as nominal concentrations expressed in μM for all the target substances.

3.2.5. Major anions and cations concentrations

Chemical characterization of groundwater from the aquifer was determined through the analysis of major anions and cations. Aliquots of samples were preserved with nitric acid to measure total concentrations of Fe, Ca, Mg, K and Na by inductively coupled plasma-optic emission spectrometry (ICP-OES, Optima 3200 RL) and by inductively coupled plasma mass spectrometry (ICP-MS, Elan 6000) at *Centres Científics i Tecnològics* of *Universitat de Barcelona* (CCiT-UB). HCO_3^- was determined by titration (METROHM 702SM Titrino). NO_3^-, Cl^- and SO_4^{-2} concentrations were analysed by high-performance liquid chromatography (HPLC) using a WATERS 515 HPLC pump with an IC-PAC anion column and a WATERS detector (mod 432) at CCiT-UB.

3.2.6. Volatile organic fatty acids (VFAs)

VFAs (lactate, pyruvate, acetate, formate and/or propionate) were measured from 1 mL filtered liquid samples (0.22 μm, Millex). The analysis was

performed with a Dionex 3000 Ultimate HPLC (Thermofisher) equipped with a UVD 170S UV detector set at 210 nm. The chromatographic separation was achieved in an ICE-COREGEL 87H3 column (300 × 4.6 mm, Transgenomic) which was set at a temperature of 40 °C. The eluent was an acidic solution of 320 µL/L H_2SO_4, pumped at a flow rate of 0.5 mL/min, and the analysis was isocratic. Injection of samples was carried out with a Dionex autosampler and the injection volume was of 20 µL.

Calibration curves

Standards were prepared as aqueous stock solutions with the chemical standards of interest and based on the concentrations of choice. Calibration curves were calculated by plotting peak areas versus the selected concentrations.

3.2.7. Compound-specific stable isotope analysis (CSIA) of CVOCs

The isotopic compositions of carbon and chlorine are reported in delta notation ($\delta^h E$, in ‰), relative to the international standards VPDB (Vienna Pee Dee Belemnite) and SMOC (Standard Mean Ocean Chloride) (Coplen, 1996; Kaufmann et al., 1984), respectively (Eq. 1)

$$\delta^h E = \left(\frac{R_{sample}}{R_{std}} - 1 \right) \qquad (1)$$

where R_{sample} and R_{std} are the isotope ratios (i.e. $^{13}C/^{12}C$, $^{37}Cl/^{35}Cl$) of the sample and the standard of an element E, respectively (Elsner, 2010).

Carbon stable isotope analysis

Stable carbon isotope analyses were performed with an Agilent 6890 GC equipped with a split/splitless injector, coupled to a Delta Plus isotope ratio

mass spectrometer (IRMS) through a GC-Combustion III interface (Thermo Finnigan) at CCiT-UB. The GC was equipped with a DB-624 column (60 m × 0.32 mm, 1.8 μm film thickness, Supelco). The injector was set at 250 °C in split mode (1:10). The oven temperature program was kept at 60 °C for 5 min, heated to 220 °C at a rate of 8 °C/min, and finally held at 220 °C for 5 min. Helium was used as a carrier gas with a flow rate of 1.8 mL/min. Aliquots of liquid sample were extracted and placed in 20 mL vials to a final volume of 10 mL (samples were diluted according to CVOCs concentrations). Vials contained a 30 mm PTFE-coated stir bar. Diluted samples were later stirred at room temperature and CVOCs were extracted during 20 min by headspace solid-phase microextraction (HS-SPME) using a manual sampler holder equipped with a 75 μm Carboxen-PDMS fibre (Supelco). All samples were measured at least in duplicate and corrected for slight carbon isotopic fractionation induced by the HS-SPME with respect to daily aqueous control standards of CVOCs with known carbon isotope ratios. The $\delta^{13}C$ of these pure in-house standards was determined previously using a Flash EA1112 (Carlo-Erba) elemental analyser (EA) coupled to a Delta C Finnigan MAT IRMS (Thermo Finnigan) through a Conflo III interface (Thermo Finnigan) using six international reference materials (NBS 19, IAEA-CH-6, USGS40, IAEA-600, IAEACH-7, L-SVEC) with respect to the VPDB standard according to Coplen et al. (2006). All the CVOCs aqueous control standards that were injected together with the experimental samples had a $1\sigma < 0.5‰$ and their mean values were used to normalise the $\delta^{13}C$ of the samples, the uncertainties of which were calculated by error propagation.

Chlorine stable isotope analysis

Stable chlorine isotope ratios ($\delta^{37}Cl$) of CVOCs were analysed at Isotope Tracer Technologies Inc., Waterloo (ON, Canada) in the framework of a

short-term PhD research stay under the supervision of Dr. Orfan Shouakar-Stash. A 6890 GC (Agilent) coupled to a MAT 253 IRMS (Thermo Finnigan) was used. This IRMS, equipped with nine collectors, is a continuous flow IRMS with a dual-inlet (DI) mode option. The DI bellows are used as the monitoring gas reservoir and reference peaks were introduced at the beginning of each analysis run (Shouakar-Stash et al., 2006). For the analysis of chlorine isotope ratios of chloroform (CF), the two main ion peaks (m/z 83 and 85) were used, which correspond to isotopologue pairs that differ by one heavy chlorine isotope ($[^{35}\text{Cl}_2{}^{12}\text{C}^1\text{H}]^+$ and $[^{37}\text{Cl}^{35}\text{Cl}^{12}\text{C}^1\text{H}]^+$, respectively) (Breider and Hunkeler, 2014). For dichloromethane (DCM), the chlorine isotopic composition was determined from two ion peaks of the molecular group (m/z 84 and 86) corresponding to $[^{35}\text{Cl}_2{}^{12}\text{C}^1\text{H}_2]^+$ and $[^{37}\text{Cl}^{35}\text{Cl}^{12}\text{C}^1\text{H}_2]^+$, respectively. Similarly to carbon isotopes analysis, the analytes were extracted by HS-SPME, as shown elsewhere (Palau et al., 2017). Samples and standards were diluted at similar concentrations and measured in duplicate. The $\delta^{37}\text{Cl}$ values of pure in-house standards were calibrated to SMOC using an offline methodology (Holt et al., 1997; Shouakar-Stash et al., 2006), and were later used to correct all measurements from samples. Precision (1σ) of the analysis was ≤0.2‰ for $\delta^{37}\text{Cl}$.

Interpretation of isotopic data

A simplified version of the Rayleigh equation in the logarithmic form (Eq. 2) correlates changes in the isotopic composition of an element in a compound (R_t/R_0) with changes in its concentration for a given reaction ($f = C_t/C_0$), which allows to determine the corresponding isotopic fractionation for that element ($\varepsilon^h E$) (Coplen, 2011; Elsner, 2010).

$$\ln\left(\frac{R_t}{R_0}\right) = \varepsilon \cdot \ln(f) \qquad (2)$$

R_t/R_0 can be expressed as $(\delta^h E_t + 1) / (\delta^h E_0 + 1)$ according to $\delta^h E$ definition and the uncertainty corresponds to the 95% confidence interval (CI). The $\varepsilon^h E$ value for an element E is characteristic for a given degradation pathway and can provide information into the reactions that are taking place in the field (Elsner, 2010). Additionally, the $\varepsilon^h E$ value can be used to quantify the extent of biodegradation of a target contaminant if a site-specific $\varepsilon^h E$-value can be obtained (Elsner, 2010).

For a target contaminant, the extent of degradation (D%) in the field can be evaluated with Eq. 3, which is derived from the Rayleigh equation (Eq. 2),

$$D\% = \left[1 - \left(\frac{\delta^h E_t + 1000}{\delta^h E_0 + 1000} \right)^{\frac{1000}{\varepsilon^h E}} \right] \cdot 100 \qquad (3)$$

where $\varepsilon^h E$ refers to the isotopic fractionation, $\delta^h E_t$ are the isotope data from groundwater samples, and $\delta^h E_0$ is the most depleted value found at the field site, assumed to be the most similar to the original source. To this regard, differences in isotope values in the field for both carbon and chlorine ($\varDelta \delta^{13}C$, $\varDelta \delta^{37}Cl$) must be >2‰ for degradation to be considered significant (Hunkeler et al., 2008). Laboratory derived $\varepsilon^h E$ values can either be site-specific (i.e. from microcosm experiments prepared with soil and/or groundwater from the contaminated site) or obtained from the literature.

The dual element isotope correlation, $\varLambda$ (e.g. $\varLambda^{C/Cl}$ for C and Cl), can be obtained from the slope of the linear regression in the dual element isotope plot (e.g. $\varDelta \delta^{13}C / \varDelta \delta^{37}Cl$), and the uncertainty is the 95% CI (Elsner, 2010).

The isotopic mass balance for a specific element can be calculated for the sequential dechlorination of family of contaminants, i.e. the parent compound and its degradation products (e.g. chlorinated ethenes or methanes). In the

present work, the carbon isotopic mass balance was calculated for the sequential reductive dechlorination of chlorinated ethenes, as follows

$$\delta^{13}C_{sum} = x_{PCE} \cdot \delta^{13}C_{PCE} + x_{TCE} \cdot \delta^{13}C_{TCE} + x_{DCE} \cdot \delta^{13}C_{DCE} + x_{VC} \cdot \delta^{13}C_{VC} \quad (4)$$

where x refers to the molar fraction of each compound with respect to the total molar mass (sum of chlorinated ethenes from which isotopic data is available) at the sampling event.

Chapter 4

Site 1

Assessment of the biodegradation potential of an aquifer contaminated with chlorinated ethenes through a multi-method approach

List of contents

Part of this chapter was **published** as:

"Multi-method assessment of the intrinsic biodegradation potential of an aquifer contaminated with chlorinated ethenes at an industrial area in Barcelona (Spain)"

in the journal **Environmental Pollution**.

Abstract

The intrinsic bioremediation potential of an aquifer contaminated with tetrachloroethene (PCE) was assessed by combining hydrogeochemical data of the site, microcosm studies, concentrations of metabolites, compound-specific stable carbon isotope analysis and the identification of selected reductive dechlorination biomarker genes. The characterization of the site evidenced that leaked PCE came from two distinct sources and was transformed to trichloroethene (TCE) and *cis*-dichloroethene (*cis*-DCE) via hydrogenolysis. In addition, the detection of the biomarkers linked to the reductive dechlorination of chlorinated ethenes (CEs) indicated the presence of indigenous bacteria capable of detoxification. However, the *cis*-DCE stall observed was consistent with the geochemistry of the aquifer (positive redox potentials (Eh); presence of dissolved oxygen, nitrate, and sulphate; absence of ferrous iron), which was thermodynamically favourable to dechlorinate highly CEs but not *cis*-DCE and vinyl chloride (VC) to ethene (ETH), which require lower Eh. Accordingly, the addition of organic substrates (e.g. lactate) as electron donors in field-derived anoxic microcosms increased the dechlorination rates and were capable of degrading CEs beyond *cis*-DCE up to ETH, unlike the natural attenuation observed at the field. The array of techniques used in this chapter provided complementary lines of evidence to suggest that an enhanced biologic reductive dechlorination using lactate as electron donor is a feasible strategy to successfully detoxify this site.

4.1. Introduction

PCE and TCE are two CEs that are widely used as degreasing agents in the industry and are frequently detected in aquifers due to their improper disposal or accidental spills. The lesser CEs, dichloroethene (DCE) and VC, are usually found in groundwater after the incomplete reductive dechlorination reaction of PCE and TCE, in a phenomenon commonly referred to as "DCE or VC stall" (Bradley, 2000; Stroo and Ward, 2010). In this scenario, CEs coexist in aquifers forming hazardous chemical mixtures.

Due to their chemical properties, one of the best approaches for the detoxification of CEs is the reductive dechlorination reaction. In order to do so, both biotically and abiotically, reducing conditions (i.e. negative Eh) are required (Bouwer, 1994; Brown et al., 2009; Leeson et al., 2004). If such redox conditions are not naturally present, they can be promoted with the addition of organic fermentable substrates such as lactate, acetate, methanol, ethanol, butyrate, or benzoate (section 1.5, Figure 1.5) (Adrian and Löffler, 2016b; da Silva et al., 2006; Fennell and Gossett, 1998; Gao et al., 1997; Gibson and Sewell, 1992; He et al., 2002; Leeson et al., 2004; Steffan and Schaefer, 2016).

Abiotically, CEs can be degraded by chemical reductants (i.e. reduced minerals) such as magnetite, green rust, iron sulphides (i.e. ferrous iron) and zero-valent iron (ZVI), which reductively dechlorinate CEs through complex mechanisms that can result in a great variety of end-products (Brown, 2010; Brown et al., 2009; Herrero et al., 2019). This process is referred to as *in-situ* chemical reduction (ISCR).

Biotically, CEs can be degraded anaerobically by organohalide-respiring bacteria (OHRB). If aquifer conditions are appropriate, biodegradation can occur naturally and is referred to as monitored natural attenuation (MNA). If they are

not, organic fermentable substrates or biostimulants can be added to promote reducing conditions in a process is commonly known as biostimulation or enhanced reductive dechlorination (ERD), or non-native OHRB can be inoculated into the aquifer in a bioaugmentation approach. Some of the OHRB that can partially dechlorinate PCE to TCE or *cis*-DCE anaerobically include *Clostridium* sp., *Dehalobacter* sp., *Desulfitobacterium* sp., *Desulfuromonas* sp., *Geobacter* sp., or *Sulfurospirillum* sp. (Löffler et al., 2012), but several strains of the *Dehalococcoides* (*Dhc*) genus are the only ones capable of fully dechlorinating PCE to innocuous ETH (Cupples et al., 2003; He et al., 2005; Sung et al., 2006b). Nevertheless, a *Dehalogenimonas* sp. has been recently reported to dechlorinate TCE to ETH (Yang et al., 2017b), thus, it may be possible that other bacteria, still unknown to date, are able to detoxify CEs.

Different approaches allow for the characterization and monitoring of *in-situ* biodegradation of organochlorides (Bombach et al., 2010; Nijenhuis and Kuntze, 2016). However, the limitations presented by a single-line-of-evidence approach (section 1.7) reinforce the use of a multidisciplinary assessment, an integrated study that provides different and complementary lines of evidence for the assessment of the intrinsic potential of contaminated sites to fully dechlorinate chlorinated solvents (Badin et al., 2016; Courbet et al., 2011; Stelzer et al., 2009).

In this chapter, the bioremediation potential of a site only contaminated by CEs, located at an industrial area in Barcelona (Spain), was assessed by means of a multi-method approach. To this end, several techniques were used, including (1) the assessment of the hydrogeochemical conditions of the aquifer, (2) the analysis of the carbon isotopic composition of CEs, (3) the establishment of anoxic field-derived microcosms to evaluate the effect of different biostimulants to detoxify groundwater samples, (4) the use of polymerase chain reaction (PCR) primers targeting specific functional genes, and (5) 16S rRNA gene sequencing.

4.2. Materials and methods

4.2.1. Materials

Pure chlorinated solvents and other chemicals used in this chapter are listed in Table 3.1.

4.2.2. Hydrogeochemical description of the aquifer

The studied aquifer is located in the province of Barcelona (Spain). This site was significantly contaminated with PCE due to improper disposal practices after its former use as a degreasing agent at an industrial plant. A preliminary site characterization revealed a significant PCE plume, accompanied by minor amounts of TCE, *cis*-DCE and VC.

The aquifer is an unconfined bedrock mainly consisting of Tertiary sediments. For the geological and hydrogeological characterization of the studied area, 55 rotational probes between 10 to 20 m depth with continuous sample extraction were carried out and habilitated as piezometers. According to the probes, from the bottom to top, mainly three main lithological facies were differentiated: i) a lower layer of red clay loams located at 10 to 3 m depth, ii) an intermediate layer of brown clays and silty clays at 6 to 2 m depth, and iii) a higher level represented by ochre silty clays that are located up to 0.5 to 5 m depth. Figure 4.1 presents a schematic hydrogeological cross section of the site where the three lithological facies can be identified. An intermediated layer of silty clays with sandstone beds is developed in the south part of the site, and it locally evolves to a sandstone – micro-conglomerate strata that probably corresponds to an old Tertiary sedimentary paleochannel. This most transmissive layer is intersected at the piezometer MW-7 (Figure 4.2). Such Tertiary formation is locally covered by Quaternary deposits including sands, silts and clays with a variable vertical extension and anthropogenic materials (concrete, etc.).
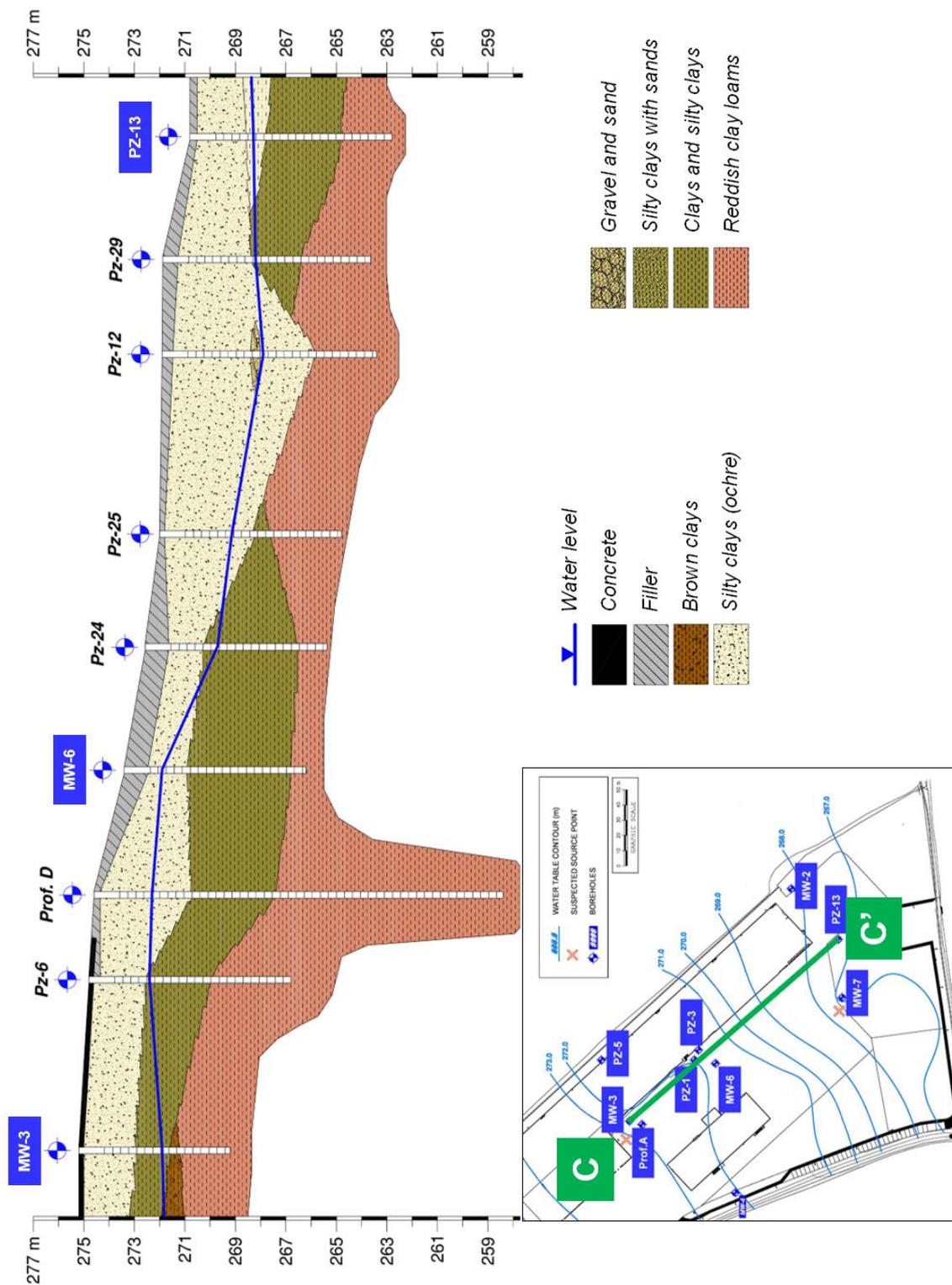
Figure 4.1. Schematic hydrogeological cross section of the site along transect C-C'.
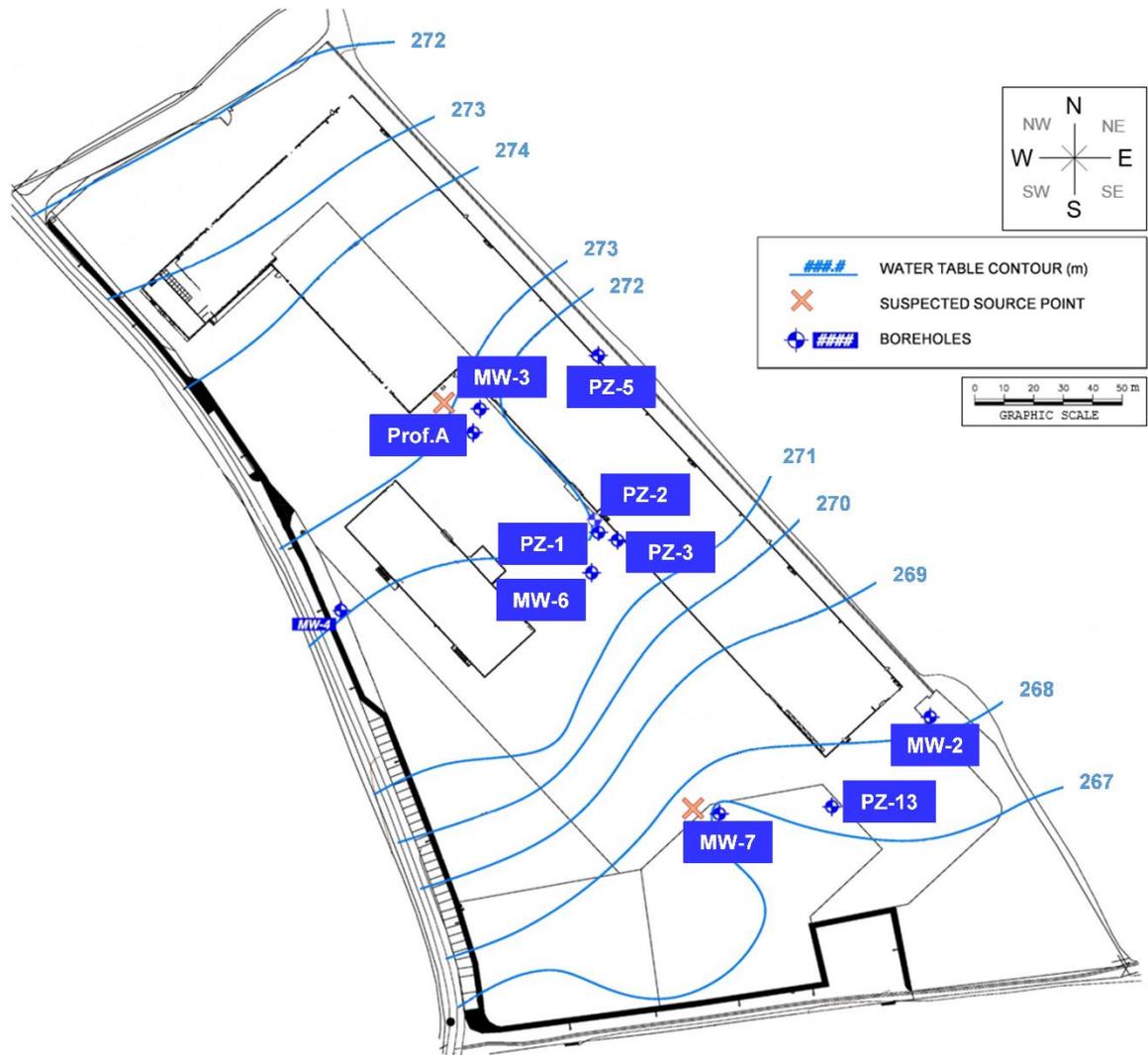
Figure 4.2. Head contour lines, groundwater flow direction, location of boreholes and suspected source points at the industrial contaminated area.

For the preliminary site characterization and further monitoring, 55 wells that were completely screened were installed. The water table is located at depths ranging between 2.5 and 7.5 m below ground surface (266 to 274 m.a.s.l.) (Figure 4.2). Groundwater is mainly concentrated in the sandstone or microconglomerate intervals that intercalate with the mudstone matrix forming a multi-layered aquifer. Due to the limited continuity of the permeable stratum, the potential hydrological exploitation of the area is low. Locally, when monitoring wells intersect layers of sandstone, silty sandstones, silty mudstones and microconglomerates, the hydraulic conductivity increases to

medium–low. Pumping tests determined that aquifer transmissivity ranged from 0.1 to 0.8 m²/day, and hydraulic conductivity from 0.02 to 0.32 m/day.

4.2.3. Collection of groundwater samples

The groundwater sampling campaign for the characterization of the plume and the establishment of microcosms was carried out in May 2016 for all the wells depicted in Figure 4.2 except for PZ-2, which was sampled on October 2016. Groundwater samples were collected as described in section 3.2.1. Concentration of dissolved oxygen (DO) was measured with a Dissolved Oxygen Meter HI 9147 (Hanna Instruments). Samples for carbon stable isotope analysis (C CSIA) were preserved with NaOH (pH>10) to prevent further biodegradation reactions.

4.2.4. Set up of microcosms

To study whether organic fermentable substrates could enhance the biodegradation of CEs to ETH, three different treatments were prepared on May 2016 in triplicate with groundwater from MW-2 as described in section 3.2.2: (1) control containing only groundwater, (2) groundwater with a mixture of methanol plus ethanol (3 mM each), and (3) groundwater with Lactate-1 (3 mM). Similarly, for microcosms from October 2016 with groundwater from well PZ-2, four different treatments were set up, at least in duplicate: (1) control containing only groundwater, (2) groundwater with Lactate-1 at 3 mM, (3) groundwater with Lactate-2 at 3 mM, and (4) groundwater with Lactate-2 at 15 mM. Microcosms that fully dechlorinated CEs were reamended with TCE and transferred to sterilized anaerobic synthetic medium (3–7% v/v) during the exponential degradation phase of CEs, as reported in section 3.2.3.

To determine the site-specific carbon isotopic fractionation ($\varepsilon^{13}C$) during anaerobic reductive dechlorination of PCE, two separate experiment lines of

six parallel cultures were simultaneously prepared as described in section 3.2.3, using as inoculum (1.5% v/v) groundwater from well MW-2 and PZ-2, respectively. Each MW-2 and PZ-2 microcosm was spiked with PCE (160 and 235 μM, respectively), and sacrificed with NaOH (10 M) at different time points of PCE degradation. In this experiment, three different controls were included, in duplicate: (1) NaOH-killed controls with inoculum and PCE; (2) NaOH-killed controls with inoculum but without PCE, and (3) abiotic controls with PCE but without inoculum, to account for abiotic transformations and control potential impurities from the PCE stock solution.

4.2.5. Analytical methods

Field parameters for the site characterization were determined as described in section 3.2.1. Concentrations of volatile organic compounds (VOCs), major anions and cations, and volatile fatty acids (VFAs) were analysed as described in sections 3.2.4, 3.2.5 and 3.2.6, respectively. Stable C isotope ratios were obtained as described in section 3.2.7.

4.2.6. DNA extraction, PCR and 16S rRNA gene sequencing

DNA was extracted from TCE-enriched field-derived cultures inoculated with aquifer samples from MW-2 that were originally amended with Lactate-1 (3 mM). Similarly, for PZ-2, DNA was extracted from TCE-enriched field-derived cultures that were originally amended with Lactate-2 (3 mM).

Cell harvesting was carried out via centrifugation of 65 mL-samples (two consecutive steps at 5000 *g* and 16 ºC for 1 h). Genomic DNA was isolated using NucleoSpin Tissue DNA extraction kit following the instructions provided by the manufacturer (Macherey-Nagel). Primer sets used to detect *Dhc* 16S rRNA gene and *Dhc* reductive dehalogenase gene *vcrA* were previously described (Manchester et al., 2012; Ritalahti et al., 2006) (see Table 4.1).

Dehalococcoides mccartyi strain BTF08 (Pöritz et al., 2013) was used as positive control. Each 10 μL reaction mixture contained 5 μL of iQ Supermix (2x) (Bio-Rad), 250 nM of each primer (1 μL volume each) (Thermofisher) and a concentration of template DNA ranging between 5-50 ng/μl (3 μL volume). The thermal program used for PCR amplification of *Dhc* and *vcrA* genes was described elsewhere (Martín-González et al., 2015; Ritalahti et al., 2006).

Table 4.1. Designations and sequences of Dhc primer sets used in this chapter.

Gene	Primer name	Primer sequence (5' to 3')	Reference
16S rRNA	Dhc1F	GAT GAA CGC TAG CGG CG	Manchester et al. (2012)
	Dhc264R	CCT CTC AGA CCA GCT ACC GAT CGAA	Manchester et al. (2012)
vcrA	Vcr1022F	CGG GCG GAT GCA CTA TTT T	Ritalahti et al. (2006)
	Vcr1093R	GAA TAG TCC GTG CCC TTC CTC	Ritalahti et al. (2006)

To get an insight into the bacteria responsible for the full dechlorination of CEs, the dilution-to-extinction method (Löffler et al., 2005) was applied as described in section 3.2.3, using *cis*-DCE as electron acceptor and 1 mL of active TCE-enriched field-derived culture as inoculum. After four dilution series for the MW-2 microcosms, and three dilution series for the PZ-2 microcosms, the more diluted vial showing activity against 10 μM of *cis*-DCE and ETH formation was used as inoculum for serum bottle microcosms. When these microcosms consumed 30 μM *cis*-DCE, DNA was extracted from the whole serum bottle as described above, and amplicons of the region V3–V4 for 16S rRNA genes were amplified with primers S-D-Bact-0341-b-S-17 and S-D-Bact-0785-a-A-21 (Klindworth et al., 2013) with the Illumina MiSeq

sequencing platform at *Serveis de Genòmica i Bioinformàtica* from *Universitat Autònoma de Barcelona* (Spain).

4.3. Results

4.3.1. Physicochemical characterization of the site

The hydrogeochemical data obtained from the collected groundwater from wells MW-2, MW-3, MW-4, MW-6, MW-7, PZ-1, PZ-3, PZ-5, PZ-13, and Prof.A on May 2016 are shown in Table 4.2. According to the results, MW-4 was never impacted by CEs contamination and, therefore, is considered to be a sample of the natural background of the groundwater of the area, which belongs to the magnesium-calcium-bicarbonate facies.

The distribution of native potential electron acceptors in the aquifer varied among the different monitoring wells. DO concentrations ranged from 0.2 to 2.0 mg/L, total Fe was insignificant (<0.1 mg/L), nitrate concentration exceeded 25 mg/L in all piezometers except in PZ-1 and Prof.A, and sulphate was detected at elevated levels in most of the wells (values ranging from 94 to 1435 mg/L) (Table 4.2). Such results suggested that the aquifer was naturally at nitrate-reducing conditions, thus, it needed to change to sulphate-reducing or methanogenic conditions to favour the complete reductive dechlorination of PCE to ETH. In addition, elevated levels of chloride were detected in most of the wells (up to 1053 mg/L at the most contaminated well PZ-5), whereas MW-4, considered the natural background, showed the lowest value (30.5 mg/L), which pointed towards the release of chloride ions in the contaminated wells (Table 4.2). On its side, the averaged concentration of bicarbonate, an indicator of the natural buffering capacity of the aquifer, was 459 ± 146 mg/L.

Table 4.2. Hydrogeochemistry of the studied wells and groundwater samples (May 2016).

	MW-2	MW-3	MW-4	MW-6	MW-7	PZ-1	PZ-2*	PZ-3	PZ-5	PZ-13	Prof.A
Well depth (m)	7.0	6.0	8.0	7.2	8.0	6.8	8.0	6.0	11.2	8.0	15.0
WT (m.b.g.l.)	2.6	5.9	5.5	4.3	5.5	1.9	4.9	2.2	n.m.	2.7	4.0
WT (m.a.s.l.)	268.2	269.3	270.4	269.1	265.5	272.2	269.3	271.8	n.m.	268.1	271.1
T (°C)	17.6	24.5	16.5	19.1	18.8	20.7	20.2	20.3	18.3	18.4	18.9
pH	7.4	7.8	7.5	7.2	7.7	7.2	6.9	7.5	7.3	7.4	7.3
EC (mS/cm)	2.8	1.5	1.1	1.5	2.0	3.4	1.1	1.4	4.3	2.2	3.4
DO (mg/L)	0.2	n.m.	n.m.	1.8	n.m.	1.2	2.1	1.0	2.0	1.5	n.m.
Eh (mV)	247	337	392	288	266	469	n.m.	401	361	273	94
SO_4^{-2} (mg/L)	301.9	199.2	105.0	94.2	159.6	1435.1	n.m.	182.4	179.2	181.7	144.3
NO_3^- (mg/L)	49.3	60.8	24.9	31.2	72.7	<20	n.m.	130.5	41.3	116.8	<20
Fe (mg/L)	<0.1	<0.02	<0.02	<0.02	<0.02	<0.1	n.m.	<0.02	<0.1	<0.02	<0.1
Cl^- (mg/L)	382.2	205.8	30.5	125.0	372.9	96.0	n.m.	114.3	1053.0	368.6	711.3
HCO_3^- (mg/L)	605.3	251.9	585.3	652.3	260.1	543.4	n.m.	351.3	369.1	364.5	605.3
Na^+ (mg/L)	412.7	149.2	32.9	58.2	167.4	336.7	n.m.	57.8	383.2	186.1	266.0
K^+ (mg/L)	0.7	1.3	0.6	1.8	1.9	0.5	n.m.	0.3	0.5	1.8	1.9
Ca^{+2} (mg/L)	121.1	125.0	77.9	122.0	166.9	287.0	n.m.	118.6	275.3	173.3	135.6
Mg^{+2} (mg/L)	27.3	29.0	74.9	88.4	58.2	138.9	n.m.	69.6	110.9	61.6	166.5

*WT = water table, m.b.g.l. = meters below ground level, m.a.s.l. = meters above sea level, T = temperature, EC = electrical conductivity, DO = dissolved oxygen, Eh = redox potential, n.m. = not measured. * PZ-2 well was sampled on October 2016.*

Lastly, pH and temperature values were on average 7.4 ± 0.2 and 19 ± 2 ℃, respectively (Table 4.2). The field parameters of the monitoring well PZ-2 that was sampled on October 2016 are also presented in Table 4.2 but, in this case, other hydrochemistry data is not available.

The concentration analyses of CEs across the site showed that PCE was the main VOC in the aquifer (concentrations ranging from 2.1 to 77 μM), but it was always accompanied by minor amounts of TCE and *cis*-DCE (see Table 4.3, Figure 4.3). Interestingly, traces of *trans*-DCE and VC were only detected in MW-2 and, as expected, no CEs were detected in MW-4 (Table 4.3).

4.3.2. Carbon stable isotope analysis of CEs at the site

The carbon isotopic compositions ($\delta^{13}C$) of PCE and its dechlorination products were analysed at the different monitoring wells on May 2016 to investigate the relevance of biodegradation processes at the contaminated site.

As presented in Figure 4.3, $\delta^{13}C$ ranged from -32.6 to -26.4‰, -37.7 to -29.7‰, and -33.0 to -26.0‰ for PCE, TCE, and *cis*-DCE, respectively (Table 4.3). In the case of PCE, which is the source of the contamination plume, all values were within the range of commercial solvents (-37.2 to -23.2‰) (Jendrzejewski et al., 2001; van Warmerdam et al., 1995).

The isotopic mass balance was calculated at each well considering the concentration-weighted $\delta^{13}C$ compositions of the CEs and assuming they were transformed via hydrogenolysis ($\delta^{13}C_{sum}$, Eq. 4, see section 3.2.7). $\delta^{13}C_{sum}$ from wells at the field site were compared to assess potential point sources of PCE in the aquifer (Table 4.3, Figure 4.3). Obtained results revealed that wells MW-7 and Prof.A exhibited similar isotopic balances of -26.4 ± 0.6‰ and -26.0 ± 0.7‰, respectively. However, the $\delta^{13}C_{sum}$-values for the rest of the sampled wells were within the same average value of -31 ± 1‰.

Table 4.3. Concentrations (μM), carbon stable isotopic composition (δ¹³C, ‰) and mass isotopic balance (δ¹³C$_{sum}$, ‰) of CEs in groundwater samples from May 2016.

	MW-2	MW-3	MW-4	MW-6	MW-7	PZ-1	PZ-3	PZ-5	PZ-13	Prof.A
PCE	25 ± 4	29 ± 5	< 0.1	18 ± 3	61 ± 14	3.9 ± 0.4	5.7 ± 0.5	77.1[a]	3.1 ± 0.6	2.1[a]
TCE	3.3 ± 0.3	0.49 ± 0.07	< 0.1	5.1 ± 0.5	0.6 ± 0.1	0.97 ± 0.01	2.8 ± 0.1	2.6[a]	< 0.2	< 0.2
cis-DCE	12.4 ± 0.8	0.56 ± 0.01	< 0.1	2.35 ± 0.09	0.56 ± 0.01	0.56 ± 0.01	4.70 ± 0.01	1.9[a]	2.0 ± 0.3	0.8[a]
trans-DCE	0.30 ± 0.01	< 0.2	< 0.1	< 0.2	< 0.2	< 0.2	< 0.2	< 0.2	< 0.2	< 0.2
VC	0.52 ± 0.09	< 0.3	< 0.1	< 0.3	< 0.3	< 0.3	< 0.3	< 0.3	< 0.3	< 0.3
ETH	< 0.2	< 0.2	n.m.	< 0.2	< 0.2	< 0.2	< 0.2	< 0.2	< 0.2	< 0.2
δ¹³C$_{PCE}$	-32.6 ± 0.4	-31.0 ± 0.7	n.m.	-32.0 ± 0.5	-26.4 ± 0.6	-29.0 ± 0.5	-31.5 ± 0.4	-29.8 ± 0.4	-30.1 ± 0.4	n.a.
δ¹³C$_{TCE}$	-29.9 ± 0.4	n.a.	n.m.	-35.1 ± 0.6	n.a.	-37.7 ± 0.6	-32.5 ± 0.6	-29.7 ± 0.5	n.a.	n.m.
δ¹³C$_{cis-DCE}$	-30.7 ± 0.7	n.a.	n.m.	n.a.	n.a.	-31.4 ± 0.8	-31.3 ± 0.7	-33.0 ± 0.7	-27.7 ± 0.6	-26.0 ± 0.7
δ¹³C$_{sum}$	-32 ± 4	-31.0 ± 0.7	n.m.	-33 ± 6	-26.4 ± 0.6	-31 ± 3	-32 ± 2	-29.8 ± 0.4	-29 ± 5	-26.0 ± 0.7

[a] Values from a single measurement and sample. n.m.: not measured. n.a.: measurement and/or calculation not applicable due to low concentrations and/or analytical uncertainty.
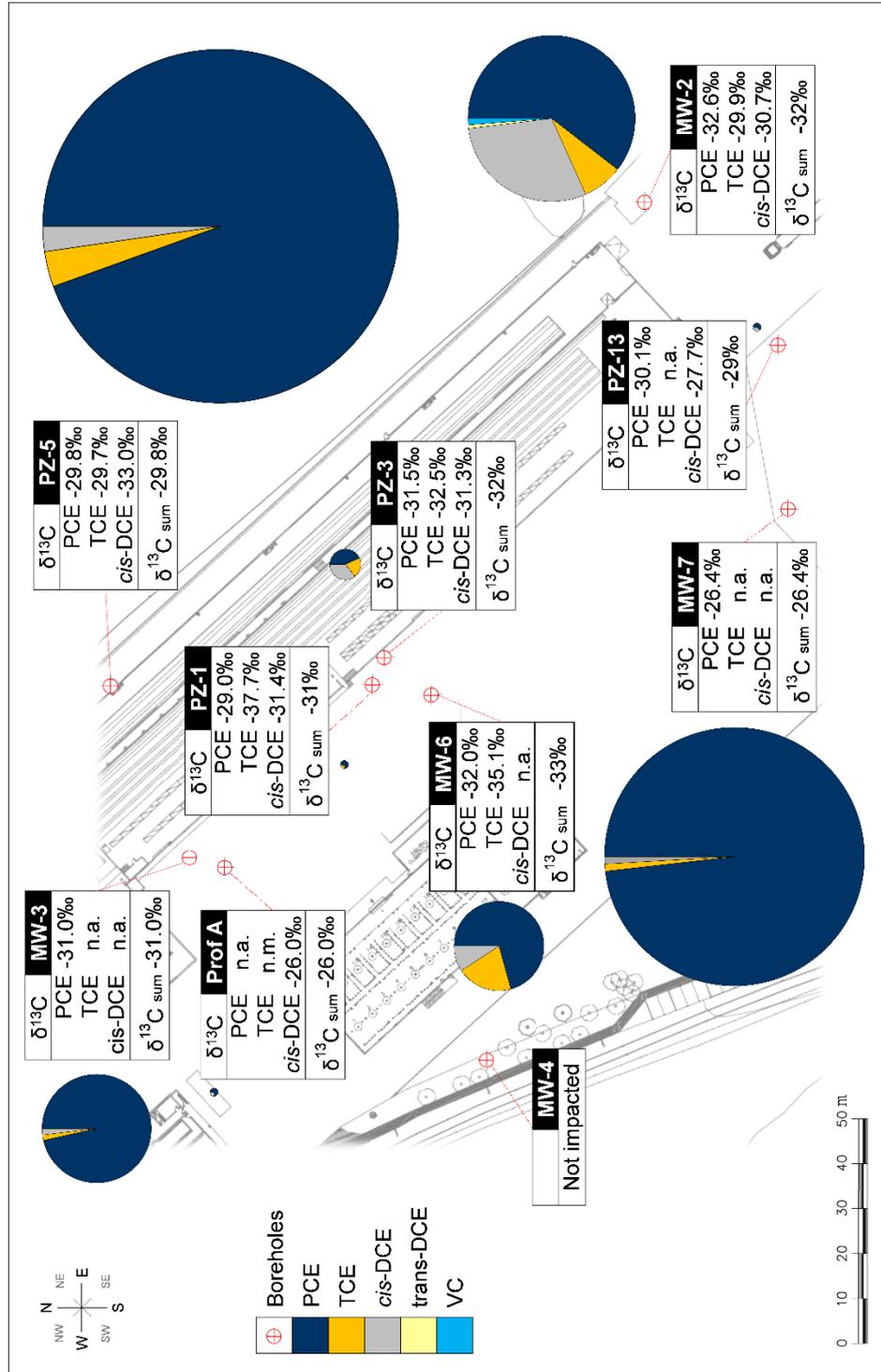
Figure 4.3. Distribution of molar concentrations and carbon isotopic compositions (δ¹³C) of CEs at the industrial contaminated area on May 2016. The pie charts are proportionally sized according to the total concentration of CEs in each well (from 2.8 to 82 μM). The carbon isotopic mass balance (δ¹³C_sum) included all CEs detected and it was calculated using Eq. 4. Detailed information about the concentration and δ¹³C of CEs in all monitoring wells can be found in Table 4.3.

4.3.3. Field-derived microcosms amended with several biostimulants

On May 2016, three different microcosm treatments were prepared with groundwater from well MW-2 to test whether different fermentable organic substrates (Lactate-1, methanol and ethanol) could enhance the reductive dechlorination of PCE to ETH.

The non-amended microcosms used as natural biodegradation controls fully converted PCE to *cis*-DCE by day 150, but the reaction remained stalled at this stage without ETH formation (Figure 4.4A).
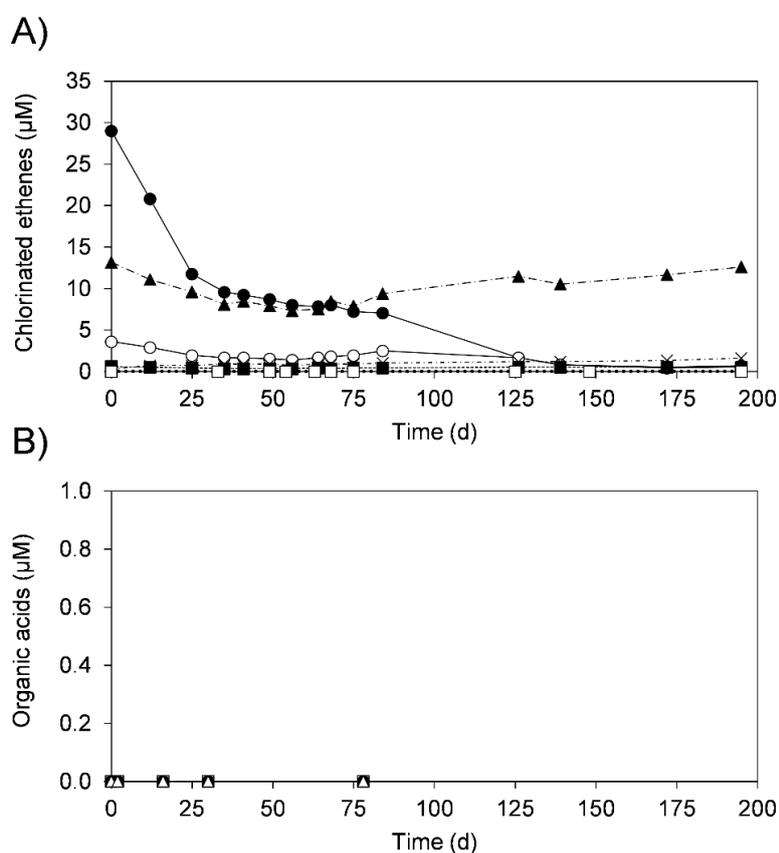
*Figure 4.4. Time-course in a non-amended microcosm constructed with aquifer materials from well MW-2. (A) Reductive dechlorination of CEs (●: PCE, ○: TCE, ▲: cis-DCE, ✕: trans-DCE, ■: VC, and □: ETH). (B) VFAs (●: lactate, □: pyruvate, Δ: acetate, ◆: formate). Concentrations of CEs and ETH are presented as nominal concentrations. Data presented is from an individual microcosm, but it is representative of triplicate microcosms.*

In the microcosms with methanol and ethanol, PCE was degraded within the first week to *cis*-DCE and it accumulated for 85 days. At day 125, *cis*-DCE and VC disappeared. At day 139, the microcosm was spiked with 75 μM of TCE and, after 60 days, all CEs were sequentially transformed (Figure 4.5A). Here, detection of ETH was initially hampered by the high amount of methane generated (see discussion below), which overlapped the ETH signal in the gas chromatograph. However, after the dechlorination of the amended TCE (see arrow in Figure 4.5A), the increased ETH signal was finally detected at day 200 (data not shown), but quantification was not possible.
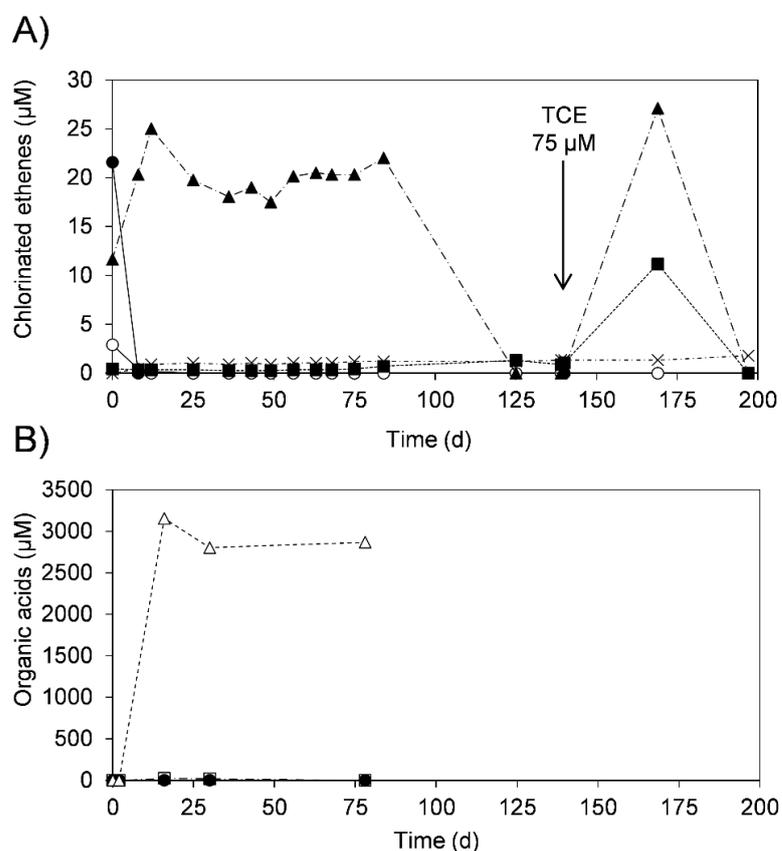
Figure 4.5. Time-course in a microcosm constructed with aquifer materials from well MW-2 and amended with ethanol and methanol (3 mM each). (A) Reductive dechlorination of CEs (●: PCE, ○: TCE, ▲: cis-DCE, ✕: trans-DCE, ■: VC, and □: ETH). (B) VFAs (●: lactate, □: pyruvate, Δ: acetate, ◆: formate). Concentrations of CEs and ETH are presented as nominal concentrations. Data presented is from an individual microcosm, but it is representative of triplicate microcosms.

Microcosms amended with Lactate-1 also transformed PCE to *cis*-DCE within the first week and, as observed in the alcohol-amended microcosms, the latter accumulated in the medium (Figure 4.6A). At day 63, VC was detected and, at day 75, ETH was observed for the first time. After 125 d, ETH was the only remaining compound in the microcosms (Figure 4.6A).
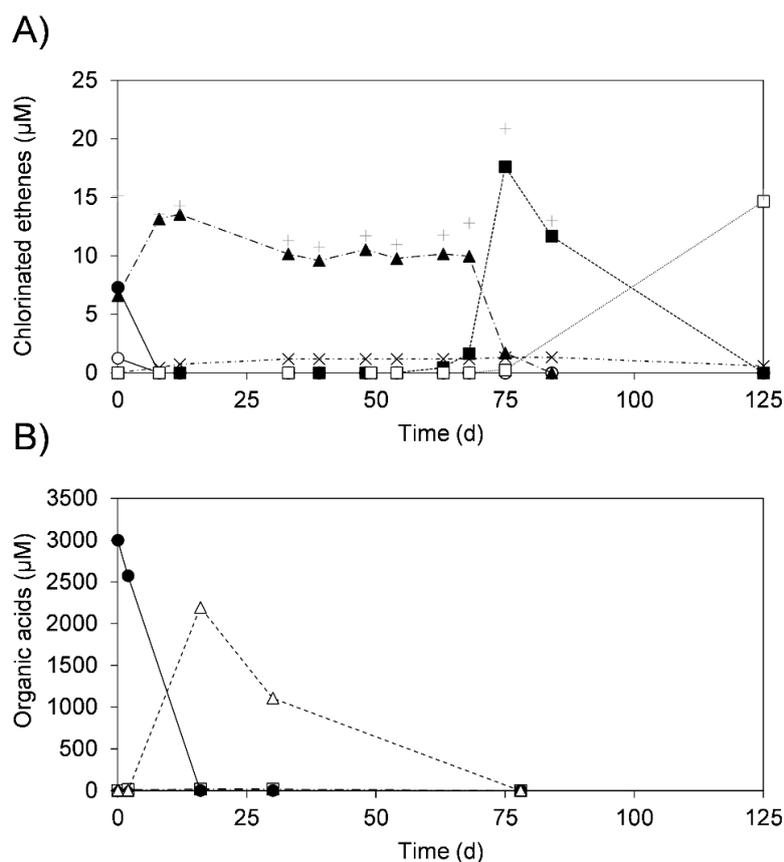
Figure 4.6. Time-course in a lactate-amended microcosm prepared with aquifer materials from well MW-2. (A) Reductive dechlorination of CEs (●: PCE, ○: TCE, ▲: cis-DCE, ✕: trans-DCE, ■: VC, □: ethene and +: sum of CEs plus ETH). (B) VFAs (●: lactate, □: pyruvate, Δ: acetate, ◆: formate). Concentrations of CEs and ETH are presented as nominal concentrations. Data presented is from an individual microcosm, but it is representative of triplicate microcosms.

To get an insight into the predominant fermentation pathways used by native microbial populations for Lactate-1, methanol and ethanol, VFAs (i.e. lactate, pyruvate, acetate, and formate) were monitored during the time-course experiments. VFAs were not detected in the non-amended microcosms

(Figure 4.4B). In the microcosms amended with ethanol plus methanol, approximately 3 mM of acetate was produced after 15 days and it remained in the medium without a significant decrease for approximately two months (Figure 4.5B). Lastly, in the microcosms amended with Lactate-1, lactate was fermented to near-stoichiometric amounts of acetate, which was slowly consumed in the microcosms, and it was completely depleted after 75 days (Figure 4.6B).

A remarkable difference observed between the microcosms amended with lactate and the mixture of ethanol plus methanol was the vigorous generation of methane in the latter treatment. As depicted in Figure 4.7, methane was not detected in the control and it was barely produced in the lactate-amended microcosms but, in the treatment with the alcohols, methane concentration remarkably increased after approximately 50 days without reaching a plateau in the monitored period.
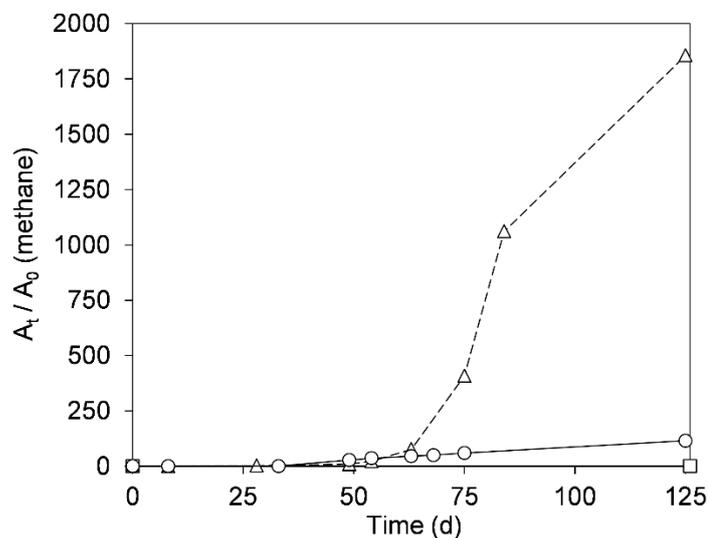
Figure 4.7. Generation of methane in the microcosms constructed with groundwater from well MW-2: non-amended control (□), microcosm amended with lactate (○), and microcosm amended with a mixture of ethanol plus methanol (△). Results are expressed as A_t/A_0, where A_t is the peak area of methane at different time points and A_0 is the peak area at time zero. Data presented is from an individual microcosm, but it is representative of triplicate microcosms.

On October 2016, microcosms were prepared with groundwater from well PZ-2 to test whether reductive dechlorination of CEs to ETH was also feasible here. In this case, both groundwater from well PZ-2 and Lactate-2 (a food-grade, commercial sodium lactate, Table 3.1) were selected for the microcosms experiments because they were the candidates to be used in a foreseeable future *in-situ* biostimulation pilot test.

Besides the control, which accounted for MNA, two different isomeric forms of sodium lactate (DL-/Lactate-1 and L-/Lactate-2) were used to test their effect on the lactate fermentation potential of the native microbial community. Additionally, Lactate-2 was amended at two different doses to discard any inhibition effects. The selection of lactate as electron donor in the preparation of these microcosms (instead of methanol and ethanol) was based on the insights obtained from the previous MW-2 microcosms.

Results showed that the unamended controls transformed PCE to *cis*-DCE and VC within 15 days, but ETH was not detected. When microcosms were reamended with TCE (35 µM) at day 25, dechlorination barely passed VC, but ETH was detected at low concentrations after 50 days (Figure 4.8A). In contrast to the microcosms that mimicked natural conditions, all lactate-amended treatments fully dechlorinated PCE to ETH within 15 days and exhibited similar rates independently of the isomeric form and dose (Figure 4.8, B–D). After adding TCE in all the lactate-amended microcosms at days 25 and 45 (albeit in different amounts, as depicted in Figure 4.8), the dechlorination remained active with the consecutive transformations to *cis*-DCE and VC, and the accumulation of ETH (Figure 4.8, B–D).

Regarding the substrates added, amended Lactate-1 at 3 mM and Lactate-2 at 15 mM were totally consumed and transformed to acetate within 10 days (Figure 4.9B and D), while the controls did not show production of VFAs

(Figure 4.9A). In the microcosms with Lactate-2 at 3 mM, both lactate and acetate were barely detected (Figure 4.9C). This was associated to an experimental error, as the amount of lactate added was much lower than the theoretically calculated. Nonetheless, results demonstrated that this lactate concentration was enough to fully dechlorinate CEs at similar rates than those observed in the microcosms at higher lactate concentrations (Figure 4.9).
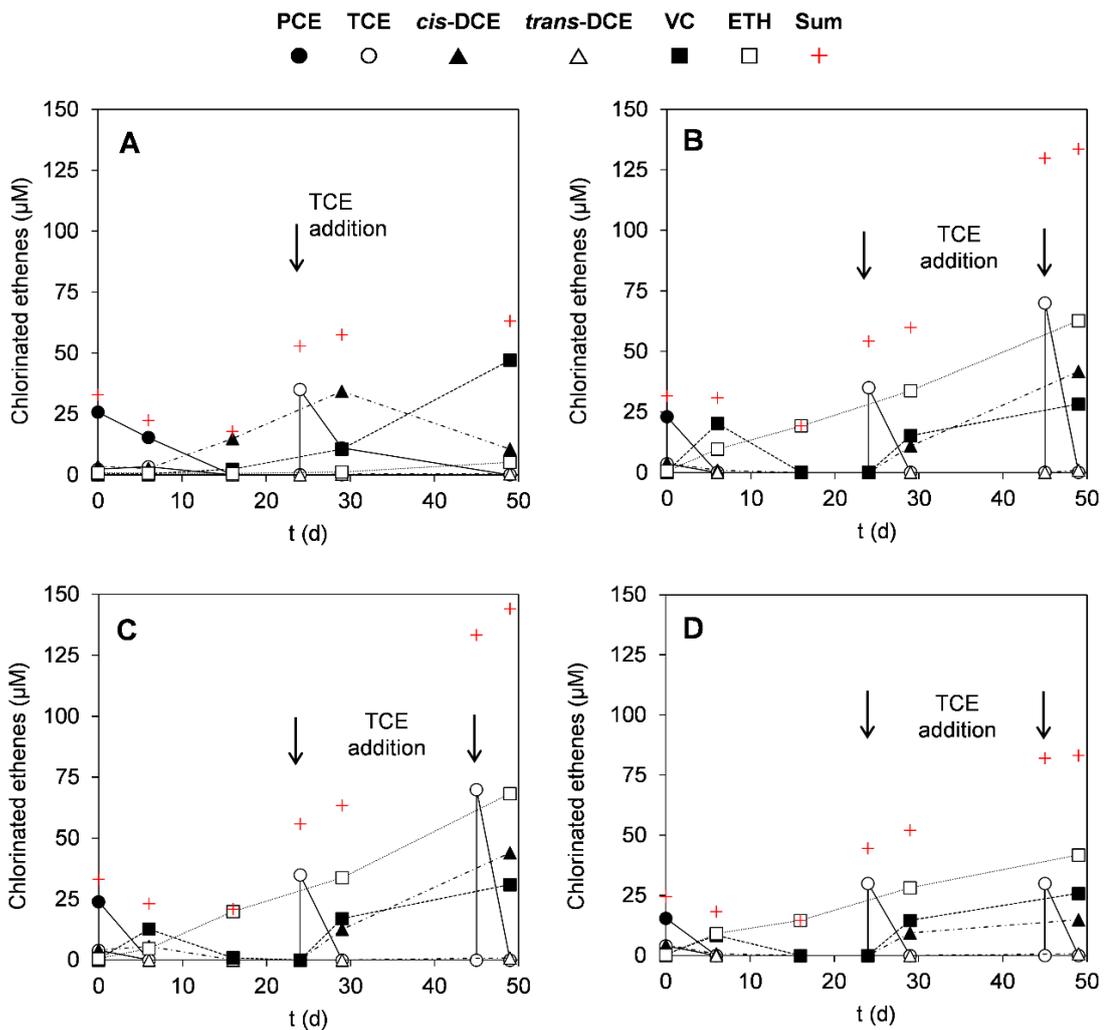
Figure 4.8. Time-course of CEs in microcosms with groundwater from well PZ-2: (A) unamended control (only groundwater); (B) amended with Lactate-1 at 3 mM; (C) amended with Lactate-2 at 3 mM, and (D) amended with Lactate-2 at 15 mM. Results for only one replicate but it is representative of all of them. The microcosms received several additions of TCE, as indicated by the arrows. Sum (+): sum of CEs and ETH.
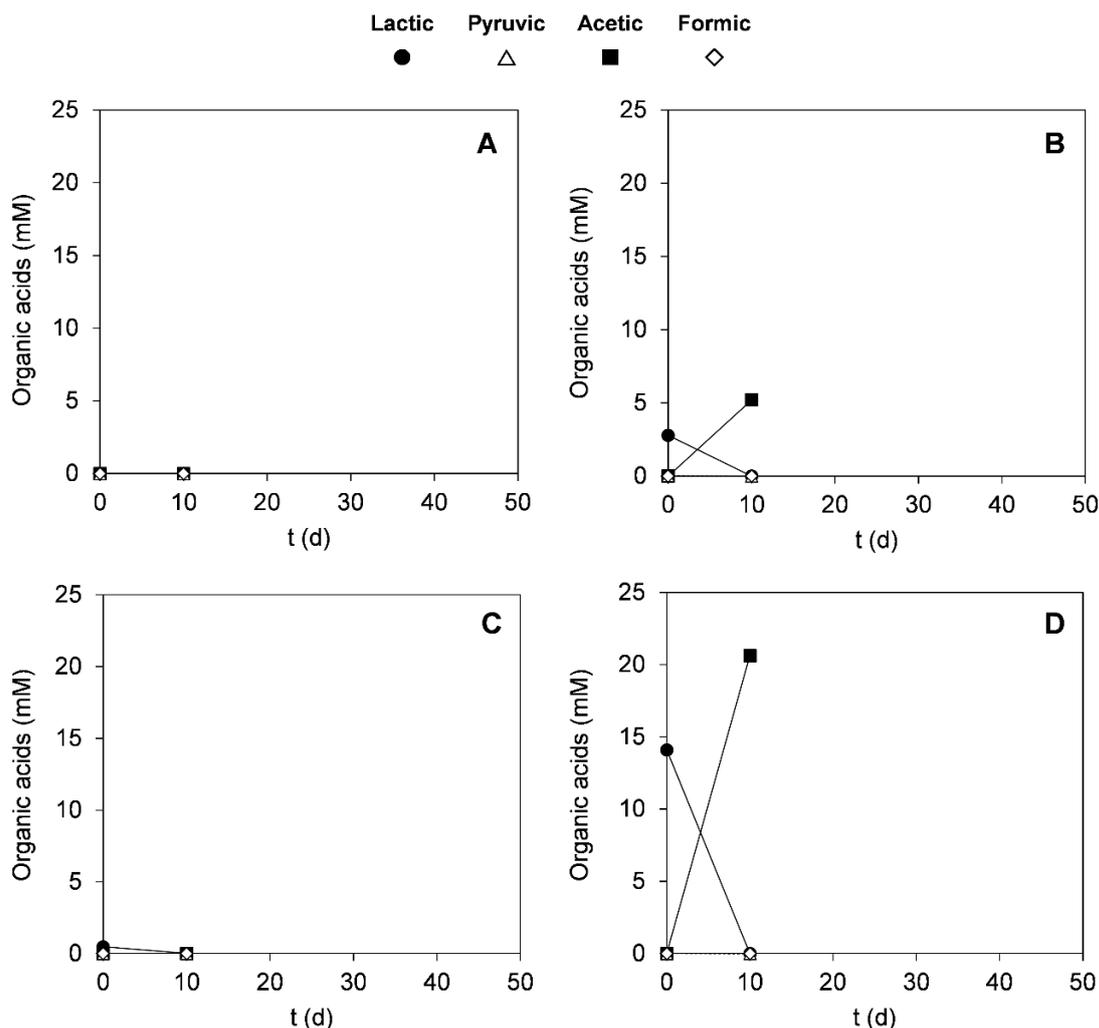
Figure 4.9. Time-course of VFAs (organic acids) in microcosms with groundwater from well PZ-2: (A) non-amended control (only groundwater); (B) amended with Lactate-1 at ~ 3 mM; (C) amended with Lactate-2 at ~ 3 mM* and (D) amended with Lactate-2 at ~ 15 mM. Results for only one replicate but it is representative of all of them. *Lactate should have been at a theoretical concentration of 3 mM, but it was lower due to experimental error.

However, as previously observed in the microcosms prepared with groundwater from well MW-2 and amended with a mixture of methanol plus ethanol, higher concentrations of lactate (in this case, of Lactate-2) produced higher concentrations of H_2, which in turn promoted methanogenesis, resulting in a vigorous formation of methane in the microcosm with 15 mM of Lactate-2 (Figure 4.10).
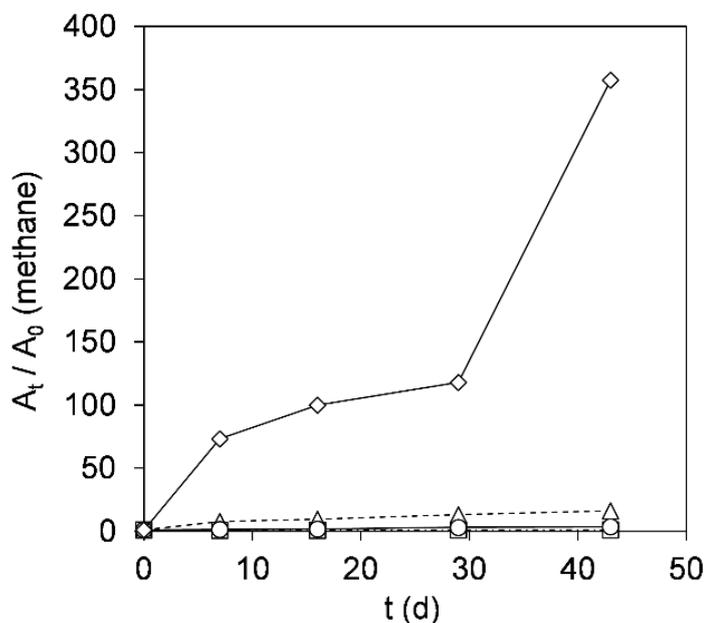
Figure 4.10. Generation of methane in microcosms from PZ-2: unamended control (□), microcosm with Lactate-1 at ~ 3 mM (△), microcosm with Lactate-2 at ~ 3 mM (○), and at ~ 15 mM (◇). Results are expressed as A_t/A_0, where A_t is the peak area of methane at different time points and A_0 is the peak area at time zero. Data presented is from an individual microcosm, but it is representative of replicate microcosms.

4.3.4. Identification of key rdh genes and native OHRB

Dhc are keystone bacteria for the detoxification of CEs to non-toxic ETH. PCR amplifications with the *Dhc* 16S rRNA and *vcrA* gene-targeted primers were run to investigate whether the *vcrA* gene and *Dhc* sp. were present in the TCE-enriched field-derived cultures.

The *Dhc* and *vcrA* targeted primers yielded amplicons of 300 bp and 100 bp, respectively, in DNA samples extracted from the TCE-enriched cultures derived from well MW-2, indicating that this groundwater contained *Dhc* implicated in the VC-to-ETH dechlorination step (Figure 4.11A). In the case of samples enriched with TCE from the well PZ-2, only the *vcrA* gene was studied, and it also yielded an amplicon at 100 bp, confirming the presence of this VC-to-ETH reductive dehalogenase (Figure 4.11B)
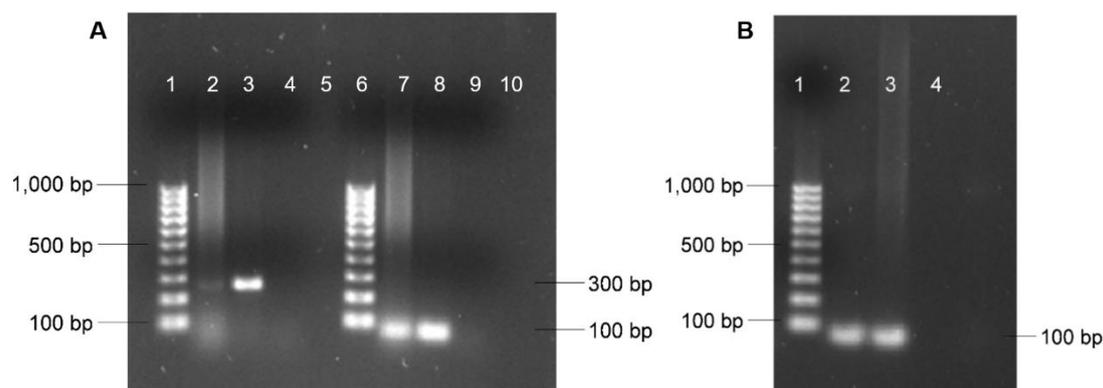
Figure 4.11. (A) Detection of Dhc 16S rRNA genes (lanes 2-4) and vcrA genes (lanes 7-9) in enriched microcosms from well MW-2. Lanes 1 and 6: ladder, lane 2 and 7: positive control (DNA from Dehalococcoides mccartyi strain BTF08), lane 3 and 8: PCR product generated using genomic DNA from the microcosm, lane 4 and 9: negative controls. (B) Detection of vcrA genes (lanes 1-4) in enriched microcosms from well PZ-2. Lane 1: ladder, lane 2: positive control (DNA from Dehalococcoides mccartyi strain BTF08), lane 3: PCR product generated using genomic DNA from the microcosm, lane 4: negative control.

To get an insight into the bacterial population responsible for the *cis*-DCE dechlorination up to ETH, 16S rRNA gene amplicon sequencing was performed on DNA samples extracted from cultures derived from wells MW-2 and PZ-2 enriched with *cis*-DCE using the dilution-to-extinction method. The taxonomic assignments of the 16S rRNA gene amplicon sequencing obtained for well MW-2 revealed that the community was constituted by the following five predominant genera: *Geobacter* (57%), *Rhodoplanes* (16%), *Dehalococcoides* (7%), *Dechloromonas* (4%) and *Bacteroides* (3%) (Figure 4.12). From those five, *Rhodoplanes* sp. have been described as phototrophic bacteria that are capable of complete denitrification (Hiraishi and Ueda, 1994), while *Dechloromonas* sp. have been described as (per)chlorate-reducing bacteria (Achenbach et al., 2001). In regards to the OHRB present and, thus, the suspected genera for being responsible of the PCE dechlorination, *Geobacter* sp. and *Dhc* are capable of degrading PCE to *cis*-DCE and PCE to ETH, respectively (Adrian and Löffler, 2016b). *Geobacter* sp. can derive energy from acetate oxidation coupled to PCE-to-*cis*-DCE dechlorination,

but it is also capable of growing on a wide range of non-halogenated electron acceptors (Atashgahi et al., 2016; Sanford et al., 2016).
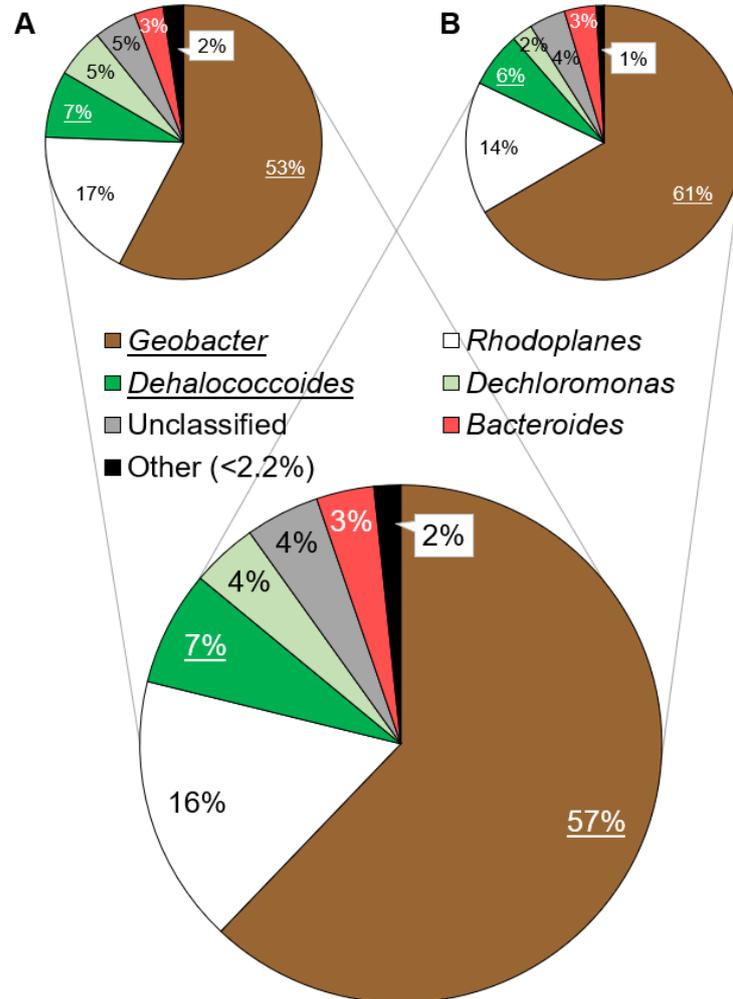
Figure 4.12. Microbial population in enriched cultures derived from groundwater from well MW-2. Average composition obtained from two cultures (A and B) that were enriched with PCE and TCE first, and later with cis-DCE for several consecutive dilution series. Total sequence reads for the genera Geobacter and Dehalococcoides (underlined) were, respectively, 68573/128355 and 9334/128355 in replicate A, and 83109/135149 and 8142/135149 in replicate B. Genera with abundance <2.2% are grouped in "Other".

In the PZ-2 enriched microcosms, the 16S rRNA gene amplicon sequencing and the taxonomic assignments revealed that the five predominant genera were *Pleomorphomonas* (50%), described as nitrogen-fixing bacteria (Im et al., 2006; Madhaiyan et al., 2013; Xie and Yokota, 2005); *Desulfomicrobium* (18%),

which are sulphate-reducing bacteria (Sharak Genthner et al., 1997, 1994); the CEs-degrading OHRB *Geobacter* (14%) and *Dehalococcoides* (3%); and *Bacteroides* (4%) (Figure 4.13).
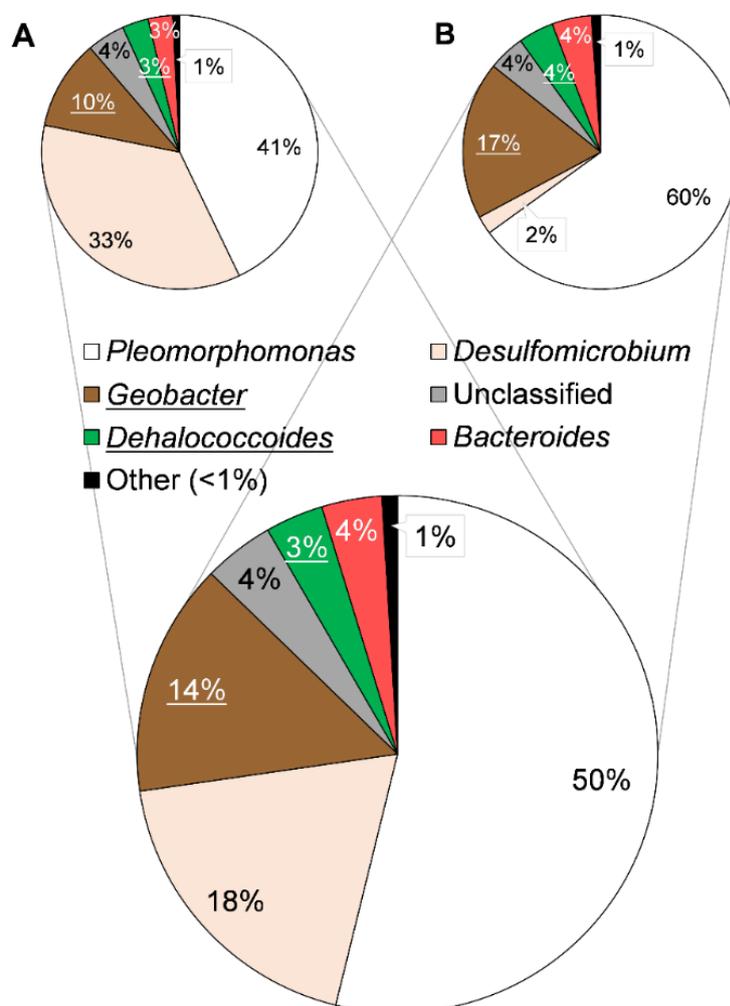
Figure 4.13. Microbial population in enriched cultures derived from well PZ-2. Average composition obtained from two cultures (A and B) that were enriched with TCE first, and later with cis-DCE for several consecutive dilution series. Total sequence reads for the genera Geobacter and Dehalococcoides (underlined) were, respectively, 24232/140088 and 5393/140088 in replicate A, and 10421/103805 and 3023/103805 in replicate B. Genera with abundance <1% are grouped in "Other".

The presence of *Dhc* in both MW-2 and PZ-2 enriched cultures was consistent with the detection of the *vcrA* reductive dehalogenase genes (Figure 4.11) and ETH generation (Figures 4.6 and 4.8) in all the lactate-amended microcosms.

4.3.5. Site-specific ε^{13}C for PCE degradation

The analysis of site-specific ε^{13}C can help estimate the extent of the *in-situ* biodegradation of contaminants in the field (Elsner, 2010).

In an attempt to determine the site-specific ε^{13}C for PCE dechlorination in this aquifer, six parallel cultures inoculated with groundwater from well MW-2, and another six with groundwater from PZ-2, were prepared. The ones from well MW-2 were killed at 0, 7, 21, 46, 79, 81 and 82% of PCE degradation, while the ones from PZ-2 were killed at 0, 1, 6, 77, 88, 96 and 97% of PCE degradation, approximately. Afterwards, the δ^{13}C of CEs was analysed.
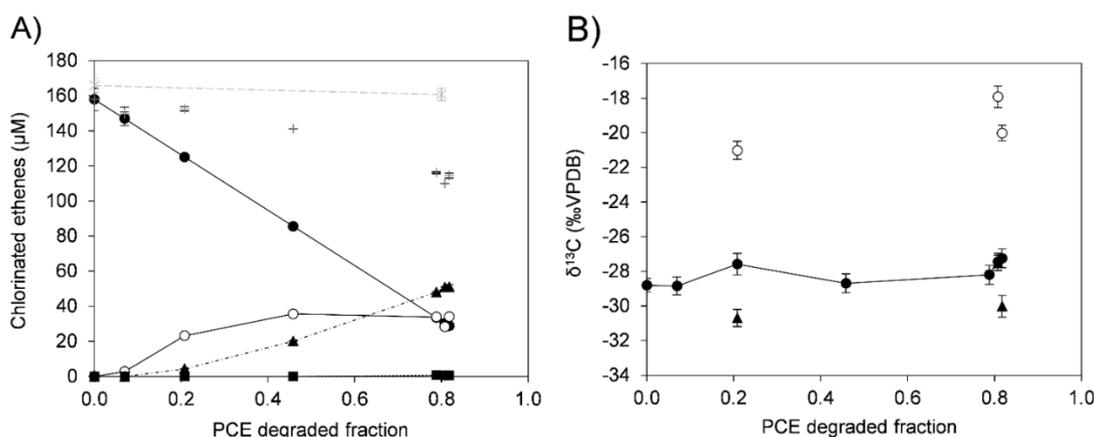
Figure 4.14. Changes in concentration (A) and carbon isotope composition (B) during anaerobic reductive dechlorination of PCE in microcosms with defined medium inoculated with 1.5% v/v MW-2 groundwater. Symbols: PCE (●), TCE (○), cis-DCE (▲), VC (■), sum of CEs (✚), PCE concentration in abiotic and killed controls (grey ✕). Error bars take into account the one standard deviation (1σ) for duplicate measurements and error propagation calculations. Concentrations of chlorinated solvents and ethene are presented as nominal concentrations.

In the MW-2 isotope experiments, abiotic and NaOH-killed controls showed no PCE degradation as its concentration remained constant throughout the whole experiment (163 $\pm$ 5 µM, n=7, Figure 4.14A). From the microcosms that were killed at different points of PCE degradation (Figure 4.14A), it was observed that the $\delta^{13}C_{PCE}$ only shifted 1.6‰ after 82% degradation (Figure

4.14B). The one standard deviation (1σ) for duplicate measurements was below total instrumental uncertainty of 0.5‰ for all samples (Sherwood Lollar et al., 2007). According to the results, dechlorination of PCE to TCE did not fit the Rayleigh model, as the data exhibited poor linearity ($R^2=0.46$) when plotted according to Eq. 2 (see section 3.2.7). The calculated $\varepsilon^{13}C$ was -0.6 ± 0.8‰, showing a 95% confidence interval bigger than the value itself, hence, $\varepsilon^{13}C$ was deemed as not significant. In contrast to PCE, TCE showed a stronger enrichment when degrading to *cis*-DCE (Figure 4.14B).
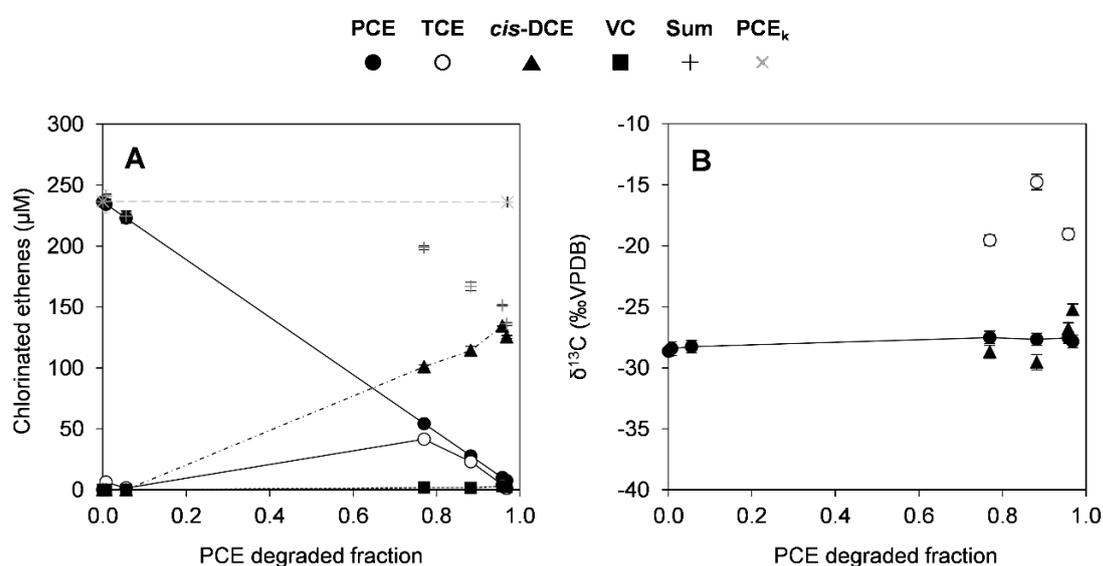

Figure 4.15. Changes in concentration (A) and carbon isotopic composition (B) during anaerobic reductive dechlorination of PCE in microcosms with defined medium and inoculated with 1.5% v/v PZ-2 groundwater. PCE_k refers to the PCE concentration in abiotic and killed controls and + to the sum of CEs. Error bars consider the one standard deviation (1σ) for duplicate measurements and error propagation calculations.

In the PZ-2 experiment, PCE was depleted in the microcosms (Figure 4.15A) but dechlorination was not accompanied by a significant change in its isotopic composition ($\delta^{13}C_{PCE}$) either (Figure 4.15B). In detail, $\delta^{13}C_{PCE}$ shifted only 0.81‰ and 1σ for duplicate measurements were, for all samples, below total instrumental uncertainty of 0.5‰ (Sherwood Lollar et al., 2007). The dechlorination reaction did not fit the Rayleigh model (Eq. 2, see section 3.2.7,

$R^2 = 0.63$, $\varepsilon^{13}C = -0.2 \pm 0.2$‰), which deemed this site-specific $\varepsilon^{13}C$ as not significant. In contrast, a stronger enrichment in ^{13}C was observed when the produced TCE was further degraded to *cis*-DCE (Figure 4.15B). Abiotic and NaOH-killed controls did not show PCE losses or degradation as its concentration did not vary significantly throughout the whole experiment (236 ± 8 µM, n=6, Figure 4.15A) and no degradation products were detected.

4.4. Discussion

From the beginning, obtained results from the hydrochemical characterization of the site served as qualitative evidence for the occurrence of natural anaerobic reductive dechlorination. For instance, the concentration of chloride ions detected in the aquifer due to the likely release of chloride from the C–Cl bond breakage, which was between 3 and 30 times higher in the impacted monitoring wells compared to the non-impacted well MW-4, which served as a background control (Table 4.2). An additional indicator of *in-situ* PCE biodegradation was provided by the presence of the degradation products of the hydrogenolysis pathway of PCE in the monitoring wells, since PCE was the only degreasing solvent used on site (Table 4.3). Furthermore, measured temperature and pH showed neutral and temperate shallow groundwater conditions, which are quite optimal for bioremediation purposes (Table 4.2) (Adrian and Löffler, 2016b).

The detection of low concentrations of DO, the relatively high concentrations of nitrate and sulphate, and the non-detection of iron (Table 4.2) indicated that the aquifer mainly exhibited hypoxic to nitrate- or iron-reducing conditions, which are thermodynamically appropriate to reduce highly chlorinated compounds such as PCE or TCE to *cis*-DCE, but not to fully dechlorinate to harmless ETH (Bouwer, 1994). The optimum Eh for a complete reductive dechlorination is less than -100 mV (Figure 1.8) (Elsner and Hofstetter, 2011)

but, as indicated in Table 4.2, no negative Eh were measured in the monitored wells, although higher reducing microenvironments in the aquifer cannot be discarded.

Since PCE was the unique chlorinated precursor released in this aquifer and it was assumed to be sequentially transformed via reductive dechlorination to TCE, *cis*-DCE and minor amounts of VC, the weighted average of the isotope composition of the CEs had to remain constant if VC was not further degraded (to ETH), and PCE released over the years had identical isotopic composition (Aeppli et al., 2010; Hunkeler et al., 1999; Palau et al., 2014b). As the values of $\delta^{13}C_{sum}$ in 7 of 9 wells (Table 4.3, Figure 4.3) were within the same average value (-31 ± 1‰), results indicated that PCE biodegradation beyond *cis*-DCE was not significant at natural conditions (the balance should have become heavier as the production of lighter VC was not taken into account). Additionally, results suggested that these seven wells shared the same source of contamination and it discarded the existence of important alternate degradation pathways or production of unidentified by-products. In contrast, the $\delta^{13}C_{sum}$ observed in the two distal wells MW-7 and Prof.A (Table 4.3, Figure 4.3) had an average value of $\delta^{13}C_{sum}$ of -26.2 ± 0.5‰ (obtained from different CEs in each well), which was statistically different from the rest (ANOVA, p < 0.0009). Such results suggested that a second source of PCE could have been leaked at this industrial area.

The extent of *in-situ* PCE biodegradation could not be quantified using the site-specific $\varepsilon^{13}C$ of PCE because the variation of $\delta^{13}C$ values obtained from the stablished microcosms at different degradation stages of PCE was not linear. Several $\varepsilon^{13}C$ values have been reported for the biodegradation of PCE under anoxic conditions in the literature. They range from strong isotope fractionation (e.g. -16.7‰ by *Desulfitobacterium* sp.) to very weak (-0.4 to -1.7‰) or even not significant isotope fractionation (e.g. by *Sulfurospirillum*, *Desulfuromonas* or *Geobacter*

species, all belonging to *ε-Proteobacteria*, Table 4.4). In particular, the reported ε^{13}C of PCE during anaerobic reductive dechlorination by *Dhc* isolates or *Dhc*-containing cultures ranges from -1.6 to -6.0‰ (Table 4.4). The non-linear low fractionation (<2‰) obtained in the MW-2 and PZ-2 enrichments (Figures 4.14B and 4.15B) were most likely a combination of the degradation of several bacterial species present in the aquifer with a major contribution of the non-fractionating species. This agrees with results obtained in the metagenomic analysis, as the predominance of *Geobacter* sp. over *Dhc* in the cultures (Figures 4.12 and 4.13) could suggest a higher contribution of *Geobacter* sp. in the PCE-to-TCE dechlorination step, and this scenario could be linked to the not significant fractionation observed (Table 4.4) (Cichocka et al., 2008).

The results obtained in the MW-2 and PZ-2 isotope experiments from the microcosms, where ε^{13}C was not significant, differ a bit from the isotopic shift of 3.6‰ for PCE that was observed on-site among the different monitoring wells with equal isotopic balance (Figure 4.3, excluding MW-7 and Prof.A). This suggested that such shift could be due to a major activity of the higher fractionating species depending on specific well conditions. Moreover, the remarkable isotopic enrichments observed in the same wells for TCE (8.1‰) and *cis*-DCE (5.3‰) agreed with the observations in both the MW-2 and PZ-2 isotope experiments (Figures 4.14 and 4.15) and pointed clearly to *in-situ* biodegradation processes (Figure 4.3, excluding MW-7 and Prof.A).

The detection of the *Dhc* biomarker genes 16S rRNA and *vcrA*, which are implicated in the VC-to-ETH transformation (Löffler et al., 2012), in the field-derived microcosms (Figure 4.11), and *Dhc* genera in the enriched cultures (Figures 4.12 and 4.13), indicated that the aquifer contained *Dhc* with the potential to detoxify PCE. However, natural groundwater geochemistry of the aquifer exerted a primary control over anaerobic dechlorination reactions.

Table 4.4. Carbon isotopic fractionation (ε13C) for the dechlorination of PCE to TCE by several OHRB and mixed cultures containing OHRB.

Strain	Phylogeny	PCE $\varepsilon^{13}C$ (‰)	Reference
Sulfurospirillum multivorans	ε-Proteobacteria	-0.4 ± 0.2	Nijenhuis et al. (2005)
Sulfurospirillum halorespirans	ε-Proteobacteria	-0.5 ± 0.2	Cichocka et al. (2007)
Desulfuromonas michiganensis	ε-Proteobacteria	ns	Cichocka et al. (2008)
Desulfuromonas michiganensis	ε-Proteobacteria	-1.7 ± 0.1	Renpenning et al. (2015)
Geobacter lovleyi strain SZ	ε-Proteobacteria	ns	Cichocka et al. (2008)
Desulfitobacterium hafniense strain PCE-S	Firmicutes	-5.2 ± 1.5	Nijenhuis et al. (2005)
Desulfitobacterium sp. strain Viet1	Firmicutes	-16.7± 4.5	Cichocka et al. (2008)
Dehalococcoides ethenogenes strain 195	Chloroflexi	-6.0 ± 0.7	Cichocka et al. (2008)
Dehalococcoides mccartyi sp. strain CBDB1	Chloroflexi	-1.6 ± 0.3	Marco-Urrea et al. (2011)
Mixed culture KB-1 (with Dhc)	-	-5.5 ± 0.8	Bloom et al. (2000)
Mixed culture TP	-	-2.7 to -5.2	Slater et al. (2001)

ns = fractionation was not significant, the observed shift in isotopic composition was within the instrumental error and, therefore, the $\varepsilon^{13}C$ could not be calculated.

The aquifer geochemical conditions are expected to improve, and allow efficient anaerobic dechlorination reactions by OHRB, with the decrease in Eh, as oxygen, nitrate, and sulphate are consumed (Figure 1.5B). However, the reduction of these electron acceptors can be hampered by the lack of electron donor in groundwater (Yu et al., 2018). According to these hypotheses, the addition of easily fermentable organic substrates (Lactate-1, Lactate-2 and the mixture of ethanol plus methanol) to the microcosms from wells MW-2 and PZ-2 enhanced the dechlorination of PCE with respect to the controls by shortening the lag phase of PCE dechlorination and overcoming the "DCE or VC stall" observed at natural conditions, which permitted the full dechlorination to ETH (Figures 4.5A, 4.6A and 4.8B–D).

Lactate, ethanol, and methanol can be potentially transformed by native bacteria using different pathways (Fennell et al., 1997). The production of acetate and hydrogen from fermentation reactions is preferred to stimulate growth of OHRB because they can serve as carbon source and electron donor, respectively. In the MW-2 microcosms, the production of $\sim$ 3 mM of acetate in the microcosms with a mixture of ethanol and methanol (Figure 4.5B) was consistent with the stoichiometric transformation of ethanol (3 mM) to acetate and hydrogen ($C_2H_6O + H_2O \rightarrow C_2H_3O_2^- + H^+ + 2H_2$), and the fermentation of methanol to carbon dioxide and hydrogen ($CH_4O + 2H_2O \rightarrow CO_2 + H_2O + 4H_2$). Similarly, the near stoichiometric conversion of Lactate-1 to acetate observed in Figure 4.6B agreed with the fermentation reaction $C_3H_5O_3^- + 2H_2O \rightarrow C_2H_3O^{-2} + HCO^- + H^+ + 2H_2$, and the same was observed in the PZ-2 microcosms (Figure 4.9), amended with either Lactate-1 or Lactate-2.

The absence of VFAs in the microcosms used as controls corroborated that acetate was only produced from the fermentation of the organic amendments added (Figures 4.4 and 4.8A).

The acidity generated from the fermentation reactions of the organic substrates (lactate, methanol and ethanol) and the dechlorination reactions (i.e. HCl) can affect the success of the biodegradation of the lesser CEs (Christ et al., 2004). The successful reductive dechlorination of PCE to ETH observed in the amended MW-2 and PZ-2 microcosms suggested that the aquifer was naturally well-buffered (Table 4.2) and it can be assumed that pH was maintained within the range of 6-8, which is described as optimal for dechlorinators (Yang et al., 2017a).

Similarly to the results obtained here, previous studies showed that methane production also developed more slowly in lactate rather than ethanol-amended microcosms (Fennell et al., 1997). Such pattern may be correlated with the amount of hydrogen released per mole of ethanol and methanol, which is larger than that produced from lactate (Fennell et al., 1997). In the MW-2 microcosms, since the concentration of fermentable organic substrates was higher in the microcosms with ethanol plus methanol (6 mM total) than in the lactate ones (3 mM), the high amount of hydrogen released in the microcosms amended with the alcohols could have caused a rapid shift to methanogenic conditions and stimulate the activity of hydrogenotrophic methanogens with the subsequent methane production (Figure 4.7). Likewise, an exaggerate methane production was observed in the PZ-2 microcosms that were amended with excess of Lactate-2, hence, a higher hydrogen release (Figure 4.10).

4.5. Conclusions

In this chapter, the use of an integrated approach that combined different complementary techniques provided insights into the intrinsic biodegradation potential of a site contaminated with CEs (i.e. if a bioremediation treatment was feasible).

The work started on May 2016 with the hydrogeochemical characterization of the field site. The application of carbon stable isotopic balances and a statistical analysis of the results suggested that two sources of PCE were responsible for the contamination plume in this industrial area, but they had not been mixed, and that PCE was transformed, in any case, via the hydrogenolysis pathway to *cis*-DCE.

The field-derived microcosms prepared with groundwater from monitoring well MW-2 allowed for the identification of *Dhc* 16S rRNA and *vcrA* genes, which provided evidence of the aquifer potential to detoxify PCE to ETH. However, the geochemistry of groundwater suggested that activity of *Dhc* in the *cis*-DCE stalled aquifer was impeded by the lack of sufficient electron donors to lower the Eh.

This was further corroborated with the time-course monitoring of the MW-2 microcosms, which were amended with different fermentable substrates (Lactate-1, methanol and ethanol). The results obtained discouraged natural attenuation as a remediation strategy in this contaminated site due to the *cis*-DCE stall observed in the microcosms mimicking the natural conditions of the aquifer (non-amended controls). In contrast, the two treatments with organic amendments (Lactate-1 and the mixture of ethanol plus methanol) accelerated the dechlorination of PCE and produced ETH, but methane was vigorously produced in the microcosm containing methanol and ethanol.

In light of these results, and also because methane production is not safe in an industrial environment, an enhanced anaerobic bioremediation injecting lactate as electron donor seems recommended to detoxify this contaminated site. For this reason, a second set of field-derived microcosms were prepared in October 2016, with groundwater from well PZ-2 and Lactate-2 (a commercial lactate product), which were candidates in a foreseeable future *in-situ* pilot test. In this

case, different isomeric forms and dosages of lactate (Lactate 1 and 2) were tested to investigate their effect on dechlorination rates. Results obtained agreed with the observations from MW-2 microcosms and provided additional evidence on the stall at *cis*-DCE and VC due to the lack of electron donors, and the production of methane due to their application in excess (i.e. excess of hydrogen).

In all, this multidisciplinary methodology used to diagnose the feasibility of biodegradation at the site for full reductive dechlorination of CEs was useful to get an insight into the idiosyncrasies of the aquifer and establish the best remediation approach.

Chapter 5

Site 1

Enhanced reductive dechlorination with lactate: *in-situ* pilot test and full-scale implementation in an aquifer contaminated with chlorinated ethenes

List of contents

Part of this chapter has been **submitted** for publication as:

"Integrative isotopic and molecular approach for the diagnosis and implementation of an efficient *in-situ* enhanced biological reductive dechlorination of chlorinated ethenes"

in the journal **Water Research**.

Abstract

An industrial site contaminated with tetrachloroethene (PCE) and its degradation products (trichloroethene (TCE), *cis*-dichloroethene (*cis*-DCE) and vinyl chloride (VC)) was investigated in Chapter 4 to assess its bioremediation potential (i.e. the full reductive dechlorination of PCE to ethene (ETH)). Based on these results, an *in-situ* enhanced reductive dechlorination (ERD) pilot test consisting of a single injection of lactate as electron donor in a monitoring well was performed and monitored for 190 days. The methodology used to follow the performance of the ERD was more complete than the integrative approach used in Chapter 4. Thus, the monitoring comprised the analysis of i) hydrochemistry, including the redox potential (Eh), and the concentrations of redox sensitive species, chlorinated ethenes (CEs), lactate, and acetate; ii) stable isotope composition of carbon of CEs, and sulphur and oxygen of sulphate; and iii) 16S rRNA gene sequencing from groundwater samples. This demonstrated that the injection of electron donor promoted sulphate-reducing conditions, with the subsequent decrease in Eh, which allowed for the full reductive dechlorination of CEs to ETH in the injection well. Such transformation was also confirmed by the enrichment of ^{13}C and carbon isotopic mass balances and, in accordance with the addition of an easily fermentable substrate (i.e. lactate), it was observed that the microbial population shifted towards the predominance of fermentative bacteria. Given the success of the *in-situ* biostimulation pilot test, a full-scale ERD with lactate was implemented at the site. After one year of treatment, CEs concentrations and δ^{13}C were analysed to evaluate the success of the treatment and, through the calculation of carbon isotopic mass balances, it was confirmed that PCE dechlorination and the VC-to-ETH reaction were occurring. The combination of techniques used in this chapter proved reliable to implement an efficient *in-situ* biological ERD of CEs at the field scale.

5.1. Introduction

As mentioned in previous chapters of this thesis, CEs are among the most ubiquitous anthropogenic groundwater contaminants due to their widespread use in industry and recalcitrance under oxic conditions. However, under anoxic conditions, CEs can undergo reductive dechlorination and, if the reaction is complete, be sequentially transformed to the non-toxic end-product ETH.

In Chapter 4, an industrial site contaminated with PCE and its degradation products (TCE, *cis*-DCE and VC) was studied to assess the feasibility of a bioremediation treatment as a strategy for the detoxification of the aquifer. The investigation, which comprised the analysis of several chemical, isotopic (CSIA), and molecular parameters to obtain separate lines of evidence of biodegradation, proved that the biological reduction of the CEs present was possible, but only with the addition of an organic fermentable substrate, which would act as an electron donor. Of the substrates that were tested, lactate showed the best results (independently of its isomeric form) because ETH was produced without an exaggerate methane generation (when lactate was not added in excess).

In subsurface ecosystems, when organohalide-respiring bacteria (OHRB) are present but hydrogen availability is limited, the contaminants detected in groundwater can show little to no dechlorination, resulting in the accumulation of toxic intermediates (e.g. the DCE or VC stall for CEs) (Bradley, 2000; Stroo and Ward, 2010). As already mentioned, this can be avoided by the conditioning of groundwater with organic fermentable substrates, which can generate reducing equivalents that promote reductive dechlorination reactions (e.g. the sequential dechlorination of CEs to ETH). This bioremediation approach is commonly referred to as biostimulation or ERD, which stands for enhanced reductive dechlorination (Adrian and Löffler, 2016b; Leeson et al., 2004).

Carbon CSIA was used in Chapter 4 of this thesis to gather complementary lines of evidence of biodegradation of CEs in groundwater (Aelion et al., 2009; Hermon et al., 2018; Hunkeler et al., 1999; Nijenhuis et al., 2007; Palau et al., 2014b). This technique can be used to confirm and quantify *in-situ* biodegradation and distinguish degradation pathways (Elsner, 2010). Similarly, the isotopic composition of potential non-halogenated electron acceptors can be used to trace changes in the redox conditions (i.e. Eh) of the aquifer, which is one of the key factors controlling reductive dechlorination reactions. For instance, a dual isotope approach can be used to measure the extent of sulphate reduction because this reaction results in an enrichment in both ^{34}S and ^{18}O in the residual sulphate (Wu et al., 2011).

To date, many studies have focused on laboratory methodologies, such as the ones used in Chapter 4, to evaluate the intrinsic bioremediation potential of CEs-polluted sites by OHRB (Buchner et al., 2015; Courbet et al., 2011; Ebert et al., 2010; Kuder et al., 2013; Lee et al., 2016; Lu et al., 2009; Matteucci et al., 2015; Nijenhuis et al., 2007; Slater et al., 2001; Tarnawski et al., 2016; Yu et al., 2018), but few have reported results after applying ERD and CSIA at the field scale (Herrero et al., 2019; Hirschorn et al., 2007; Song et al., 2002).

In this regard, several guidelines and research articles have been published for practitioners to consult when considering the design parameters of an *in-situ* bioremediation application (e.g. treatability of pollutants by OHRB, monitoring parameters, type and concentration of amendment, injection frequency, or treatment duration) (Dugat-Bony et al., 2012; Kueper et al., 2014; Leeson et al., 2013, 2004; Stroo and Ward, 2010) but, ultimately, they mostly are case-specific.

This chapter aims to apply an integrated isotopic and molecular approach that provides complementary lines of evidence to implement and monitor an efficient *in-situ* ERD with lactate at the field scale. In particular, the detoxification of the

aquifer contaminated by PCE, and the lesser CEs, of the same industrial site studied in Chapter 4, which is in Barcelona (Spain). To do so, the monitoring of the progress of the *in-situ* pilot test and the qualitative assessment of the efficiency of the full-scale treatment was performed via (1) the acquisition of hydrogeochemical data, (4) stable isotopes of sulphate (as model redox sensitive species), and carbon from the target contaminants (CEs), and (3) molecular techniques (i.e. identification of selected biomarkers and 16S rRNA high-throughput sequencing of groundwater samples).

5.2. Materials and methods

5.2.1. Materials

Pure chlorinated solvents and other chemicals used in this chapter are listed in Table 3.1.

5.2.2. Study site

The studied site is located in the Barcelona province (Spain) and a detailed hydrogeochemical description of the aquifer can be found in Chapter 4 (section 4.2.2) of this thesis. The original contamination plume, containing PCE, TCE, *cis*-DCE and traces of VC, had been treated by a combination of pump and treat (P&T) and dual-phase extraction (DPE, vapour and groundwater). Pumped groundwater was later treated through an air stripping system, where polluted groundwater was cleaned by transferring the volatile organic compounds (VOCs) into an air stream. This air stream and the vapours extracted via DPE were lastly passed through activated carbon, which adsorbed the VOCs present. These P&T and DPE systems were halted partially during the *in-situ* pilot test carried out in this chapter, and completely stopped for the full-scale bioremediation.

Figure 5.1 presents the water table and the location of the wells studied in this chapter. As depicted, the natural groundwater flow path of the aquifer followed a general NW–SE direction (Figure 5.1); however, under the ongoing remediation, all the extraction points (i.e. monitoring wells or piezometers) were almost dried due to the low productivity of the aquifer.
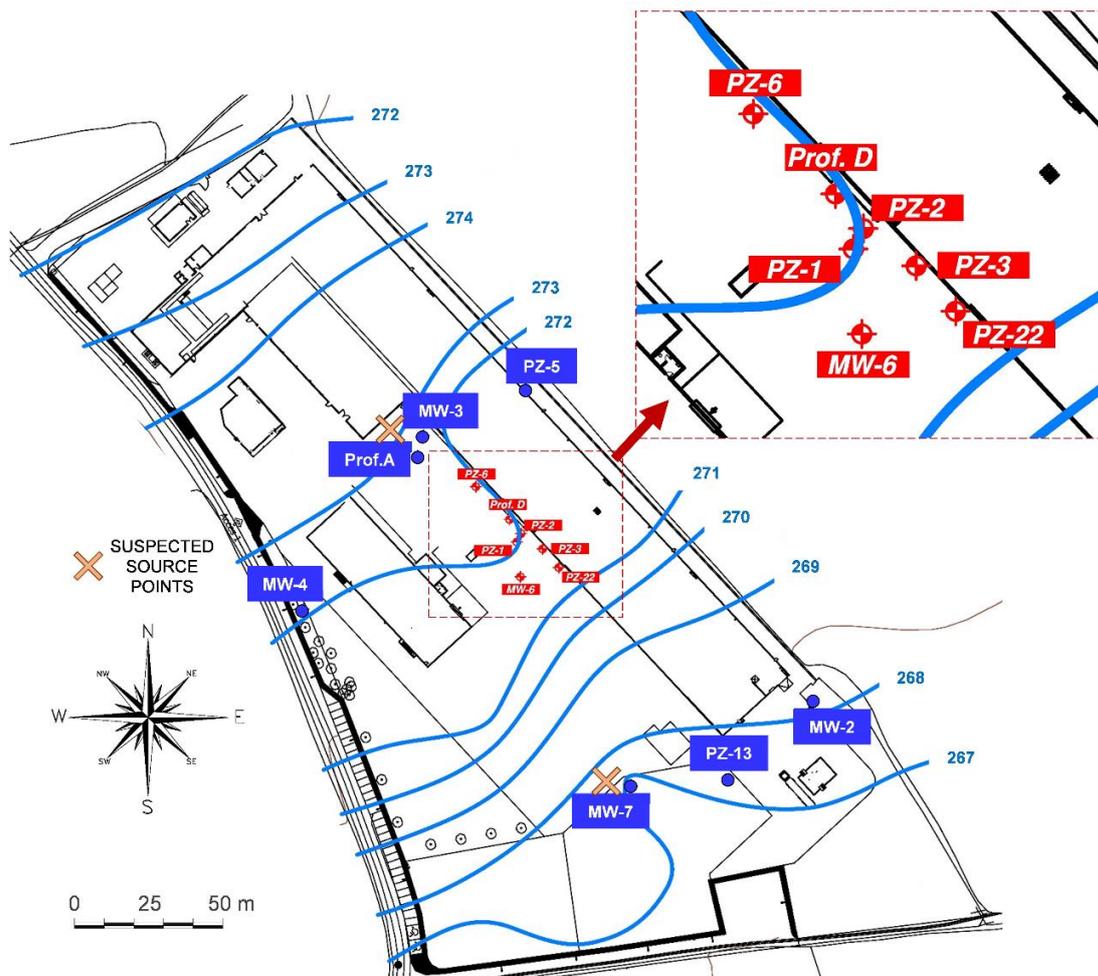
Figure 5.1. Water table (blue lines, in m.a.s.l.) representative of the natural groundwater flow at the site and location of monitoring wells. Red numerical codes refer to the wells monitored during the in-situ pilot test described in this chapter. Well PZ-2 is the injection well.

5.2.3. Implementation of the ERD *in-situ* pilot test

The pilot test consisted of a unique injection of lactate in well PZ-2 (Figure 5.1) on October 25th, 2016 (t_0). The product injected was an aqueous solution

of Lactate-2 diluted with the aquifer groundwater that was outflowing from the air stripping system installed at the site. This type of sodium lactate was chosen because it was a food-grade commercial cost-effective alternative that had been successfully tested in the laboratory prior to the field-scale application (see Chapter 4 for more details). The total volume of substrate solution injected was lower than 10% of the treatment zone volume to avoid a significant displacement of the contamination plume, for example, outside of the site limits and to the surrounding lands. The design parameters of the *in-situ* pilot test were based on the recommendations from Leeson et al. (2004) and Dugat-Bony et al. (2012).

5.2.4. Monitoring of the ERD *in-situ* pilot test

Field parameters (i.e. Eh, pH, temperature (T), and electric conductivity (EC)) were measured *in-situ* and groundwater was collected with a peristaltic pump from the injection well PZ-2 and nearby wells PZ-1, PZ-3, PZ-6, PZ-22, MW-6, and Prof.D (Figure 5.1) as described in section 3.2.1. Sampling campaigns were carried out the day before the injection of lactate (t_{-1}, October 24th, 2016) and the following 2, 9, 20, 50, 86, 142 and 190 days after the injection (hereinafter, t_i), thus, the pilot test lasted 6 months and a half, approximately. Samples collected for both CSIA and CEs concentration were immediately killed with NaOH (pH>10) and stored at 4ºC until analysed. Volatile fatty acids (VFAs) including lactate and acetate were analysed from groundwater samples filtered on site (0.20 μm) and stored in borosilicate tubes at 4ºC until analysed.

5.2.5. Isotopic evaluation of the full-scale ERD treatment

A full-scale ERD treatment was implemented by Litoclean, S.L. on August 2017. The bioremediation strategy consisted in the injection of Lactate-2 every

three months for the period of a year, approximately. Out of a total of 66 existing monitoring wells at the site, between 30 and 50 of them received the substrate injection at every injection campaign. However, the distribution of the injections varied between campaigns to ensure the maximum coverage of the contamination plume area. On September 2018, after one year of treatment, groundwater was sampled from wells PZ-3, PZ-5, PZ-22, MW-3, MW-6, and MW-7 (Figure 5.1) following the same methodology described in section 5.2.4. Samples were analysed for CEs concentrations and CSIA, and obtained results were compared to the chemical and isotopic data available for each well before the *in-situ* pilot test (Chapter 4 of this thesis and t$_{-1}$ of this chapter).

5.2.6. Analytical methods

Field parameters for the site characterization (t$_{-1}$) and during the monitoring of the *in-situ* pilot test were determined as described in section 3.2.1. Concentrations of VOCs, major anions and cations, and VFAs were analysed as described in sections 3.2.4, 3.2.5 and 3.2.6, respectively.

The predominant equilibrium systems controlling the Eh were investigated via Eh–pH predominance diagrams, which were prepared with PHREEQC and the MEDUSA code (Puigdomènech, 2010).

Stable carbon isotopes of CEs were obtained as described in section 3.2.7. For field results, increments in isotopic values must be >2‰ to consider that the reaction taking place is significant (Hunkeler et al., 2008).

Dissolved SO_4^{-2} present in groundwater was precipitated as $BaSO_4$ as reported in Dogramaci et al. (2001), and its sulphur and oxygen isotopic compositions were analysed following Rodríguez-Fernández et al. (2018b). Results are presented in delta notation ($\delta^{34}S$-SO_4^{-2} and $\delta^{18}O$-SO_4^{-2}, in ‰), relative to the

international standards, Vienna Canyon Diablo Troillite (VCDT) for δ^{34}S and Vienna Standard Mean Oceanic Water (VSMOW) for δ^{18}O.

5.2.7. 16S rRNA gene amplicon sequencing

To characterize the impact of lactate injection on the bacterial community distribution after the *in-situ* pilot test, an approximate total volume of 80 mL of groundwater was collected from wells PZ-2, PZ-1, and PZ-22 (Figure 5.1) at t_{-1} and t_{142}. Samples were stored at -20ºC until DNA extraction and 16S rRNA gene high-throughput sequencing were performed at AllGenetics & Biology (A Coruña, Spain). For DNA extraction, samples were centrifuged at 5000 g for 1 h and the pellet was transferred to PowerBead tubes of the DNeasy Powersoil DNA isolation kit (Qiagen). DNA was isolated following the instructions of the manufacturer. For library preparation, a fragment of the bacterial 16S rRNA region of around 450 bp was amplified using primers Bakt_341F and Bakt_805R (Herlemann et al., 2011). The pool was sequenced in a MiSeq PE300 run (Illumina).

5.3. Results and discussion

5.3.1. Hydrochemistry changes induced by the lactate injection

Concentrations of major ions in groundwater were monitored to get an insight into the occurring redox reactions, which can be used as an indicator of Eh. This is relevant because, as already mentioned, reducing conditions past sulphate-reduction are necessary for the detoxification of CEs. Therefore, SO_4^{-2}, NO_3^-, HCO_3^-, Cl^-, Na^+, K^+, Ca^{+2}, Mg^{+2} were analysed at t_{-1}, t_{20}, t_{86} and t_{190} to understand the effect of lactate injection on the hydrochemistry of the aquifer (see Figure 5.1 for the location of the injection and monitored wells).

Figure 5.2 presents the time-course of SO_4^{-2} and NO_3^- before and after the injection of lactate in well PZ-2. At this well, NO_3^- and SO_4^{-2} were depleted after the addition of the Lactate-2 (Figure 5.2A), while Na^+, Ca^{+2}, Mg^{+2} and EC increased, as a response to the injected sodium lactate (Table 5.1).

At the monitoring wells PZ-1, PZ-6 and MW-6, NO_3^- concentrations were depleted as well (or were naturally very low already), but different trends were observed for SO_4^{-2} (Figure 5.2A, B). In detail, SO_4^{-2} concentrations were naturally very low and somehow decreased after the substrate injection in wells PZ-6 and MW-6, whereas they slightly increased in well PZ-1.

In contrast, no significant changes occurred for those anions in wells PZ-3, PZ-22, and Prof.D (Figure 5.2C). In well PZ-3, which is nearby of the injection well PZ-2, both NO_3^- and SO_4^{-2} concentrations increased after the injection, but they decreased and almost went back to natural values with time. Similarly, but in a lesser extent due to the distance to the injection well PZ-2, monitoring well PZ-22 also exhibited such an increase/decrease pattern after the lactate injection, while Prof.D remained non-impacted.

The change in the reducing conditions was also investigated through the modelling of the geochemical conditions and the construction of Eh–pH predominance diagrams. Such an approach showed that the aquifer was at nitrate-reducing conditions before injection and that the addition of lactate promoted a shift towards sulphate-reducing and methanogenic conditions (Figure 5.3). This shift was more extreme in the injection well PZ-2 (at t_{20}) as well as in monitoring wells PZ-1 (at t_{86}), and PZ-6 and MW-6 (both at t_{190}), which agrees with the decrease observed in NO_3^- and SO_4^{-2} concentrations (Figure 5.2). In addition, results suggested that the system was controlled by calcite ($CaCO_3(s)$) (Figure 5.3B), as the pH was maintained within the range of 6–8, the optimal for OHRB (Yang et al., 2017a).
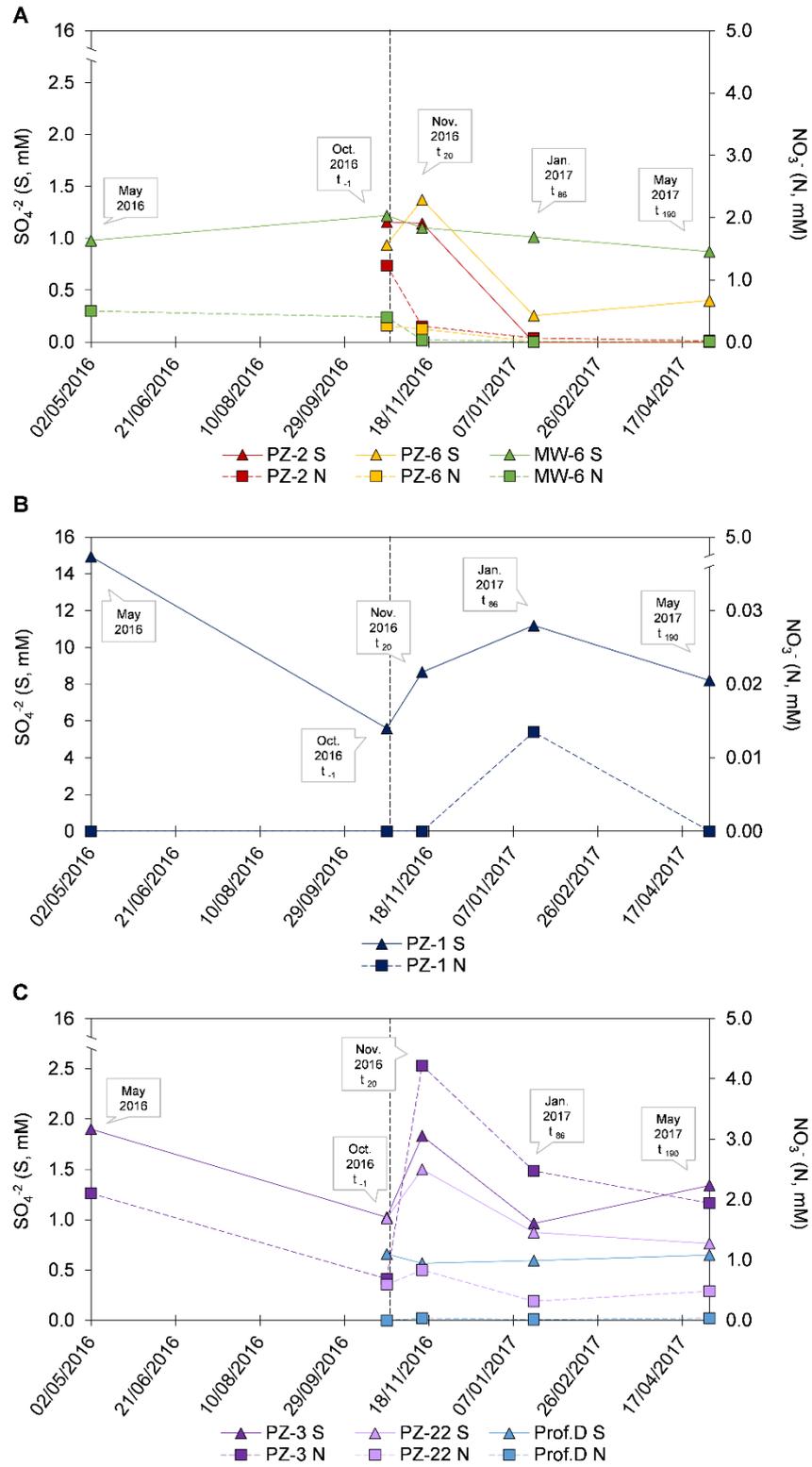
Figure 5.2. Time-course of SO₄⁻² and NO₃⁻ concentrations, before (May 2016 and t₋₁) and after (t₂₀, t₈₆ and t₁₉₀) the injection of lactate in PZ-2 (indicated with a vertical black dashed line), for wells (A) PZ-2, PZ-6 and MW-6, (B) PZ-1, (C) PZ-3, PZ-22 and Prof.D. The rest of the physicochemical parameters of groundwater are in Table 5.1. Legend: S: SO₄⁻², N: NO₃⁻.

Table 5.1. Physicochemical parameters of groundwater before (May 2016 and t_{-1}) and after (t_{20}, t_{86} and t_{190}) the in-situ ERD pilot test with lactate (injection at PZ-2). Time-course of NO_3^- and SO_4^{-2} concentrations are depicted in Figure 5.2.

Groundwater sample	Sampling date	Event (t_i)	T (ºC)	EC (µS/cm)	Cl^- (mM)	HCO_3^- (mM)	Na^+ (mM)	K^+ (mM)	Ca^{+2} (mM)	Mg^{+2} (mM)
Air stripping	24/10/2016	-1	21	2010	13	7	11	0.02	1	3
MW-6	02/05/2016	n.a.	19	1530	4	11	3	0.05	3	4
MW-6	24/10/2016	-1	22	1768	5	13	3	0.04	2	4
MW-6	14/11/2016	20	19	1915	5	14	3	0.04	2	4
MW-6	19/01/2017	86	16	1666	5	12	4	0.04	1	4
MW-6	03/05/2017	190	16	1596	5	12	3	0.08	1	3
Prof-D	24/10/2016	-1	18	2520	20	11	10	0.04	0.7	5
Prof-D	14/11/2016	20	18	2570	15	11	11	0.04	2	5
Prof-D	19/01/2017	86	17	2520	14	12	11	0.04	2	5
Prof-D	03/05/2017	190	18	2360	14	11	10	0.04	2	5
PZ-1	02/05/2016	n.a.	21	3410	3	9	15	0.01	7	6
PZ-1	24/10/2016	-1	22	2300	4	10	9	0.02	3	4
PZ-1	14/11/2016	20	21	2940	5	blq	14	0.02	6	5
PZ-1	19/01/2017	86	18	3560	3	10	20	0.01	5	4
PZ-1	03/05/2017	190	17	2770	3	9	17	0.01	2	4
PZ-2	24/10/2016	-1	22	1266	3	7	3	0.02	1	3
PZ-2	14/11/2016	20	20	19820	12	blq	297	0.3	29	24
PZ-2	19/01/2017	86	18	12200	8	blq	94	0.1	12	13
PZ-2	03/05/2017	190	18	5920	7	blq	34	0.06	5	6
PZ-22	24/10/2016	-1	20	1094	3	7	3	0.02	2	2
PZ-22	14/11/2016	20	20	1212	4	7	3	0.02	1	2
PZ-22	19/01/2017	86	18	1193	3	8	3	0.02	1	2
PZ-22	03/05/2017	190	18	843	2	6	2	0.04	2	2
PZ-3	02/05/2016	n.a.	20	1370	3	6	3	0.01	3	3
PZ-3	24/10/2016	-1	21	1296	5	8	2	0.01	2	3
PZ-3	14/11/2016	20	21	1319	5	5	2	0.01	2	3
PZ-3	19/01/2017	86	17	1405	3	6	2	0.01	2	3
PZ-3	03/05/2017	190	17	1226	4	4	2	0.02	2	3
PZ-6	24/10/2016	-1	19	1822	11	8	6	0.06	0.9	5
PZ-6	14/11/2016	20	19	1833	15	10	5	0.04	2	5
PZ-6	19/01/2017	86	17	1895	9	11	5	0.03	2	5
PZ-6	03/05/2017	190	17	1435	8	7	4	0.02	2	4

Air stripping: groundwater collected from across the aquifer, and treated through an air stripping system, that was mixed with lactate and injected into well PZ-2 for the *in-situ* pilot test.
n.a.: not applicable, blq: below limit of quantification.
Data from the site characterization on May 2016 is reported in Chapter 4.
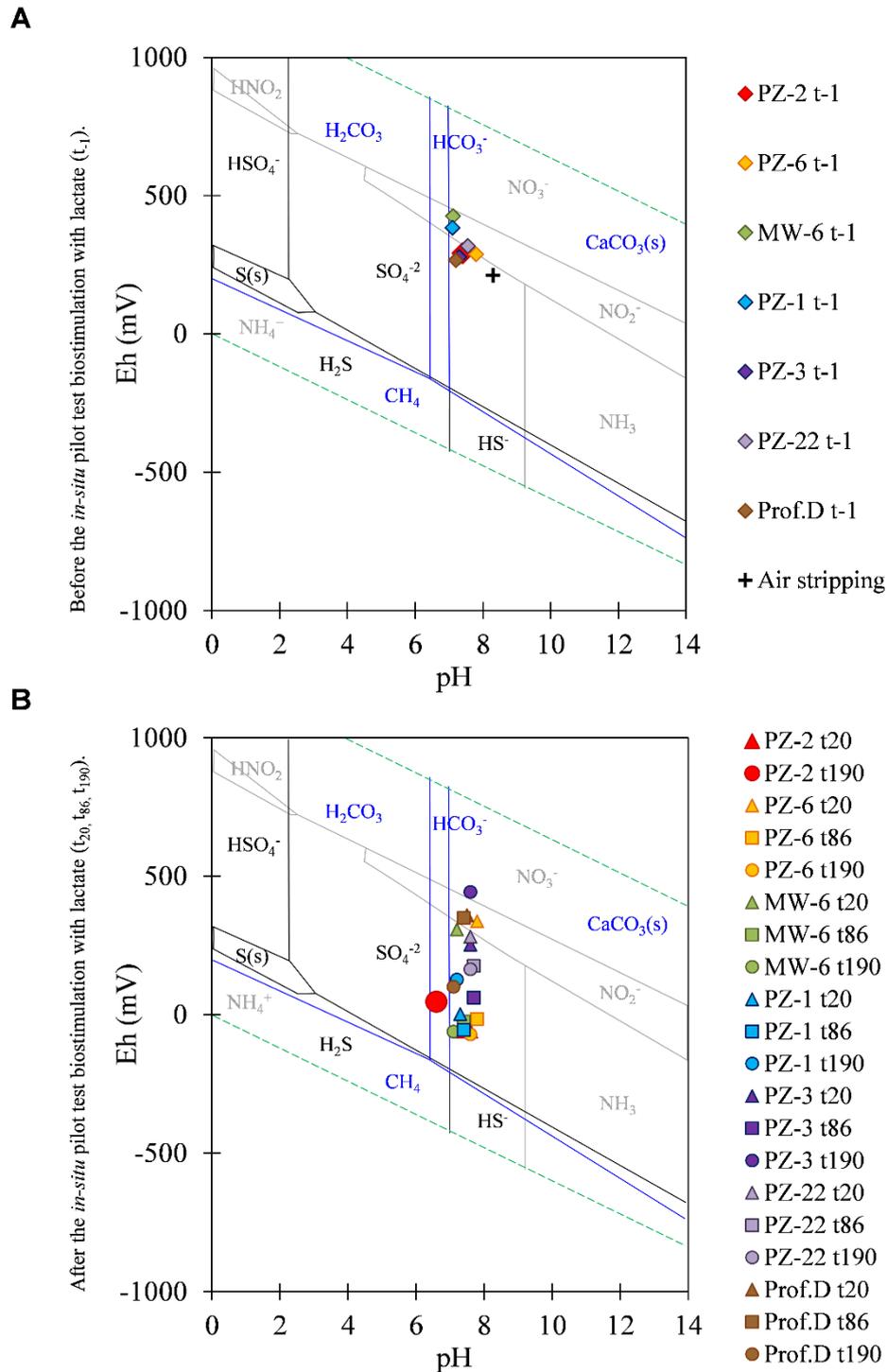
Figure 5.3. Eh–pH diagram of the systems S–H₂O (in black), Ca–C–H₂O (in blue) and N–H₂O (in grey) before lactate injection (A) and after lactate injection (B). Calculations were performed with $[Cl^-]_{tot} = 4 \cdot 10^{-3}$ M, $[NO_3^-]_{tot} = 5 \cdot 10^{-4}$ M, $[SO_4^{-2}]_{tot} = 2 \cdot 10^{-3}$ M, $[CO_3^{-2}]_{tot} = 7 \cdot 10^{-3}$ M, $[Na^+]_{tot} = 5 \cdot 10^{-3}$ M, $[Mg^{+2}]_{tot} = 4 \cdot 10^{-3}$ M, $[Ca^{+2}]_{tot} = 3 \cdot 10^{-3}$ M, $[K^+]_{tot} = 3 \cdot 10^{-5}$ M, CaCO₃(s), T = 25ºC, and using PHREEQC and the MEDUSA code (Puigdomènech, 2010). Dashed green lines stand for water stability field.

Another line of evidence for the occurrence of sulphate-reduction reactions is the analysis of S–O isotopes of SO_4^{-2}. For this reason, $\delta^{34}S$ and $\delta^{18}O$ values of dissolved SO_4^{-2} from t_{-1} at each monitoring well were compared with the ones obtained after the lactate injection (t_{20}, t_{86} or t_{190}).

Before the injection, the S and O isotopic composition of SO_4^{-2} at the site showed diverse values corresponding to a mixture among geogenic composition (Triassic or Tertiary recycled gypsum) in well Prof.D, synthetic fertilizers, and an unknown source (with the lowest ^{34}S and ^{18}O values) that could be related to agricultural uses of manure (Otero et al., 2008). This variability points out to a heterogeneity in the origin of the dissolved sulphate in the aquifer (Figure 5.4).

In the injection well PZ-2, isotopic compositions at t_{20} became significantly more enriched with a shift of $\varDelta\delta^{34}S = +3.0‰$ and $\varDelta\delta^{18}O = +3.2‰$ resulting in a slope of 1.1 (Figure 5.4). These $\delta^{34}S$ and $\delta^{18}O$ values of sulphate seemed influenced by the mixing with the sulphate isotopic composition of the injected water (Figure 5.4). Unluckily, no values could be obtained for t_{86} or t_{190} due to concentrations being below the limit of quantification.

An even larger shift was measured in monitoring wells PZ-6 and MW-6 because the slower decrease of SO_4^{-2} concentrations allowed the measurement of more points. By t_{190}, PZ-6 showed the most ^{34}S enriched value measured at the site, also with respect to its t_{-1} ($\varDelta\delta^{34}S = +14.4‰$), but with a small $\delta^{18}O$ enrichment ($\varDelta\delta^{18}O = +1.0‰$) (Figure 5.4). For MW-6, the most enriched $\delta^{34}S$ was measured in t_{86} ($\varDelta\delta^{34}S = +7.4‰$), while the largest $\varDelta\delta^{18}O$, of +4.7‰, was measured in t_{190} (Figure 5.4).

In contrast, $\varDelta\delta^{34}S$ and $\varDelta\delta^{18}O$ in monitoring wells PZ-1, PZ-3, PZ-22, and Prof.D were not significant (Figure 5.4).
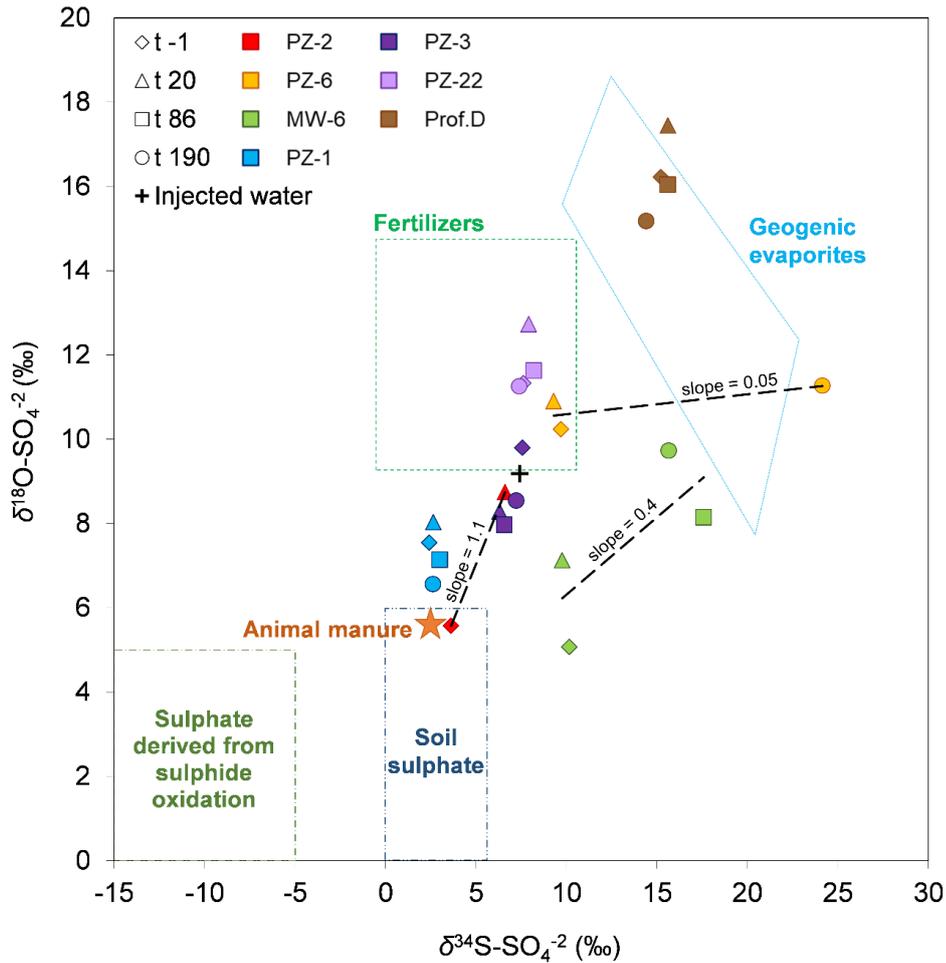
Figure 5.4. Dual S–O isotopic compositions of SO_4^{-2} during the in-situ ERD pilot test in all monitored wells. "Injected water" refers to the groundwater collected from across the aquifer, treated through an air stripping system, later mixed with Lactate-2, and injected into well PZ-2 for the pilot test. Samples t_{86} and t_{190} for PZ-2 had too low SO_4^{-2} concentration for isotopic measurements, while sample t_{86} for PZ-6 was lost. Dashed black lines represent the slopes estimated for each well with the available values. Shapes of symbols indicate different monitoring events, while colours indicate different monitoring wells.

A wide range of dual S–O slopes has been described for bacterial sulphate reduction in different natural environments (from 0.23 to 1.7) (Antler et al., 2013; Mizutani and Rafter, 1973). These differences have been linked to the net sulphate reduction rate and to the recycling of intermediate species (such as sulphite, which facilitates the oxygen isotope exchange with H_2O) back to sulphate. In environments where sulphate reduction is fast, this sulphite re-

oxidation is minimal, resulting in lower slopes due to sulphur isotopes increasing faster than oxygen isotopes (Antler et al., 2013). Therefore, obtained results with the available data points demonstrated that sulphate reduction was occurring, after the lactate injection, only in wells PZ-6 and MW-6 by isotopic enrichment, rather than pure mixing with injected water. Thermodynamically, the achievement of sulphate-reducing conditions suggested that the lesser chlorinated ethenes could be fully degraded to ETH *in-situ* (Bouwer, 1994).

5.3.2. Enhanced biodegradation of CEs at the injection well PZ-2

Concentrations of CEs and VFAs, Eh, and the carbon isotopic compositions of CEs were monitored to understand the effect of lactate injection and demonstrate whether detoxification could be achieved.

As depicted in Figure 5.5A, PCE was the main toxic substance dissolved in groundwater of well PZ-2 before lactate injection. After biostimulation, Eh decreased from +300-400 mV to ~ -50 mV by t_{20} (Figure 5.5D) and acetate was detected for the first time by t_{50} (Figure 5.5C). The generation of reducing equivalents from lactate fermentation and the subsequent dramatic decrease of Eh favoured dechlorination past *cis*-DCE and VC up to ETH by t_{190} (Figure 5.5A).

The full dechlorination of CEs to ETH by t_{190} was also confirmed by the enrichment in the isotopic mass balance ($\delta^{13}C_{sum}$, Eq. 4, section 3.2.7), which changed from -33 ± 2‰ to -9.0 ± 0.5‰ (Figure 5.5B). This difference in the $\delta^{13}C_{sum}$ is due to not considering the isotopic composition of ETH after VC degradation (which would be depleted as lighter isotopes react faster). Hence, $\delta^{13}C_{sum}$ became less negative as VC to ETH reaction progressed.

In detail, the PCE to TCE reaction at PZ-2 did not change $\delta^{13}C_{PCE}$ significantly and remained constant throughout the whole monitoring period (Figure 5.5B),

emulating the results of the microcosm experiments ($\varepsilon^{13}C$ = not significant) (Chapter 4, section 4.3.5). Conversely, TCE and *cis*-DCE showed variations in $\delta^{13}C$ during the *in-situ* dechlorination process, which were up to +7‰ for TCE, and +16‰ for *cis*-DCE at the measured times (Figure 5.5B). Lastly, VC could be nicely traced, exhibiting a remarkable variation of $\delta^{13}C$ (shift up to +49‰), which responded to its formation from *cis*-DCE and degradation to ETH by t_{190} (Figure 5.5B).
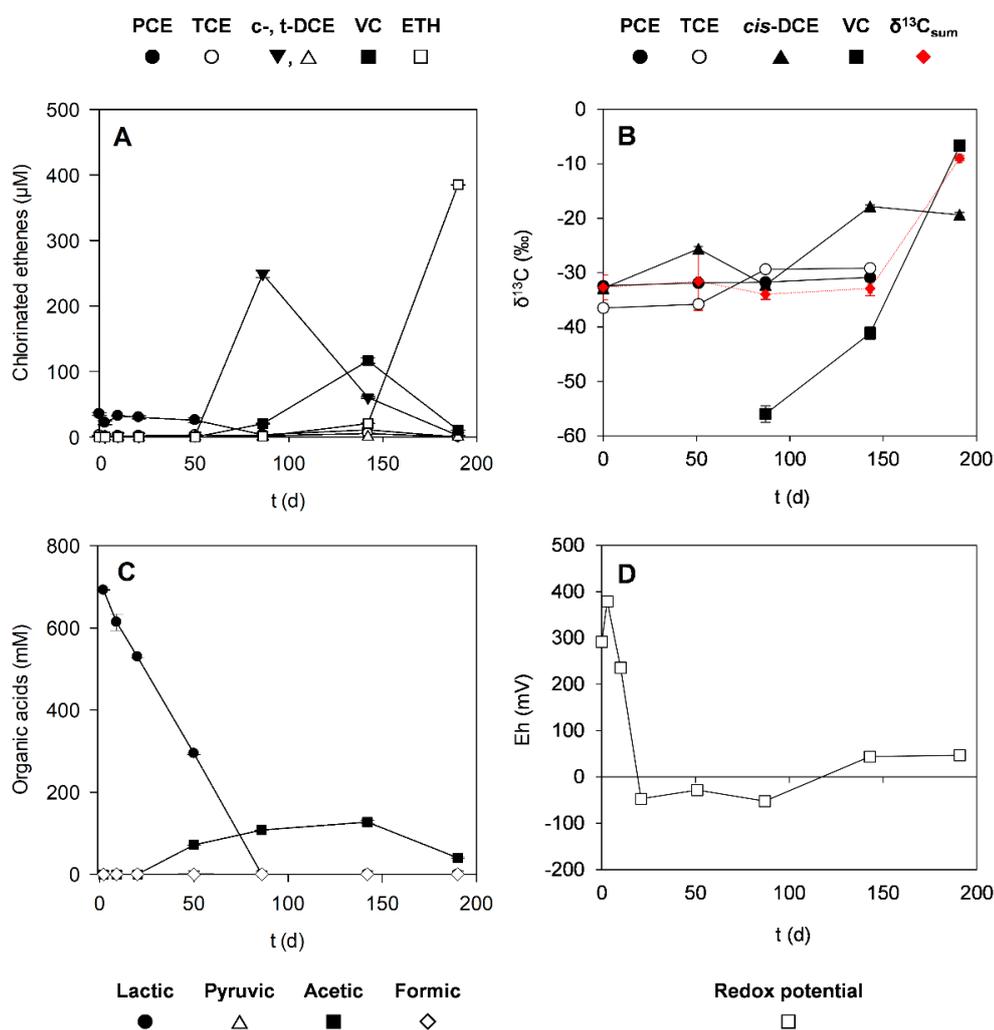
Figure 5.5. Time-course of monitored parameters in well PZ-2 during the in-situ pilot test: (A) concentration of CEs; (B) carbon isotopic composition and balance; (C) concentration of organic acids (VFAs), and (D) redox potential (Eh). Data presented is an average of each monitoring event and include error bars showing the one standard deviation (1σ) for duplicate measurements. δ¹³Csum: carbon isotopic mass balance.

5.3.3. Impact of the *in-situ* ERD pilot test at wells within the direct radius of influence of the lactate injection

Monitoring data obtained from nearby wells of the lactate injection was assessed in a similar manner to that of the injection well. Results allowed for the distinction between monitoring wells within and outside the direct radius of influence of the injection, and this criterion is used for their presentation.
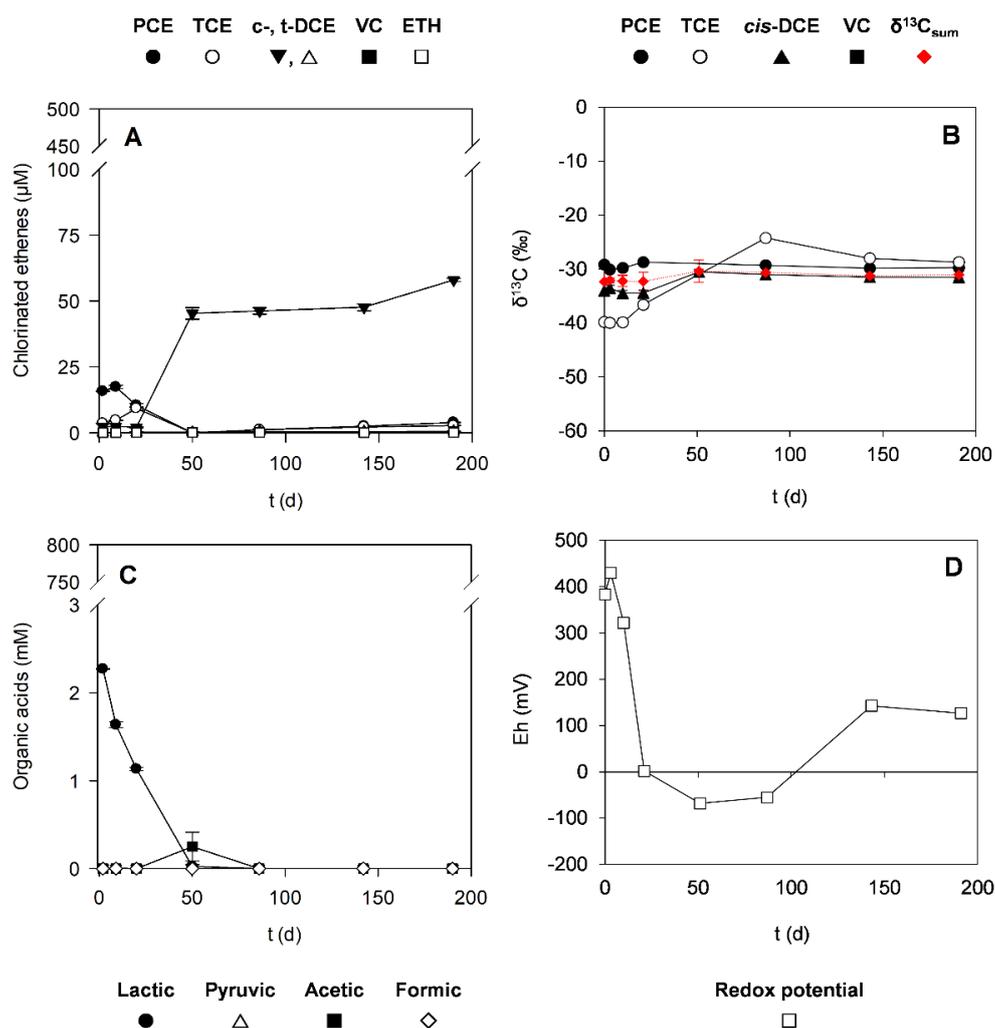
Figure 5.6. Time-course of monitored parameters in well PZ-1 during the in-situ pilot test: (A) concentration of CEs; (B) carbon isotopic composition and balance; (C) concentration of organic acids (VFAs), and (D) redox potential (Eh). Data presented is an average of each monitoring event and includes error bars showing the one standard deviation (1σ) for duplicate measurements.

Lactate, which was added in well PZ-2, and/or acetate, which is the product of its fermentation, were progressively detected in wells PZ-1 (at t_2, Figure 5.6C), PZ-6 (at t_{20}, Figure 5.7C) and MW-6 (at t_{142}, Figure 5.8C). This indicated the arrival of the injected solution of lactate through the preferential groundwater flow paths, which had a stronger N–S direction than at natural conditions (Figure 5.1), and drew the direct radius of influence of the *in-situ* ERD pilot test.
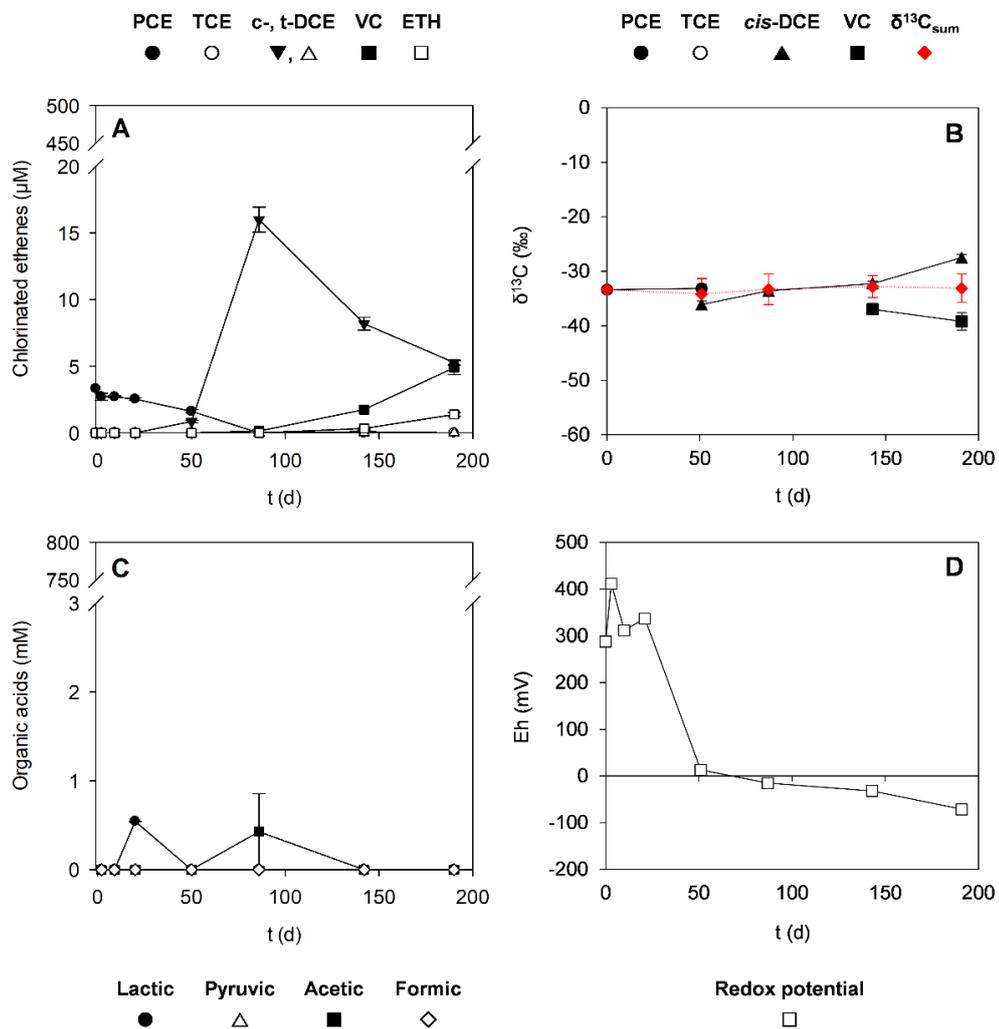
*Figure 5.7. Time-course of monitored parameters in well PZ-6 during the in-situ pilot test: (A) concentration of CEs; (B) carbon isotopic composition and balance; (C) concentration of organic acids (VFAs), and (D) redox potential (Eh). Data presented is an average of each monitoring event and includes error bars showing the one standard deviation (1σ) for duplicate measurements.*

Another evidence for the effect of the injection at these wells was the dramatic decrease in Eh like the one observed in the injection well PZ-2 (Figures 5.6D, 5.7D, 5.8D). However, even when reaching similar negative Eh values (down to -100 mV), the PCE reductive dechlorination mainly stalled at *cis*-DCE (Figures 5.6A, 5.7A, 5.8A, 5.9). This was more evident at well PZ-1, while in PZ-6, which was the farthest from PZ-2, *cis*-DCE started to pass to VC and ETH by t_{190} (Figure 5.7A).
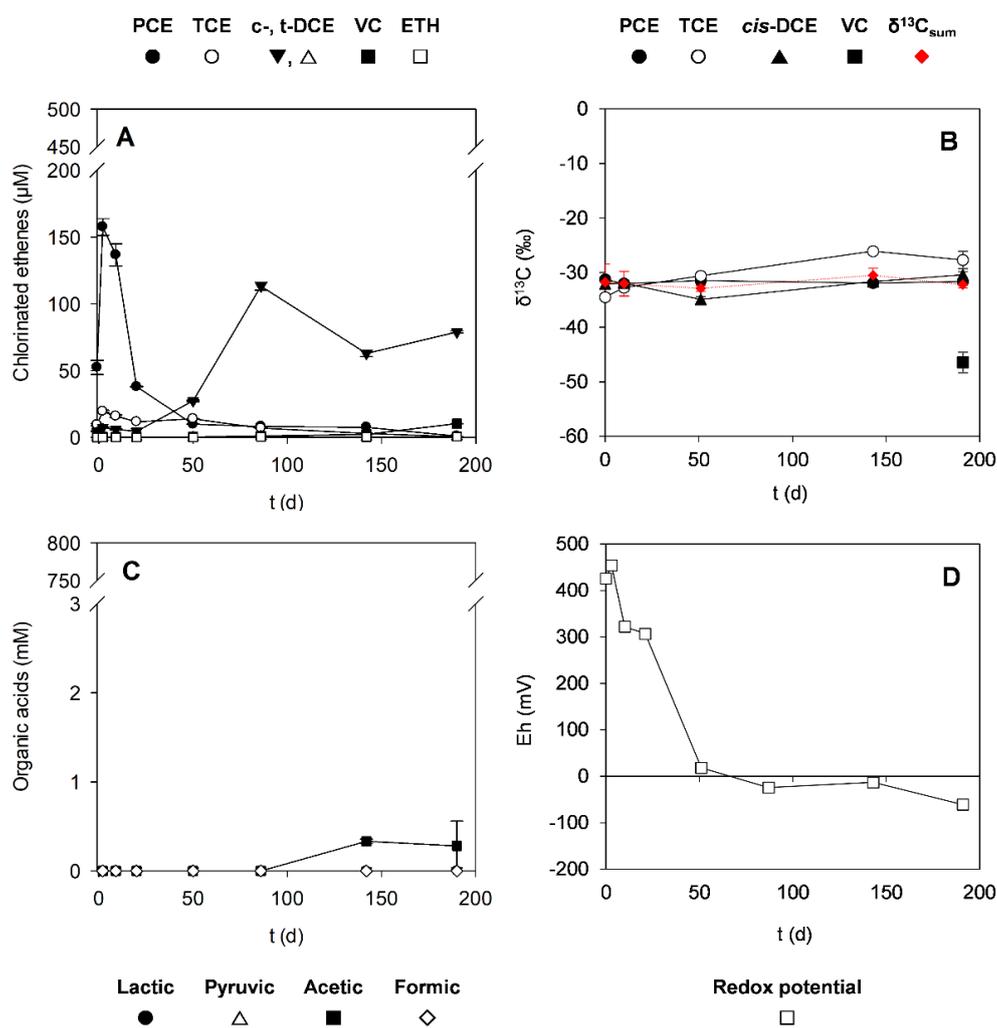

*Figure 5.8. Time-course of monitored parameters in well MW-6 during the in-situ pilot test: (A) concentration of CEs; (B) carbon isotopic composition and balance; (C) concentration of organic acids (VFAs), and (D) redox potential (Eh). Data presented is an average of each monitoring event and includes error bars showing the one standard deviation (1σ) for duplicate measurements.*

The concentration data that are presented in panel A of Figures 5.6, 5.7, and 5.8 agree with $\delta^{13}C_{sum}$ (Eq. 4, section 3.2.7) of CEs remaining constant in the three wells (~ -32‰ over 190 days, Figures 5.6B, 5.7B, 5.8B, 5.9), so there were no significant alternative degradation pathways besides hydrogenolysis and ETH generation was still minor compared to PZ-2.
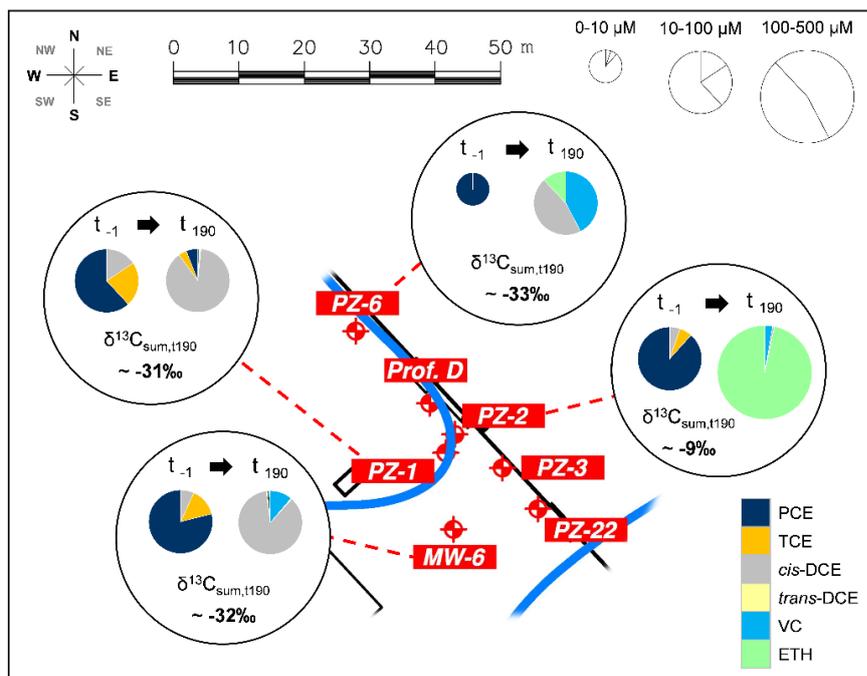
Figure 5.9. Location of the lactate injection well (PZ-2) and the monitoring wells under the influence of the biostimulation, indicating the molar fraction shift of CEs + ETH and the final carbon isotopic mass balance ($\delta^{13}C_{sum,t190}$). The size of the pie charts is related to the total concentration of CEs + ETH in each well and t_i. For details, see Figures 5.5, 5.6, 5.7 and 5.8.

Curiously, the most inefficient ERD (*cis*-DCE stall confirmed by no changes in its $\delta^{13}C_{cis\text{-}DCE}$ after t_{50}) occurred in PZ-1, where the initial drop in the Eh was followed by a rebound to more positive values after t_{86} (Figure 5.6D). This was most likely caused by the consumption and absence of electron donor from t_{86} onwards. In contrast, and possibly due to the combination of preferential flow paths and the remediation systems (P&T and DPE) that were active in the wells located outside the pilot test area, Eh in PZ-6 and MW-6 remained negative, allowing further degradation to VC (Figure 5.7D, 5.8D).

5.3.4. Impact of the *in-situ* ERD pilot test at wells outside the direct radius of influence of the injection

Following the same scheme of the previous section, lactate and acetate were not detected in wells PZ-3, PZ-22, and Prof.D (Figures 5.10C, 5.11C and 5.12C). Accordingly, Eh did not reach negative values in any of them (Figures 5.10D, 5.11D and 5.12D), preventing to prove a direct effect of the *in-situ* ERD pilot test.
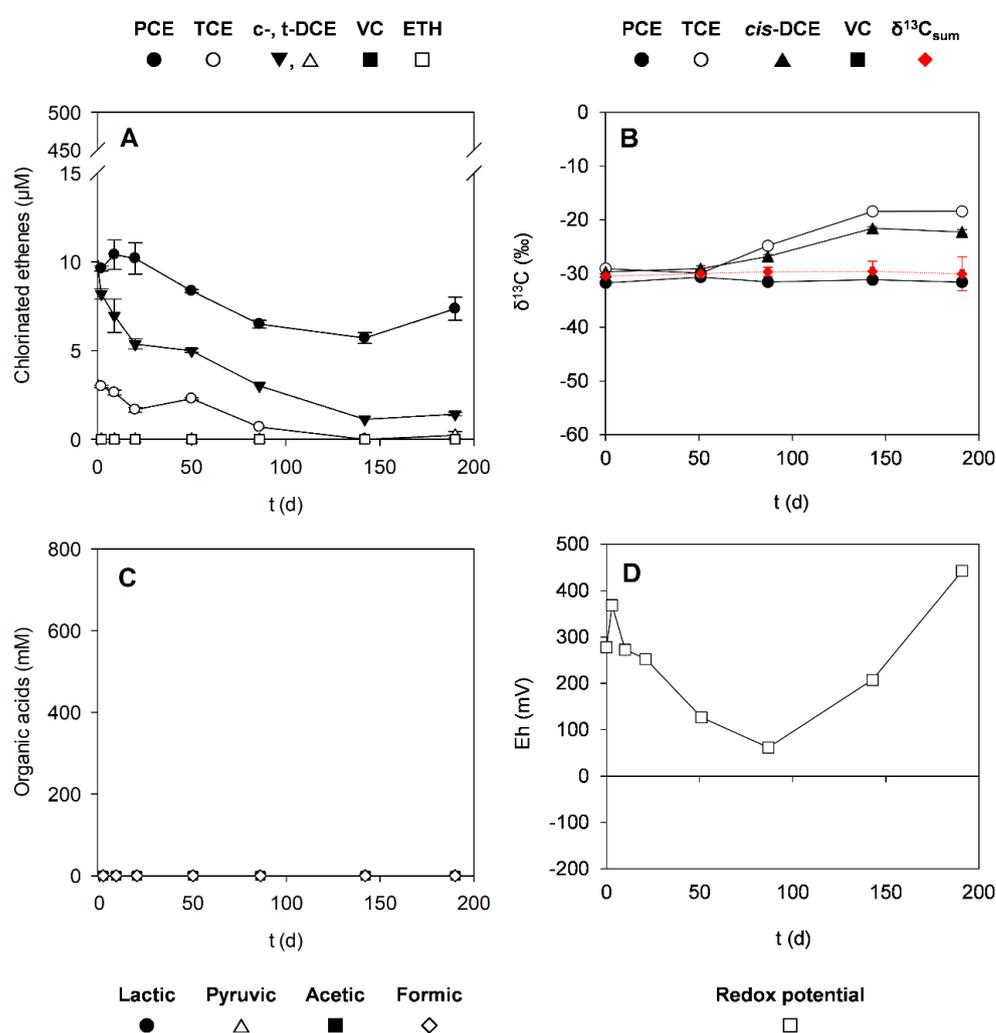

Figure 5.10. Time-course of monitored parameters in well PZ-3 during the in-situ pilot test: (A) concentration of CEs; (B) carbon isotopic composition and balance; (C) concentration of organic acids (VFAs), and (D) redox potential (Eh). Data presented is an average of each monitoring event and includes error bars showing the one standard deviation (1σ) for duplicate measurements.
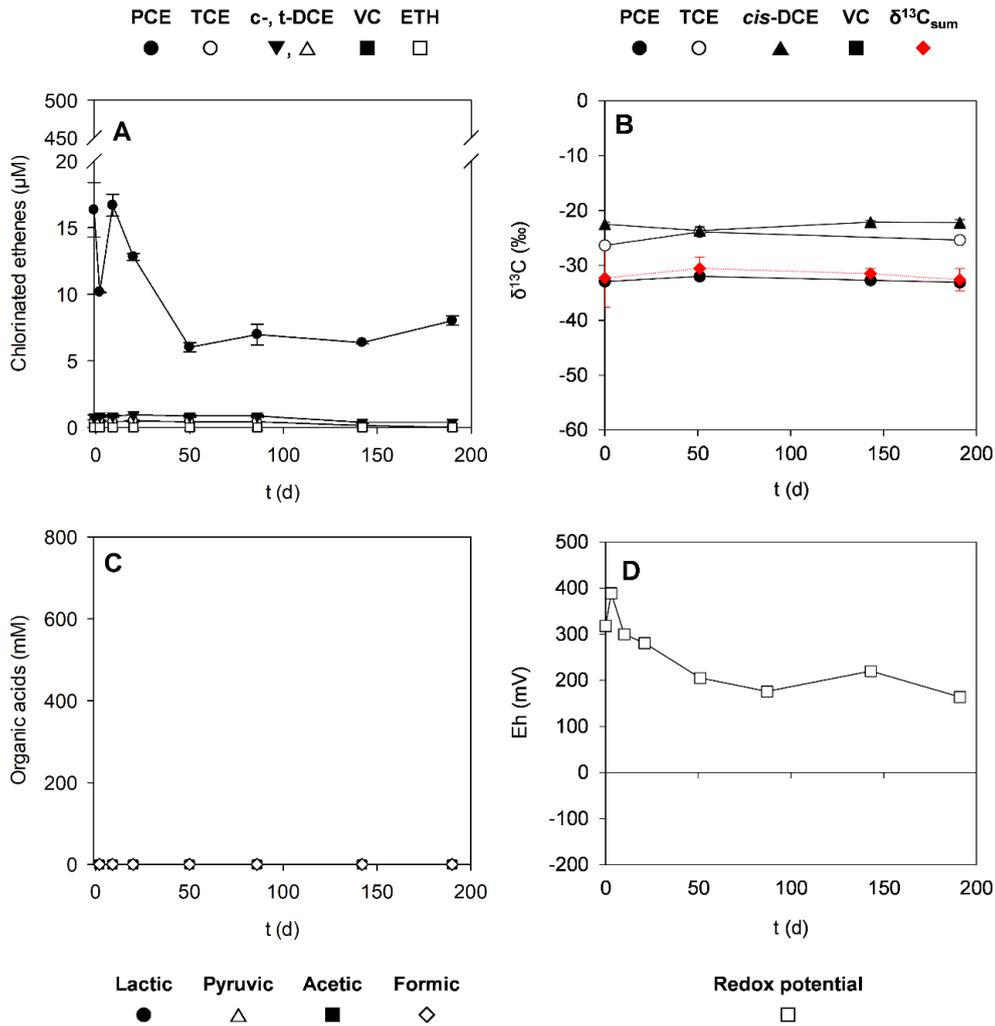
Figure 5.11. Time-course of monitored parameters in well PZ-22 during the in-situ pilot test: (A) concentration of CEs; (B) carbon isotopic composition and balance; (C) concentration of organic acids (VFAs), and (D) redox potential (Eh). Data presented is an average of each monitoring event and includes error bars showing the one standard deviation (1σ) for duplicate measurements. δ¹³Csum: carbon isotopic mass balance.

In well PZ-3, Eh decreased to +60 mV at t_{86} but it rebounded to initial conditions by t_{190} (Figure 5.10D). Curiously, CEs concentrations decreased globally in PZ-3 and PZ-22, but PCE molar fraction increased in respect to the lesser CEs, which could indicate a solubilization and dilution of the PCE absorbed to the soil due to the injected volume (Figure 5.13). Therefore, the ^{13}C enrichments observed for TCE and *cis*-DCE in PZ-3 (by +11.5‰ and +8.1‰, respectively, Figure 5.10B) could be attributed to reductive

dechlorination in the well or, most probably, associated to the dispersion from upstream contaminants that had been previously enriched in ^{13}C.
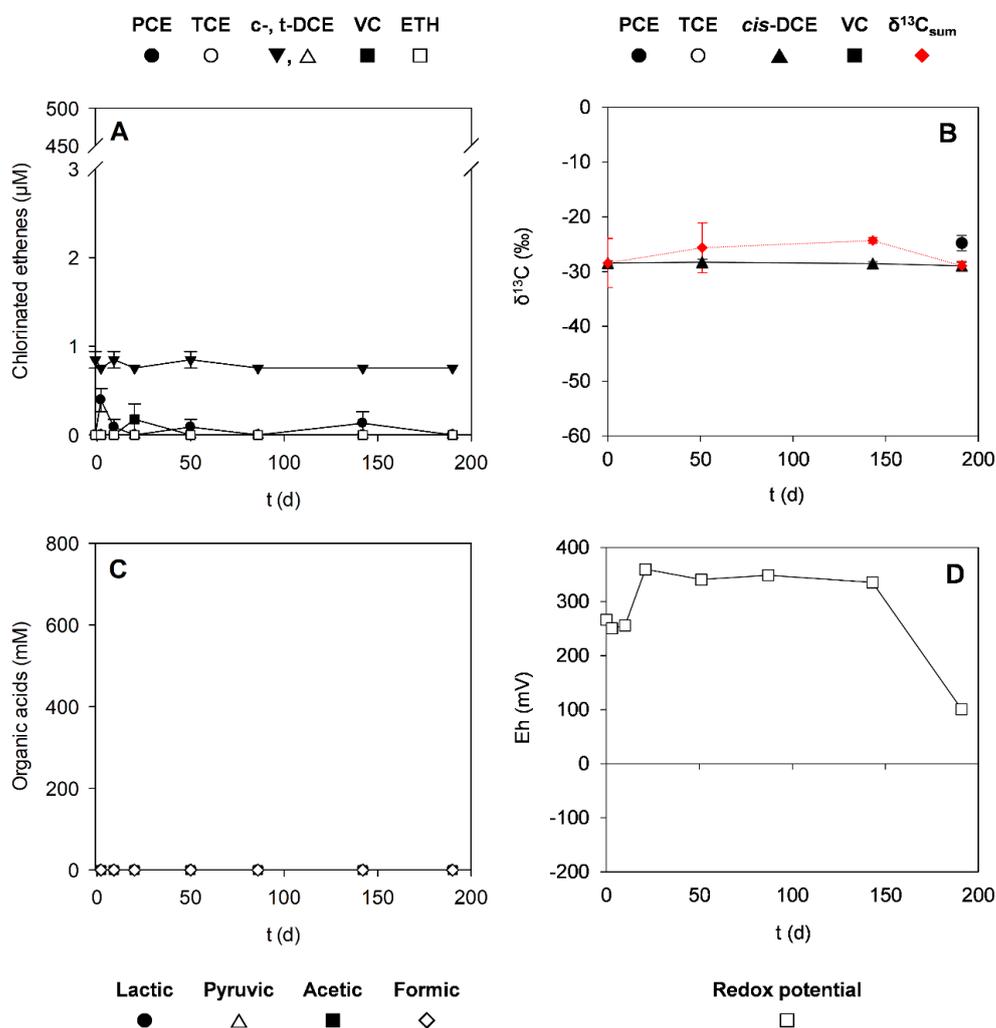

Figure 5.12. Time-course of monitored parameters in well Prof.D during the in-situ pilot test: (A) concentration of CEs; (B) carbon isotopic composition and balance; (C) concentration of organic acids (VFAs), and (D) redox potential (Eh). Data presented is an average of each monitoring event and includes error bars showing the one standard deviation (1σ) for duplicate measurements.

In line with the previous conclusions, changes in CEs concentrations in both PZ-22 and Prof.D wells (Figures 5.11A and 5.12A) were not associated to significant shifts in ^{13}C values (Figures 5.11B and 5.12B), which confirmed this dilution effect. In detail, Eh in PZ-22 decreased from +300-400 mV to ~ +200 mV after lactate injection in well PZ-2 (Figure 5.11), but such a shift

in the redox conditions was not even enough to promote the degradation of PCE to TCE and *cis*-DCE, which require less strict reducing conditions than the *cis*-DCE to VC and ETH reactions. Lastly, well Prof.D showed a unique behaviour, possibly due to its constructive characteristics, as it was twice as deep than the rest of the wells and, thus, reached different units of the aquifer.
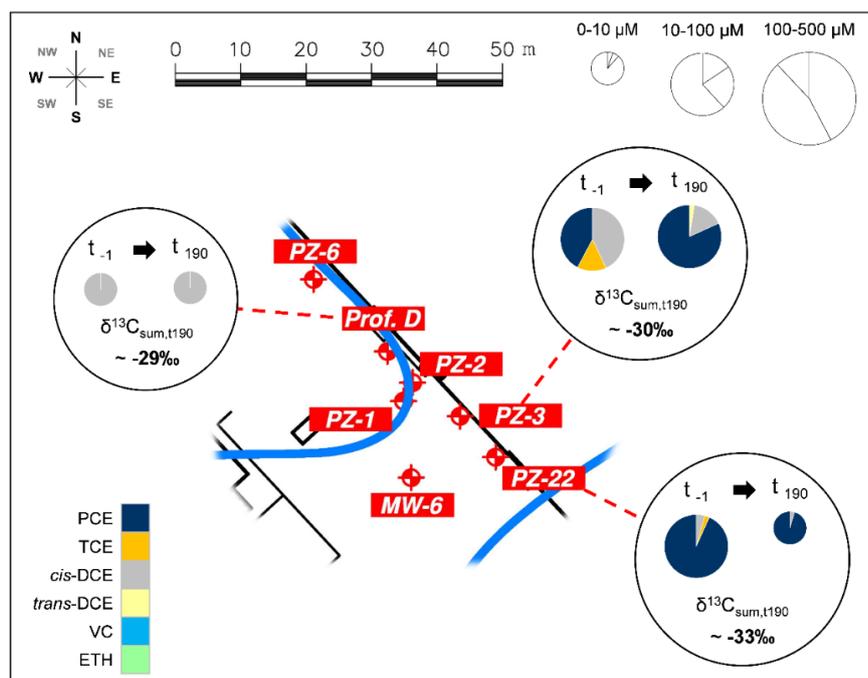
Figure 5.13. Location of the lactate injection well (PZ-2) and the monitoring wells outside the influence of the biostimulation, indicating the molar fraction shift of CEs + ETH and the final carbon isotopic mass balance ($\delta^{13}C_{sum,t190}$). The size of the pie charts is related to the total concentration of CEs + ETH in each well and t_i. See Figures 5.10, 5.11 and 5.12 for details.

5.3.5. Shift in the native microbial community induced by the *in-situ* ERD pilot test

As demonstrated in Chapter 4 of this thesis, another line of evidence for biodegradation can be obtained through molecular data. In this case, the effect of lactate injection on the microbial community of the aquifer was investigated by high-throughput sequencing of the 16S rRNA region of selected groundwater samples. Samples from wells PZ-2, PZ-1 and PZ-22 at t_{-1} and t_{142}

were chosen based on the results obtained in the pilot test, as they represented three different scenarios: i) PCE-to-ETH reaction at the injection well (PZ-2), ii) *cis*-DCE stall (PZ-1), and iii) a well not directly impacted by the injection of lactate (PZ-22).

In PZ-2, the most abundant phyla at t_{-1} were *Proteobacteria* (58%), *Planctomycetes* (11%), *Bacteroidetes* (6%), *Verrucomicrobia* (6%), *Chlamydiae* (4%), *Actinobacteria* (4%), and *Acidobacteria* (2%), whereas at t_{142}, the community shifted to *Firmicutes* (67%), *Bacteroidetes* (14%), *Proteobacteria* (14%), and *Tenericutes* (2%) (Figure 5.14, Table 5.2). Within *Firmicutes*, bacteria from the family *Veillonellaceae* (26%), and *Erysipelotrichaceae* (9%) were the most abundant; and the same occurred for the genus *Desulfovibrio* (3%), from the *Proteobacteria* phylum (data not shown). The microbial composition after the injection of lactate was dominated by fermenting bacteria that were probably induced by the injection of lactate (Fennell et al., 1997; He et al., 2007; Tegtmeier et al., 2016).

In contrast, the abundance of the *Firmicutes* phylum was very limited in well PZ-1 (abundance of 4% at t_{142}) and almost insignificant in well PZ-22 (Figure 5.14, Table 5.2), which agrees with the chemical and isotopic results discussed before.

When comparing PZ-2 results obtained in this chapter to the ones obtained in Chapter 4, during the laboratory integrative assessment of the feasibility of PCE biodegradation for the detoxification of this site, great differences can be detected. For instance, in the enriched cultures derived from wells MW-2 and PZ-2 (the latter is the injection well in this chapter), the most abundant phyla were *Proteobacteria*, *Bacteroidetes* and *Chloroflexi* (i.e. the *Dehalococcoides* sp. phylum), while *Firmicutes* only placed fourth with a very low relative abundance (~ 3%, data not shown).

Table 5.2. 16S rRNA gene sequencing detailed results in relative abundance (%) at the phylum level at t_{-1} and t_{142}. Results presented in this table correspond to data represented in Figure 5.14.

| Legend	Taxonomy	Total %	PZ-2 t_{-1} %	PZ-2 t_{142} %	PZ-1 t_{-1} %	PZ-1 t_{142} %	PZ-22 t_{-1} %	PZ-22 t_{142} %
	Unclassified; Other	0.1%	0.0%	0.0%	0.0%	0.0%	0.0%	0.8%
	Archaea; Other	0.0%	0.0%	0.0%	0.0%	0.0%	0.0%	0.2%
	Archaea; *Crenarchaeota*	0.0%	0.0%	0.0%	0.0%	0.0%	0.0%	0.2%
	Archaea; *Euryarchaeota*	0.1%	0.4%	0.0%	0.0%	0.0%	0.0%	0.0%
	Bacteria; Other	2.2%	2.3%	1.4%	0.0%	7.0%	0.6%	1.9%
	Bacteria; *Acidobacteria*	1.8%	2.4%	0.0%	1.9%	0.0%	3.7%	2.8%
	Bacteria; *Actinobacteria*	1.3%	4.2%	0.3%	0.0%	0.2%	0.6%	2.4%
	Bacteria; *Bacteroidetes*	5.4%	6.1%	13.6%	0.0%	9.3%	1.1%	2.2%
	Bacteria; *Chlamydiae*	1.9%	4.4%	0.0%	0.0%	1.0%	1.1%	4.8%
	Bacteria; *Chlorobi*	0.3%	0.6%	0.0%	0.0%	0.4%	0.0%	1.0%
	Bacteria; *Chloroflexi*	0.5%	0.3%	1.0%	0.0%	1.1%	0.0%	0.4%
	Bacteria; *Cyanobacteria*	0.0%	0.0%	0.0%	0.0%	0.0%	0.3%	0.0%
	Bacteria; *Elusimicrobia*	0.2%	0.8%	0.0%	0.0%	0.0%	0.2%	0.1%
	Bacteria; *Firmicutes*	11.9%	0.0%	66.9%	0.0%	4.4%	0.0%	0.0%
	Bacteria; GN02	0.1%	0.0%	0.0%	0.0%	0.3%	0.0%	0.3%
	Bacteria; *Gemmatimonadetes*	1.3%	0.9%	0.0%	0.0%	0.2%	5.6%	0.9%
	Bacteria; *Lentisphaerae*	0.2%	0.0%	0.8%	0.0%	0.4%	0.0%	0.0%
	Bacteria; NKB19	0.1%	0.0%	0.0%	0.0%	0.0%	0.4%	0.2%
	Bacteria; *Nitrospirae*	0.2%	0.0%	0.0%	0.0%	0.0%	0.0%	0.9%
	Bacteria; OD1	5.9%	0.5%	0.3%	0.0%	27.2%	0.0%	7.2%
	Bacteria; OP1	0.0%	0.0%	0.0%	0.0%	0.0%	0.0%	0.3%
	Bacteria; OP11	0.1%	0.0%	0.0%	0.0%	0.6%	0.0%	0.0%
	Bacteria; OP3	0.2%	1.0%	0.0%	0.0%	0.0%	0.2%	0.2%
	Bacteria; *Planctomycetes*	2.8%	11.2%	0.0%	0.0%	0.8%	3.2%	1.4%
	Bacteria; *Proteobacteria*	56.3%	58.1%	13.2%	73.1%	44.5%	80.9%	68.0%
	Bacteria; SBR1093	0.1%	0.2%	0.0%	0.0%	0.0%	0.0%	0.3%
	Bacteria; TM6	0.7%	0.2%	0.0%	0.5%	2.3%	0.3%	1.1%
	Bacteria; TM7	4.4%	0.0%	0.0%	24.4%	0.5%	0.0%	1.4%
	Bacteria; *Tenericutes*	0.3%	0.0%	2.0%	0.0%	0.0%	0.0%	0.0%
	Bacteria; *Verrucomicrobia*	1.5%	5.8%	0.4%	0.0%	0.0%	1.7%	1.1%
	Bacteria; WWE1	0.0%	0.0%	0.2%	0.0%	0.0%	0.0%	0.0%
	Bacteria; ZB3	0.1%	0.7%	0.0%	0.0%	0.0%	0.0%	0.0%
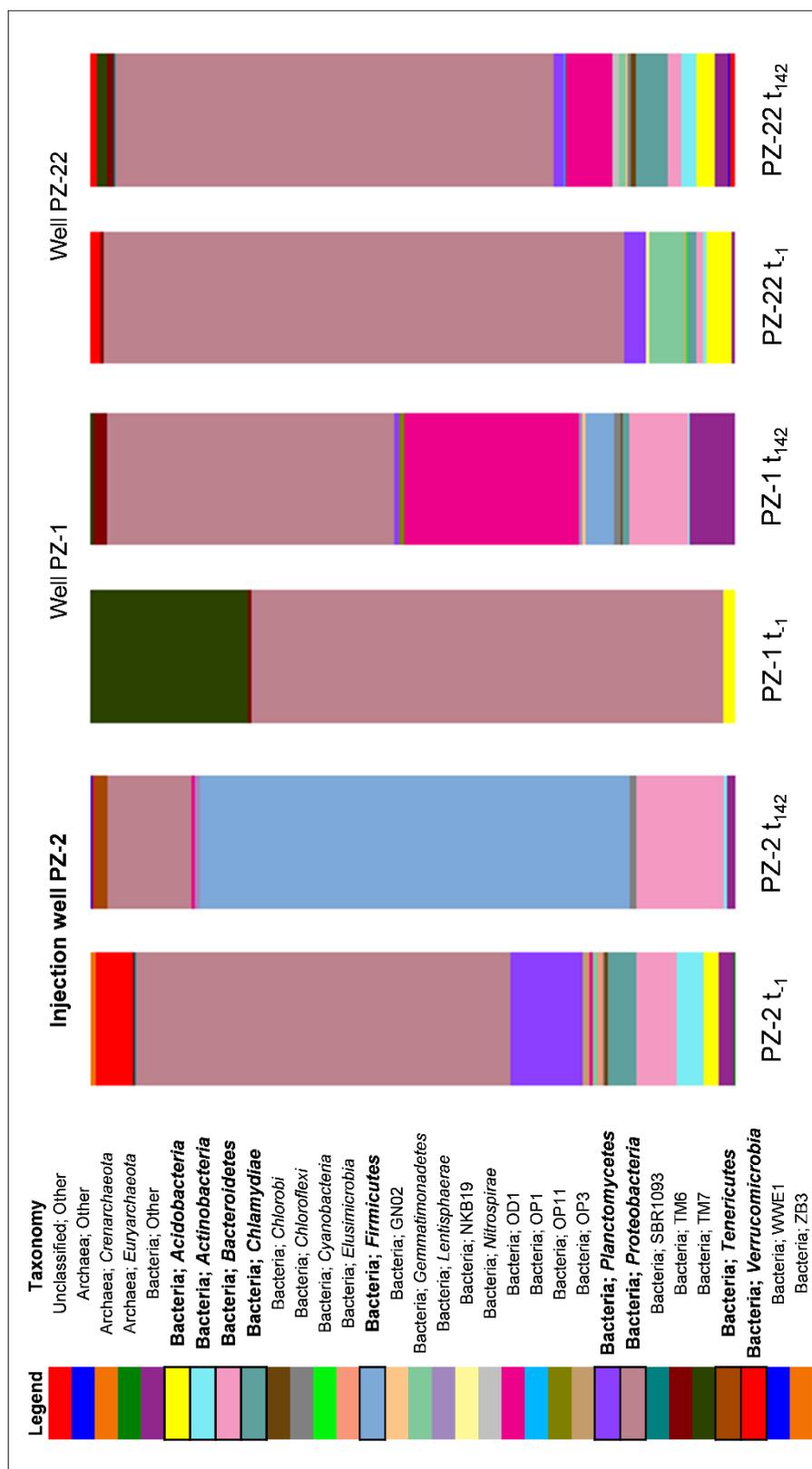
Figure 5.14. 16S rRNA high-throughput sequencing results at the phylum level for wells PZ-2, PZ-1, and PZ-22 before lactate injection (t-1) and after injection (t142). Detailed abundance (in %) is presented in Table 5.2. Phyla in bold are the most abundant in PZ-2 (either at t-1 or t142).

These observed discrepancies are due to the different conditions in which the microbial populations were subjected to. In broad terms, in the case of the laboratory microcosms, cultures were enriched with PCE, TCE and *cis*-DCE, hence, the OHRB population (including *Geobacter* sp. and *Dehalococcoides* sp.) was promoted because they can use CEs as electron acceptors. Additionally, the medium was specially designed for the growth of OHRB and, thus, was anoxic from the beginning and did not require the presence of other bacteria (e.g. fermentative) to promote a decrease in Eh. In contrast, in the aquifer, the decrease of Eh was a requirement for OHRB to grow and, thus, other bacteria were needed to condition the ecosystem. Another relevant aspect that differed between the laboratory and the field results was the presence of the *Chloroflexi* phylum. In the field samples, *Chloroflexi* were barely detected due to their low natural abundance, compared to the total number of microorganisms present in aquifers. By comparison, and after several extinction series in the laboratory, *Chloroflexi* accounted for ~ 5% of the microbial community.

5.3.6. Isotopic evaluation of the full-scale ERD with lactate

After the *in-situ* ERD pilot test, which finished in June 2017, a full-scale ERD with Lactate-2 was implemented by Litoclean, S.L. on August 2017. After one year of full-scale treatment (from August 2017 to September 2018), an isotopic mass balance of CEs ($\delta^{13}C_{sum}$) was calculated for 6 selected monitoring wells (PZ-3, PZ-5, PZ-22, MW-3, MW-6, MW-7, Figure 5.1) to evaluate the extent and success of the full-scale ERD.

Results revealed that PCE, which originally was the main pollutant at the site, and TCE were completely depleted in 5 out of the 6 monitoring wells and VC and ETH were the major end products, with *cis*-DCE still detected in some wells (Table 5.3). Originally, $\delta^{13}C_{sum}$ at the site was, in average, of -30 ± 2‰, which responded to the original $\delta^{13}C$ composition of PCE (see Chapter 4).

Table 5.3. Molar concentrations (in μM) and δ¹³C (in ‰) of the target contaminants and isotopic mass balances (δ¹³C$_{sum}$) in September 2018, after one year of full-scale ERD with lactate at the site. Results obtained can be compared with the results obtained in the field characterizations that were carried out before any biostimulation treatment (either in May 2016 from Chapter 4, or t$_{-1}$ from this chapter).

Well	Campaign	PCE (μM)	TCE (μM)	*cis*-DCE (μM)	VC (μM)	ETH (μM)
PZ-3	t$_{-1}$	10.4 ± 0.5	3.6 ± 0.1	10.5 ± 0.4	< 0.3	< 0.2
	Sept. 2018	< 0.2	< 0.2	0.6 ± 0.1	< 0.3	0.2 ± 0.1
PZ-5	May 2016	77.1	2.6	1.9	< 0.3	< 0.2
	Sept. 2018	< 0.2	< 0.2	3.1 ± 0.1	10.6 ± 0.8	34 ± 3
PZ-22	t$_{-1}$	16 ± 2	0.42 ± 0.01	0.8 ± 0.2	< 0.3	< 0.2
	Sept. 2018	< 0.2	< 0.2	4.7 ± 0.1	0.7 ± 0.1	1.02 ± 0.01
MW-3	May 2016	29 ± 5	0.49 ± 0.07	0.56 ± 0.01	< 0.3	< 0.2
	Sept. 2018	< 0.2	< 0.2	0.6 ± 0.1	29 ± 1	24.8 ± 0.3
MW-6	t$_{-1}$	52 ± 5	9.4 ± 0.8	4.5 ± 0.4	< 0.3	< 0.2
	Sept. 2018	< 0.2	< 0.2	< 0.3	< 0.3	0.9 ± 0.1
MW-7	May 2016	61 ± 14	0.6 ± 0.1	0.56 ± 0.01	< 0.3	< 0.2
	Sept. 2018	1.7 ± 0.1	0.8 ± 0.1	15.9 ± 0.3	56 ± 3	17 ± 2

Well	Campaign	PCE δ¹³C (‰)	TCE δ¹³C (‰)	*cis*-DCE δ¹³C (‰)	VC δ¹³C (‰)	δ¹³C$_{sum}$ (‰)
PZ-3	t$_{-1}$	-31.7 ± 0.5	-29.1 ± 0.5	-29.7 ± 0.5	n.d.	-30 ± 1
	Sept. 2018	n.d.	n.d.	-16.7 ± 0.4	n.d.	-16.7 ± 0.4
PZ-5	May 2016	-29.8 ± 0.4	-29.7 ± 0.5	-33.0 ± 0.7	n.d.	-29.8 ± 0.4
	Sept. 2018	n.d.	n.d.	-14.3 ± 0.4	-23.5 ± 0.6	-21 ± 2
PZ-22	t$_{-1}$	-32.9 ± 0.5	-26.3 ± 0.6	-22.5 ± 0.3	n.d.	-32 ± 5
	Sept. 2018	n.d.	n.d.	-23.2 ± 0.5	n.d.	-23.2 ± 0.5
MW-3	May 2016	-31.0 ± 0.7	n.d.	n.d.	n.d.	-31.0 ± 0.7
	Sept. 2018	n.d.	n.d.	-10.4 ± 0.6	-12.8 ± 0.3	-13 ± 1
MW-6	t$_{-1}$	-31.2 ± 0.4	-34.5 ± 0.6	-32.1 ± 0.5	n.d.	-32 ± 3
	Sept. 2018	n.d.	n.d.	n.d.	n.d.	n.a.
MW-7	May 2016	-26.4 ± 0.6	n.d.	n.d.	n.d.	-26.4 ± 0.6
	Sept. 2018	-27.1 ± 0.4	-25.1 ± 0.4	-23.0 ± 0.6	-25.2 ± 0.6	-25 ± 2

May 2016 campaign: results from the field site characterization reported in Chapter 4 of this thesis. n.d.: not detected due to concentrations being below the limit of quantification.
n.a.: not applicable.

After one year of full-scale ERD, and with the sequential reductive dechlorination of CEs still ongoing, calculated $\delta^{13}C_{sum}$ in those 5 wells were enriched in ^{13}C (ranging from -23.2 ± 0.5‰ to -13 ± 1‰) with respect to the initial value (Table 5.3). This trend in $\delta^{13}C_{sum}$ of becoming more positive was also observed in well PZ-2 during the *in-situ* pilot test and responds to ETH production.

In the case of well MW-7, the calculated $\delta^{13}C_{sum}$ remained constant and was different from the rest of the wells, a phenomenon that had been already observed in the characterization campaign carried out in May 2016 and described in Chapter 4 of this thesis. Notwithstanding, biodegradation until VC was also observed after one year of full-scale ERD, as PCE concentrations had largely decreased in the well, and *cis*-DCE, VC and ETH could be detected (Table 5.3). Therefore, these results obtained from monitoring wells located all over the site confirmed that the reductive dechlorination of CEs to ETH was occurring across the site, albeit at different extents in each well.

5.4. Conclusions

In this chapter, a multidisciplinary methodology to monitor biodegradation of CEs at the field scale was validated, as it was able to evidence that full reductive dechlorination of PCE to ETH was achieved at the injection well within 190 days. Furthermore, it was also observed that the reaction followed a different pace in the surrounding monitoring wells, thus, the hydrodynamic characteristics of the aquifer possibly dominated the distribution of electron donor, affecting the outcome of the biodegradation reaction in the studied surrounding wells.

Such an integrative approach was useful, as well, to characterize the changes that were induced by the electron donor injection in the hydrochemistry of

groundwater and in the microbial population. This was achieved through the analysis of major anions and cations, Eh, pH, S–O stable isotopes from dissolved sulphate, and 16S rRNA metagenomics. As an electron donor, lactate enhanced the achievement of sulphate-reducing conditions, with the consequent decrease in Eh and occurrence of the dechlorination reactions past *cis*-DCE. On the contrary, when lactate became limited, the aquifer could not be properly conditioned and a *cis*-DCE stall was observed. The availability of lactate was also observed in the microbial community evolution, as fermentative bacteria barely increased in the monitoring wells with electron donor limitation, compared to the injection well PZ-2.

Finally, the initial isotopic characterization of the site (Chapter 4) allowed for applying isotope-mass balance calculations to unequivocally demonstrate ETH generation after the full-scale ERD via lactate injection. This stable isotope-based technique can overcome the difficulties related to the traditional mass balance approaches which are often hindered by natural processes (e.g. dilution, sorption, volatilization).

In all, the methodology proposed here can be easily integrated as a tool in the monitoring and the success evaluation of *in-situ* bioremediation applications. Moreover, it can reduce the uncertainties regarding the ongoing processes that are occurring in groundwater ecosystems.

Chapter 6

Sites 2 and 3

Assessment of the biodegradation potential at two complex multi-contaminated sites via an isotopic and molecular approach

List of contents

This chapter was published as:

"Use of dual element isotope analysis and microcosm studies to determine the origin and potential anaerobic biodegradation of dichloromethane in two multi-contaminated aquifers"

in the journal **Science of the Total Environment**.

Abstract

In this chapter, a multi-method approach was used to provide lines of evidence of natural attenuation processes and potential setbacks in the implementation of bioremediation strategies in complex multi-contaminated aquifers. First, this study determined i) the carbon and chlorine isotopic compositions (δ^{13}C, δ^{37}Cl) of several commercial pure phase chlorinated compounds, and ii) the chlorine isotope fractionation (ε^{13}Cl = -5.2 ± 0.6‰) and the dual C–Cl isotope correlation ($\Lambda^{C/Cl}$ = 5.9 ± 0.3) during dichloromethane (DCM) degradation by a *Dehalobacterium*-containing culture. Such data provide valuable information for practitioners to support the interpretation of stable isotope analyses derived from polluted sites. Second, the bioremediation potential of two industrial sites contaminated with a mixture of organic pollutants (mainly DCM, chloroform (CF), trichloroethene (TCE), and monochlorobenzene (MCB)) was evaluated. Hydrochemistry, dual carbon and chlorine (C–Cl) isotope analyses, laboratory microcosms, and microbiological data were used to investigate the origin and fate of chlorinated methanes (CMs) and the feasibility of bioremediation strategies. At Site 2, δ^{13}C and δ^{37}Cl compositions from field samples were consistent with laboratory microcosms, which showed complete degradation of CF, DCM and TCE, while MCB remained. Identification of *Dehalobacter* sp. in CF-enriched microcosms further supported the biodegradation capability of the aquifer to remediate CMs. At Site 3, hydrochemistry and δ^{13}C and δ^{37}Cl compositions from field samples suggested little DCM, CF and TCE transformation; however, laboratory microcosms evidenced that their degradation was severely inhibited, probably by co-contamination. A dual C–Cl isotopic assessment using results from this study and reference values from the literature allowed to determine the extent of degradation and elucidated the origin of CMs.

6.1. Introduction

In Chapter 4 of this thesis, a site that was only polluted with chlorinated ethenes (CEs) was investigated for a potential bioremediation application. The positive results that were obtained motivated the full-scale treatment through a biological enhanced reductive dechlorination (ERD) with lactate that was described in Chapter 5.

However, many aquifers around the world are impacted not only by one family of contaminants but by several of them, forming complex mixtures that become very difficult to remediate. For this reason, it is common to find aquifers where CEs co-occur with chlorinated methanes and benzenes, other halogenated substances, BTEX (benzene, toluene, ethylbenzene and xylene), fuel oxygenates such as methyl tert-butyl ether (MTBE) and ethyl tert-butyl ether (ETBE), and total petroleum hydrocarbons (TPH), among others.

In this chapter, two sites that were polluted by multiple substances widely used in the industry were investigated for their bioremediation potential. Given the scope of this thesis on toxic substances and chlorinated solvents, only CEs, which were previously discussed in Chapters 4 and 5, the CMs DCM and CF, and MCB (in a lesser extent) were the target contaminants of this chapter.

DCM can be naturally released by oceanic sources, wetlands, volcanoes and macroalgae (Gribble, 2010), but its detection in groundwater is often a result of its extensive use in chemical, pharmaceutical, and petroleum industrial facilities, among others (Marshall and Pottenger, 2016). Numerous bacteria capable of using DCM as a growth substrate under aerobic conditions have been identified, including various strains of *Hyphomicrobium* (Heraty et al., 1999; Hermon et al., 2018; Nikolausz et al., 2006) and *Methylobacterium* (Torgonskaya et al., 2019). The aerobic pathway for DCM biodegradation begins with a glutathione S-transferase

producing formaldehyde, which is partially oxidized to CO_2 and chloride (Muller et al., 2011).

To date, anaerobic biodegradation of DCM has been solely reported for bacteria affiliated with the *Peptococcaceae* family: *Dehalobacterium* (*Dhb*), *Dehalobacter*, and *Candidatus* Dichloromethanomonas elyunquensis (D. elyunquensis). *Dehalobacterium formicoaceticum* (*Dhb f.*) is the only pure culture described using DCM as carbon and energy source under anoxic conditions, and produces formate and acetate as end products (Mägli et al., 1998). Recently, mixed bacterial cultures containing *Dehalobacter* sp. and/or D. elyunquensis have been reported to ferment DCM to mainly acetate (Chen et al., 2017; Justicia-Leon et al., 2012; Kleindienst et al., 2017; Lee et al., 2015, 2012).

Besides direct release into groundwater, DCM can also be produced by dehalogenation of the higher CMs, i.e. carbon tetrachloride (CT) or CF. Under anoxic conditions, DCM might derive from the hydrogenolysis of CF by the organohalide-respiring bacteria (OHRB) *Dehalobacter* sp. and *Desulfitobacterium* sp. (Chan et al., 2012; Ding et al., 2014; Tang and Edwards, 2013; Wong et al., 2016). Also, the anaerobic degradation of CF by *Acetobacterium* sp. comprises both a reductive branch leading to DCM, and an oxidative pathway leading to CO_2 (Egli et al., 1990, 1988; Wanner et al., 2018). Lastly, DCM can also be produced co-metabolically by, for example, *Methanosarcina* sp. or *Clostridium* sp. (Egli et al., 1988; Gälli and McCarty, 1989; Krone et al., 1989b, 1989a; Mikesell and Boyd, 1990).

As previously mentioned, chlorinated solvents are commonly found in groundwater from contaminated sites within complex mixtures rather than as individual chemicals. In those scenarios, microbial degradation can be affected and even inhibited by co-contaminants. This information is relevant to foresee the efficiency of natural attenuation or enhanced bioremediation strategies. For

instance, the inhibitory effects of CF on key microbial processes such as methanogenesis and microbial dechlorination reactions of CEs and chlorinated ethanes are well known (Weathers and Parkin, 2000; Wei et al., 2016). In addition, it has also been reported that CT and CF inhibit their mutual biodegradation (da Lima and Sleep, 2010; Grostern et al., 2010; Justicia-Leon et al., 2014).

Compound-specific stable isotope analysis (CSIA) is a useful tool that allows bioremediation practitioners to assess the effectiveness of remediation treatments. This technique may be used for source apportionment as well as the monitoring of transformation processes in the field (Elsner, 2010). In addition, a quantitative estimation of contaminant transformation extent in the field can be possible, provided that the isotope fractionation (ε) for a given compound and degradation pathway are known and well constrained (Aelion et al., 2009).

Dual element isotope analysis has some advantages over a single element isotope approach. On the one hand, by improving the identification of the source (either related to commercial solvents release or from parent compound degradation); on the other, by allowing the elucidation of the fate of pollutants in the field. During biodegradation processes, single element intrinsic isotope effects related to C–Cl bond cleavage can be masked due to the occurrence of previous rate-limiting steps such as preceding enzymatic reactions (Sherwood Lollar et al., 2010), bioavailability of electron donor and/or acceptor (Aeppli et al., 2009; Kampara et al., 2008; Thullner et al., 2008), substrate uptake and transport through the cell membrane (Cichocka et al., 2007; Renpenning et al., 2015), among others. During these processes both elements (e.g. C and Cl) are affected similarly, hence, by taking the ratio of the isotope shift for the two elements (e.g. $\Lambda = \Delta\delta^{13}C / \Delta\delta^{37}Cl$), their masking effect is cancelled out and these slopes reflect better the ongoing degradation mechanisms (Elsner, 2010). While single element isotope fractionation could provide insight into the

underlying reaction mechanisms in laboratory biodegradation experiments, this is not possible under field conditions. The reason is that contaminant concentration changes at the field are also related to processes other than its transformation (such as sorption and hydrodynamic dispersion), preventing accurate calculation of ε values (Eq. 2, section 3.2.7). Thus, Λ values determined from laboratory studied reactions can be compared with those obtained from groundwater samples to investigate degradation processes at the field scale (Badin et al., 2014; Hermon et al., 2018; Hunkeler et al., 2009; Palau et al., 2017; Rodríguez-Fernández et al., 2018b).

Several laboratory studies have applied dual C–Cl isotope analysis to describe biotic and abiotic transformation mechanisms for DCM (Chen et al., 2018; Heraty et al., 1999; Torgonskaya et al., 2019) and CF (Heckel et al., 2017a, 2019; Rodríguez-Fernández et al., 2018a; Torrentó et al., 2017) but, to the best of the author's knowledge, the application of a dual isotope approach in DCM-contaminated sites has not been reported yet.

The purpose of the work presented in this chapter is two-fold. First, it aims to determine i) the $\Lambda^{C/Cl}$ value for the anaerobic degradation of DCM by a *Dehalobacterium*-containing culture, and ii) the carbon and chlorine isotopic compositions ($\delta^{13}C$, $\delta^{37}Cl$) of several commercial pure phase DCM and CF. These new isotope data enrich the database to which dual C–Cl isotopes slopes measured in the field can be compared to elucidate degradation mechanisms. Second, a multi-method approach was used at two industrial sites impacted with DCM, CF, TCE and MCB to investigate their origin, fate and intrinsic biodegradation potential. To this end, hydrochemical conditions in groundwater, concentrations of target contaminants and their stable isotope ratios ($\delta^{13}C$, $\delta^{37}Cl$) in field samples were analysed. Afterwards, a dual C–Cl isotopic assessment using the results from this study and reference values from the literature was performed

to reveal the origin and fate of DCM and CF. Lastly, field-derived microcosms testing for biostimulation as well as bioaugmentation, and 16S rRNA high-throughput sequencing were performed to assess the intrinsic biodegradation potential of the target contaminants at the sites.

6.2. Materials and methods

6.2.1. Materials

Pure chlorinated compounds isotopically characterized and other chemicals used in this chapter are listed in Table 3.1. CF (Sigma Aldrich) was used for the enrichment of field-derived cultures.

Samples of the time-course degradation of DCM in a *Dhb*-containing culture were obtained from a study reported elsewhere (Trueba-Santiso et al., 2017).

Two different commercial bacterial consortia were used for the microcosm bioaugmentation tests. Detailed information about the products cannot be disclosed due to commercial confidentiality reasons. Commercial inoculum "S" was reported to degrade CF to DCM, and fully dechlorinated CEs to ethene (ETH). Commercial inoculum "M" was reported to degrade CF to methane via DCM and chloromethane.

6.2.2. Hydrogeochemistry of the studied sites

The sites are located in the Catalan Coastal Ranges, which are characterized by an echelon fault system, subparallel to the coast, that affected the Hercynian basement and the Mesozoic overlying sediments. The Neogene extension created a "horst and graben" system filled by Miocene and Quaternary sediments. Both sites are located in the Neogene basin, one of them in the Miocene sediments, and the other in the granitic basement.
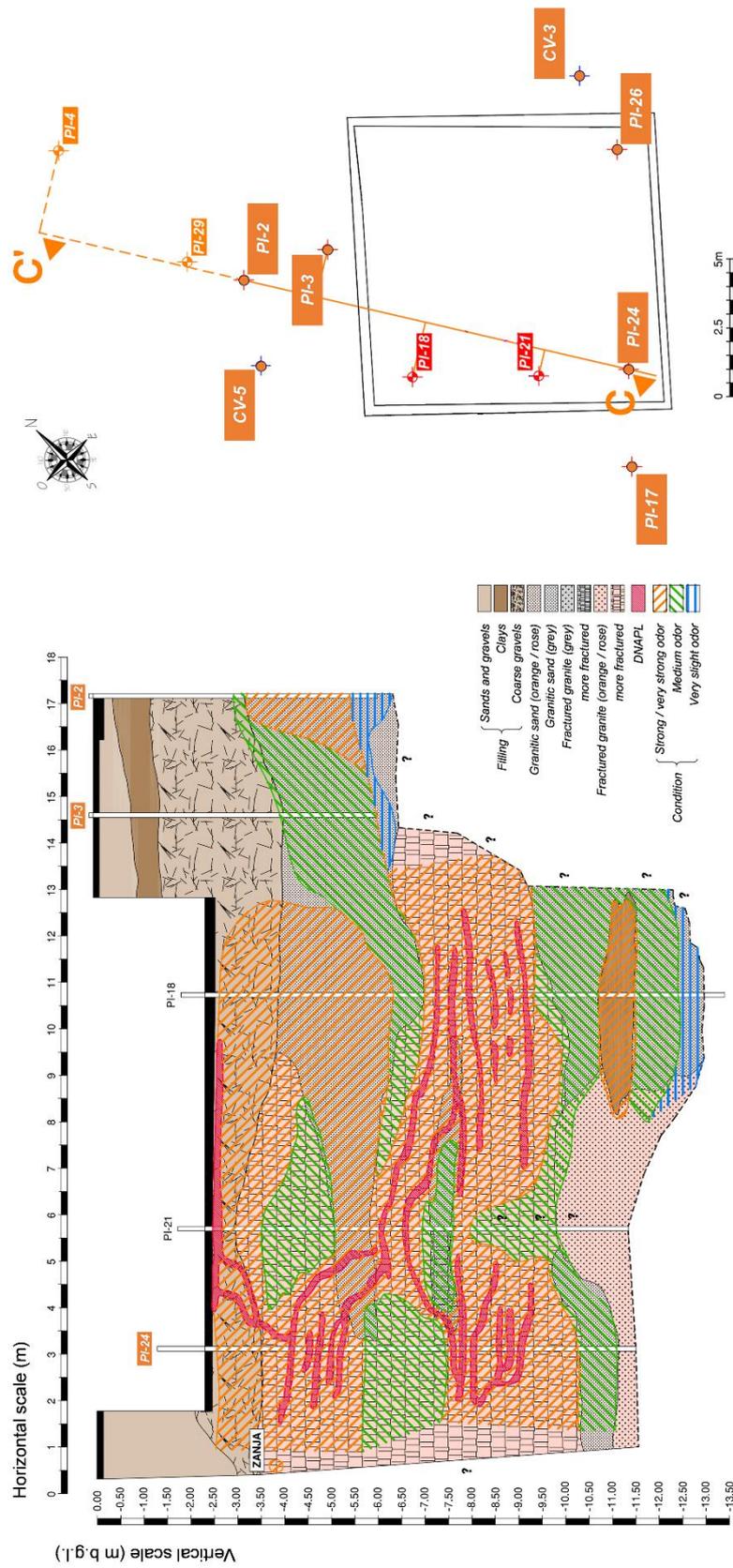
Figure 6.1. Schematic geological cross section of Site 2 along transect C-C'.
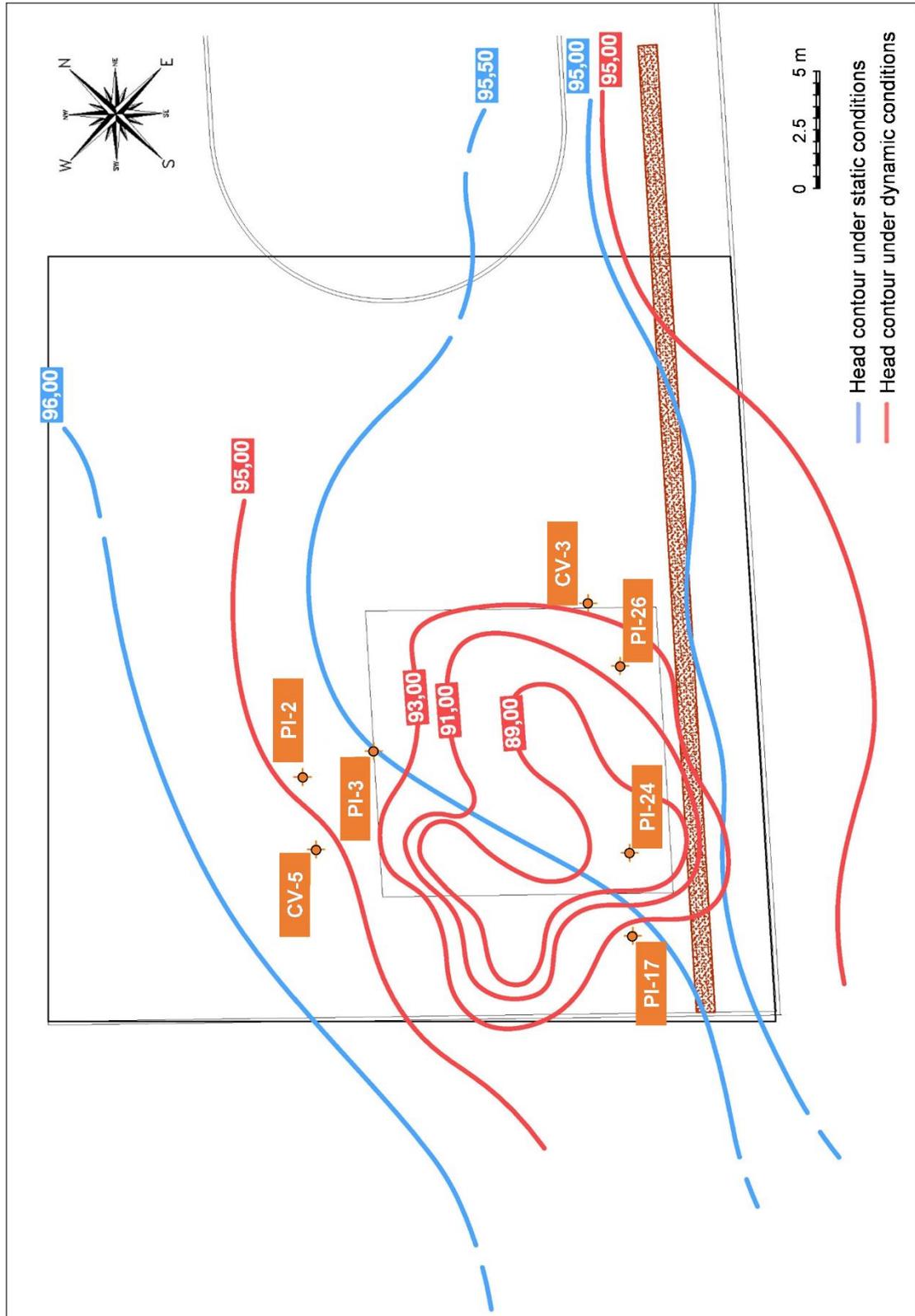
Figure 6.2. Site 2 head contour and location of boreholes / monitoring wells. Lines refer to the water table (in m.a.s.l.) at natural / static conditions (blue) and under active remediation system / dynamic conditions (red).

Site 2

The studied site is located at an industrial area in the Barcelona province (Spain). Geologically, it is constituted by clays and conglomerates of quaternary age overlying unconformable upper Miocene siliciclastic sediments that dip 15–20° in the NW direction. Petrologically, the Miocene sediments are represented by clay and sands composed of abundant quartz grains, mica and kaolinized feldspars and, locally, by some conglomerates. Hydrogeologically, the Miocene aquifer has an average transmissivity of 5–180 m^2/d, less than the alluvial aquifer. A geological cross section of the studied area can be found in Figure 6.1.

A previous characterization of the site detected high loads of contaminants and dense nonaqueous phase liquid (DNAPL) in groundwater, which was originated after improper storage of the substances (Figure 6.1). The main organic halogenated compounds included DCM, CF, TCE, and MCB, but *cis*-dichloroethene (*cis*-DCE), vinyl chloride (VC), tetrachloroethene (PCE), acetone, BTEX, and tetrahydrofuran were also detected. The contamination plume was considered finite and contained. After the initial site characterization, a pump and treat (P&T) remediation system (groundwater extraction) was implemented. Under this ongoing treatment, groundwater flowed radially towards the extraction points and a total of seven conventional fully screened monitoring wells were sampled for this study (Figure 6.2).

Site 3

This site is also located at an industrial zone in the Barcelona province (Spain), but more than 30 km apart from Site 2. Geologically, it is constituted by Quaternary alluvial sediments represented by sands and gravels that overlie unconformably the basement of the Neogen basin made by later-Hercynian

intrusive granites. Hydrogeologically, groundwater flows mainly from the alluvial gravels to the river freshwater and, to a lesser extent, through the more fractured and weathered granite. A conceptual site model of the studied area can be found in Figure 6.3.

Like in Site 2, it was previously confirmed that the contamination plume in Site 3, originated due to improper management, contained DNAPL (Figure 6.3). The most abundant contaminants in groundwater included DCM, CF, TCE, and MCB, but acetone, toluene, PCE, CT, VC, tetrahydrofuran and benzene were also detected in groundwater. After the initial site characterization, dual-phase extraction (DPE) and P&T remediation systems were implemented and ongoing during this study. For the hydrochemical characterization carried out in the present work, nine conventional fully screened monitoring wells were sampled (Figure 6.4). At that time, the groundwater flow direction was E–W, and radially towards the extraction points due to DPE and P&T, and the contamination source was reported to be still active (Figure 6.4).

6.2.3. Collection of groundwater samples

Hydrochemical parameters (redox potential (Eh), pH, temperature (T) and electric conductivity (EC)) were measured *in-situ* and groundwater samples from selected monitoring wells (Figures 6.2 and 6.4) were collected as described in section 3.2.1. Samples for chemical and isotopic analysis were collected in different sampling containers on July 11th and 12th, 2017, from Site 2 and Site 3, respectively. Samples for C–Cl CSIA were preserved with HNO_3 (pH~2) (Badin et al., 2016) to prevent biodegradation processes. For the establishment of microcosms, groundwater with fine sediments from wells PZ-9, PZ-19 and PZ-36 from Site 3 (Figure 6.4), and well PI-2 from Site 2 (Figure 6.2), was sampled on the 18th and 19th of June 2018, respectively.
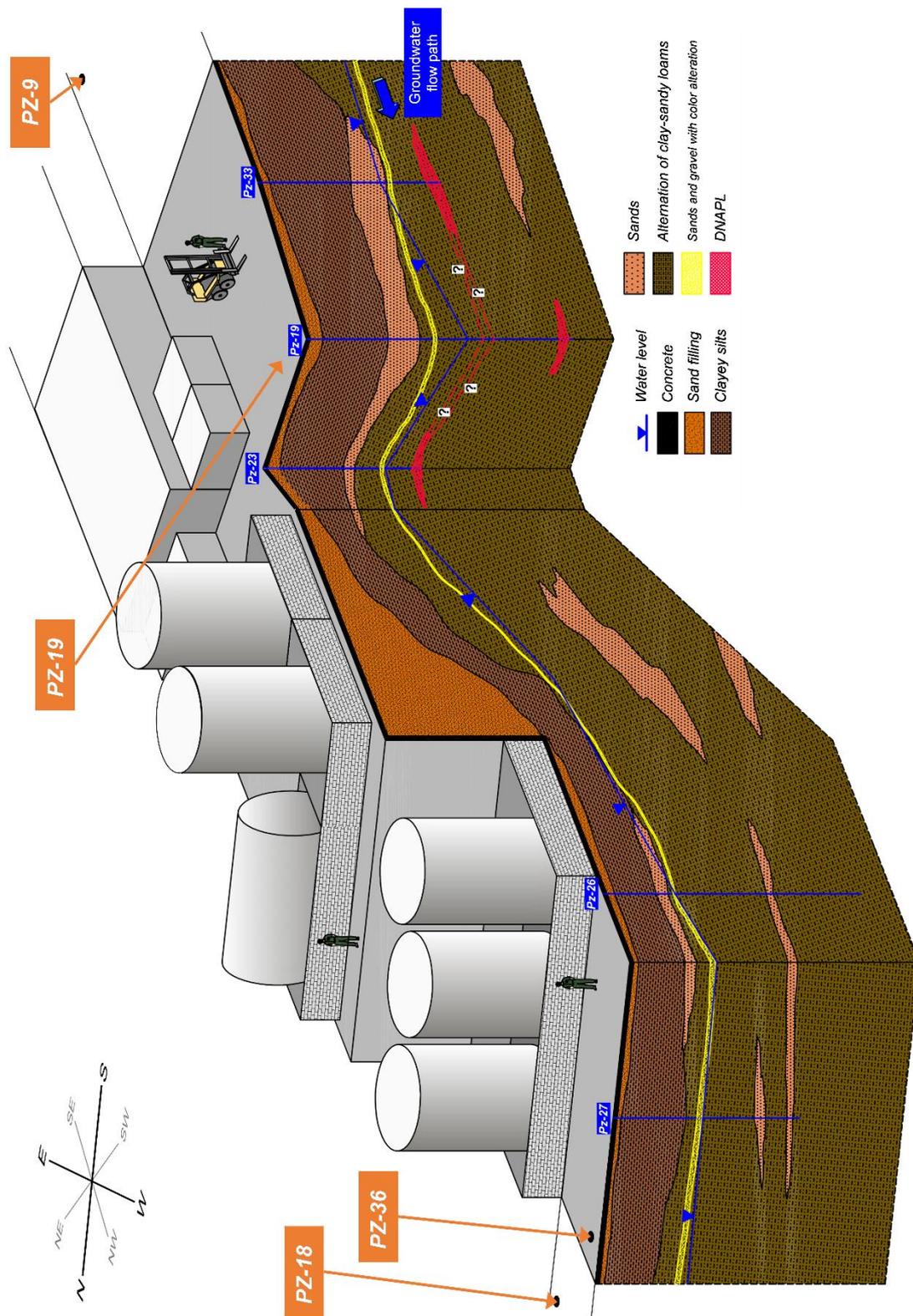
Figure 6.3. Conceptual site model of Site 3.
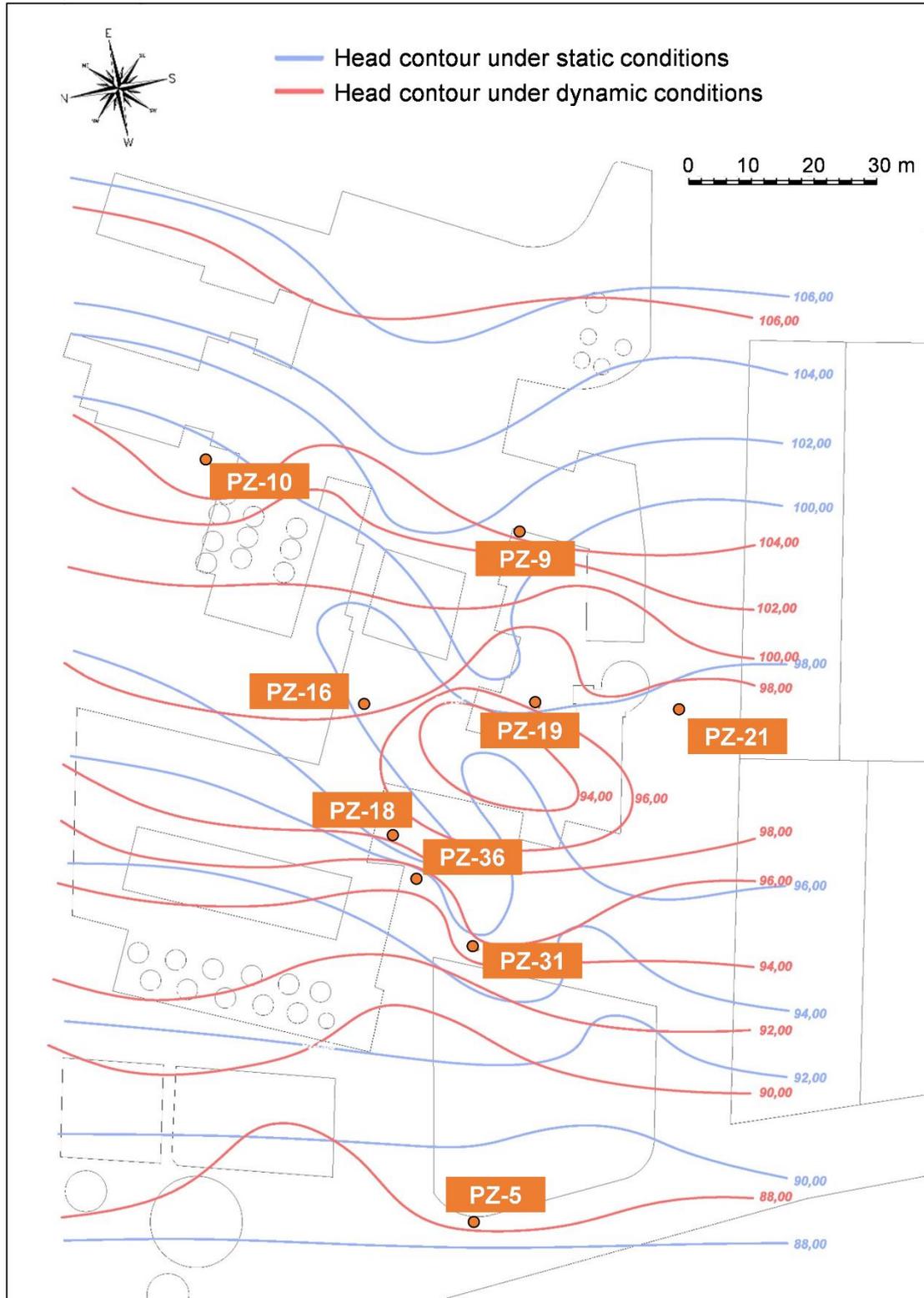
Figure 6.4. Site 3 head contour and location of boreholes / monitoring wells. Lines refer to the water table (in m.a.s.l.) at natural / static conditions (blue) and under active remediation system / dynamic conditions (red).

6.2.4. Establishment of laboratory microcosms

The microcosms were prepared within the following two days after sampling, as described in section 3.2.2.

To investigate whether a potential bioremediation treatment would be feasible at the investigated sites, three different experiments were prepared in triplicate: (i) a control containing only groundwater from the site, which tested for monitored natural attenuation (MNA); (ii) groundwater with Lactate-2 (~4 mM), which tested for biostimulation; and (iii) groundwater inoculated with the commercial bacterial consortia described in section 6.2.1 at a concentration of 10^6–10^7 cells/mL, approximately, plus Lactate-2 (~4 mM), which tested for bioaugmentation.

For the samples from wells PZ-19 and PZ-36 (Site 3, Figure 6.4), two different bioaugmentation tests were established, i.e. one with each commercial inoculum, whereas only one bioaugmentation test (using the commercial inoculum "S") was performed with samples from wells PZ-9 (Site 3, Figure 6.4) and PI-2 (Site 2, Figure 6.2).

To identify the bacteria responsible for CF degradation, specific active field-derived microcosms that showed CF dechlorinating activity were selected for cultivation to maintain the degrading microbial population. Enrichment of the degrading culture was performed with the dilution-to-extinction method, described in section 3.2.3, and using CF as electron acceptor.

After four extinction series, the more diluted vial showing activity against CF was used as inoculum for serum bottle microcosms, which were selected for 16S rRNA analysis after consuming 1 mM CF. The serum bottle microcosms were prepared as described in section 3.2.3.

6.2.5. DNA extraction and 16S rRNA gene amplicon sequencing

Biomass was harvested from active whole serum bottle microcosms in sterile falcon tubes that were centrifuged for 40 min at 7000 *g* and 10 ºC in an Avanti J-20 centrifuge. The pellets were resuspended in sterile PBS buffer and, afterwards, DNA was extracted with the Gentra Puregene Yeast/Bact kit (Qiagen) following the instructions of the manufacturer. Extraction and analysis of the DNA of each microcosm was performed separately. The regions V3–V4 of the 16S rRNA genes were amplified with primers S-D-Bact-0341-b-S-17 and S-D-Bact-0785-a-A-21 (Klindworth et al., 2013) with the Illumina MiSeq platform at *Serveis de Genòmica i Bioinformàtica* from *Universitat Autònoma de Barcelona*.

6.2.6. Analytical methods

Hydrogeochemical field parameters of groundwater were determined as described in section 3.2.1. Concentrations of volatile organic compounds (VOCs) and volatile fatty acids (VFAs) were analysed as described in sections 3.2.4 and 3.2.6, respectively. Stable C and Cl isotope ratios ($\delta^{13}C$ and $\delta^{37}Cl$) of pure in-house standards and target chlorinated compounds were obtained as described in section 3.2.7. $\varepsilon^{37}Cl$ and $\Lambda^{C/Cl}$ for the degradation of DCM by the stable enrichment culture containing *Dhb* was obtained from the slope of the linear regression according to Eq. 2 and the slope in the dual C–Cl isotope plot, respectively, as described in section 3.2.7. Lastly, the extent of degradation (D%) in the field was evaluated with Eq. 3 (section 3.2.7).

6.2.7. Dual C–Cl isotopic assessment based on selected $\Lambda^{C/Cl}$

A dual C–Cl isotopic assessment (Badin et al., 2016; Hunkeler et al., 2008) was performed to investigate the potential origin and fate of DCM and CF at each site, based on $\delta^{13}C$ and $\delta^{37}Cl$ data of field and commercial compounds, the

definition of D% (Eq. 3, section 3.2.7), and $\varepsilon^{13}C$, $\varepsilon^{37}Cl$ and $\Lambda^{C/Cl}$ from the literature (Tables 6.1 and 6.2). As shown in Figure 6.5C, the expected C and Cl isotopic compositions of CF and DCM (coloured areas) were estimated for the considered reactions with D% values ranging from 35 to 98%.

The procedure followed to determine the expected isotopic compositions in the dual isotope plot is explained step by step below.

For CF:

- *Initial isotopic signature (CF$_0$)*: the $\delta^{13}C$ and $\delta^{37}Cl$ signature of the original CF at each site was defined considering the most negative $\delta^{13}C_{CF}$ and $\delta^{37}Cl_{CF}$ values measured in groundwater samples (see "original CF" black triangle in Figure 6.5C as an example).

- *Isotopic composition of degraded CF$_0$*: potential $\delta^{13}C$ and $\delta^{37}Cl$ values for degraded CF were determined based on CF$_0$ and the selected range of $\Lambda^{C/Cl}$ for CF degradation, from 6.6 to 17 for reductive dechlorination by *Dehalobacter* sp. and oxidation, respectively ("CF degradation" orange area in Figure 6.5C).

For DCM:

- *Initial isotopic signature (DCM$_0$)*: the commercial DCM that could have been spilled at the site is depicted as "original DCM" (black dot) in Figure 6.5C.

- *Isotopic composition of degraded DCM$_0$*: following the same methodology than for CF, the potential C and Cl isotopic compositions of commercial DCM being affected by aerobic and anaerobic biodegradation were calculated (see "Commercial DCM aerobic deg." dark green dashed area and "Comm. DCM anaerobic deg." light green shaded area in Figure 6.5C for details). In this case, the whole isotopic range of commercial DCM was considered.
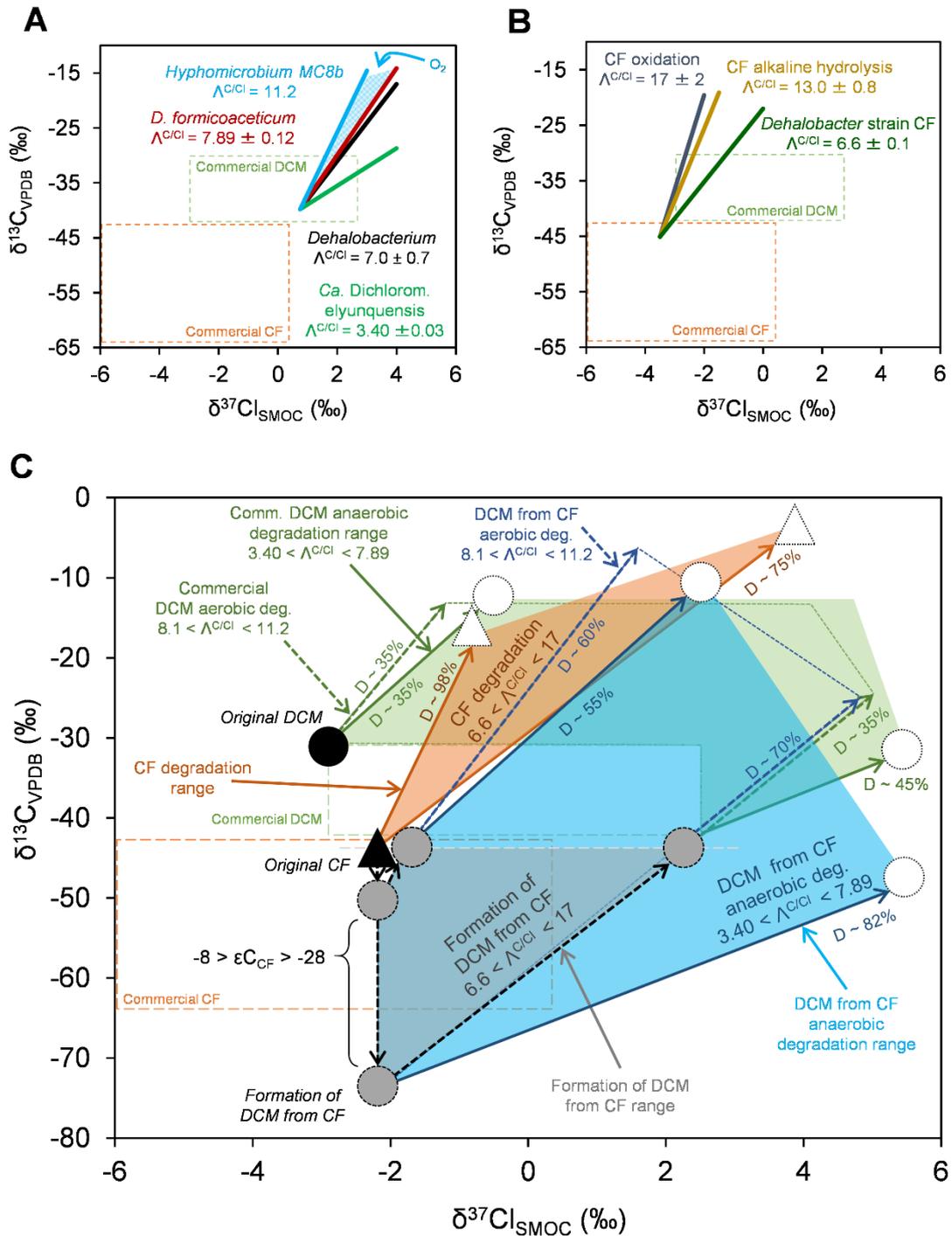
Figure 6.5. (A) Selection of $\Lambda^{C/Cl}$ reported for DCM aerobic and anaerobic degradation mechanisms (Table 6.2). (B) Selection of $\Lambda^{C/Cl}$ reported for several biotic and abiotic CF degradation processes (Table 6.2). (C) Example of the dual C–Cl isotopic assessment for CF and DCM degradation based on an assumed isotopic composition of CF (CF$_0$) and reported isotopic values (Tables 6.1 and 6.2). The green and orange rectangles in all panels represent the $\delta^{13}C$ and $\delta^{37}Cl$ ranges for commercial DCM and CF solvents, respectively (Table 6.1).

- *Isotopic composition of DCM produced by CF degradation (not further transformed)*:
  based on the isotope signature of CF_0 and the $\varepsilon^{13}C_{CF}$ range for CF oxidation
  and biodegradation reactions, from -8 to -28‰, the spectrum of initial $\delta^{13}C$
  values of DCM produced by CF degradation (DCM_{ini}) was estimated as
  $\delta^{13}C_{DCM,ini} = \delta^{13}C_{CF,0} + \varepsilon^{13}C_{CF}$. For chlorine, secondary isotope effects were
  neglected and, therefore, there is no isotopic discrimination between the
  instantaneously formed DCM and the CF from which it is formed (Elsner
  and Hunkeler, 2008). This means that the $\delta^{37}Cl_{DCM,ini}$ is the same as that of
  original CF (i.e. $\delta^{37}Cl_{CF,0} = \delta^{37}Cl_{DCM,ini}$). Secondary isotope effects are
  typically small compared to primary isotope effects. For CF, a bulk
  secondary Cl isotopic fractionation value as low as -0.44 $\pm$ 0.06‰ was
  measured during degradation via C–H bond oxidation (Torrentó et al.,
  2017). However, relatively high secondary chlorine isotope effects may also
  occur (e.g. Chen et al. (2018), Swiderek et al. (2012), Palau et al. (2014b)).
  For instance, a bulk secondary Cl isotopic fractionation value
  of -3.8 $\pm$ 0.2‰ was measured during anaerobic degradation of 1,2-DCA
  (C–H bond oxidation) by *Pseudomonas* sp. strain DCA1 (Palau et al., 2014a).
  Then, the approximate isotopic composition area for produced DCM from
  CF degradation ("Formation of DCM from CF" grey area in Figure 6.5C)
  was determined considering the same range of $\Lambda^{C/Cl}$ for CF degradation
  reactions, having in mind that, at the completion of such reactions, the final
  $\delta^{13}C_{DCM}$ value will be the same as the original CF (i.e. $\delta^{13}C_{CF,0}$) for reasons
  of isotopic mass balance.

- *Isotopic composition of DCM produced by CF degradation (affected by further
  transformation)*: similarly to what was done for CF degradation, potential $\delta^{13}C$
  and $\delta^{37}Cl$ values for aerobic and anaerobic DCM (from CF) degradation
  were determined considering the widest $\Lambda^{C/Cl}$ spectrum for DCM
  biodegradation and the estimated DCM_{ini} range. For aerobic DCM

biodegradation, $\varLambda^{C/Cl}$ values from 8.1 to 11.2, approx., were used ("DCM from CF aerobic deg." dark blue dashed area in Figure 6.5C), whereas for the anaerobic reactions, $\varLambda^{C/Cl}$ from 3.40 to 7.89 were considered ("DCM from CF anaerobic deg." light blue area in Figure 6.5C).

Once the potential isotopic composition ranges of CF and DCM were depicted in the dual C–Cl plot (Figure 6.5C), measured isotopic field data from each site were added to evaluate whether they were consistent with DCM and CF sources and considered degradation pathways.

6.3. Results and discussion

6.3.1. $\delta^{13}C$ and $\delta^{37}Cl$ of pure in-house commercial standards

Different pure in-house DCM and CF commercial solvents were analysed to determine their $\delta^{13}C$ and $\delta^{37}Cl$ isotopic compositions (Table 6.1). The $\delta^{13}C$ values for the DCM solvents that were measured in this investigation ranged from -35.4 $\pm$ 0.2 to -41.71 $\pm$ 0.08‰, while $\delta^{37}Cl_{DCM}$ ranged from +2.1 $\pm$ 0.3 to -2.7 $\pm$ 0.1‰. Similarly, the $\delta^{13}C$ values for CF ranged from -47.96 $\pm$ 0.06 to -52.7 $\pm$ 0.1‰, while $\delta^{37}Cl_{CF}$ ranged from -2.6 $\pm$ 0.1 to -5.9 $\pm$ 0.2‰. From the obtained results, a significant variation was observed among the different DCM and CF commercial standards analysed in this chapter, but also when compared to some of the values reported in the literature (Table 6.1). For instance, the $\delta^{37}Cl_{DCM}$ value obtained for the Fisher standard (-2.7 $\pm$ 0.1‰) is more depleted in $^{37}Cl_{DCM}$ than the values available to date (Table 6.1). This emphasizes the relevance of having the reference isotopic compositions of the pure products provided in this chapter for future field data interpretation.

Likewise, $\delta^{13}C$ for TCE and MCB pure commercial solvents was also analysed and resulted in -25.40 $\pm$ 0.03‰ and -27.09 $\pm$ 0.07‰, respectively (Table 6.1).

Table 6.1. $\delta^{13}C$ and $\delta^{37}Cl$ (in ‰) of commercial pure-phase CF, DCM, TCE and MCB.

DCM	$\delta^{13}C$ (‰/VPDB)	$\delta^{37}Cl$ (‰/SMOC)	Reference
Fisher	-41.71 ± 0.08	-2.7 ± 0.1	This study
Sigma Aldrich	-	+0.75 ± 0.05	This study
SDS	-35.4 ± 0.2	+1.27 ± 0.01	This study
Merck	-39.0 ± 0.1	-	This study
unknown	-39.78 ± 0.08	-	This study
unknown	-	+1.3 ± 0.2	This study
unknown	-	+2.1 ± 0.3	This study
unknown	-31.5 ± 0.3	+2.13 ± 0.03	Jendrzejewski et al. (2001)
unknown	-31.8 ± 0.5	+2.3 ± 0.2	Jendrzejewski et al. (2001)
unknown	-34.19 ± 0.02	+1.555 ± 0.005	Holt et al. (1997)
unknown	-40.4 ± 0.5	-	Holt et al. (1997)

CF	$\delta^{13}C$ (‰/VPDB)	$\delta^{37}Cl$ (‰/SMOC)	Reference
Merck[a]	-48.93 ± 0.08	-	This study
Merck[a]	-52.7 ± 0.1	-	This study
Sigma Aldrich	-	-2.6 ± 0.1	This study
Alfa	-47.96 ± 0.06	-5.9 ± 0.2	This study
Alfa	-47.88 ± 0.08	-5.4 ± 0.3	Breider (2013)
unknown	-43.21 ± 0.04	-1.52 ± 0.01	Holt et al. (1997)
Fluka	-48.7 ± 0.1	-3.0 ± 0.2	Rodríguez-Fernández et al. (2018b), Heckel et al. (2017b)
Acros	-49.76 ± 0.08	-	Rodríguez-Fernández et al. (2018b)
unknown	-51.7 ± 0.4	+0.32 ± 0.08	Jendrzejewski et al. (2001)
Fisher	-53.23 ± 0.09	-	Rodríguez-Fernández et al. (2018b)
Sigma Aldrich	-63.6 ± 0.1	-	Breider (2013)

TCE	$\delta^{13}C$ (‰/VPDB)	$\delta^{37}Cl$ (‰/SMOC)	Reference
unknown	-25.40 ± 0.03	-	This study
unknown	-27.18 ± 0.01	-1.42 ± 0.10	Holt et al. (1997)
PPG	-27.37 ± 0.09	-2.8 ± 0.1	Shouakar-Stash et al. (2003)
unknown	-27.90 ± 0.08	+2.0 ± 0.1	Jendrzejewski et al. (2001)
StanChem	-29.1 ± 0.1	-3.19 ± 0.07	Shouakar-Stash et al. (2003)
ICI	-31.01 ± 0.09	+2.71 ± 0.08	Shouakar-Stash et al. (2003)
Dow	-31.57 ± 0.01	+3.55 ± 0.05	Shouakar-Stash et al. (2003)
Dow	-31.90 ± 0.05	+4.1 ± 0.3	van Warmerdam et al. (1995)
Sigma Aldrich	-33.49 ± 0.08	+3.8 ± 0.1	Jendrzejewski et al. (2001)

MCB	$\delta^{13}C$ (‰/VPDB)	$\delta^{37}Cl$ (‰/SMOC)	Reference
Sigma Aldrich	-27.09 ± 0.07	-	This study
Sigma Aldrich	-25.6[b]	-	Liang et al. (2011)

[a] Solvent with the same reference number but from different batches. [b] $\delta^{13}C$ (‰) value for MCB was obtained from a microcosm experiment where changes in $\delta^{13}C$ by biodegradation of MCB were measured. The initial $\delta^{13}C$ is not considered to be affected by degradation and, therefore, can be assumed as representative of the commercial MCB. VPDB: Vienna Pee Dee Belemnite, SMOC: Standard Mean Ocean Chloride.

Table 6.2. $\varepsilon^{13}C$, $\varepsilon^{37}Cl$ and $\Lambda^{C/Cl}$ of DCM and CF degradation by several mechanisms[a].

DCM	$\varepsilon^{13}C$ (‰)	$\varepsilon^{37}Cl$ (‰)	$\Lambda^{C/Cl}$	Reference
Mixed culture containing *Dehalobacterium* sp. (*Dhb*)	-31 ± 3*	-5.2 ± 0.6	+5.9 ± 0.3	* See note below
Dehalobacterium formicoaceticum (*Dhb.f.*)	-42.4 ± 0.7	-5.3 ± 0.1	+7.89 ± 0.12	Chen et al. (2018)
Consortium RM harboring *Ca.* Dichloromethanomonas elyunquensis	-18.3 ± 0.2	-5.2 ± 0.1	+3.40 ± 0.03	Chen et al. (2018)
Mixed culture containing *Dehalobacter* sp. (DCMD)	-16 ± 2	n.a.[b]	n.a.	Lee et al. (2015)
Hyphomicrobium sp. strain MC8b	-42.4[c,d]	-3.8[c,d]	+11.2[c,d]	Heraty et al. (1999)
Hyphomicrobium strains, *Methylobacterium*, *Methylopila*, *Methylophilus*, and *Methylorhabdus* strains	-41.2 to -66.3[d] / -45.8 to -61.0[e]	n.a.	n.a.	Nikolausz et al. (2006) / Nikolausz et al. (2006)
Hyphomicrobium strains	-22 to -46[d] / -26 ± 5[e]	n.a.	n.a.	Hermon et al. (2018) / Hermon et al. (2018)
Methylobacterium extorquens DM4 (average between high and low density cell suspensions)	-66.6[d,f]	-7.0[d,f]	+9.5[d,f]	Torgonskaya et al. (2019)
DM4 DCM dehalogenase (average between high and low activity)	-48.4[d,f]	-5.7[d,f]	+8.5[d,f]	Torgonskaya et al. (2019)
DM11 DCM dehalogenase (average between high and low activity)	-45.4[d,f]	-5.6[d,f]	+8.1[d,f]	Torgonskaya et al. (2019)

CF	$\varepsilon^{13}C$ (‰)	$\varepsilon^{37}Cl$ (‰)	$\Lambda^{C/Cl}$	Reference
Oxidation	-8 ± 1	-0.44 ± 0.06	+17 ± 2	Torrentó et al. (2017)
Alkaline hydrolysis	-57 ± 5	-4.4 ± 0.4	+13.0 ± 0.8	Torrentó et al. (2017)
Hydrogenolysis plus reductive elimination with Fe (0)	-33 ± 11	-3 ± 1	+8 ± 2	Torrentó et al. (2017)
Biodegradation with vitamin B_{12}	-14 ± 4	-2.4 ± 0.4	+7 ± 1	Rodríguez-Fernández et al. (2018a)
Outer-sphere single electron transfer (OS-SET)	-17.7 ± 0.8	-2.6 ± 0.2	+6.7 ± 0.4	Heckel et al. (2017a)
Dehalobacter strain CF	-28 ± 2	-4.2 ± 0.2	+6.6 ± 0.1	Heckel et al. (2019)
Dehalobacter strain UNSWDHB	-3.1 ± 0.5	+2.5 ± 0.3	-1.2 ± 0.2	Heckel et al. (2019)
Mixed culture containing *Dehalobacter* strain UNSWDHB	-4.3 ± 0.5	n.a.	n.a.	Lee et al. (2015)

* This study and $\varepsilon^{13}C$ re-calculated from Trueba-Santiso et al. (2017). [a]Uncertainties of ε and Λ values correspond to the 95% confidence interval (CI). [b]n.a.: values were not analysed. [c]$\Lambda^{C/Cl}$ values were calculated based on reported $\varepsilon^{13}C$ and $\varepsilon^{37}Cl$ data by the referenced authors. [d]Values were measured under oxic conditions. [e]Values were measured under nitrate-reducing conditions. [f]$\varepsilon^{13}C$ and $\varepsilon^{37}Cl$ values were calculated here based on reported aC and aCl data and definitions ($\varepsilon C,Cl = (1/aC,Cl - 1) \cdot 1000$) by the referenced authors, and the $\Lambda^{C/Cl}$ values were calculated from the here estimated $\varepsilon^{13}C$ and $\varepsilon^{37}Cl$ values ($\Lambda^{C/Cl} \sim \varepsilon C/\varepsilon Cl$).

6.3.2. $\varepsilon^{37}Cl$ and $\Lambda^{C/Cl}$ during anaerobic DCM degradation by a *Dhb*-containing culture

Samples of a *Dhb*-containing culture, which were previously killed to analyse the decrease in concentration and the carbon isotope fractionation ($\varepsilon^{13}C$) associated to the degradation of DCM (Trueba-Santiso et al., 2017), were used in this section to determine $\varepsilon^{37}Cl$ first, and $\Lambda^{C/Cl}$ later. In this case, the degradation of DCM occurred via its fermentation to acetate and formate (Trueba-Santiso et al., 2017), rather than its reductive dechlorination.

The $\delta^{37}Cl$ values obtained during DCM fermentation increased from -5.7 ± 0.2 to +7.2 ± 0.2‰ after 97% transformation (Figure 6.6), but neither changes in concentration nor in $\delta^{37}Cl$ (average -5.7 ± 0.2‰) were observed in the abiotic controls (data not shown).
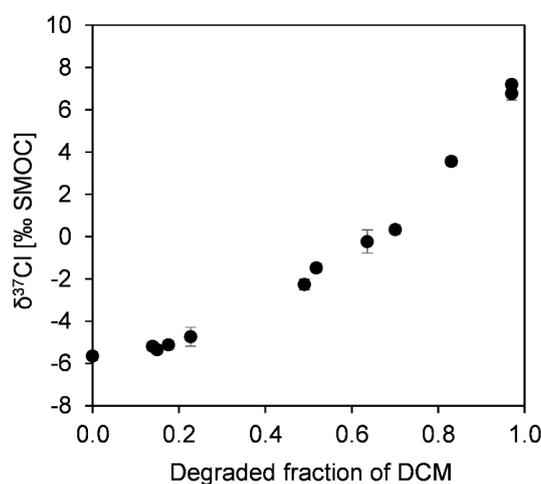
Figure 6.6. Chlorine isotopic composition (●) during DCM fermentation by a Dehalobacterium-containing culture. The error bars show the one standard deviation (1σ) for duplicate measurements.

For the calculation of $\varepsilon^{37}Cl$, however, the last $\delta^{37}Cl$ point (corresponding to the 97% of DCM degradation, Figure 6.6) was excluded because it appeared to be deviated from the linear regression that resulted from all the available data points ($R^2=0.95$, Eq. 2, section 3.2.7). Instead, the best-fitting linear regression

was obtained for $\delta^{37}Cl$ values up to 84% of DCM degradation ($R^2=0.98$), which lead to a $\varepsilon^{37}Cl$ of -5.2 ± 0.6‰ (Figure 6.7A). This phenomenon had been observed previously by Mundle et al. (2013), who reported that a higher uncertainty could be present in the ε values calculated at the later stages of the reactions, and suggested examining the linearity of the fits over shorter reaction progress intervals.

To date, there is still no $\varepsilon^{37}Cl$ value available for a DCM-degrading *Dehalobacter*, but the $\varepsilon^{37}Cl$ value of -5.2 ± 0.6‰ obtained in this chapter for *Dhb* is not significantly different from those reported for D. elyunquensis (-5.2 ± 0.1‰), *Dhb f.* (-5.3 ± 0.1‰), and the purified dehalogenases of *M. extorquens* DM4 and *Methylophilus leisingeri* DM11 (-5.7 and -5.6‰, respectively) (Chen et al., 2018; Torgonskaya et al., 2019), as per the student's t-test (8 degrees of freedom, p=0.05). In contrast, the $\varepsilon^{37}Cl$ obtained here is significantly different than those reported for *Hyphomicrobium* sp. strain MC8b (-3.8‰) and *Methylobacterium extorquens* DM4 (-7.0‰) (Heraty et al., 1999; Torgonskaya et al., 2019) (Table 6.2).

Contrary to the variations observed in R^2 during the calculation of $\varepsilon^{37}Cl$, the re-calculated $\varepsilon^{13}C$ for the 84% of DCM degradation by *Dhb*, which resulted in -31 ± 3‰ ($R^2=0.986$), did not vary much from the previously published value of -27 ± 2‰ ($R^2=0.985$) (Trueba-Santiso et al., 2017). Even with those adjustments, $\varepsilon^{13}C$ for the fermentation of DCM by *Dhb* still differed from the reported (at that time) anaerobic DCM-fermentative *Dehalobacter* (-16 ± 2‰) (Lee et al., 2015), and the aerobic methylotrophic bacteria (Heraty et al., 1999; Nikolausz et al., 2006) (Table 6.2). However, recent studies on *Hyphomicrobium* sp. strains (Hermon et al., 2018) and *Methylobacterium extorquens* DM4 (Torgonskaya et al., 2019) have widened the $\varepsilon^{13}C$ range for DCM degradation by methylotrophic bacteria from -22 to -66.6‰, preventing the distinction

only by carbon isotopes between the hydrolytic transformation of DCM via glutathione-dependent dehalogenases from the fermentation pathway (Table 6.2).
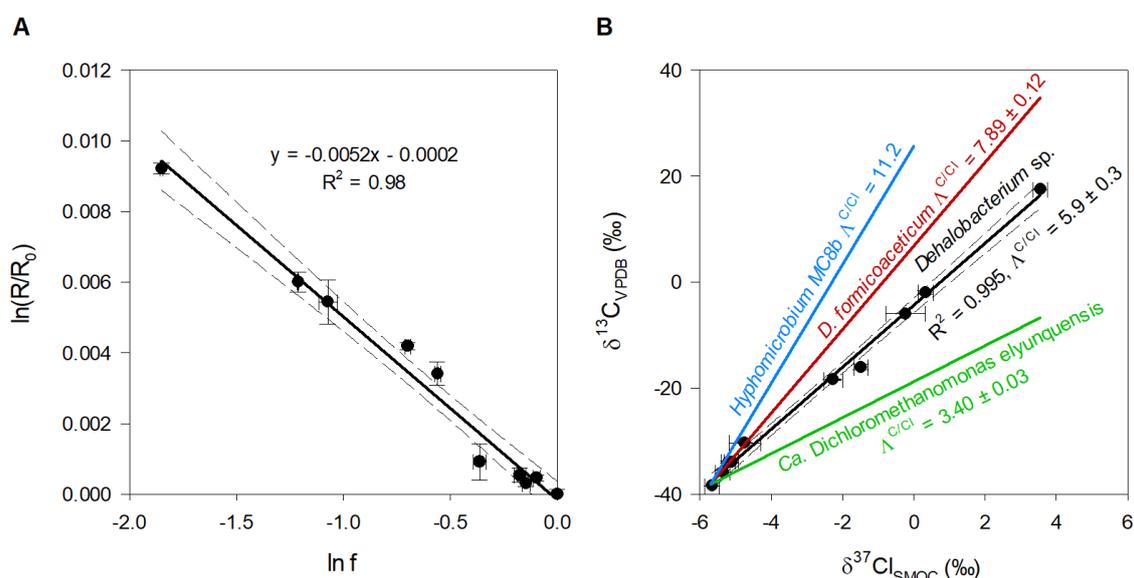
Figure 6.7. Double logarithmic Rayleigh plot for chlorine isotope data (A) and dual C–Cl isotope plot (B) for the anaerobic degradation of DCM by the Dhb containing culture investigated in this study. Solid black lines for the Dhb culture in each panel depict the corresponding linear regression and dashed lines represent the associated 95% CI. In panel B, the trend lines reported for DCM degradation by Hyphomicrobium strain MC8b (Heraty et al., 1999), Dhb f. and D. elyunquensis (Chen et al., 2018) are shown for comparison. Data points show the error bars from duplicate measurements.

In the calculation of $\Lambda^{C/Cl}$, a very good linear correlation (R^2=0.995) was also obtained in the dual C–Cl isotope plot for $\delta^{13}C$ against $\delta^{37}Cl$ values (up to 84% of DCM degradation) that resulted of 5.9 ± 0.3 (Figure 6.7B). This $\Lambda^{C/Cl}$ value obtained for the *Dhb*-containing culture is significantly different from those reported for D. elyunquensis ($\Lambda^{C/Cl}$ = 3.40 ± 0.03) and for *Dhb f.* ($\Lambda^{C/Cl}$ = 7.89 ± 0.12) (Chen et al., 2018) (Figure 6.7B) as per the student's t-test (8 degrees of freedom, p=0.05). The difference between *Dhb* and D. elyunquensis is in accordance with recent proteogenomic findings suggesting that both genera have distinct DCM degradation pathways

(Kleindienst et al., 2019). However, the difference observed between *Dhb* and *Dhb f.* may suggest that they have mechanistic disparities during DCM degradation, even though they both belong to the same genus.

Higher $\Lambda^{C/Cl}$ values ranging from 8.1 to 11.2 have been reported for the aerobic *Hyphomicrobium* sp. strain MC8b (Heraty et al., 1999), *Methylobacterium extorquens* DM4, and DM4 and DM11 DCM dehalogenases (Torgonskaya et al., 2019). To date, these values hint at the distinction between aerobic (11.2 to 8.1) and anaerobic (7.89 to 3.40) pathways (Figure 6.7B). However, further research on this topic would be needed to confirm such hypothesis. See Table 6.2 for a detailed review of literature values.

6.3.3. Investigation of the complex multi-contaminated field sites

With an enriched and widened isotopic database, thanks to the results obtained for pure-phase chlorinated solvents and for the DCM-degrading *Dhb* culture in the above sections (6.3.1 and 6.3.2), field data from both studied sites were investigated aiming to elucidate the origin and fate of DCM, CF, TCE and MCB in the groundwater of each aquifer, and the intrinsic biodegradation potential of each site.

Site 2

This site was first sampled for an hydrogeochemical characterization on July 2017. At that time, the aquifer exhibited mixed redox conditions, since Eh ranged from +250 to -52 mV. Nevertheless, most of the studied wells were in anoxic conditions (Table 6.3), which are expected to be conducive to reductive dechlorination reactions. In addition, temperature and pH were considered homogeneous throughout the aquifer and appropriate for OHRB survival (21.1 ± 0.7 ºC and 6.8 ± 0.3, respectively) (Table 6.3).

Table 6.3. Field parameters measured at each sampling event (left) and molar concentrations of chlorinated solvents and acetate (right) in Site 2.

Well	Sampling date	Experiment	D (m)	WT (m.b.g.l.)	WT (m.a.s.l.)	T (°C)	pH	EC (mS/cm)	Eh (mV)
Site 2									
PI-2	June 2018	Microcosms	6.0	3.2	95.3	21.1 [a]	n.m.	n.m.	+250 [b]
PI-3	July 2017	Characterization	6.0	3.0	95.5	22.0	6.7	1.8	+276
PI-17	July 2017	Characterization	7.0	2.8	95.8	20.2	7.0	1.2	-52
PI-24	July 2017	Characterization	11.5	1.9	94.3	20.2	6.7	1.8	-52
PI-26	July 2017	Characterization	7.5	1.7	94.4	21.2	6.8	2.6	-45
CV-3	July 2017	Characterization	6.0	3.2	95.3	21.7	7.3	3.9	+13
CV-5	July 2017	Characterization	5.0	2.6	95.8	21.3	6.3	1.3	-10

D = well depth, WT = water table in meters below ground level (m.b.g.l.) and meters above sea level (m.a.s.l.), EC = electric conductivity, Eh = corrected redox potential (T dependent, section 3.2.1), n.m. = not measured.
[a] Average groundwater T at the site (T at this well is not available).
[b] Eh estimated using the average groundwater T at the site.

Well	Sampling date	PCE (μM)	TCE (μM)	*cis*-DCE (μM)	*trans*-DCE (μM)	VC (μM)	ETH (μM)	CF (μM)	DCM (μM)	MCB (μM)	Acetate (μM)
Site 2											
PI-2	2018 (M)	blq	28.8 ± 0.7	6.56 ± 0.01	blq	3.09 ± 0.09	0.3 ± 0.01	116 ± 2	blq	46 ± 1	blq
PI-3	2017 (C)	blq	0.55 ± 0.01	blq	blq	blq	blq	blq	blq	4.1 ± 0.7	blq
PI-17	2017 (C)	blq	17.7 ± 0.2	0.56 ± 0.01	blq	1.44 ± 0.04	7.5 ± 0.6	34.1 ± 0.6	blq	106 ± 2	blq
PI-24	2017 (C)	blq	12.41 ± 0.07	0.75 ± 0.01	blq	2.18 ± 0.09	23.5 ± 0.2	115.0 ± 0.6	3.85 ± 0.01	72.8 ± 0.9	blq
PI-26	2017 (C)	blq	123 ± 2	4.4 ± 0.3	0.89 ± 0.01	11.4 ± 0.4	21 ± 2	1450 ± 20	17.3 ± 0.4	375 ± 3	0.249 ± 0.003
CV-3	2017 (C)	0.17 ± 0.01	359 ± 5	5.17 ± 0.09	0.52 ± 0.07	4.8 ± 0.1	blq	3800 ± 56	8.48 ± 0.01	734 ± 4	0.8 ± 0.2
CV-5	2017 (C)	blq	55 ± 3	4.8 ± 0.3	blq	15.6 ± 0.2	8 ± 1	1617 ± 90	4.2 ± 0.4	77 ± 7	blq

(C): samples used for characterization of the sites, (M): samples used for microcosm experiments, blq: below limit of quantification. Concentrations in the microcosm experiments refer to the initial concentrations (time zero). Acetate concentrations refer to the initial concentrations of the non-amended microcosms (time zero of the controls). Time-course of chlorinated solvents and acetate in the microcosms is depicted in the following pages (section 6.3.3).

Table 6.4. δ¹³C and δ³⁷Cl compositions of target chlorinated solvents in Site 2.

Well	Sampling date	TCE $\delta^{13}C$ (‰)	TCE $\delta^{37}Cl$ (‰)	CF $\delta^{13}C$ (‰)	CF $\delta^{37}Cl$ (‰)	DCM $\delta^{13}C$ (‰)	DCM $\delta^{37}Cl$ (‰)	MCB $\delta^{13}C$ (‰)	MCB $\delta^{37}Cl$ (‰)
Site 2									
PI-2	June 2018 (M)	n.a.	n.a.	n.a.	n.a.	n.a.	n.a.	n.a.	n.a.
PI-3	July 2017 (C)	-28.2 ± 0.4	n.a.	n.d.	n.d.	n.d.	n.d.	-27.2 ± 0.4	n.a.
PI-17	July 2017 (C)	-32.4 ± 0.4	n.a.	-40.7 ± 0.6	-2.1 ± 0.2	n.d.	n.d.	-25.4 ± 0.3	n.a.
PI-24	July 2017 (C)	-32.0 ± 0.4	n.a.	-42.9 ± 0.6	-1.3 ± 0.2	n.d.	+4.4 ± 0.4	-25.3 ± 0.3	n.a.
PI-26	July 2017 (C)	-32.1 ± 0.4	n.a.	-40.9 ± 0.7	-1.6 ± 0.2	-32.8 ± 1.1	+3.0 ± 0.4	-26.0 ± 0.4	n.a.
CV-3	July 2017 (C)	-32.5 ± 0.4	n.a.	-41.8 ± 0.5	-2.2 ± 0.2	n.d.	+3.3 ± 0.2	-26.5 ± 0.6	n.a.
CV-5	July 2017 (C)	-31.8 ± 0.4	n.a.	-43.9 ± 0.5	-2.2 ± 0.2	n.d.	+5.3 ± 0.2	-26.7 ± 0.4	n.a.

(C): characterization experiment, (M): microcosm experiment, n.d.: could not be determined based on their low concentration, n.a.: not analysed.

Regarding the contamination plume, CF was the chlorinated solvent detected at the highest concentration (454 mg/L), followed by MCB (82.7 mg/L), TCE (47.2 mg/L), and DCM (1.47 mg/L) (Figure 6.12A). Molar concentrations of the target contaminants can be found in Table 6.3.

The C–Cl isotopic composition of CF could only be determined in 5 out of 7 monitoring wells (Table 6.4, Figure 6.12A), since CF concentration in well PI-3 was below the limit of quantification, and well PI-2 was not included in this first phase of the investigation. According to the results, obtained $\delta^{13}C$ values for CF showed a relatively small but significant variation ($\Delta\delta^{13}C_{CF}$) of 3.2‰ between samples of wells PI-17 and CV-5, which exhibited the most enriched and depleted $\delta^{13}C_{CF}$, respectively (Table 6.4). Since this difference in the carbon isotope composition was >2‰, this result could be related to *in-situ* CF transformation (Hunkeler et al., 2008). In contrast, the widest $\Delta\delta^{37}Cl_{CF}$ observed at the site, which was between samples of wells CV-5 and PI-24, was lower than 2‰. This result agreed with previous research showing that $\varepsilon^{13}C$ values are usually greater than $\varepsilon^{37}Cl$ during CF biodegradation (Table 6.2). Moreover, the isotopic composition of CF in the analysed groundwater samples fell outside the isotopic range of commercial CF solvents, except for the samples that were collected in well CV-5 (Figure 6.8). Therefore, results for CF C–Cl isotopic compositions in groundwater supported a potential *in-situ* transformation of CF at the site.

In the case of DCM, only the one C–Cl isotopic composition in well PI-26 could be determined. This was due to the fact that DCM concentration in most of the samples was too low for carbon CSIA, but enough for, at least, the determination of $\delta^{37}Cl$ in 4 out of 7 wells (Table 6.4, Figure 6.12A). With the available isotopic data, it was observed that obtained $\delta^{37}Cl$ for DCM showed a significant variation in $^{37}Cl/^{35}Cl$ ratios of $\Delta\delta^{37}Cl_{DCM} = 2.3$‰

between wells CV-5 and PI-26 (Table 6.4, Figure 6.12A), which could be indicative of DCM *in-situ* transformations. Moreover, these δ^{37}Cl values were enriched in ^{37}Cl (more positive) compared to those of commercial DCM (Table 6.1), further supporting a potential DCM degradation in groundwater. As mentioned earlier, no $\Delta\delta^{13}C_{DCM}$ can be provided for δ^{13}C since only one value could be obtained, but this value was also enriched in ^{13}C compared to most of the δ^{13}C reported for commercial DCM (Table 6.1). Hence, this dual C–Cl isotopic composition obtained for DCM in the analysed groundwater of well PI-26 fell outside the isotopic range of commercial DCM, suggesting a potential transformation of DCM at the site as well (Figure 6.8). When comparing these results to the literature, the low carbon enrichment observed in the field (compared to that of chlorine) could indicate that the bacteria responsible for DCM degradation have a ε^{13}C that is in the lower range (e.g. *Dehalobacter* sp., which has the lowest reported ε^{13}C as presented in Table 6.2).
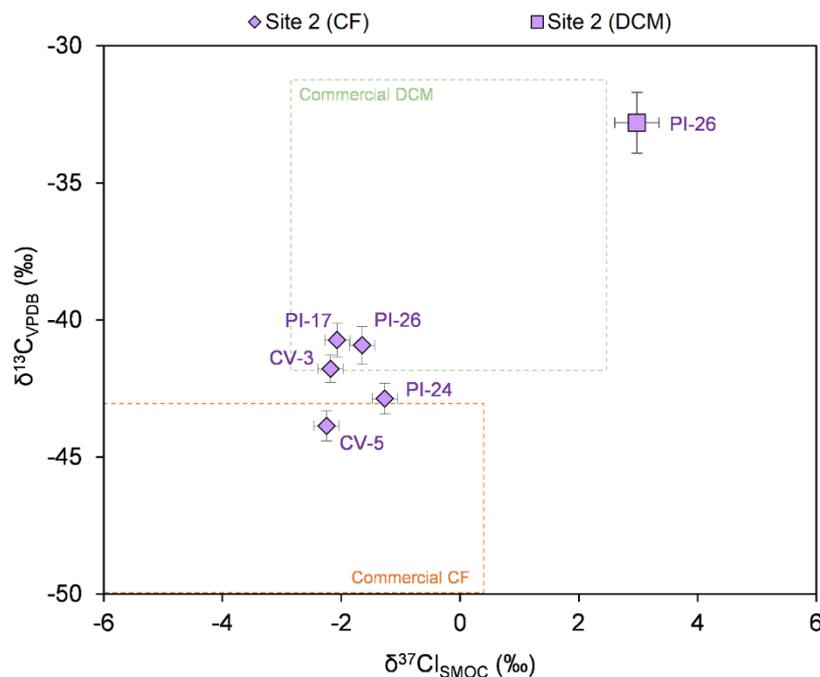
*Figure 6.8. Distribution of measured δ¹³C and δ³⁷Cl of CF and DCM at Site 2. Isotopic ranges for commercial CF and DCM solvents are depicted with the green and orange rectangles, respectively, using isotopic values shown in Table 6.1.*

An additional evidence pointing towards *in-situ* DCM biodegradation was the detection of acetate in wells PI-26 and CV-3 (Table 6.3, Figure 6.12A), which is the main by-product of DCM fermentation (Justicia-Leon et al., 2012; Lee et al., 2015; Mägli et al., 1998; Trueba-Santiso et al., 2017).

Following the same methodology used for CF and DCM, the isotopic compositions of TCE and MCB were also investigated. Interestingly, $\delta^{13}C$ for TCE in the wells that also contained CF ranged between -32.5 and -31.8‰ but was significantly enriched in ^{13}C in the unique well (PI-3) that lacked CF ($\delta^{13}C_{TCE}$ = -28.2‰, Table 6.4, Figure 6.12A). This may be in agreement with several studies suggesting that CF can significantly inhibit microbial reductive dechlorination of CEs, as reviewed by Wei et al. (2016). However, *cis*-DCE, VC and ETH were also detected in most of the monitored wells (Table 6.3) indicating that, despite this potential inhibition effect suggested by the isotopic analysis, full dechlorination of TCE could occur. Lastly, no significant carbon isotope fractionation was observed for MCB ($\angle\delta^{13}C_{MCB}$ < 2‰, Table 6.4), and obtained $\delta^{13}C$ values were within the available range of commercial MCB solvents (Table 6.1), indicating that this compound was, most likely, not being degraded.

To investigate the biodegradation potential of Site 2, three different microcosm treatments were prepared with groundwater from well PI-2 (Figures 6.1 and 6.2). In this case, groundwater samples were collected in June 2018, one year after those collected and used for the chemical and isotopic characterization that was just discussed in the above lines.

As depicted in Figure 6.9A1, the non-amended microcosms used as natural attenuation controls fully degraded CF and DCM in less than 30 days and transformed TCE to VC via *cis*-DCE after 75 days (Figure 6.9A2). Similarly, an additional amendment of CF was eliminated as well (Figure 6.9A1).
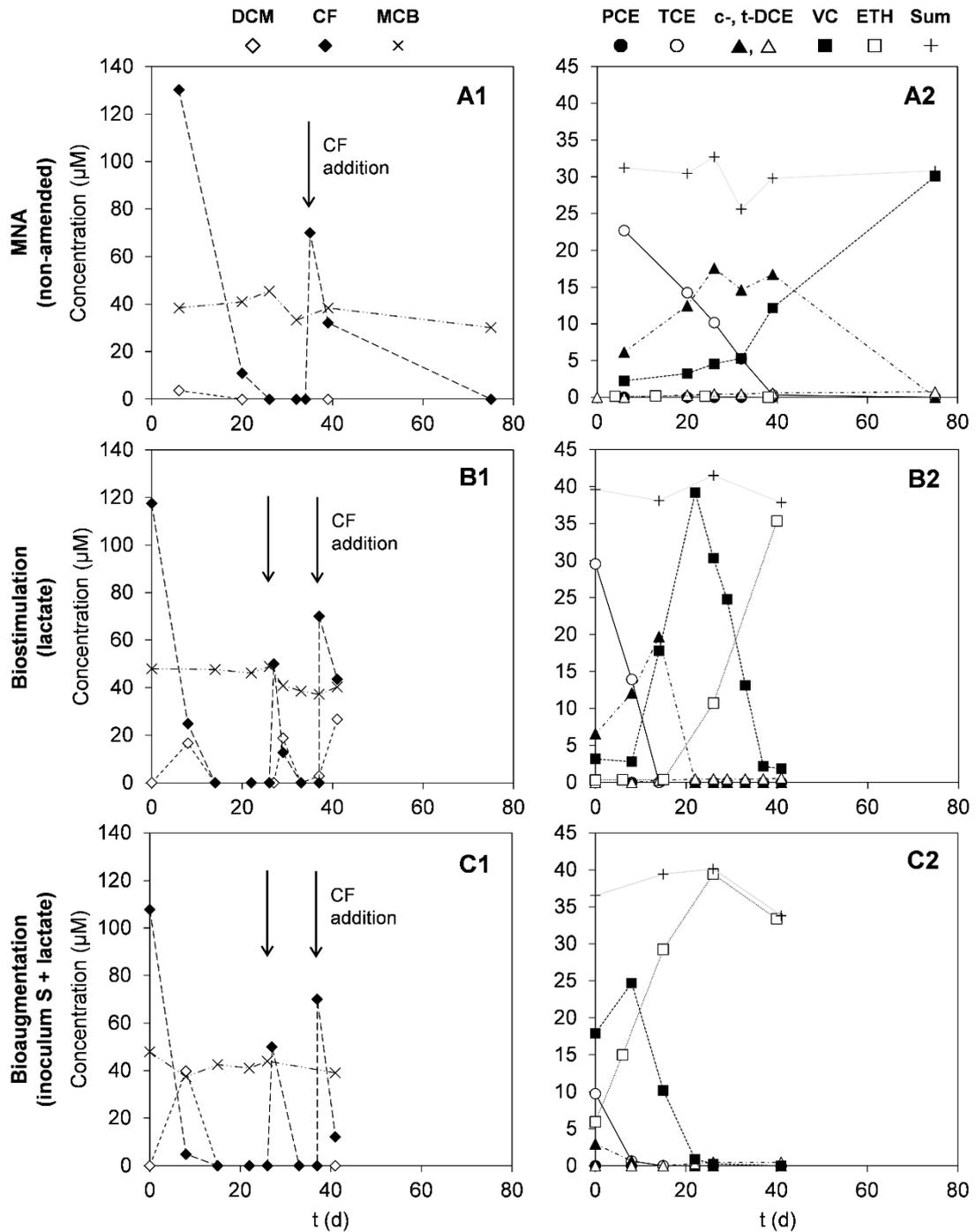
Figure 6.9. Time-course of contaminants in microcosms from well PI-2. Data presented is from an individual microcosm, but it is representative of triplicates.

The microcosms amended with either only Lactate-2 (biostimulation), or Lactate-2 plus the "S" inoculum (bioaugmentation), increased the degradation rate of CF, DCM, TCE and, more importantly, fully dechlorinated the latter

to stoichiometric amounts of ETH (Figure 6.9B and C). Both CMs and CEs elimination occurred simultaneously, and the two reamendments of CF proved that CF was degraded to DCM (Figure 6.9B1). These results confirmed the feasibility of *in-situ* CF, DCM and TCE biodegradation, and agreed with the information obtained from the isotopic field data that was just discussed.

In contrast to the observations for CEs and CMs, MCB always accumulated in the medium of the microcosms and was not degraded (Figure 6.9A1, B1, and C1). Such evidence further supports the conclusions obtained from the isotopic field data, which pointed towards the recalcitrance of the pollutant. Thus, it could be discarded that benzene, which was detected in the preliminary characterization of this aquifer, was derived from MCB biodegradation.
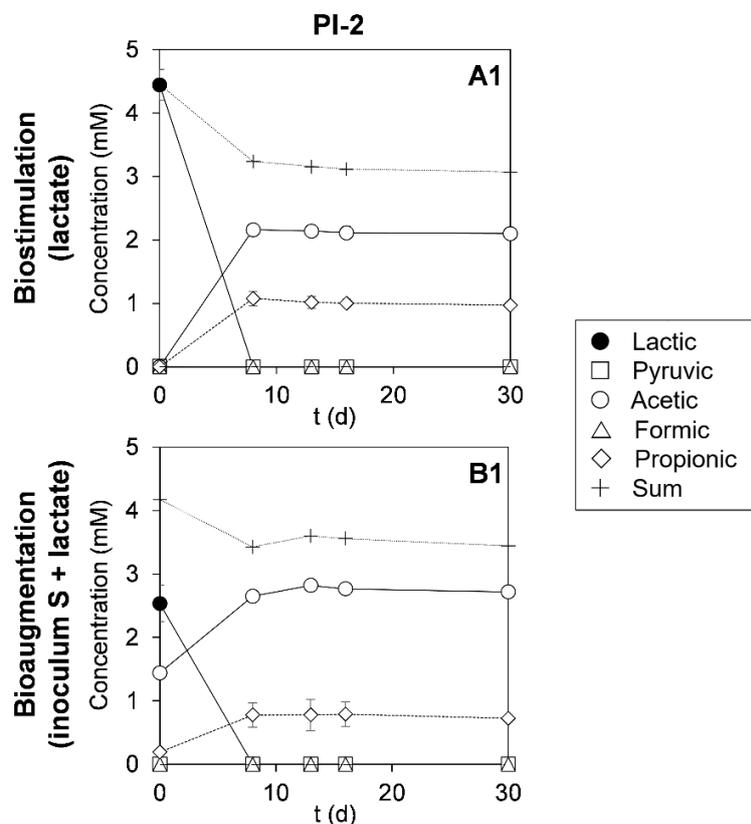
Figure 6.10. Time-course of VFAs in the microcosm experiments from well PI-2. No VFAs were detected in the controls and that is why it is not presented. Error bars indicate the 1σ for triplicates.

Regarding the fate of the amended lactate, results demonstrated that it was converted to acetate (major product) and propionate in all the amended microcosms (Figure 6.10).
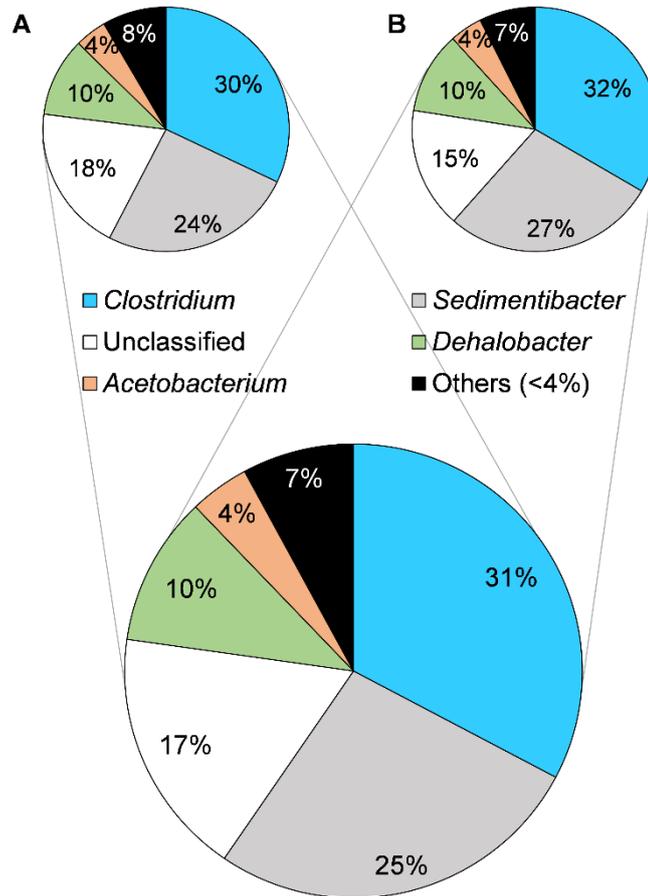
Figure 6.11. Averaged composition of the bacterial community in well PI-2 (Site 2). Averaged composition at the genus level was obtained from two cultures that were enriched with CF for four consecutive extinction series. Total number of reads for Dehalobacter sp. at A and B replicates were of 6110/61977 and 6048/58951, respectively. Genera <4% are included in Others.

The composition of the degrading microbial community in cultures derived from Site 2 was assessed by 16S rRNA high-throughput sequencing. The analysis was performed on groundwater samples that were collected from well PI-2 and were enriched with CF for four consecutive dilution series. As depicted in Figure 6.11, the taxonomic assignments of 16S rRNA sequences revealed that the four predominant genera were *Clostridium* (31%),

Sedimentibacter (25%), *Dehalobacter* (10%) and *Acetobacterium* (4%). The presence of *Dehalobacter* sp., a well-known CF and DCM degrader (Justicia-Leon et al., 2012; Lee et al., 2015), further supports the intrinsic biodegradation potential of the aquifer to remediate CMs. In addition, results also suggested that *Clostridium* sp. and *Acetobacterium* sp. could be involved in the degradation of CF as well, as described elsewhere (Egli et al., 1990, 1988; Gälli and McCarty, 1989; Wanner et al., 2018). No predominant genera related to the degradation of CEs were obtained, nor was expected to, because the cultures were enriched with CF only and, thus, the microbial community linked to CEs degradation was not cultivated.

With the evidences discussed above and aiming to better understand the fate of CF and DCM at this site, a dual C–Cl isotopic assessment was performed. Such an approach was based on the assumption that CF in well CV-5 reflected the initial isotopic composition of CF (CF$_0$), as it possessed the most depleted $\delta^{13}C$ and $\delta^{37}Cl$ values (Figure 6.12A). As depicted in Figure 6.12B, the dual isotope fractionation pattern observed for CF in CV-3, PI-17 and PI-26 was consistent with the degradation of leaked commercial CF, since the data points for those wells fell within the estimated potential range of isotopic compositions for a degraded CF (orange area).

Following the methodology described in section 6.2.7, the values for a DCM that would be initially produced from the degradation of a leaked CF (i.e. DCM$_{ini}$) would range between -50.9‰ and -73.9‰ for $\delta^{13}C$ and would be of -2.2‰ for $\delta^{37}Cl$ (Figure 6.12B). From those DCM$_{ini}$ values, the area that would correspond to the formation of DCM from the degradation of CF was depicted (grey colour, Figure 6.12B). Accordingly, as presented in Figure 6.12B, the isotopic composition of the DCM detected in well PI-26 (Table 6.4) was enriched in ^{37}Cl compared to that of commercial DCM (green dashed

rectangle, Table 6.1), and in both ^{13}C and ^{37}Cl compared to that of DCM produced by CF degradation (grey area). These results suggest that, independently of its origin, DCM could be subject to biodegradation. Regarding the main source of the detected DCM at the site, and considering the historical industrial activity at the area, obtained results point to a potential spill of DCM at the site being more likely than DCM production from CF degradation. However, neither could be confirmed through this investigation. See section 6.2.7 for the methodology details.

In the scenario discussed above (i.e. confirmed degradation of CF by isotopic and microcosm studies, and detection of *Dehalobacter* sp. in the field-derived CF-enriched cultures), and assuming *Dehalobacter* sp. was the responsible for CF biotransformation, the estimated extent of biodegradation (D%, Eq. 3, section 3.2.7) for CF in the wells CV-3, PI-17 and PI-26 (where $\varDelta\delta^{13}C$ was > 2‰, Table 6.4) ranged between 7–11%, considering the $\varepsilon^{13}C$ data reported for *Dehalobacter* strain CF ($\varepsilon^{13}C$ = -28 ± 2) (Table 6.2). Data for *Dehalobacter* strain CF was used for this calculation because its $\varLambda^{C/Cl}$ was more coherent with the field results from Site 2 (i.e. the isotopic pattern of positive dual C–Cl slopes observed for CF measurements), than the $\varLambda^{C/Cl}$ of *Dehalobacter* strain UNSWDHB (Table 6.2) (Heckel et al., 2019). Nevertheless, further research needs to be done on this culture to better understand the roles of *Dehalobacter*, *Clostridium* and *Acetobacterium* bacteria, and elucidate the biodegradation mechanisms of CF, which would allow an improved assessment and quantification of D% at the field. Likewise, the estimation of D% was not carried out for the DCM available data point (well PI-26) because the degradation mechanism of DCM and the responsible degrader are still not confirmed, even though it was demonstrated in the microcosms that DCM (as a result of CF degradation) could be eliminated as well (Figure 6.9).
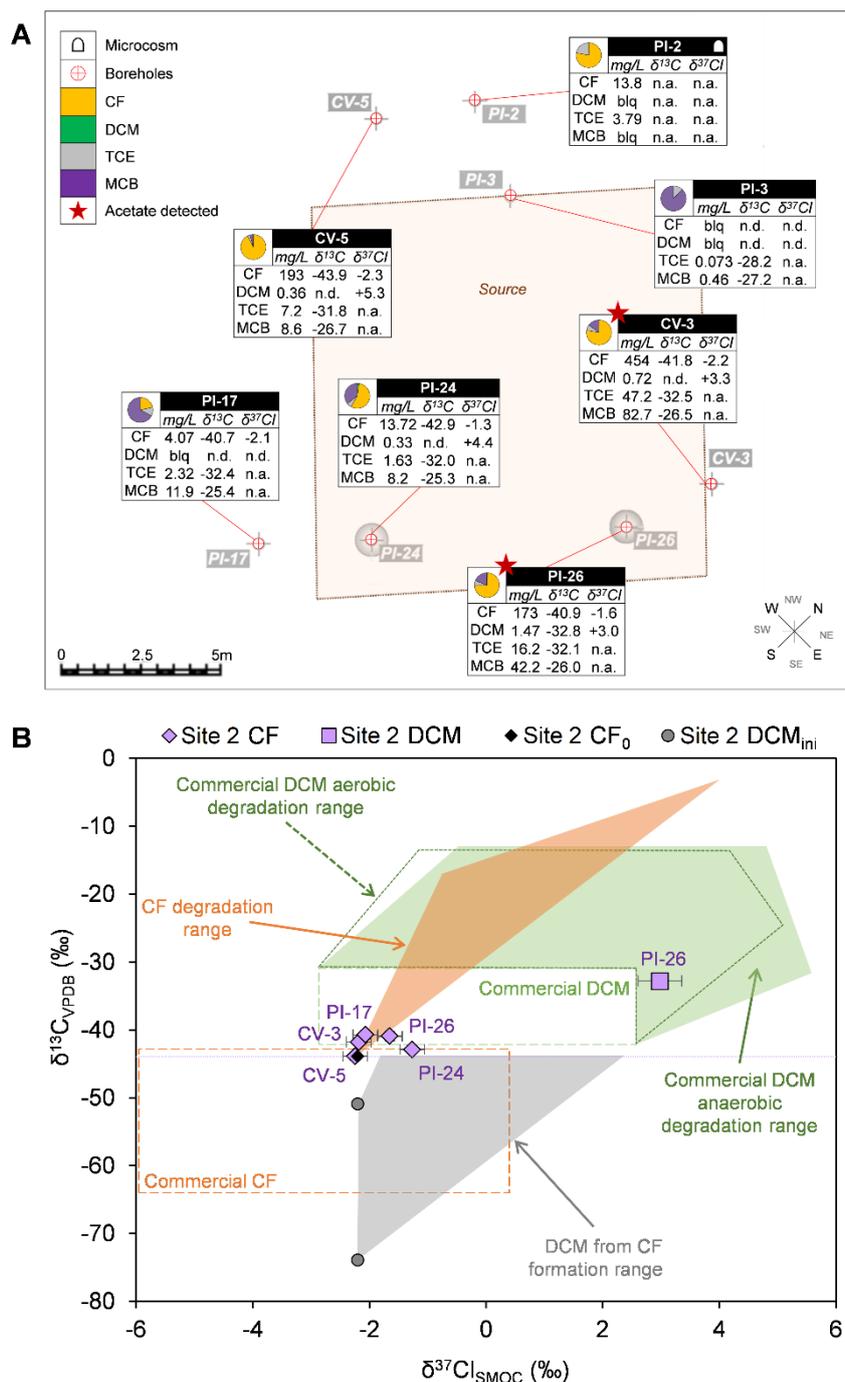
Figure 6.12. (A) Concentrations (in mg/L) and δ¹³C and δ³⁷Cl compositions (in ‰) of CF, DCM, TCE and MCB from Site 2. Pie charts show the molar distribution of contaminants at each well. Detailed concentrations (in μM) and isotopic compositions are available in Tables 6.3 and 6.4, respectively. "n.d." means "could not be determined based on their low concentration"; "n.a." means "not analysed". (B) Dual C–Cl isotopic assessment for DCM and CF field data from Site 2. Both CF₀ and the range for DCMₐₙₐ are represented. Green and orange dashed rectangles depict the δ¹³C and δ³⁷Cl ranges of commercial DCM and CF solvents, respectively (see Table 6.1 for details).

Site 3

Similarly to Site 2, Site 3 was investigated as well to assess the biodegradation potential of the aquifer. During the first sampling campaign, on July 2017, Eh ranged from +254 to -118 mV. However, even though several wells exhibited negative redox potentials, groundwater in most of the wells was oxic, which limits the occurrence of reductive dechlorination reactions (Table 6.5). Nevertheless, temperature and pH were homogeneous across the site and averaged 24 ± 2 °C and 6.8 ± 0.3, respectively (Table 6.5), so they were within the optimal range for the growth of OHRB.

Of the target contaminants, CF was detected at the highest concentrations (272 mg/L) and was followed by DCM (27 mg/L), TCE (1.7 mg/L) and MCB (0.88 mg/L) (Figure 6.18A). Molar concentrations of the studied contaminants can be found in Table 6.6.

In this case, $\delta^{13}C$ and $\delta^{37}Cl$ of CF could only be determined in 7 out of 9 wells because the concentration of CF in PZ-5 and PZ-31 was below the limit of quantification (Table 6.7). According to the results presented in Table 6.7, the $\varDelta\delta^{13}C_{CF} > 2‰$ observed between wells PZ-9 and PZ-18 and the $\varDelta\delta^{37}Cl_{CF} < 2‰$ observed between wells PZ-10 and PZ-18, which are the maximum differences detected in the field for each element, could be related to CF transformation in groundwater (Hunkeler et al., 2008) considering the low $\varepsilon^{37}Cl$ reported for CF transformation (Table 6.2). However, most of the C–Cl isotope compositions that were obtained for CF were within the isotopic range for pure commercial CF solvents (Figure 6.13). Therefore, results could also indicate that measured $\delta^{13}C$ and $\delta^{37}Cl$ belonged to a leaked and not degraded CF (i.e. the observed differences in $\delta^{13}C$ and $\delta^{37}Cl$ could be due to CF industrial manufacture rather than its degradation in the aquifer).

Table 6.5. Field parameters measured at each sampling event in Site 3.

Well	Sampling date	Experiment	D (m)	WT (m.b.g.l.)	WT (m.a.s.l.)	T (°C)	pH	EC (mS/cm)	Eh (mV)
Site 3									
PZ-5	July 2017	Characterization	12.6	10.5	88.3	n.m.	n.m.	n.m.	n.m.
PZ-9	July 2017	Characterization	15.3	13.3	92.7	22.1	7.5	4.4	+210
PZ-9	June 2018	Microcosms	15.3	6.8	99.1	24.0	n.m.	n.m.	+200
PZ-10	July 2017	Characterization	15.3	5.9	99.6	23.4	6.7	2.0	+254
PZ-16	July 2017	Characterization	16.0	6.9	98.7	27.9	6.7	2.1	+116
PZ-18	July 2017	Characterization	15.3	3.6	98.8	21.7	6.3	2.6	-118
PZ-19	July 2017	Characterization	16.0	7.2	98.6	26.4	7.0	5.0	+27
PZ-19	June 2018	Microcosms	16.0	7.3	98.5	23.5	n.m.	n.m.	+230
PZ-21	July 2017	Characterization	16.0	7.9	97.8	23.5	6.7	3.8	+137
PZ-31	July 2017	Characterization	15.0	7.8	94.1	22.9	6.7	3.2	-45
PZ-36	July 2017	Characterization	14.5	1.1	101.1	21.2	6.7	4.8	-52
PZ-36	June 2018	Microcosms	14.5	9.7	92.5	24 [a]	n.m.	n.m.	+237 [b]

D = well depth, WT = water table in meters below ground level (m.b.g.l.) and meters above sea level (m.a.s.l.), EC = electric conductivity, Eh = corrected redox potential (T dependent, section 3.2.1), n.m. = not measured.

[a] Average groundwater T at the site (T at this well is not available).

[b] Eh estimated using the average groundwater T at the site.

Table 6.6. Molar concentrations of chlorinated solvents and acetate in groundwater of Site 3.

Well	Sampling date	PCE (µM)	TCE (µM)	cis-DCE (µM)	trans-DCE (µM)	VC (µM)	ETH (µM)	CF (µM)	DCM (µM)	MCB (µM)	Acetate (µM)
Site 3											
PZ-5	July 2017 (C)	blq	blq	blq	0.74 ± 0.01	blq	blq	blq	blq	7.9 ± 0.5	blq
PZ-9	July 2017 (C)	1.35 ± 0.04	1.0 ± 0.1	blq	2.5 ± 0.2	blq	blq	89 ± 2	2 ± 2	1.06 ± 0.05	blq
PZ-9	June 2018 (M)	0.83 ± 0.03	0.27 ± 0.05	blq	0.69 ± 0.07	blq	blq	46 ± 4	blq	1.9 ± 0.1	blq
PZ-10	July 2017 (C)	blq	blq	blq	0.44 ± 0.01	blq	2 ± 2	128.9 ± 1.3	blq	blq	blq
PZ-16	July 2017 (C)	blq	blq	blq	0.96 ± 0.07	blq	blq	4 ± 1	blq	blq	blq
PZ-18	July 2017 (C)	blq	0.83 ± 0.01	blq	0.44 ± 0.01	blq	blq	7.9 ± 0.3	9.3 ± 0.8	2.27 ± 0.05	43.09 ± 0.09
PZ-19	July 2017 (C)	blq	6.73 ± 0.07	blq	2.66 ± 0.01	blq	blq	525 ± 6	28.1 ± 0.4	0.55 ± 0.01	blq
PZ-19	June 2018 (M)	blq	31 ± 3	blq	0.44 ± 0.01	blq	blq	7614 ± 711	29 ± 2	2 ± 1	0.126 ± 0.009
PZ-21	July 2017 (C)	blq	blq	blq	blq	blq	blq	5 ± 2	blq	blq	blq
PZ-31	July 2017 (C)	blq	blq	blq	1.92 ± 0.01	blq	blq	blq	blq	4.58 ± 0.05	blq
PZ-36	July 2017 (C)	blq	13 ± 1	1.22 ± 0.09	1.6 ± 0.2	0.74 ± 0.04	blq	2276 ± 185	313 ± 25	blq	7.99 ± 0.09
PZ-36	June 2018 (M)	blq	1.9 ± 0.2	blq	blq	blq	blq	115 ± 10	blq	0.40 ± 0.04	blq

(C): samples used for characterization of the sites, (M): samples used for microcosm experiments, blq: below limit of quantification. Concentrations in the microcosm experiments refer to the initial concentrations (time zero). Acetate concentrations refer to the initial concentrations of the non-amended microcosms (time zero of the controls). Time-course of chlorinated solvents and acetate in the microcosms is depicted in the following pages (section 6.3.3).

Table 6.7. $\delta^{13}C$ and $\delta^{37}Cl$ compositions of target chlorinated solvents in groundwater of Site 3.

Well	Sampling date	TCE		CF		DCM		MCB	
		$\delta^{13}C$ (‰)	$\delta^{37}Cl$ (‰)	$\delta^{13}C$ (‰)	$\delta^{37}Cl$ (‰)	$\delta^{13}C$ (‰)	$\delta^{37}Cl$ (‰)	$\delta^{13}C$ (‰)	$\delta^{37}Cl$ (‰)
Site 3									
PZ-5	July 2017 (C)	n.d.	n.a.	n.d.	n.d.	n.d.	n.d.	n.d.	n.a.
PZ-9	July 2017 (C)	-24.5 ± 0.5	n.a.	-45.1 ± 0.6	-2.1 ± 0.2	n.d.	+0.9 ± 0.2	n.d.	n.a.
PZ-9	June 2018 (M)	n.a.	n.a.	n.a.	n.a.	n.a.	n.a.	n.a.	n.a.
PZ-10	July 2017 (C)	n.d.	n.a.	-44.2 ± 0.5	-3.5 ± 0.2	n.d.	n.d.	n.d.	n.a.
PZ-16	July 2017 (C)	n.d.	n.a.	-42.8 ± 0.6	-2.6 ± 0.2	n.d.	n.d.	n.d.	n.a.
PZ-18	July 2017 (C)	n.d.	n.a.	-42.5 ± 0.6	-1.7 ± 0.2	n.d.	+3.1 ± 0.4	n.d.	n.a.
PZ-19	July 2017 (C)	-18.7 ± 0.2	n.a.	-44.2 ± 0.6	-2.7 ± 0.2	-45.8 ± 0.4	+2.3 ± 0.3	n.d.	n.a.
PZ-19	June 2018 (M)	n.a.	n.a.	n.a.	n.a.	n.a.	n.a.	n.a.	n.a.
PZ-21	July 2017 (C)	-23.2 ± 0.3	n.a.	-43.4 ± 0.5	-2.6 ± 0.2	n.d.	n.d.	n.d.	n.a.
PZ-31	July 2017 (C)	n.d.	n.a.	n.d.	n.d.	n.d.	n.d.	n.d.	n.a.
PZ-36	July 2017 (C)	-22.6 ± 0.5	n.a.	-43.6 ± 0.3	-2.3 ± 0.2	-39.7 ± 0.3	+1.9 ± 0.2	n.d.	n.a.
PZ-36	June 2018 (M)	n.a.	n.a.	n.a.	n.a.	n.a.	n.a.	n.a.	n.a.

(C): characterization experiment, (M): microcosm experiment, n.d.: could not be determined based on their low concentration, n.a.: not analysed.

On its side, the DCM that was detected in groundwater presented a higher variation for both C and Cl isotope ratios, which were of $\varDelta\delta^{13}C_{DCM}$ = 6.1‰ (between wells PZ-19 and PZ-36) and of $\varDelta\delta^{37}Cl_{DCM}$ = 2.2‰ (between wells PZ-9 and PZ-18) and could be indicative of potential *in-situ* transformations (Table 6.7). In this case, however, the isotopic composition that was measured in well PZ-36 fell within the commercial DCM solvents range, but the one measured on well PZ-19 did not, as depicted in Figure 6.13 (see further discussion on this topic in the following pages).
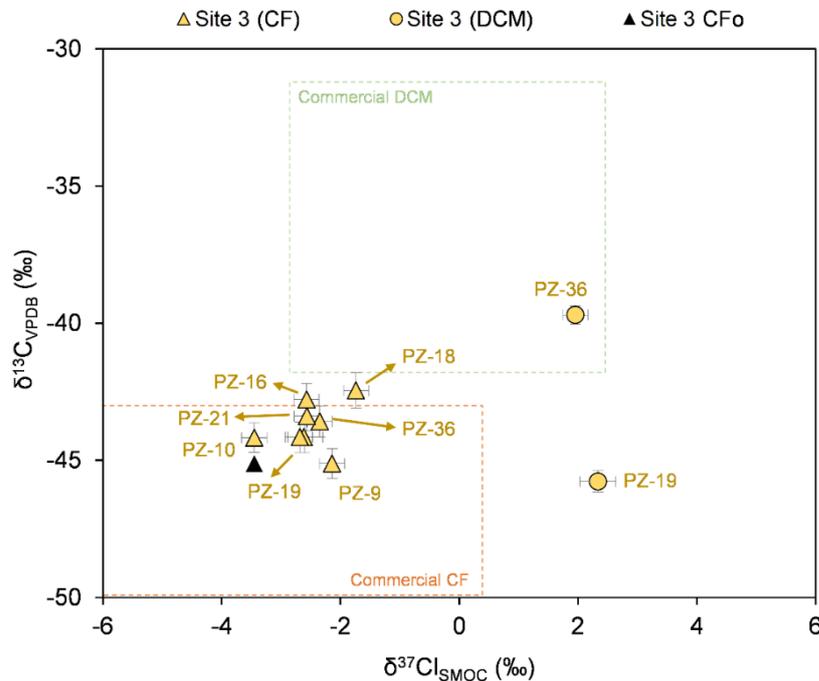

Figure 6.13. Distribution of measured $\delta^{13}C$ and $\delta^{37}Cl$ of CF and DCM at Site 3. Isotopic ranges for commercial CF and DCM solvents are depicted with the green and orange rectangles, respectively, using isotopic values shown in Table 6.1.

Following the same methodology used for CF and DCM, $\varDelta\delta^{13}C$ for TCE was of 5.8‰ (Table 6.7), which could be related to TCE transformation in groundwater (Hunkeler et al., 2008). Additionally, available isotopic data for pure TCE solvents (Table 6.1) allowed the comparison with the measured $\delta^{13}C_{TCE}$ field values. This revealed that the latter were more enriched in ^{13}C

than those for commercial TCE, which would be in agreement with a potential TCE degradation *in-situ*. However, the reductive dechlorination products of TCE (dichloroethene (DCE), VC, and ETH) were only detected occasionally and at very low concentrations (Table 6.6). Lastly, MCB was detected at this site (Table 6.6) but concentrations were too low for the analysis of $\delta^{13}C$ and $\delta^{37}Cl$.

Given that this site was larger than Site 2 and aiming to have an appropriate representativity of the field conditions, microcosm experiments were prepared with groundwater from three different wells: PZ-9, PZ-19 and PZ-36.

Microcosms for well PZ-9 did not show significant degradation of neither CF nor CEs, and no major differences were observed between the non-amended, biostimulated and the bioaugmented treatments after 150 days (Figure 6.14). However, traces of DCM and VC, a slight decrease in PCE and TCE, and formation of *trans*-dichloroethene (*trans*-DCE) were observed throughout the course of the study (Figure 6.14).

In the microcosms prepared with groundwater from well PZ-19, no significant elimination of contaminants was observed in any of the treatments either. Nevertheless, TCE did exhibit a decrease in all microcosms and traces of *cis*-DCE, *trans*-DCE and VC were detected in some of them (Figure 6.15). Interestingly, these microcosms presented a higher concentration of CF (Figure 6.15 A1–D1) compared to the other two wells PZ-9 and PZ-36. Given that P&T was active at the site and PZ-19 was close to what would seem an extraction point (Figure 6.4), the high CF concentration detected in this well could be attributed to a nearby accumulation of groundwater due to pumping.

In the case of the PZ-36 microcosms, a different evolution of the pollutants was observed, at least in the bioaugmented (with "S") treatment (Figure

6.16C). In this case, in the 150 days of monitoring, CF exhibited a decrease with the transient production of DCM, and TCE was completely transformed (within the first days of the experiment) to VC and *trans*-DCE, which remained accumulated for the rest of the study (Figure 6.16C2). In this microcosm, even ETH was detected, albeit not in significant concentrations that could confirm VC-to-ETH activity (Figure 6.16C2). In contrast, the rest of the treatments (the non-amended, biostimulated and bioaugmented ("M") microcosms) neither degraded CF nor CEs significantly, although traces of DCM and formation of *trans*-DCE were observed (Figure 6.16 A, B and D), like in the PZ-9 and PZ-19 microcosms.

Regarding the fermentation pathway of the amended lactate (Lactate-2), it was observed that it was totally consumed and mainly transformed to acetate in both PZ-9 and PZ-36 field-derived microcosms (Figure 6.17). In PZ-19, however, lactate did decrease but was not completely consumed during the monitoring period. Regardless, its decrease was followed by acetate and propionate production in both bioaugmentation tests, while no significant changes were observed in the biostimulation treatment (i.e. only lactate) (Figure 6.17).

Considering the results obtained in the microcosms, one of the most relevant aspects is that not even the bioaugmentation treatments, which were inoculated with commercialized bacterial consortia, were able to degrade the contaminants that were present in groundwater. Such inability of the inoculated bacteria to efficiently degrade these chlorinated solvents suggested that it was probably due to inhibition issues. A plausible explanation for such inhibition could be the co-contamination that was present in groundwater. Specifically, it is possible that inhibition was mainly driven by CT, which had been detected in this aquifer (in the site characterizations that were carried out

prior to this thesis, section 6.2.2) and is a known inhibitor of microbial activity and CF degradation in particular (da Lima and Sleep, 2010; Grostern et al., 2010; Justicia-Leon et al., 2014; Wei et al., 2016).
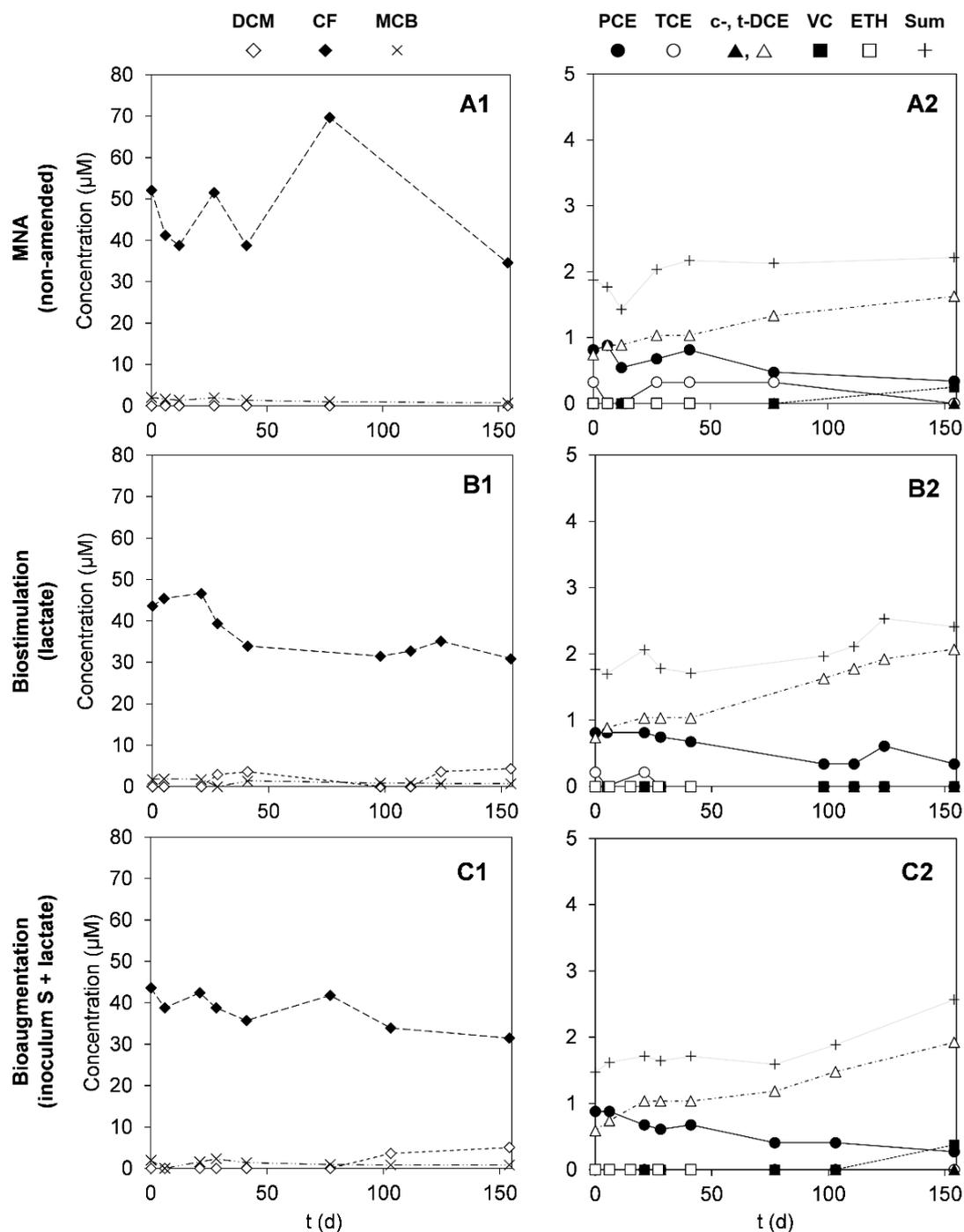
Figure 6.14. Time-course of contaminants in microcosms from well PZ-9. Data presented is from an individual microcosm, but it is representative of triplicates.
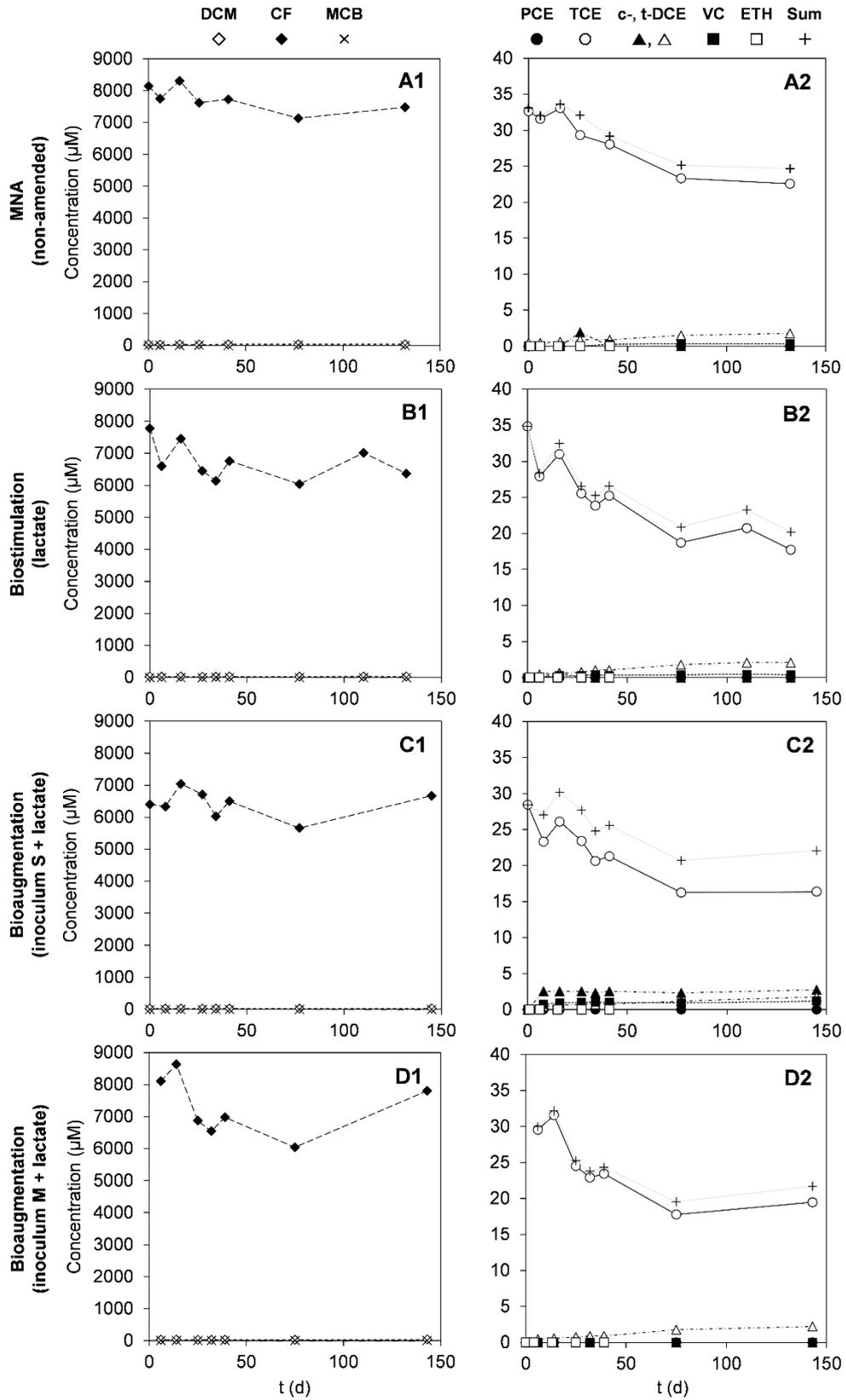
Figure 6.15. Time-course of contaminants in microcosms from well PZ-19. Data presented is from an individual microcosm, but it is representative of triplicates.
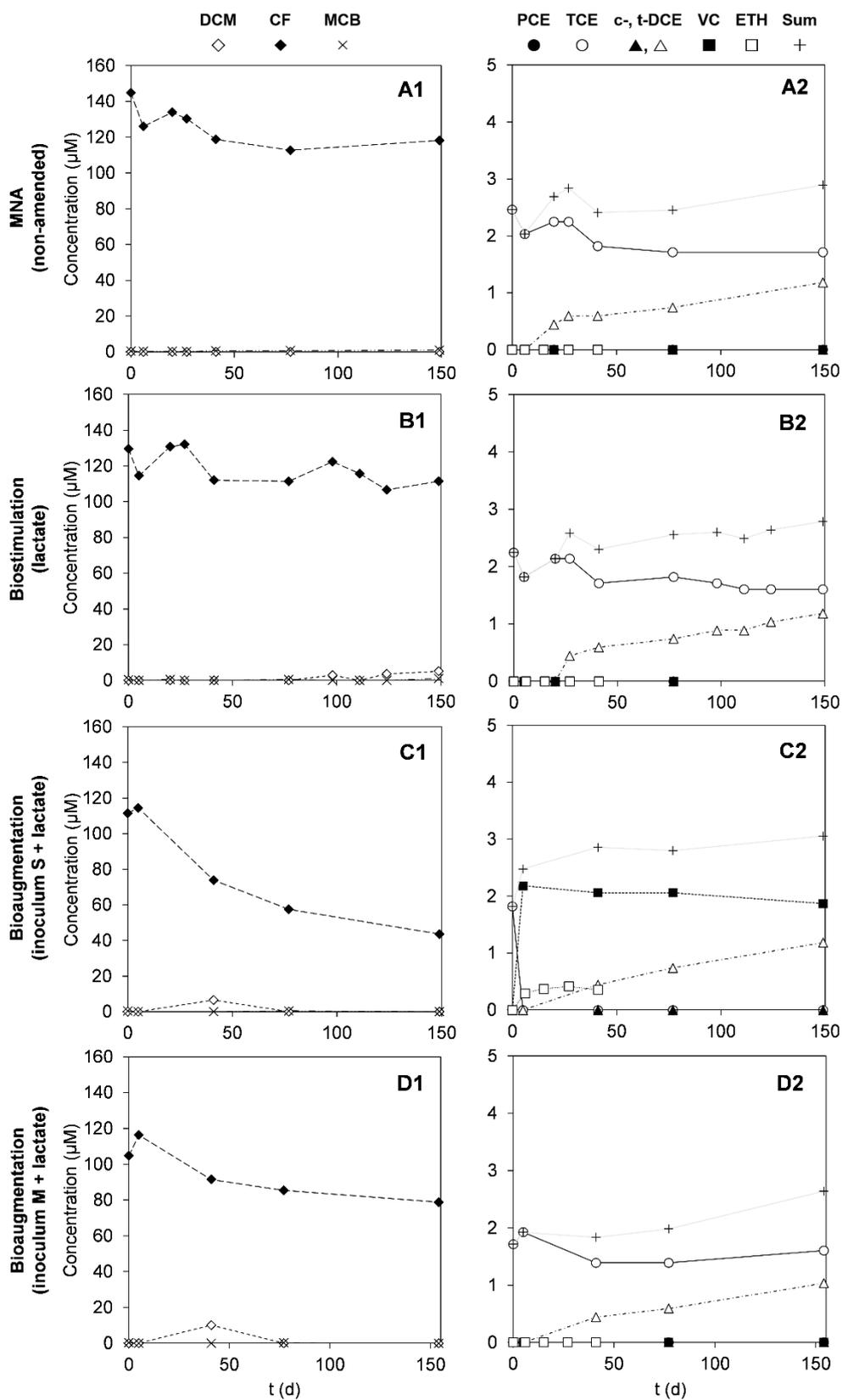
Figure 6.16. Time-course of contaminants in microcosms from well PZ-36. Data presented is from an individual microcosm, but it is representative of triplicates.
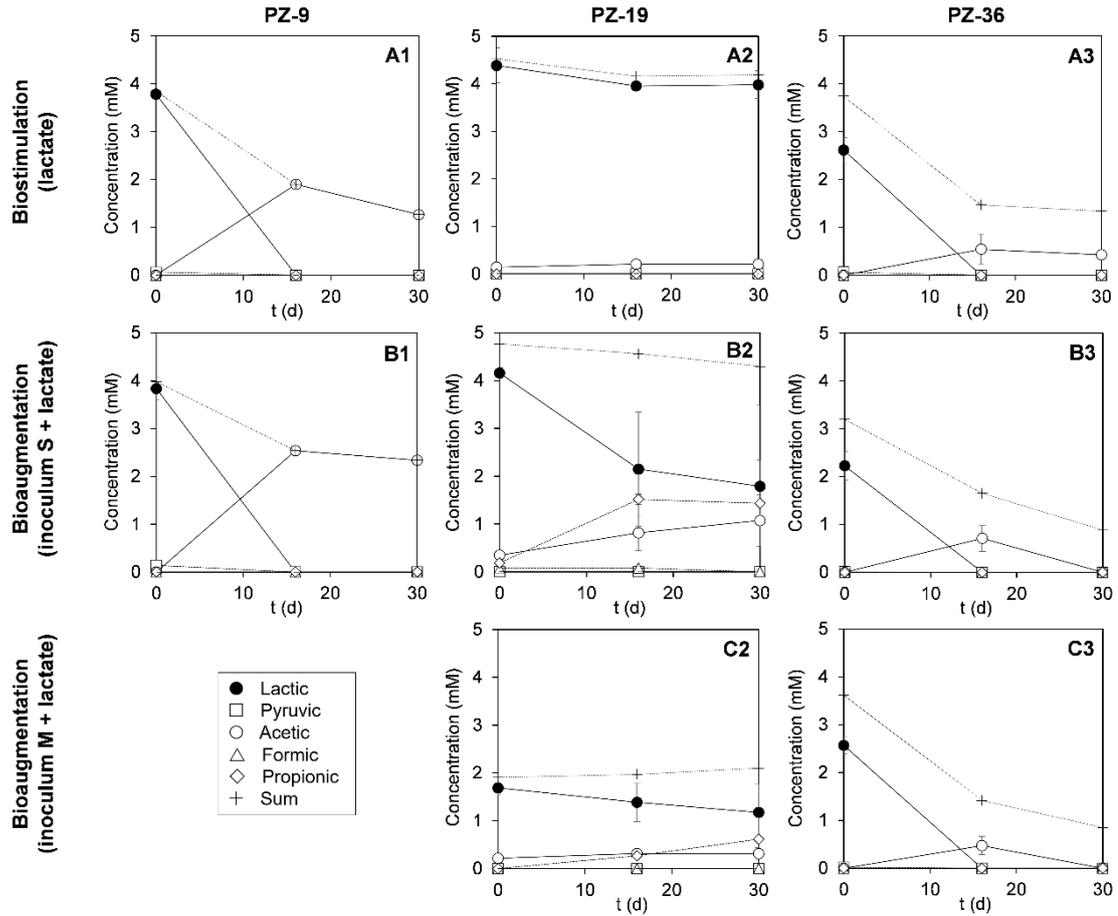
Figure 6.17. Time-course of VFAs in the microcosm experiments of Site 3. No VFAs were detected in the controls, except for traces of acetate in PZ19. Data is an average of triplicates and the 1σ.

In all, the results obtained with these microcosm experiments suggested that, under the studied conditions, degradation of contaminants was very slow and inefficient but possible to some extent, as demonstrated by the trace concentrations of some degradation by-products. Such conclusions agree with the information obtained from the isotopic field data that was discussed above.

Aiming to shed some light into the reactions that might be naturally occurring at this site, a dual C–Cl isotopic assessment was performed. In this case, it was based on the assumption that the original C–Cl composition of CF (CF_0) was of $\delta^{13}C$ = -45.1‰ (from well PZ-9) and $\delta^{37}Cl$ = -3.5‰ (from well PZ-10), as

they were the most depleted values measured (Figure 6.18A). As depicted in Figure 6.18B, the dual isotope fractionation pattern observed for CF was not consistent with the degradation of leaked commercial CF (orange area), which would be in agreement with the conclusions obtained from the microcosms. It should be noted, however, that $\delta^{37}Cl_{CF}$ values were enriched respect to CF_0 signature. This could be attributable to Cl isotope fractionation processes in the unsaturated zone due to diffusion-controlled vaporization (Jeannottat and Hunkeler, 2012; Palau et al., 2016) or to the leakage of CF from different providers with distinct isotopic signatures. Moreover, it must be considered that this release of CF was still active at the site and a potential CF degradation could be masked by a more depleted CF input. This scenario would agree with the fact that all measured C–Cl isotopic data points for CF fell within the range of commercial pure CF solvents (Figure 6.18B).

In the hypothetical case that CF were biologically degraded, and following the methodology described in section 6.2.7, the calculated isotopic range for DCM_{ini} (i.e. the formation of DCM from CF degradation) would range from -52.1‰ to -75.1‰ for carbon, and -3.5‰ for chlorine (Figure 6.18B). From those DCM_{ini} values, the area that would correspond to the formation of DCM from the degradation of CF was depicted (grey colour, Figure 6.18B). According to this, the isotopic composition of the DCM that was detected in groundwater (Table 6.7) was very enriched in both ^{37}Cl and ^{13}C compared to that of a hypothetical initial DCM that were produced by CF degradation (Figure 6.18B). In detail, DCM detected in well PZ-36 (with the highest DCM concentration, Figure 6.18A) was within the range of commercial DCM (Figure 6.18B), pointing to a potential release of DCM at the site. However, this DCM could be subject to a little biodegradation as acetate, the main by-product of DCM fermentation, was detected in the well PZ-36, and in PZ-18 as well (Table 6.6).
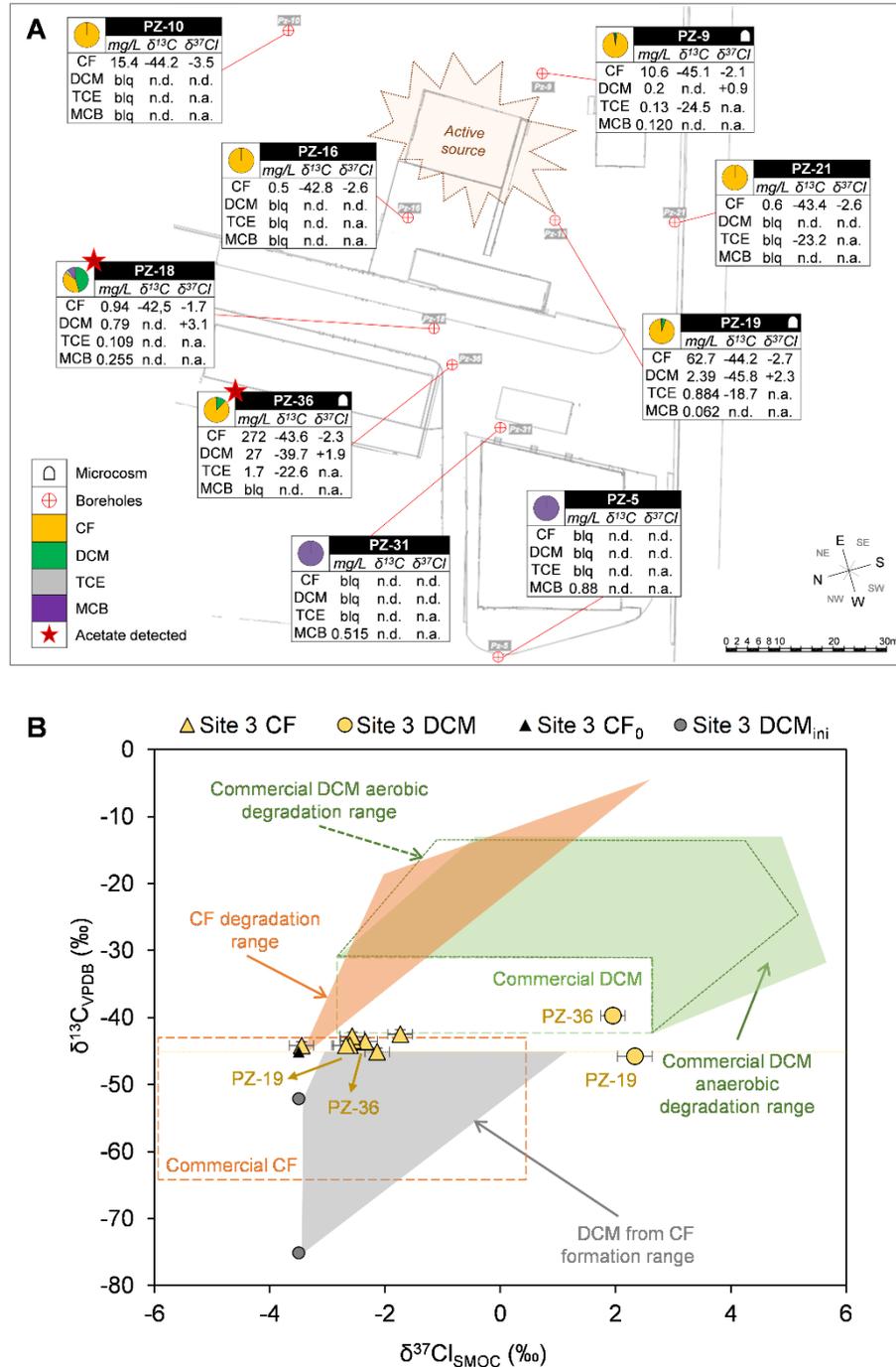
Figure 6.18. (A) Concentrations (in mg/L) and $\delta^{13}C$ and $\delta^{37}Cl$ compositions (in ‰) of CF, DCM, TCE and MCB from Site 3. Pie charts show the molar distribution of contaminants at each well. Detailed concentrations (in μM) and isotopic compositions are available in Tables 6.6 and 6.7, respectively. "n.d." means "could not be determined based on their low concentration"; "n.a." means "not analysed". (B) Dual C–Cl isotopic assessment for DCM and CF field data from Site 3. Both CF_0 and the range for DCM_{ini} are represented. Green and orange dashed rectangles depict the $\delta^{13}C$ and $\delta^{37}Cl$ ranges of commercial DCM and CF solvents, respectively (see Table 6.1 for details).

On its side, for well PZ-19, the $\delta^{13}C_{DCM}$ value that was measured was slightly depleted in ^{13}C, while the $\delta^{37}Cl_{DCM}$ value was slightly enriched in ^{37}Cl, compared to those measured in PZ-36 (Figure 6.18B). Such behaviour could be explained similarly to CF. On the one hand, DCM could be an impurity in the CF raw source, with its isotopic signature changing over time due to changes in CF providers or manufacturing processes. On the other, the isotopic composition of DCM could have changed by the effect of vaporization and diffusion processes in the unsaturated zone (Jeannottat and Hunkeler, 2012; Palau et al., 2016). As noted above, the release of CF (and probably DCM) was still active at the site.

Taking all these evidences into account, the extent of biodegradation (D%) was not estimated neither for CF nor DCM, as the results would not be representative of CF or DCM degradation processes.

6.4. Conclusions

The study presented in this chapter provides additional data on isotope C and Cl compositions for different commercial CMs, widening the known range for these solvents and proving the utility of these results for data interpretation. In addition, the C and Cl isotopic fractionation values for the anaerobic degradation of DCM by a *Dhb*-containing culture were also determined. These results enrich the available database that can be used by practitioners to provide diagnostic information about CMs biodegradation in contaminated aquifers. The value of $\Lambda^{C/Cl}$ obtained for the investigated *Dhb*-containing culture (5.9 ± 0.3) was right in between and was significantly different to those described for *Dhb f.* and D. elyunquensis, which would allow the distinction of these DCM degradation mechanisms through dual isotope analyses.

The pumping regimes that were active at both studied sites probably impacted the geographical distribution of the chlorinated compounds and their corresponding isotopic compositions. For this reason, the focus of this work was not on the flow path of the plume, but on the correlation between the isotopic composition of the chlorinated solvents and the biodegradation information obtained from microcosms experiments for each monitoring well. For this, the use of an integrative approach that combined C–Cl CSIA, laboratory microcosms, and 16S rRNA high-throughput sequencing demonstrated the intrinsic biodegradation potential of Site 2 to fully transform CF, DCM, and CEs, but not MCB. In contrast, results for Site 3 suggested that inhibition was preventing the efficient elimination of CMs, CEs and MCB at tested conditions. Nevertheless, the dual C–Cl isotopic assessment proved useful, as well, to elucidate the origin and fate of DCM and CF at both sites. Considering these results, a biostimulation (e.g. enhanced reductive dechlorination with lactate) could be applied at Site 2 to degrade both CMs and CEs. However, the persistence of MCB at this site, and the inhibition of biodegradation observed at Site 3, suggested that a treatment train (i.e. a combination or sequence of different remedial strategies targeting different groups of contaminants) could possibly be the optimal approach for the detoxification of these aquifers.

This work shows that such a multi-method approach allows for the collection of data that can help making decisions in the field. In this case, it is a valuable tool to evaluate the feasibility of biodegradation strategies to remediate chlorinated solvents in complex multi-contaminated aquifers, as it can provide the lines of evidence required to demonstrate whether bacteria can successfully detoxify groundwater and identify any potential setbacks. The microcosm tests can provide a positive indication that complete dechlorination can be achieved by native microbial populations and is useful to predict the effect of bioremediation treatments (biostimulation or bioaugmentation) to detoxify the

aquifer. Changes in carbon and chlorine isotope composition among the residual fraction of the chlorinated compounds in the monitoring wells can provide field evidence for microbial degradation. Lastly, the positive molecular identification of key organohalide-respiring bacteria (e.g. *Dehalobacter*) can provide additional evidence that chlorinated solvents can be fully dechlorinated in the aquifer. Notwithstanding, there is a need for additional laboratory studies that correlate the metabolism of microbial transformations with stable isotope fractionation of multiple elements to support the interpretation of CSIA data obtained from contaminated groundwaters, as well as the potential inhibitory effects of co-contaminants over bacteria degrading chlorinated solvents.

Chapter 7

General conclusions and future work

List of contents

7.1. General conclusions

The main objective of this thesis was to deepen the understanding of *in-situ* anaerobic bioremediation processes of chlorinated solvents and improve the application of these technologies at polluted sites. An integrative approach combining hydrogeochemical data, microcosm experiments, and molecular and isotopic techniques with samples from three different contaminated sites – from more simple (Site 1, old tetrachloroethene (PCE) spill) to more complex scenarios (multi-contaminant sites with no active source vs. active source, Site 2 and 3, respectively) – was used throughout this thesis, both at the laboratory and field scale, to achieve the specific objectives of this work.

The main achievements and general conclusions that can be drawn from this thesis are:

- Hydrogeochemical conditions of aquifers such as the redox potential (Eh) exert a primary control over anaerobic biodegradation reactions. This was observed at Sites 1 and 2, where the addition of an electron donor such as lactate was necessary to complete the reductive dechlorination of chlorinated ethenes (CEs) to ethene (ETH) by organohalide-respiring bacteria (OHRB). Without the electron donor, the accumulation of even more toxic intermediates was observed (dichloroethene (DCE) and vinyl chloride (VC) stall). Additionally, it was demonstrated that, in the *in-situ* pilot test at Site 1, the lactate addition induced the change from nitrate- to sulphate-reducing conditions, promoting the activity of anaerobic OHRB.

- Compound-specific stable isotope analysis (CSIA) is a versatile technique that proved useful at the three studied sites to monitor the biodegradation process and provide relevant information about the potential reactions taking place *in-situ*. In this thesis, CSIA was used i) to determine whether

biochemical transformations were naturally occurring in the studied aquifers, ii) to demonstrate that the enrichment of the database on the isotopic composition of pure phase chlorinated solvents and the isotopic fractionation during their degradation is a key point to properly interpret *in-situ* field data, iii) for source apportionment, and iv) as a qualitative tool to assess the extent and success of a biodegradation process (i.e. if detoxification is occurring). The last two were achieved in Site 1 through the calculation of the carbon isotopic mass balance of a family of contaminants (i.e. the parent compound and its degradation products) such as CEs. However, even with all these possibilities, CSIA still has some limitations when used alone. For instance, significant shifts in delta values can also indicate the leakage of solvents from different providers with distinct isotopic signatures, or Cl isotope fractionation processes in the unsaturated zone due to diffusion-controlled vaporization (as discussed for the results from Site 3). Moreover, the co-occurrence of different (bio)chemical transformations can result in the overlapping of each C–Cl isotopic plot, preventing the unequivocal identification of the responsible pathway or degrader. Additionally, the low isotopic fractionation produced by certain species, or the continuous leakage in scenarios where the source is still active, can mask *in-situ* biodegradation, which would need to be proved through other approaches.

- Techniques such as 16S rRNA metagenomics and polymerase chain reaction (PCR) are useful to identify bacterial species and enzymes associated with the detoxification of contaminants (e.g. *Dehalococcoides*, *Dehalobacter* and the *vcrA* gene in this thesis). These can be used as *in-situ* biomarkers to confirm the presence of the required genes for the complete biodegradation of the target pollutants. Moreover, such molecular

approaches are also useful to investigate the evolution of the microbial diversity during *in-situ* bioremediation treatments (e.g. after the addition of lactate in Site 1). However, these techniques present some limitations, such as the need of a minimum amount of DNA in order to detect those genes but, more importantly, that such detection does not confirm bacterial activity and, thus, the ability to perform the reaction. For this purpose, transcriptomic techniques are more appropriate.

- Field-derived microcosms (i.e. microcosms constructed with sampled groundwater) can fairly reproduce aquifer conditions and, thus, exhibit the processes that could take place *in-situ*. In addition, treatability studies (with microcosms) can anticipate the success, or failure, of a potential biostimulation or bioaugmentation field application before amendments (substrate or bacterial inoculum) are used in the field, which can save a lot of time and money. In this thesis, anoxic field-derived microcosms were established with groundwater from the three sites and, at Sites 1 and 2, confirmed that the addition of an organic fermentable substrate such as lactate was necessary to complete the degradation of the target contaminants. With these experiments, the accumulation of toxic intermediates was discarded, and the degradation pathways of the majority of the pollutants were identified. In contrast, the microcosms prepared with samples from Site 3 revealed a strong biodegradation inhibition (even with the commercial inoculum, possibly due to co-contamination), which suggested that both biostimulation and bioaugmentation remediation approaches would fail in the field.

- An integrative assessment of the field samples obtained with the techniques mentioned above allows an improved understanding of the groundwater ecosystem under study, so that strengths and weaknesses, in light of a future

bioremediation treatment, can be identified. For instance, at Site 3, the isotopic results and the hydrogeochemical data were not conclusive about the occurrence of natural biodegradation and was only with the microcosm experiments that inhibition issues were detected, even for a bioaugmentation strategy. Similarly, at Site 1, the lines of evidence for biodegradation obtained with the isotopic and molecular techniques pointed to a feasible natural attenuation and the potential for detoxification. However, only when integrating those conclusions with the hydrogeochemical data and the microcosms results, it became evident that i) PCE was not fractionating, but it was indeed naturally transformed, but only to ii) *cis*-DCE and VC, two toxic intermediates that accumulated due to the natural Eh conditions, and iii) the addition of lactate was necessary to complete the degradation of PCE to ETH efficiently. In addition, such an integrative laboratory study was able to predict the biodegradation process that was later observed at the field during the *in-situ* pilot test. This demonstrated the utility and reliability of the methodology for the assessment of the intrinsic biodegradation potential and, thus, the feasibility of bioremediation strategies at sites polluted by chlorinated solvents. For this reason, and based on these conclusions, the full-scale enhanced reductive dechlorination (ERD) with lactate was confidently applied by Litoclean, SL at Site 1.

- The diagnostic techniques that were used to gather the lines of evidence for biodegradation in the laboratory can also be used in the field for a proper monitoring of an *in-situ* biodegradation process. By using such a multi-method methodology in the *in-situ* pilot test at Site 1, all the relevant parameters were tracked and any deviation or setback in the process could be detected and addressed, if needed. For instance, hydrochemical data and

stable isotopes of sulphur and oxygen from sulphate indicated that the injection of electron donor promoted a shift towards sulphate-reducing conditions, required by OHRB to perform the reductive dechlorination of CEs. In line with this, the recovery of Eh to more positive values could indicate the need of an additional injection of electron donor in the near future if the biodegradation process is to be continued. Similarly, the combined use of chemical and isotopic data confirmed that biodegradation was occurring and discarded dilution processes as the reason behind the decrease in the concentration of metabolites. Lastly, molecular techniques confirmed that the conditioning of the aquifer modified the microbial community towards fermentative bacteria, which are responsible for the metabolism of the electron donor (i.e. lactate) and, thus, the release of hydrogen that is needed to promote all these microbial-mediated reactions.

In all, the conclusions obtained in this thesis support and validate the use of an integrative methodology such as the one used here to evaluate the feasibility and monitor bioremediation strategies in field studies, even with different degrees of complexity.

7.2. Future work

This thesis has covered many aspects related to the anaerobic biodegradation of chlorinated solvents and the application of bioremediation strategies in the field. For this reason, some of the limitations that need to be addressed in order to fully exploit the strengths of the microbe-mediated remediation approaches were also detected throughout this transdisciplinary investigation.

Some of these aspects that would need to be addressed, or further investigated, include:

- The assessment of the biodegradation potential of the most recalcitrant compound found in this study, monochlorobenzene (MCB) or other industry or fuel-originated co-contaminants frequently detected in aquifers such as the fuel oxygenates methyl tert-butyl ether (MTBE) and ethyl tert-butyl ether (ETBE); benzene, toluene, ethylbenzene and the three xylene isomers (BTEX); total petroleum hydrocarbons (TPH); and insecticides and pesticides, among others. For instance, Sites 2 and 3 were two complex multi-contaminated sites and, in this thesis, chlorinated solvents were the main target substances. However, in order to achieve complete detoxification, these other organic contaminants should be targeted as well. Thus, their biodegradability and potential co-metabolism in the hydrogeochemical conditions of the aquifers should be investigated, possibly through a diagnostic study such as the one performed for the chlorinated solvents.

- The effect of co-contamination in aquifers of Sites 2 and 3 on the degrading bacteria and the potential degradation processes that may occur in complex multi-contaminated aquifers. These type of interactions among contaminants and microorganisms have not been thoroughly studied yet but are very relevant, as they can compromise the bioremediation success, for example, due to inhibition issues.

- The efficient application of consecutive remediation strategies to optimize the detoxification of aquifers, for instance, with the use of treatment-train approaches. The bioremediation of a multi-contaminated aquifer could be dependent on the presence of different bacteria which, in turn, could require diverse hydrogeochemical aquifer conditions. In this sense, the treatment train could include the addition of several stimulants to adequate

aquifer conditions to the different native bacteria, or combine biotic with abiotic techniques, such as zero-valent iron (ZVI), *in-situ* chemical oxidation (ISCO) or *in-situ* chemical reduction (ISCR), to create a synergy among the different remediation strategies used and take advantage of the cooperative interactions that might occur. For example, carbon tetrachloride (CT) could be the inhibitor in Site 3, therefore, it should be targeted and eliminated first, maybe with the addition of vitamin B_{12} (Rodríguez-Fernández et al., 2018a), which could be used later for the biodegradation of other families of contaminants such as CEs. Another interesting aspect of treatment trains would be the combination of oxic and anoxic strategies (e.g. aerobic and anaerobic biodegradation), considering the different redox conditions that can be found along a contamination plume, and the diversity of degradation mechanisms of the metabolites that can potentially be produced.

- Basic science, which would support applied science and the bioremediation decision-making process. In this regard, it is necessary to find new degradation mechanisms of the chemical substances that are extensively used in industries and frequently detected in the subsoil and groundwater (e.g. at Sites 2 and 3). Research should include the investigation of new biomarkers, both for the bacteria and functional enzymes that degrade these contaminants, which may be present at the studied sites but have not been considered because they have not been described yet. Additionally, the study of the multi-element isotopic fractionation of new degrading bacteria, or bacteria that are specific from studied sites, will be useful in the interpretation of field data and the design of an appropriate remediation strategy.

- Funding for applied research and for research collaborations between universities, or research institutes, and companies. The bioremediation

technology is a mature, efficient and solid science that has been studied for decades but, sadly, the percentage of aquifers that have been remediated through biological treatments is still very low in Catalonia. In the author's opinion, this is due to the gap between science and industry, which could be bridged by promoting applied research and knowledge transfer among the responsible administration/authorities, consultancies, and academia. Such collaborations would have an impact on the actual application of *in-situ* bioremediation, as demonstrated with the results obtained in this thesis.

Acknowledgements – Agradecimientos – Agraïments

Primer de tot, voldria agrair a tots els involucrats (que no sé exactament qui són) la creació d'aquesta gran oportunitat que ha significat tant per a mi, tant de Litoclean com de la Universitat Autònoma de Barcelona. I, en especial, al programa de Doctorats Industrials, que ha sabut generar un espai molt necessari d'investigació, desenvolupament i de col·laboració entre empresa i universitat. No sabeu els anys que feia que ho buscava.

Voldria aturar-me un moment i fer una menció molt especial als meus directors de tesi "oficials", l'Ernest Marco, la Teresa Vicent i la Mònica Rosell, i als "no tant oficials" però que han tingut un paper igualment rellevant, el Marçal Bosch i el Joan Varias, de Litoclean. Us agraeixo de tot cor l'oportunitat que em vau brindar fa tres anys i *pico*, el lideratge, l'ajuda i recolzament, els diàlegs i els debats, els bon moments, l'honestedat i, sobretot, l'immens coneixement que m'enduc. He gaudit d'aquest projecte com si fos una nena que ha rebut el regal de reis que demanava. És el que volia. I tot i que hi ha hagut ratxes una mica *durilles*, em sap molt greu que s'acabin les piles de la meva joguina preferida. Per sort, em sembla que he trobat piles de recanvi. Moltes, moltes i moltes gràcies.

A més, he tingut la sort de col·laborar amb molta gent i amb la que les he vist de varis colors. Sota la pluja, *plagats* de mosques, mostrejos que surten fatal, equips que es rebel·len contra nosaltres, i també grans sessions de solàrium perfumat a quasi 40ºC de temperatura i vestits amb uns *monos* blancs que eren *estupendos*. També les hem vist de molts colors, en aquest cas sobre la taula: amanida de xató, la paella dels dijous, l'escudella, la sèpia a la planxa i, com no, les galtes. No em queixo pas, tot al contrari, més records per l'àlbum del doctorat. Per tant, Marc i Sergi (Litoclean), i Roger i Diana (UB): *a sus pies*.

També vull agrair a l'Albert Soler i al Jordi Palau tot el seu *input*. El significat darrera d'aquesta paraula no té res a veure amb les poques lletres que la formen. *Bua*, el que és aprendre molt i adonar-se que no en saps prou encara. M'encanta.

Gràcies a tots els membres del grup de recerca BioRem (ehem, tòxics), som poquets però ben avinguts. Que algú li tradueixi al Kaidi :) Al David, Jesica, Oriol, Aina, Jan, Diego i Marta... gràcies per salvar-me la vida tantes i tantes vegades. Siti: *thank you for teaching me how to deal with those devils and showing me the way. You and your work motivated me a lot when I still didn't know what I was doing (not saying that I do now).* Alba: *otra de las que he aprendido mogollón y aún siento que no sé nada. Aún hoy, pienso: tengo que preguntárselo a Alba. Lo siento porque me voy a quedar corta. Se me amontonan las cosas y no sé cuál es la más representativa. Así que lo voy a dejar en "gracias por ser mi guía espiritual, mi inspiración y aspiración, y mi fuente de conocimiento". Muchas gracias y mucha suerte.*

He d'agrair també a totes les persones que han col·laborat en aquest treball d'una forma o altra: Pilar, Pili, Anna, Cristina, Clara, Sara, Marc, Manuel, Pili i Rosi. I faig extensa aquesta gratitud a tot el Departament d'Enginyeria Química, Biològica i Ambiental de la UAB, com el Departament de Mineralogia, Petrologia i Geologia Aplicada de la UB.

Special thanks to Orfan Shouakar-Stash from Isotope Tracer Technologies, Inc. for the crazy opportunity that he gave me. It was only for two months, but the whole thing felt like it was a lot more. I felt super welcomed from the first second. Thank you for the knowledge, the scientific contribution and the life experience. The feelings that come to mind are "good vibes" and "warmth", so I guess that's a great sign considering that I almost froze to death :) I must mention the amazing people that worked there and made me feel like I was one of you, so: Irem, Nart, Adam, Jackie, Richard, Mirna, and Shamila... Thaaaaaaank you. IT² people, I miss the beer, the wings!, the burgers, the shawarmas... and you, of course. It was great fun.

Sylwia: THANK YOU. Thank you for being my sister and friend while I was in Waterloo. That didn't feel like a two-month relationship. It was all very cheesy-movie-like. I had a great time, you were an amazing host, an amazing roomie, and amazing overall. I can't thank you enough and your family, really. I'm counting the days to see you again. Like, truly.

A tots els companys del dia a dia al DEQBA i "víctimes" del doctorat: ¡*sí se puede*!

Thank you to all the international people that I've met along the years (in Copenhagen, Uppsala, New Zealand, or wherever we were at the time) and are dear to my heart: you give me hope (it's a long story...). Thank you for leaving your mark on me, it's made me who I am. Special mention to Nathalie, Denis, Dimitry, Henni and Jenni: I expect to see you all relatively soon. No option here. Gracias también a Ana, Rochi, Cris, i a la Sílvia, la Sara i la Sandra. Esteu dins del sac internacional :)

Merci a totes aquelles persones que em coneixeu de fa molt temps, amb qui hem compartit moltes coses i en seguim compartint, encara que sigui massa de tant en tant. Ja sabeu com sóc. La vida, de vegades, no és gaire agradable, però es fa menys difícil amb vosaltres a prop. Merci a tots. Hem connectat!

A las locas del patinaje: gracias por darme vida, vidilla, locura, cordura, y de todo, en cada segundo que compartimos. Ya sea en el foro, en los chats, en París, Barcelona, Estocolmo, Viena, Bratislava, Marsella, Vielha, Ostrava, Helsinki, Milán, Hannover... esperad que miro la agenda: Zaragoza, Graz, Valladolid... y todo lo que queda por venir. Os amo. Firmado: Jodidas pero contentas.

Al *tantu* que ve la *frikada*: voldria agrair també i esmentar a les persones i/o personalitats que van encendre la flama, m'han inspirat professionalment al llarg del temps i que han fet que, gràcies al seu granet de sorra en el seu moment, avui sigui on sóc i encara no m'hagi rendit del tot. *Voy a ello*: el Capità Enciam, Jordi Carmona, Francesc Vélez, Joan Puig, Dian Fossey, Cristina Yacoub, Brian Huser,

Javier Fernández, Aljona Savchenko, Jane Goodall i Dian Fossey mil vegades més. El més sincer dels agraïments. *Gracias. Danke. Thank you.*

La família. La família és complicada, molt maca, però complicada. Però per molt complicada que sigui, me l'estimo molt. Què hi farem. En els tres anys i *pico* del doctorat... hem rebut uns quants pals. N'havíem rebut abans, però aquests s'han notat més i ha sigut tot una mica muntanya russa. Però els sotracs a vegades porten coses bones, i aquest ha estat el meu cas. Així doncs, brindo perquè seguim creixent, aprenent i gaudint tots junts. I a l'Enric i a la Júlia, un *xupito* gratis.

I, per acabar, gràcies a la persona que fa més de mitja vida que és amb mi, al meu costat. M'has ensenyat, ajudat, encoratjat, recolzat, acompanyat, suportat, criticat, entès, m'has fet riure i plorar (de riure també) i mil verbs més. Hem crescut junts, viatjat i compartit moltes experiències. A vegades, les coses no han estat gens fàcils però, probablement, no seria aquí si no fos per tu. Per tot això, i molt més... ILD.

Curriculum vitae of the author

Natàlia Blázquez Pallí

Contact information: blazquez.palli@gmail.com

PhD candidate

Doctorats Industrials predoctoral grant (2015). Starting date: April 4th, 2016. Joint industrial PhD project between Litoclean, S.L. and BioRem Research Group from Departament d'Enginyeria Química, Biològica i Ambiental at Escola d'Enginyeria of Universitat Autònoma de Barcelona (UAB), Barcelona (Spain). Student of the Environmental Science and Technology PhD program.

Research stay at Isotope Tracer Technologies, Inc. (Waterloo, ON, Canada) under the supervision of Dr. Orfan Shouakar-Stash (Dec 2017 – Feb 2018).

Thesis title: "*Assessing the feasibility of bioremediation strategies in aquifers polluted by chlorinated solvents*". Supervisors: Dr. Ernest Marco Urrea, Dra. M. Teresa Vicent Huguet, and Dra. Mònica Rosell Linares.

Previous research experience

Jan 2015 – Jun 2015. Research student at the Department of Aquatic Sciences and Assessment of the Swedish University of Agricultural Sciences (SLU). Research on remediation and restoration strategies to reduce eutrophication in Swedish lakes. The work developed there was within the master thesis of the MSc in Agriculture and Environmental Science by University of Copenhagen and SLU. Thesis title: "*A comparison of two methods to reduce internal phosphorus cycling in lakes: aluminium versus phoslock*". Supervisor: Brian Huser.

Mar 2013 – May 2013. Research assistant at the Chemical Engineering Department of Universitat Politècnica de Catalunya (UPC). Research on the environmental conditions and ecological risks related with mining activities in the Andean region.

Jan 2011 – Oct 2012. Research student at the Chemical Engineering Department of Universitat Politècnica de Catalunya (UPC). Research on the spatial and temporal distribution of trace metals in a Peruvian river basin. The work developed there was within the final thesis of the Chemical Engineering degree by UPC. Thesis title: "*Study of the content of trace metals in the Jequetepeque basin, Peru*". Supervisor: Cristina Yacoub.

List of peer-reviewed publications

N. Blázquez-Pallí, M. Rosell, J. Varias, M. Bosch, A. Soler, T. Vicent, E. Marco-Urrea. *Integrative isotopic and molecular approach for the diagnosis and implementation of an efficient in-situ enhanced biological reductive dechlorination of chlorinated ethenes.* **Submitted** to the journal Water Research.

N. Blázquez-Pallí, O. Shouakar-Stash, J. Palau, A. Trueba-Santiso, J. Varias, M. Bosch, A. Soler, T. Vicent, E. Marco-Urrea, M. Rosell (2019). *Use of dual element isotope analysis and microcosm studies to determine the origin and potential anaerobic biodegradation of dichloromethane in two multi-contaminated aquifers.* Science of the Total Environment 696, 134066. DOI: 10.1016/j.scitotenv.2019.134066.

N. Blázquez-Pallí, M. Rosell, J. Varias, M. Bosch, A. Soler, T. Vicent, E. Marco-Urrea (2019). *Multi-method assessment of the intrinsic biodegradation potential of an aquifer contaminated with chlorinated ethenes at an industrial area in Barcelona (Spain).* Environmental Pollution 244, 165–173. DOI: 10.1016/j.envpol.2018.10.013.

C. Yacoub, N. Blazquez, A. Pérez-Foguet, N. Miralles (2013). *Spatial and temporal trace metal distribution of a Peruvian basin: recognizing trace metal sources and assessing the potential risk.* Environmental Monitoring and Assessment 185, 10, 7961–7978. DOI: 10.1007/s10661-013-3147-x.

Other publications

N. Blázquez-Pallí, O. Shouakar-Stash, J. Palau, A. Trueba-Santiso, J. Varias, M. Bosch, A. Soler, T. Vicent, E. Marco-Urrea, M. Rosell (2019). *Dual C–Cl isotopic assessment to elucidate origin, fate, and potential bioremediation treatment of chlorinated methanes at two industrial multi-contaminated aquifers.* Poster presented in the AquaConSoil 2019 conference. DOI: 10.13140/RG.2.2.20562.09921.

N. Blázquez Pallí (2016). *Ecological restoration? Yes, but to what extent?* EcoLincNZ student blog about ecology from Lincoln University (Canterbury, New Zealand). http://www.lincolnecology.org.nz/?p=1764.

N. Blázquez Pallí (2015). *A comparison of two methods to reduce internal phosphorus cycling in lakes: aluminium versus phoslock* (MSc thesis). Available from Epsilon Archive for Student Projects. http://stud.epsilon.slu.se/8596/.

N. Blázquez Pallí (2012). *Estudio de la afectación de los metales traza en la cuenca del Jequetepeque, Perú* (Final thesis). Available from UPCommons, UPC's institutional repository. http://hdl.handle.net/2099.1/17090.

Presenter on scientific conferences

AquaConSoil 15th International Conference. **Oral presentation**: *Enhanced anaerobic bioremediation of a site contaminated with chlorinated ethenes: from lab studies to full-scale implementation.* 20th – 24th May, 2019. Antwerp, Belgium.

AquaConSoil 15th International Conference. **Poster presentation**: *Dual C–Cl isotopic assessment to elucidate origin, fate, and potential bioremediation treatment of chlorinated methanes at two industrial multi-contaminated aquifers.* First prize of the Poster Awards issued by Prof. Dr. Ir. Huub Rijnaarts, Chairman of AquaConSoil 2019. 20th – 24th May, 2019. Antwerp, Belgium.

AquaConSoil 14th International Conference. **Oral presentation**: *Assessment of the bioremediation potential of groundwater contaminated with chlorinated solvents and enhanced reductive dechlorination pilot test at an industrial site in Barcelona (Spain).* 26th – 30th June, 2017. Lyon, France.

Technical seminar "*El uso de los isótopos en la resolución de problemas de contaminación ambiental*" organized by MAiMA of Universitat de Barcelona. **Oral presentation**: *Bioremediación in-situ de acuíferos contaminados per organoclorados (decloración de organoclorados mediante bacterias dehalorespiradores).* 26th April, 2017. Barcelona (Spain).

Conference "*R+D+i en l'aplicació de tecnologies de la descontaminació del subsòl. Casos pràctics*" organized by Agència de Residus de Catalunya. Oral presentation: *Bioremediació in-situ d'aqüífers contaminats per organoclorats (decloració d'organoclorats mitjançant bacteris dehalorespiradors).* 9th – 10th March, 2017. Barcelona, Spain.

Attendee on scientific conferences

Seminar *"Bacterial degradation of dichloromethane: ongoing work on long-standing blindspots"* by S. Vuilleumier from University of Strasbourg (France). 5th April, 2018. Barcelona, Spain.

Seminar *"Distribution of Dehalococcoides in marine sediments and strategies for their enrichment"* by C. Algora Gallardo from the Department of Isotope Biogeochemistry of UFZ Helmholzt Institut of Leipzig (Germany). 13th April, 2016. Barcelona, Spain.

ELLS Scientific Student Conference 2014 *"Brave new thinking, brave new sciences, brave new world"* organized by Warsaw University of Life Sciences. 14th – 15th November, 2014. Warsaw, Poland.

Education

2015. Summer School in *Ecological Restoration: remediation of degraded and contaminated land.* Lincoln University (Lincoln, Canterbury, New Zealand).

2015. Double degree MSc in Agriculture and Environmental Science, with the *Land Use, Soil and Water Resources* specialization. The MSc belongs to the EnvEuro program (European Master in Environmental Science). University of Copenhagen (Copenhagen, Denmark) and Swedish University of Agricultural Sciences (Uppsala, Sweden). 120 ECTS.

2012. Chemical Engineering. Universitat Politècnica de Catalunya. Barcelona, Spain. 302 ECTS.

Professional experience

June 2019 – Present. R+D+i, quantitative risk assessment, subsoil investigation, and soil and groundwater remediation. Litoclean, Barcelona (Spain).

Oct 2015 – Apr 2016. Writer, editor and designer of teaching guidelines for chemistry courses at secondary school level. Editorial Vicens Vives, Barcelona (Spain).

Dec 2015 – Mar 2016. Online teacher and tutor in environmental courses and programs. Fundación Universitaria Iberoamericana (FUNIBER), Barcelona (Spain).

Sep 2012 – Jun 2015. English translator (finance and accounting). Blázquez, Planas i Associats, Barcelona (Spain).

Sep 2012 – Jul 2013. Junior auditor (finance and accounting). Blázquez, Planas i Associats, Barcelona (Spain).

Nov 2004 – Nov 2012. Artistic roller-skating coach / teacher and supervisor of sport activities. Associació Esportiva l'Eixample, Barcelona (Spain).

Sep 2011 – Jul 2012. Internship. Integrated management systems (quality, environment and safety). Reciclajes Rodilla, Sant Adrià de Besòs (Spain).

Nov 2009 – Jul 2011. Internship. Administration and archive. SIAE, Universitat Politècnica de Catalunya, Barcelona (Spain).

Voluntary experience and causes

Present. *Conservation International*, *Greenpeace*, *World Wildlife Fund*, *The Dian Fossey Gorilla Fund*.

Present. Figure skating writer at an online sports blog. Sexto Anillo.

Present. Staff at an online figure skating forum. Peña Ariquitaun.

April 2017. Catering team during the ISU World Figure Skating Championships 2017, Helsinki (Finland).

2005 – 2012. *Intermon Oxfam*.

May 2003 – Jul 2007. Director and supervisor at a children and youth association. Esplai l'Olivera Rodona, Barcelona (Spain).

References

A

ACA, 2017. La contaminació de les aigües subterrànies a Catalunya.

ACA, 2010. Valors genèrics per a la restauració d'aigües subterrànies en emplaçaments contaminats per fonts d'origen puntual.

ACA, 2009. Criteris d'aplicació dels valors genèrics per a la restauració d'aigües subterrànies en emplaçaments contaminants per fonts d'origen puntual.

Achenbach, L.A., Michaelidou, U., Bruce, R.A., Fryman, J., Coates, J.D., 2001. *Dechloromonas agitata* gen. nov., sp. nov. and *Dechlorosoma suillum* gen. nov., sp. nov., two novel environmentally dominant (per)chlorate-reducing bacteria and their phylogenetic position. Int. J. Syst. Evol. Microbiol. 51, 527–533. https://doi.org/10.1099/00207713-51-2-527

Adrian, L., Löffler, F.E., 2016a. Organohalide-Respiring Bacteria—An Introduction, in: L. Adrian and F.E. Löffler (Ed) Organohalide-Respiring Bacteria. Springer Berlin Heidelberg, Berlin, Heidelberg, pp. 3–6. https://doi.org/10.1007/978-3-662-49875-0_1

Adrian, L., Löffler, F.E., 2016b. Organohalide-Respiring Bacteria, Organohalide-Respiring Bacteria. Springer Berlin Heidelberg, Berlin, Heidelberg. https://doi.org/10.1007/978-3-662-49875-0

Adrian, L., Löffler, F.E., 2016c. Outlook-the next frontiers for research on organohalide-respiring bacteria, in: L. Adrian and F.E. Löffler (Ed) Organohalide-Respiring Bacteria. Springer Berlin Heidelberg, Berlin, Heidelberg, pp. 621–627. https://doi.org/10.1007/978-3-662-49875-0_26

Adrian, L., Manz, W., Szewzyk, U., Görisch, H., 1998. Physiological characterization of a bacterial consortium reductively dechlorinating 1,2,3- and 1,2,4-trichlorobenzene. Appl. Environ. Microbiol. 64, 496–503.

Aelion, C.M., Höhener, P., Hunkeler, D., Aravena, R., 2009. Environmental isotopes in bioremediation and biodegradation. CRC Press, Boca Raton. https://doi.org/10.1159/000076616

Aeppli, C., Berg, M., Cirpka, O.A., Holliger, C., Schwarzenbach, R.P., Hofstetter, T.B., 2009. Influence of mass-transfer limitations on carbon isotope fractionation during microbial dechlorination of trichloroethene. Environ. Sci. Technol. 43, 8813–8820. https://doi.org/10.1021/es901481b

Aeppli, C., Hofstetter, T.B., Amaral, H.I.F., Kipfer, R., Schwarzenbach, R.P., Berg, M., 2010. Quantifying in situ transformation rates of chlorinated ethenes by combining compound-specific stable isotope analysis, groundwater dating, and carbon isotope mass balances. Environ. Sci. Technol. 44, 3705–3711. https://doi.org/10.1021/es903895b

Alfán-Guzmán, R., Ertan, H., Manefield, M., Lee, M., 2017. Isolation and characterization of *Dehalobacter* sp. strain TeCB1 including identification of *TcbA*: a novel tetra- and trichlorobenzene reductive dehalogenase. Front. Microbiol. 8, 558. https://doi.org/10.3389/fmicb.2017.00558

Alvarez, P.J.J., Illman, W.A., 2005a. Bioremediation technologies, in: Alvarez, P. J. J. and Illman, W. A. (Ed) Bioremediation and Natural Attenuation. John Wiley & Sons, Inc.,

Hoboken, NJ, USA, pp. 351–455. https://doi.org/10.1002/047173862X.ch8

Alvarez, P.J.J., Illman, W.A., 2005b. Introduction to bioremediation, in: Alvarez, P. J. J. and Illman, W. A. (Ed) Bioremediation and Natural Attenuation. John Wiley & Sons, Inc., Hoboken, NJ, USA, pp. 1–23. https://doi.org/10.1002/047173862X.ch1

Antler, G., Turchyn, A. V, Rennie, V., Herut, B., Sivan, O., 2013. Coupled sulfur and oxygen isotope insight into bacterial sulfate reduction in the natural environment. Geochim. Cosmochim. Acta 118, 98–117. https://doi.org/10.1016/j.gca.2013.05.005

ARC, 2016. Memòria de l'Agència de Residus de Catalunya 2016.

ARC, 2015. Memòria de l'Agència de Residus de Catalunya 2015.

ARC, 2014. Memòria de l'Agència de Residus de Catalunya 2014.

ARC, 2013. Memòria de l'Agència de Residus de Catalunya 2013.

ARC, 2012. Memòria de l'Agència de Residus de Catalunya 2012.

Atashgahi, S., Lu, Y., Smidt, H., 2016. Overview of known organohalide-respiring bacteria-phylogenetic diversity and environmental distribution, in: L. Adrian and F.E. Löffler (Ed) Organohalide-Respiring Bacteria. Springer Berlin Heidelberg, Berlin, Heidelberg, pp. 63–105. https://doi.org/10.1007/978-3-662-49875-0_5

Atlas, R.M., Philp, J.C., 2005. Bioremediation of contaminated soils and aquifers, in: Atlas, R. M. and Philp, J. C. (Ed) Bioremediation. American Society of Microbiology, pp. 139–236. https://doi.org/10.1128/9781555817596.ch5

ATSDR, 2017. Substance Priority List [WWW Document]. Agency Toxic Subst. Dis. Regist. URL https://www.atsdr.cdc.gov/SPL/index.html#2017spl (accessed 4.17.19).

Audí-Miró, C., Cretnik, S., Torrentó, C., Rosell, M., Shouakar-Stash, O., Otero, N., Palau, J., Elsner, M., Soler, A., 2015. C, Cl and H compound-specific isotope analysis to assess natural versus Fe(0) barrier-induced degradation of chlorinated ethenes at a contaminated site. J. Hazard. Mater. 299, 747–754. https://doi.org/10.1016/j.jhazmat.2015.06.052

Aulenta, F., Pera, A., Rossetti, S., Petrangeli Papini, M., Majone, M., 2007. Relevance of side reactions in anaerobic reductive dechlorination microcosms amended with different electron donors. Water Res. 41, 27–38. https://doi.org/10.1016/j.watres.2006.09.019

B

Badin, A., Broholm, M.M., Jacobsen, C.S., Palau, J., Dennis, P., Hunkeler, D., 2016. Identification of abiotic and biotic reductive dechlorination in a chlorinated ethene plume after thermal source remediation by means of isotopic and molecular biology tools. J. Contam. Hydrol. 192, 1–19. https://doi.org/10.1016/j.jconhyd.2016.05.003

Badin, A., Buttet, G., Maillard, J., Holliger, C., Hunkeler, D., 2014. Multiple dual C–Cl isotope patterns associated with reductive dechlorination of tetrachloroethene. Environ. Sci. Technol. 48, 9179–9186. https://doi.org/10.1021/es500822d

Barul, C., Fayossé, A., Carton, M., Pilorget, C., Woronoff, A.-S., Stücker, I., Luce, D., 2017. Occupational exposure to chlorinated solvents and risk of head and neck cancer in men: a population-based case-control study in France. Environ. Heal. 16, 77.

https://doi.org/10.1186/s12940-017-0286-5

Bhatt, P., Kumar, M.S., Mudliar, S., Chakrabarti, T., 2007. Biodegradation of chlorinated compounds—A review. Crit. Rev. Environ. Sci. Technol. 37, 165–198. https://doi.org/10.1080/10643380600776130

Bloom, Y., Aravena, R., Hunkeler, D., Edwards, E.A., Frape, S.K., 2000. Carbon isotope fractionation during microbial dechlorination of trichloroethene, cis-1,2-dichloroethene, and vinyl chloride: implications for assessment of natural attenuation. Environ. Sci. Technol. 34, 2768–2772. https://doi.org/10.1021/es991179k

Boada, L.D., Zumbado, M., Henríquez-Hernández, L.A., Almeida-González, M., Álvarez-León, E.E., Serra-Majem, L., Luzardo, O.P., 2012. Complex organochlorine pesticide mixtures as determinant factor for breast cancer risk: a population-based case–control study in the Canary Islands (Spain). Environ. Heal. 11, 28. https://doi.org/10.1186/1476-069X-11-28

Bombach, P., Richnow, H.H., Kästner, M., Fischer, A., 2010. Current approaches for the assessment of in situ biodegradation. Appl. Microbiol. Biotechnol. 86, 839–852. https://doi.org/10.1007/s00253-010-2461-2

Bouwer, E.J., 1994. Bioremediation of chlorinated solvents using alternate electron acceptors, in: Norris, R. D. (Ed) Handbook of Bioremediation. CRC Press, Boca Raton, pp. 149–176. https://doi.org/10.1201/9780203712764-9

Bradley, P.M., 2003. History and ecology of chloroethene biodegradation: a review. Bioremediat. J. 7, 81–109. https://doi.org/10.1080/713607980

Bradley, P.M., 2000. Microbial degradation of chloroethenes in groundwater systems. Hydrogeol. J. 8, 251–253. https://doi.org/10.1007/s100400050011

Breider, F., 2013. Investigating the origin of chloroform in soils and groundwater using carbon and chlorine stable isotopes analysis. Université de Neuchâtel (Switzerland).

Breider, F., Hunkeler, D., 2014. Investigating chloroperoxidase-catalyzed formation of chloroform from humic substances using stable chlorine isotope analysis. Environ. Sci. Technol. 48, 1592–1600. https://doi.org/10.1021/es403879e

Brown, R.A., 2010. Chemical oxidation and reduction for chlorinated solvent remediation, in: H. F. Stroo and C. H. Ward (Ed) In Situ Remediation of Chlorinated Solvent Plumes. Springer, New York, NY, pp. 481–535. https://doi.org/10.1007/978-1-4419-1401-9_15

Brown, R.A., Mueller, J.G., Seech, A.G., Henderson, J.K., Wilson, J.T., 2009. Interactions between biological and abiotic pathways in the reduction of chlorinated solvents. Remediat. J. 20, 9–20. https://doi.org/10.1002/rem.20226

Buchner, D., Behrens, S., Laskov, C., Haderlein, S.B., 2015. Resiliency of stable isotope fractionation (δ^{13}C and δ^{37}Cl) of trichloroethene to bacterial growth physiology and expression of key enzymes. Environ. Sci. Technol. 49, 13230–13237. https://doi.org/10.1021/acs.est.5b02918

C

Carson, R., 1962. Silent spring, 1st ed. Houghton Mifflin.

Carter, J.M., Lapham, W.W., Zogorski, J.S., 2008. Occurrence of volatile organic compounds in aquifers of the United States. J. Am. Water Resour. Assoc. 44, 399–416. https://doi.org/10.1111/j.1752-1688.2008.00170.x

Chan, C.C.H., Mundle, S.O.C., Eckert, T., Liang, X., Tang, S., Lacrampe-Couloume, G., Edwards, E.A., Sherwood Lollar, B., 2012. Large carbon isotope fractionation during biodegradation of chloroform by *Dehalobacter* cultures. Environ. Sci. Technol. 46, 10154–10160. https://doi.org/10.1021/es3010317

Chen, G., Kleindienst, S., Griffiths, D.R., Mack, E.E., Seger, E.S., Löffler, F.E., 2017. Mutualistic interaction between dichloromethane- and chloromethane-degrading bacteria in an anaerobic mixed culture. Environ. Microbiol. 19, 4784–4796. https://doi.org/10.1111/1462-2920.13945

Chen, G., Shouakar-Stash, O., Phillips, E., Justicia-Leon, S.D., Gilevska, T., Sherwood Lollar, B., Mack, E.E., Seger, E.S., Löffler, F.E., 2018. Dual carbon-chlorine isotope analysis indicates distinct anaerobic dichloromethane degradation pathways in two members of the *Peptococcaceae*. Environ. Sci. Technol. 52, 8607–8616. https://doi.org/10.1021/acs.est.8b01583

Chen, K., Huang, L., Xu, C., Liu, X., He, J., Zinder, S.H., Li, S., Jiang, J., 2013. Molecular characterization of the enzymes involved in the degradation of a brominated aromatic herbicide. Mol. Microbiol. 89, 1121–1139. https://doi.org/10.1111/mmi.12332

Christ, J.A., Ramsburg, C.A., Abriola, L.M., Pennell, K.D., Löffler, F.E., 2004. Coupling aggressive mass removal with microbial reductive dechlorination for remediation of DNAPL source zones: a review and assessment. Environ. Health Perspect. 113, 465–477. https://doi.org/10.1289/ehp.6932

Cichocka, D., Imfeld, G., Richnow, H.H., Nijenhuis, I., 2008. Variability in microbial carbon isotope fractionation of tetra- and trichloroethene upon reductive dechlorination. Chemosphere 71, 639–648. https://doi.org/10.1016/j.chemosphere.2007.11.013

Cichocka, D., Siegert, M., Imfeld, G.G., Andert, J., Beck, K., Diekert, G., Richnow, H.H., Nijenhuis, I., 2007. Factors controlling the carbon isotope fractionation of tetra- and trichloroethene during reductive dechlorination by *Sulfurospirillum* ssp. and *Desulfitobacterium* sp. strain PCE-S. FEMS Microbiol. Ecol. 62, 98–107. https://doi.org/10.1111/j.1574-6941.2007.00367.x

Cogliano, V.J., Baan, R., Straif, K., Grosse, Y., Lauby-Secretan, B., Ghissassi, F. El, Bouvard, V., Benbrahim-Tallaa, L., Guha, N., Freeman, C., Galichet, L., Wild, C.P., 2011. Preventable exposures associated with human cancers. J. Natl. Cancer Inst. https://doi.org/10.1093/jnci/djr483

Conesa, H.M., Evangelou, M.W.H., Robinson, B.H., Schulin, R., 2012. A critical view of current state of phytotechnologies to remediate soils: Still a promising tool? Sci. World J. 2012, 1–10. https://doi.org/10.1100/2012/173829

Coplen, T.B., 2011. Guidelines and recommended terms for expression of stable-isotope-ratio and gas-ratio measurement results. Rapid Commun. Mass Spectrom. 25, 2538–2560. https://doi.org/10.1002/rcm.5129

Coplen, T.B., 1996. New guidelines for reporting stable hydrogen, carbon, and oxygen isotope-ratio data. Geochim. Cosmochim. Acta 60, 3359–3360. https://doi.org/10.1016/0016-

7037(96)00263-3

Coplen, T.B., Brand, W.A., Gehre, M., Gröning, M., Meijer, H.A.J., Toman, B., Verkouteren, R.M., 2006. New guidelines for $\delta^{13}C$ measurements. Anal. Chem. 78, 2439–2441. https://doi.org/10.1021/ac052027c

Courbet, C., Rivière, A., Jeannottat, S., Rinaldi, S., Hunkeler, D., Bendjoudi, H., de Marsily, G., 2011. Complementing approaches to demonstrate chlorinated solvent biodegradation in a complex pollution plume: mass balance, PCR and compound-specific stable isotope analysis. J. Contam. Hydrol. 126, 315–329. https://doi.org/10.1016/j.jconhyd.2011.08.009

Crawford, R.L., Crawford, D.L., 2005. Bioremediation: principles and applications. Cambridge University Press.

Cupples, A.M., Spormann, A.M., McCarty, P.L., 2003. Growth of a *Dehalococcoides*-like microorganism on vinyl chloride and cis-dichloroethene as electron acceptors as determined by competitive PCR. Appl. Environ. Microbiol. 69, 953–959. https://doi.org/10.1128/AEM.69.2.953-959.2003

Cwiertny, D.M., Scherer, M.M., 2010. Chlorinated solvent chemistry: structures, nomenclature and properties, in: Stroo, H. F. and Ward, C. H. (Ed) In Situ Remediation of Chlorinated Solvent Plumes. Springer, New York, NY, pp. 29–37. https://doi.org/10.1007/978-1-4419-1401-9_2

D

da Lima, G.P., Sleep, B.E., 2010. The impact of carbon tetrachloride on an anaerobic methanol-degrading microbial community. Water. Air. Soil Pollut. 212, 357–368. https://doi.org/10.1007/s11270-010-0350-z

da Silva, M.L.B., Daprato, R.C., Gomez, D.E., Hughes, J.B., Ward, C.H., Alvarez, P.J.J., 2006. Comparison of bioaugmentation and biostimulation for the enhancement of dense nonaqueous phase liquid source zone bioremediation. Water Environ. Res. 78, 2456–2465. https://doi.org/10.2175/106143006X123111

Daniels, S.I., Chambers, J.C., Sanchez, S.S., La Merrill, M.A., Hubbard, A.E., Macherone, A., McMullin, M., Zhang, L., Elliott, P., Smith, M.T., Kooner, J., 2018. Elevated levels of organochlorine pesticides in South Asian immigrants are associated with an increased risk of diabetes. J. Endocr. Soc. 2, 832–841. https://doi.org/10.1210/js.2017-00480

Diamanti-Kandarakis, E., Bourguignon, J.-P., Giudice, L.C., Hauser, R., Prins, G.S., Soto, A.M., Zoeller, R.T., Gore, A.C., 2009. Endocrine-disrupting chemicals: an Endocrine Society scientific statement. Endocr. Rev. 30, 293–342. https://doi.org/10.1210/er.2009-0002

Ding, C., Zhao, S., He, J., 2014. A *Desulfitobacterium* sp. strain PR reductively dechlorinates both 1,1,1-trichloroethane and chloroform. Environ. Microbiol. 16, 3387–3397. https://doi.org/10.1111/1462-2920.12387

Dogramaci, S.., Herczeg, A.., Schiff, S.., Bone, Y., 2001. Controls on $\delta^{34}S$ and $\delta^{18}O$ of dissolved sulfate in aquifers of the Murray Basin, Australia and their use as indicators of flow processes. Appl. Geochemistry 16, 475–488. https://doi.org/10.1016/S0883-

2927(00)00052-4

Dolfing, J., 2016. Energetic considerations in organohalide respiration, in: L. Adrian and F.E. Löffler (Ed) Organohalide-Respiring Bacteria. Springer Berlin Heidelberg, Berlin, Heidelberg, pp. 31–48. https://doi.org/10.1007/978-3-662-49875-0_3

Dugat-Bony, E., Biderre-Petit, C., Jaziri, F., David, M.M., Denonfoux, J., Lyon, D.Y., Richard, J.-Y., Curvers, C., Boucher, D., Vogel, T.M., Peyretaillade, E., Peyret, P., 2012. In situ TCE degradation mediated by complex dehalorespiring communities during biostimulation processes. Microb. Biotechnol. 5, 642–653. https://doi.org/10.1111/j.1751-7915.2012.00339.x

Duhamel, M., Edwards, E.A., 2006. Microbial composition of chlorinated ethene-degrading cultures dominated by *Dehalococcoides*. FEMS Microbiol. Ecol. 58, 538–549. https://doi.org/10.1111/j.1574-6941.2006.00191.x

Duhamel, M., Wehr, S.D., Yu, L., Rizvi, H., Seepersad, D., Dworatzek, S., Cox, E.E., Edwards, E.A., 2002. Comparison of anaerobic dechlorinating enrichment cultures maintained on tetrachloroethene, trichloroethene, cis-dichloroethene and vinyl chloride. Water Res. 36, 4193–4202. https://doi.org/10.1016/S0043-1354(02)00151-3

E

Ebert, K., Laskov, C., Behrens, S., Haderlein, S.B., 2010. Assessment of chlorinated ethenes biodegradation in an anaerobic aquifer by isotope analysis and microcosm studies. IAHS Publ 342, 13–18.

Egli, C., Stromeyer, S., Cook, A.M., Leisinger, T., 1990. Transformation of tetra- and trichloromethane to CO_2 by anaerobic bacteria is a non-enzymic process. FEMS Microbiol. Lett. 68, 207–212. https://doi.org/10.1016/0378-1097(90)90152-G

Egli, C., Tschan, T., Scholtz, R., Cook, A.M., Leisinger, T., 1988. Transformation of tetrachloromethane to dichloromethane and carbon dioxide by *Acetobacterium Woodii*. Appl. Environ. Microbiol. 54, 2819–2824.

Elsner, M., 2010. Stable isotope fractionation to investigate natural transformation mechanisms of organic contaminants: principles, prospects and limitations. J. Environ. Monit. 12, 2005–2031. https://doi.org/10.1039/c0em00277a

Elsner, M., Hofstetter, T.B., 2011. Current perspectives on the mechanisms of chlorohydrocarbon degradation in subsurface environments: insight from kinetics, product formation, probe molecules, and isotope fractionation, in: Tratnyek et Al. (Ed) Aquatic Redox Chemistry. American Chemical Society, Washington, DC, pp. 407–439. https://doi.org/10.1021/bk-2011-1071.ch019

Elsner, M., Hunkeler, D., 2008. Evaluating chlorine isotope effects from isotope ratios and mass spectra of polychlorinated molecules. Anal. Chem. 80, 4731–4740. https://doi.org/10.1021/ac702543y

Enviro Wiki contributors, 2018. Biodegradation - Reductive Processes [WWW Document]. Enviro Wiki. URL https://www.enviro.wiki/index.php?title=Special:CiteThisPage&page=Biodegradation_-_Reductive_Processes&id=11326 (accessed 4.22.19).

European Commission, 2012. Priority Substances and Certain Other Pollutants according to Annex II of Directive 2008/105/EC [WWW Document]. URL http://ec.europa.eu/environment/water/water-framework/priority_substances.htm (accessed 10.31.17).

European Commission, 2008. Directive 2008/105/EC of 16 December 2008 on environmental quality standards in the field of water policy, Official Journal of the European Union. https://doi.org/http://eur-lex.europa.eu/legal-content/EN/TXT/?uri=celex:32008L0105

F

Fennell, D.E., Gossett, J.M., 1998. Modeling the production of and competition for hydrogen in a dechlorinating culture. Environ. Sci. Technol. 32, 2450–2460. https://doi.org/10.1021/es980136l

Fennell, D.E., Gossett, J.M., Zinder, S.H., 1997. Comparison of butyric acid, ethanol, lactic acid, and propionic acid as hydrogen donors for the reductive dechlorination of tetrachloroethene. Environ. Sci. Technol. 31, 918–926. https://doi.org/10.1021/es960756r

Fernàndez-Garcia, D., Carles Brangarí, A., Freixas Borrell, G., 2014. Guia tècnica per a l'avaluació de la problemàtica del subsòl associada a compostos organoclorats.

Field, J.A., 2016. Natural Production of Organohalide Compounds in the Environment, in: L. Adrian and F.E. Löffler (Ed) Organohalide-Respiring Bacteria. Springer Berlin Heidelberg, Berlin, Heidelberg, pp. 7–29. https://doi.org/10.1007/978-3-662-49875-0_2

Freitag, D., Ballhorn, L., Behechti, A., Fischer, K., Thumm, W., 1994. Structural configuration and toxicity of chlorinated alkanes. Chemosphere 28, 253–259. https://doi.org/10.1016/0045-6535(94)90122-8

Friis, A.K., Kofoed, J.L.L., Heron, G., Albrechtsen, H.J., Bjerg, P.L., 2007. Microcosm evaluation of bioaugmentation after field-scale thermal treatment of a TCE-contaminated aquifer. Biodegradation 18, 661–674. https://doi.org/10.1007/s10532-006-9098-y

Futagami, T., Furukawa, K., 2016. The genus *Desulfitobacterium*, in: L. Adrian and F.E. Löffler (Ed) Organohalide-Respiring Bacteria. Springer Berlin Heidelberg, Berlin, Heidelberg, pp. 173–207. https://doi.org/10.1007/978-3-662-49875-0_9

G

Gälli, R., McCarty, P.L., 1989. Biotransformation of 1,1,1-trichloroethane, trichloromethane, and tetrachloromethane by a *Clostridium* sp. Appl. Environ. Microbiol. 55, 837–844.

Gao, J., Skeen, R.S., Hooker, B.S., Quesenberry, R.D., 1997. Effects of several electron donors on tetrachloroethylene dechlorination in anaerobic soil microcosms. Water Res. 31, 2479–2486. https://doi.org/10.1016/S0043-1354(97)00108-5

Gibson, S.A., Sewell, G.W., 1992. Stimulation of reductive dechlorination of tetrachloroethene in anaerobic aquifer microcosms by addition of short-chain organic acids or alcohols. Appl. Environ. Microbiol. 58, 1392–1393.

Goris, T., Diekert, G., 2016. The genus *Sulfurospirillum*, in: L. Adrian and F.E. Löffler (Ed) Organohalide-Respiring Bacteria. Springer Berlin Heidelberg, Berlin, Heidelberg, pp. 209–234. https://doi.org/10.1007/978-3-662-49875-0_10

Gribble, G.W., 2010. Naturally occurring organohalogen compounds - A comprehensive update, Asian Journal of WTO and International Health Law and Policy, Fortschritte der Chemie organischer Naturstoffe / Progress in the Chemistry of Organic Natural Products. Springer Vienna, Vienna. https://doi.org/10.1007/978-3-211-99323-1

Gribble, G.W., 2004a. Amazing organohalogens: although best known as synthetic toxicants, thousands of halogen compounds are, in fact, part of our natural enviornment. Am. Sci. 92, 342–349. https://doi.org/10.2307/27858423

Gribble, G.W., 2004b. Natural organohalogens. Sci. Doss. 6. Euro Chlor 80.

Grostern, A., Duhamel, M., Dworatzek, S., Edwards, E.A., 2010. Chloroform respiration to dichloromethane by a *Dehalobacter* population. Environ. Microbiol. 12, 1053–1060. https://doi.org/10.1111/j.1462-2920.2009.02150.x

H

Harper, D.B., 2000. The global chloromethane cycle: biosynthesis, biodegradation and metabolic role. Nat. Prod. Rep. 17, 337–348. https://doi.org/10.1039/a809400d

He, J., Holmes, V.F., Lee, P.K.H., Alvarez-Cohen, L., 2007. Influence of vitamin B_{12} and cocultures on the growth of *Dehalococcoides* isolates in defined medium. Appl. Environ. Microbiol. 73, 2847–2853. https://doi.org/10.1128/AEM.02574-06

He, J., Sung, Y., Dollhopf, M.E., Fathepure, B.Z., Tiedje, J.M., Löffler, F.E., 2002. Acetate versus hydrogen as direct electron donors to stimulate the microbial reductive dechlorination process at chloroethene-contaminated sites. Environ. Sci. Technol. 36, 3945–3952. https://doi.org/10.1021/es025528d

He, J., Sung, Y., Krajmalnik-Brown, R., Ritalahti, K.M., Löffler, F.E., 2005. Isolation and characterization of *Dehalococcoides* sp. strain FL2, a trichloroethene (TCE)- and 1,2-dichloroethene-respiring anaerobe. Environ. Microbiol. 7, 1442–1450. https://doi.org/10.1111/j.1462-2920.2005.00830.x

Heckel, B., Cretnik, S., Kliegman, S., Shouakar-Stash, O., McNeill, K., Elsner, M., 2017a. Reductive outer-sphere single electron transfer is an exception rather than the rule in natural and engineered chlorinated ethene dehalogenation. Environ. Sci. Technol. 51, 9663–9673. https://doi.org/10.1021/acs.est.7b01447

Heckel, B., Phillips, E., Edwards, E.A., Sherwood Lollar, B., Elsner, M., Manefield, M.J., Lee, M., 2019. Reductive dehalogenation of trichloromethane by two different *Dehalobacter restrictus* strains reveal opposing dual element isotope effects. Environ. Sci. Technol. 53, 2332–2343. https://doi.org/10.1021/acs.est.8b03717

Heckel, B., Rodríguez-Fernández, D., Torrentó, C., Meyer, A.H., Palau, J., Domènech, C., Rosell, M., Soler, A., Hunkeler, D., Elsner, M., 2017b. Compound-specific chlorine isotope analysis of tetrachloromethane and trichloromethane by gas chromatography-isotope ratio mass spectrometry vs gas chromatography-quadrupole mass spectrometry: method development and evaluation of precision and trueness. Anal. Chem. 89, 3411–

3420. https://doi.org/10.1021/acs.analchem.6b04129

Henry, B.M., 2010. Biostimulation for anaerobic bioremediation of chlorinated solvents, in: Stroo, H. F. and Ward, C. H. (Ed) In Situ Remediation of Chlorinated Solvent Plumes. Springer New York, New York, NY, pp. 357–423. https://doi.org/10.1007/978-1-4419-1401-9_12

Heraty, L.J., Fuller, M.., Huang, L., Abrajano, T., Sturchio, N.., 1999. Isotopic fractionation of carbon and chlorine by microbial degradation of dichloromethane. Org. Geochem. 30, 793–799. https://doi.org/10.1016/S0146-6380(99)00062-5

Herlemann, D.P.R., Labrenz, M., Jürgens, K., Bertilsson, S., Waniek, J.J., Andersson, A.F., 2011. Transitions in bacterial communities along the 2000 km salinity gradient of the Baltic Sea. ISME J. 5, 1571–1579. https://doi.org/10.1038/ismej.2011.41

Hermon, L., Denonfoux, J., Hellal, J., Joulian, C., Ferreira, S., Vuilleumier, S., Imfeld, G., 2018. Dichloromethane biodegradation in multi-contaminated groundwater: insights from biomolecular and compound-specific isotope analyses. Water Res. 142, 217–226. https://doi.org/10.1016/j.watres.2018.05.057

Heron, G., Van Zutphen, M., Christensen, T.H., Enfield, C.G., 1998. Soil heating for enhanced remediation of chlorinated solvents: a laboratory study on resistive heating and vapor extraction in a silty, low- permeable soil contaminated with trichloroethylene. Environ. Sci. Technol. 32, 1474–1481. https://doi.org/10.1021/es970563j

Herrero, J., Puigserver, D., Nijenhuis, I., Kuntze, K., Carmona, J.M., 2019. Combined use of ISCR and biostimulation techniques in incomplete processes of reductive dehalogenation of chlorinated solvents. Sci. Total Environ. 648, 819–829. https://doi.org/10.1016/j.scitotenv.2018.08.184

Higgins, M.R., Olson, T.M., 2009. Life-cycle case study comparison of permeable reactive barrier versus pump-and-treat remediation. Environ. Sci. Technol. 43, 9432–9438. https://doi.org/10.1021/es9015537

Hiraishi, A., Ueda, Y., 1994. *Rhodoplanes* gen. nov., a new genus of phototrophic bacteria including *Rhodopseudomonas rosea* as *Rhodoplanes roseus* comb. nov. and *Rhodoplanes elegans* sp. nov. Int. J. Syst. Bacteriol. 44, 665–673. https://doi.org/10.1099/00207713-44-4-665

Hirschorn, S.K., Grostern, A., Lacrampe-Couloume, G., Edwards, E.A., MacKinnon, L., Repta, C., Major, D.W., Sherwood Lollar, B., 2007. Quantification of biotransformation of chlorinated hydrocarbons in a biostimulation study: added value via stable carbon isotope analysis. J. Contam. Hydrol. 94, 249–260. https://doi.org/10.1016/j.jconhyd.2007.07.001

Holliger, C., Hahn, D., Harmsen, H., Ludwig, W., Schumacher, W., Tindall, B., Vazquez, F., Weiss, N., Zehnder, A.J.B., 1998. *Dehalobacter restrictus* gen. nov. and sp. nov., a strictly anaerobic bacterium that reductively dechlorinates tetra- and trichloroethene in an anaerobic respiration. Arch. Microbiol. 169, 313–321. https://doi.org/10.1007/s002030050577

Holt, B.D., Sturchio, N.C., Abrajano, T., Heraty, L.J., 1997. Conversion of chlorinated volatile organic compounds to carbon dioxide and methyl chloride for isotopic analysis of carbon and chlorine. Anal. Chem. 69, 2727–2733. https://doi.org/10.1021/ac961096b

References

Hossaini, R., Chipperfield, M.P., Montzka, S.A., Leeson, A.A., Dhomse, S.S., Pyle, J.A., 2017. The increasing threat to stratospheric ozone from dichloromethane. Nat. Commun. 8, 15962. https://doi.org/10.1038/ncomms15962

Hug, L.A., 2016. Diversity, evolution, and environmental distribution of reductive dehalogenase genes, in: L. Adrian and F.E. Löffler (Ed) Organohalide-Respiring Bacteria. Springer Berlin Heidelberg, Berlin, Heidelberg, pp. 377–393. https://doi.org/10.1007/978-3-662-49875-0_16

Hug, L.A., Maphosa, F., Leys, D., Löffler, F.E., Smidt, H., Edwards, E.A., Adrian, L., 2013. Overview of organohalide-respiring bacteria and a proposal for a classification system for reductive dehalogenases. Philos. Trans. R. Soc. B Biol. Sci. 368, 10. https://doi.org/10.1098/rstb.2012.0322

Huling, S.G., Weaver, J.W., 1991. Groundwater Issue: Dense nonaqueous phase liquids., EPA. Washington, D.C. EPA/540/4-91-002.

Hunkeler, D., Aravena, R., Butler, B.J., 1999. Monitoring microbial dechlorination of tetrachloroethene (PCE) in groundwater using compound-specific stable carbon isotope ratios: microcosm and field studies. Environ. Sci. Technol. 33, 2733–2738. https://doi.org/10.1021/es981282u

Hunkeler, D., Meckenstock, R.U., Lollar, B.S., Schmidt, T.C., Wilson, J.T., 2008. A guide for assessing biodegradation and source identification of organic ground water contaminants using compound specific isotope analysis (CSIA), U.S. Environmental Protection Agency. Washington, D.C., EPA/600/R-08/148.

Hunkeler, D., Van Breukelen, B.M., Elsner, M., 2009. Modeling chlorine isotope trends during sequential transformation of chlorinated ethenes. Environ. Sci. Technol. 43, 6750–6756. https://doi.org/10.1021/es900579z

I

IARC, 2019. Agents classified by the IARC monographs, volumes 1-123. List of classifications. [WWW Document]. IARC Monogr. Identif. Carcinog. Hazards to Humans. URL https://monographs.iarc.fr/list-of-classifications-volumes/ (accessed 4.18.19).

Im, W.T., Kim, S.H., Kim, M.K., Ten, L.N., Lee, S.T., 2006. *Pleomorphomonas koreensis* sp. nov., a nitrogen-fixing species in the order Rhizobiales. Int. J. Syst. Evol. Microbiol. 56, 1663–1666. https://doi.org/10.1099/ijs.0.63499-0

J

Jayaraj, R., Megha, P., Sreedev, P., 2016. Organochlorine pesticides, their toxic effects on living organisms and their fate in the environment. Interdiscip. Toxicol. 9, 90–100. https://doi.org/10.1515/intox-2016-0012

Jeannottat, S., Hunkeler, D., 2012. Chlorine and carbon isotopes fractionation during volatilization and diffusive transport of trichloroethene in the unsaturated zone. Environ. Sci. Technol. 46, 3169–3176. https://doi.org/10.1021/es203547p

Jendrzejewski, N., Eggenkamp, H.G.M., Coleman, M.. L., 2001. Characterisation of chlorinated hydrocarbons from chlorine and carbon isotopic compositions: scope of

application to environmental problems. Appl. Geochemistry 16, 1021–1031. https://doi.org/10.1016/S0883-2927(00)00083-4

Jugder, B.-E., Bohl, S., Lebhar, H., Healey, R.D., Manefield, M., Marquis, C.P., Lee, M., 2017. A bacterial chloroform reductive dehalogenase: purification and biochemical characterization. Microb. Biotechnol. 10, 1640–1648. https://doi.org/10.1111/1751-7915.12745

Jugder, B.E., Ertan, H., Bohl, S., Lee, M., Marquis, C.P., Manefield, M., 2016. Organohalide respiring bacteria and reductive dehalogenases: key tools in organohalide bioremediation. Front. Microbiol. 7, 249. https://doi.org/10.3389/fmicb.2016.00249

Justicia-Leon, S.D., Higgins, S., Mack, E.E., Griffiths, D.R., Tang, S., Edwards, E.A., Löffler, F.E., 2014. Bioaugmentation with distinct *Dehalobacter* strains achieves chloroform detoxification in microcosms. Environ. Sci. Technol. 48, 1851–1858. https://doi.org/10.1021/es403582f

Justicia-Leon, S.D., Ritalahti, K.M., Mack, E.E., Löffler, F.E., 2012. Dichloromethane fermentation by a *Dehalobacter* sp. in an enrichment culture derived from pristine river sediment. Appl. Environ. Microbiol. 78, 1288–1291. https://doi.org/10.1128/AEM.07325-11

K

Kampara, M., Thullner, M., Richnow, H.H., Harms, H., Wick, L.Y., 2008. Impact of bioavailability restrictions on microbially induced stable isotope fractionation. 2. Experimental evidence. Environ. Sci. Technol. 42, 6552–6558. https://doi.org/10.1021/es702781x

Kaufmann, R., Long, A., Bentley, H., Davis, S., 1984. Natural chlorine isotope variations. Nature 309, 338–340. https://doi.org/10.1038/309338a0

Kirtland, B.C., Aelion, C.M., 2000. Petroleum mass removal from low permeability sediment using air sparging/soil vapor extraction: impact of continuous or pulsed operation. J. Contam. Hydrol. 41, 367–383. https://doi.org/10.1016/S0169-7722(99)00071-6

Kleindienst, S., Chourey, K., Chen, G., Murdoch, R.W., Higgins, S.A., Iyer, R., Campagna, S.R., Mack, E.E., Seger, E.S., Hettich, R.L., Löffler, F.E., 2019. Proteogenomics reveals novel reductive dehalogenases and methyltransferases expressed during anaerobic dichloromethane metabolism. Appl. Environ. Microbiol. 85. https://doi.org/10.1128/AEM.02768-18

Kleindienst, S., Higgins, S.A., Tsementzi, D., Chen, G., Konstantinidis, K.T., Mack, E.E., Löffler, F.E., 2017. 'Candidatus *Dichloromethanomonas elyunquensis*' gen. nov., sp. nov., a dichloromethane-degrading anaerobe of the *Peptococcaceae* family. Syst. Appl. Microbiol. 40, 150–159. https://doi.org/10.1016/j.syapm.2016.12.001

Klindworth, A., Pruesse, E., Schweer, T., Peplies, J., Quast, C., Horn, M., Glöckner, F.O., 2013. Evaluation of general 16S ribosomal RNA gene PCR primers for classical and next-generation sequencing-based diversity studies. Nucleic Acids Res. 41, e1–e1. https://doi.org/10.1093/nar/gks808

Krajmalnik-Brown, R., Hölscher, T., Thomson, I.N., Saunders, F.M., Ritalahti, K.M., Löffler,

F.E., 2004. Genetic identification of a putative vinyl chloride reductase in *Dehalococcoides* sp. strain BAV1. Appl. Environ. Microbiol. 70, 6347–6351. https://doi.org/10.1128/AEM.70.10.6347-6351.2004

Krembs, F.J., Siegrist, R.L., Crimi, M.L., Furrer, R.F., Petri, B.G., 2010. ISCO for groundwater remediation: analysis of field applications and performance. Ground Water Monit. Remediat. 30, 42–53. https://doi.org/10.1111/j.1745-6592.2010.01312.x

Krone, U., Laufer, K., Thauer, R.K., Hogenkamp, H.P.C., 1989a. Coenzyme F430 as a possible catalyst for the reductive dehalogenation of chlorinated C1 hydrocarbons in methanogenic bacteria. Biochemistry 28, 10061–10065. https://doi.org/10.1021/bi00452a027

Krone, U., Thauer, R.K., Hogenkamp, H.P.C., 1989b. Reductive dehalogenation of chlorinated C1-hydrocarbons mediated by corrinoids. Biochemistry 28, 4908–4914. https://doi.org/10.1021/bi00437a057

Kublik, A., Deobald, D., Hartwig, S., Schiffmann, C.L., Andrades, A., von Bergen, M., Sawers, R.G., Adrian, L., 2016. Identification of a multi-protein reductive dehalogenase complex in *Dehalococcoides* mccartyi strain CBDB1 suggests a protein-dependent respiratory electron transport chain obviating quinone involvement. Environ. Microbiol. 18, 3044–3056. https://doi.org/10.1111/1462-2920.13200

Kuder, T., Van Breukelen, B.M., Vanderford, M., Philp, P., 2013. 3D-CSIA: Carbon, chlorine, and hydrogen isotope fractionation in transformation of TCE to ethene by a *Dehalococcoides* culture. Environ. Sci. Technol. 47, 9668–9677. https://doi.org/10.1021/es400463p

Kueper, B.H., Vogel, C.M., Stroo, H.F., Ward, C.H., 2014. Chlorinated solvent source zone remediation, Industrial & Engineering Chemistry Research. Springer New York, New York, NY. https://doi.org/10.1007/978-1-4614-6922-3

L

Laeter, J.R. De, Böhlke, J.K., Bièvre, P. De, Hidaka, H., Peiser, H.S., Rosman, K.J.R., Taylor, P.D.P., 2003. Atomic weights of the elements: review 2000. Pure Appl. Chem. 75, 683–800.

Lee, J., Im, J., Kim, U., Löffler, F.E., 2016. A data mining approach to predict in situ detoxification potential of chlorinated ethenes. Environ. Sci. Technol. 50, 5181–5188. https://doi.org/10.1021/acs.est.5b05090

Lee, J.H., 2013. An overview of phytoremediation as a potentially promising technology for environmental pollution control. Biotechnol. Bioprocess Eng. 18, 431–439. https://doi.org/10.1007/s12257-013-0193-8

Lee, M., Low, A., Zemb, O., Koenig, J., Michaelsen, A., Manefield, M.J., 2012. Complete chloroform dechlorination by organochlorine respiration and fermentation. Environ. Microbiol. 14, 883–894. https://doi.org/10.1111/j.1462-2920.2011.02656.x

Lee, M., Wells, E., Wong, Y.K., Koenig, J., Adrian, L., Richnow, H.H., Manefield, M.J., 2015. Relative contributions of *Dehalobacter* and zerovalent iron in the degradation of chlorinated methanes. Environ. Sci. Technol. 49, 4481–4489.

https://doi.org/10.1021/es5052364

Leeson, A., Beevar, E., Henry, B.M., Fortenberry, J., Coyle, C., Parsons Corp., 2004. Principles and practices of enhanced anaerobic bioremediation of chlorinated solvents. Port Hueneme, California, ESTCP CU 0125.

Leeson, A., Stroo, H.F., Johnson, P.C., 2013. Groundwater remediation today and challenges and opportunities for the future. Groundwater 51, 175–179. https://doi.org/10.1111/gwat.12039

Lemming, G., Hauschild, M.Z., Chambon, J., Binning, P.J., Bulle, C., Margni, M., Bjerg, P.L., 2010. Environmental impacts of remediation of a trichloroethene-contaminated site: Life cycle assessment of remediation alternatives. Environ. Sci. Technol. 44, 9163–9169. https://doi.org/10.1021/es102007s

Leri, A.C., Marcus, M.A., Myneni, S.C.B., 2007. X-ray spectromicroscopic investigation of natural organochlorine distribution in weathering plant material. Geochim. Cosmochim. Acta 71, 5834–5846. https://doi.org/10.1016/j.gca.2007.09.001

Leri, A.C., Myneni, S.C.B., 2010. Organochlorine turnover in forest ecosystems: the missing link in the terrestrial chlorine cycle. Global Biogeochem. Cycles 24, n/a-n/a. https://doi.org/10.1029/2010GB003882

Liang, X., Howlett, M.R., Nelson, J.L., Grant, G., Dworatzek, S., Lacrampe-Couloume, G., Zinder, S.H., Edwards, E.A., Sherwood Lollar, B., 2011. Pathway-dependent isotope fractionation during aerobic and anaerobic degradation of monochlorobenzene and 1,2,4-trichlorobenzene. Environ. Sci. Technol. 45, 8321–8327. https://doi.org/10.1021/es201224x

Liu, Q., Wang, Q., Xu, C., Shao, W., Zhang, C., Liu, H., Jiang, Z., Gu, A., 2017. Organochloride pesticides impaired mitochondrial function in hepatocytes and aggravated disorders of fatty acid metabolism. Sci. Rep. 7, 46339. https://doi.org/10.1038/srep46339

Löffler, F.E., Ritalahti, K.M., Zinder, S.H., 2012. *Dehalococcoides* and reductive dechlorination of chlorinated solvents, in: Stroo et Al. (Ed) Bioaugmentation for Groundwater Remediation. Springer New York, New York, NY, pp. 39–88. https://doi.org/10.1007/978-1-4614-4115-1_2

Löffler, F.E., Sanford, R.A., Ritalahti, K.M., 2005. Enrichment, cultivation, and detection of reductively dechlorinating bacteria. Methods Enzymol. 397, 77–111. https://doi.org/10.1016/S0076-6879(05)97005-5

Löffler, F.E., Yan, J., Ritalahti, K.M., Adrian, L., Edwards, E.A., Konstantinidis, K.T., Müller, J.A., Fullerton, H., Zinder, S.H., Spormann, A.M., 2013. *Dehalococcoides mccartyi* gen. nov., sp. nov., obligately organohalide-respiring anaerobic bacteria relevant to halogen cycling and bioremediation, belong to a novel bacterial class, *Dehalococcoidia* classis nov., order *Dehalococcoidales* ord. nov. and famil. Int. J. Syst. Evol. Microbiol. 63, 625–635. https://doi.org/10.1099/ijs.0.034926-0

Loganathan, B.G., 2011. Global contamination trends of persistent organic chemicals: an overview, in: Loganathan, B. G. and Lam, P. K. S. (Ed) Global Contamination Trends of Persistent Organic Chemicals. CRC Press, pp. 3–31. https://doi.org/10.1201/b11098-3

Lovley, D.R., 2001. Anaerobes to the rescue. Science (80-.). 293, 1444–1446.

https://doi.org/10.1126/science.1063294

Lovley, D.R., Giovannoni, S.J., White, D.C., Champine, J.E., Phillips, E.J.P., Gorby, Y.A., Goodwin, S., 1993. *Geobacter metallireducens* gen. nov. sp. nov., a microorganism capable of coupling the complete oxidation of organic compounds to the reduction of iron and other metals. Arch. Microbiol. 159, 336–344. https://doi.org/10.1007/BF00290916

Lu, X., Wilson, J.T., Kampbell, D.H., 2009. Comparison of an assay for *Dehalococcoides* DNA and a microcosm study in predicting reductive dechlorination of chlorinated ethenes in the field. Environ. Pollut. 157, 809–815. https://doi.org/10.1016/j.envpol.2008.11.015

Lyon, D.Y., Vogel, T.M., 2013. Bioaugmentation for groundwater remediation: an overview, in: Stroo et Al. (Ed) Bioaugmentation for Groundwater Remediation. Springer New York, New York, NY, pp. 1–37. https://doi.org/10.1007/978-1-4614-4115-1_1

M

Mackay, D.M., Cherry, J.A., 1989. Groundwater contamination: pump-and-treat remediation. Environ. Sci. Technol. 23, 630–636.

Madhaiyan, M., Jin, T.Y., Roy, J.J., Kim, S.-J., Weon, H.-Y., Kwon, S.-W., Ji, L., 2013. *Pleomorphomonas diazotrophica* sp. nov., an endophytic N-fixing bacterium isolated from root tissue of *Jatropha curcas* L. Int. J. Syst. Evol. Microbiol. 63, 2477–2483. https://doi.org/10.1099/ijs.0.044461-0

Madigan, M.T., Bender, K.S., Buckley, D.H., Sattley, W.M., Stahl, D.A., 2018. Brock biology of microorganisms, 15th ed. Pearson.

Madsen, E.L., 2015. Environmental microbiology: from genomes to biogeochemistry. Wiley-Blackwell.

Mägli, A., Messmer, M., Leisinger, T., 1998. Metabolism of dichloromethane by the strict anaerobe *Dehalobacterium formicoaceticum*. Appl. Environ. Microbiol. 64, 646–650.

Maillard, J., Schumacher, W., Vazquez, F., Regeard, C., Hagen, W.R., Holliger, C., 2003. Characterization of the corrinoid iron-sulfur protein tetrachloroethene reductive dehalogenase of *Dehalobacter restrictus*. Appl. Environ. Microbiol. 69, 4628–4638. https://doi.org/10.1128/AEM.69.8.4628-4638.2003

Majone, M., Verdini, R., Aulenta, F., Rossetti, S., Tandoi, V., Kalogerakis, N., Agathos, S., Puig, S., Zanaroli, G., Fava, F., 2015. In situ groundwater and sediment bioremediation: barriers and perspectives at European contaminated sites. N. Biotechnol. 32, 133–146. https://doi.org/10.1016/j.nbt.2014.02.011

Manchester, M.J., Hug, L.A., Zarek, M., Zila, A., Edwards, E.A., 2012. Discovery of a trans-dichloroethene-respiring *Dehalogenimonas* species in the 1,1,2,2-tetrachloroethane-dechlorinating WBC-2 consortium. Appl. Environ. Microbiol. 78, 5280–5287. https://doi.org/10.1128/AEM.00384-12

Maphosa, F., de Vos, W.M., Smidt, H., 2010. Exploiting the ecogenomics toolbox for environmental diagnostics of organohalide-respiring bacteria. Trends Biotechnol. 28, 308–316. https://doi.org/10.1016/j.tibtech.2010.03.005

Marco-Urrea, E., Nijenhuis, I., Adrian, L., 2011. Transformation and carbon isotope

fractionation of tetra-and trichloroethene to trans-dichloroethene by *Dehalococcoides* sp. strain CBDB1. Environ. Sci. Technol. 45, 1555–1562. https://doi.org/10.1021/es1023459

Marshall, K.A., Pottenger, L.H., 2016. Chlorocarbons and chlorohydrocarbons, in: Ley, C. (Ed) Kirk-Othmer Encyclopedia of Chemical Technology. John Wiley & Sons, Inc., Hoboken, NJ, USA, pp. 1–29. https://doi.org/10.1002/0471238961.1921182218050504.a01.pub3

Martín-González, L., Mortan, S.H., Rosell, M., Parladé, E., Martínez-Alonso, M., Gaju, N., Caminal, G., Adrian, L., Marco-Urrea, E., 2015. Stable carbon isotope fractionation during 1,2-dichloropropane-to-propene transformation by an enrichment culture containing *Dehalogenimonas* strains and a *dcpA* gene. Environ. Sci. Technol. 49, 8666–74. https://doi.org/10.1021/acs.est.5b00929

Matteucci, F., Ercole, C., Del Gallo, M., 2015. A study of chlorinated solvent contamination of the aquifers of an industrial area in central Italy: a possibility of bioremediation. Front. Microbiol. 6, 1–10. https://doi.org/10.3389/fmicb.2015.00924

Mayer-Blackwell, K., Fincker, M., Molenda, O., Callahan, B., Sewell, H., Holmes, S., Edwards, E.A., Spormann, A.M., 2016. 1,2-dichloroethane exposure alters the population structure, metabolism, and kinetics of a trichloroethene-dechlorinating *Dehalococcoides mccartyi* consortium. Environ. Sci. Technol. 50, 12187–12196. https://doi.org/10.1021/acs.est.6b02957

McCarty, P.L., 2016. Discovery of organohalide-respiring processes and the bacteria involved, in: L. Adrian and F.E. Löffler (Ed) Organohalide-Respiring Bacteria. Springer Berlin Heidelberg, Berlin, Heidelberg, pp. 51–62. https://doi.org/10.1007/978-3-662-49875-0_4

Meckenstock, R.U., Elsner, M., Griebler, C., Lueders, T., Stumpp, C., Aamand, J., Agathos, S.N., Albrechtsen, H.-J., Bastiaens, L., Bjerg, P.L., Boon, N., Dejonghe, W., Huang, W.E., Schmidt, S.I., Smolders, E., Sørensen, S.R., Springael, D., van Breukelen, B.M., 2015. Biodegradation: updating the concepts of control for microbial cleanup in contaminated aquifers. Environ. Sci. Technol. 49, 7073–7081. https://doi.org/10.1021/acs.est.5b00715

Mikesell, M.D., Boyd, S.A., 1990. Dechlorination of chloroform by *Methanosarcina* strains. Appl. Environ. Microbiol. 56, 1198–1201.

Mizutani, Y., Rafter, T.A., 1973. Isotopic behaviour of sulphate oxygen in the bacterial reduction of sulphate. Geochem. J. 6, 183–191. https://doi.org/10.2343/geochemj.6.183

Moe, W.M., Rainey, F.A., Yan, J., 2016. The genus *Dehalogenimonas*, in: L. Adrian and F.E. Löffler (Ed) Organohalide-Respiring Bacteria. Springer Berlin Heidelberg, Berlin, Heidelberg, pp. 137–151. https://doi.org/10.1007/978-3-662-49875-0_7

Molenda, O., Quaile, A.T., Edwards, E.A., 2016. *Dehalogenimonas* sp. strain WBC-2 genome and identification of its trans-dichloroethene reductive dehalogenase, *TdrA*. Appl. Environ. Microbiol. 82, 40–50. https://doi.org/10.1128/AEM.02017-15

Moran, M.J., 2006. Occurrence and implications of selected chlorinated solvents in groundwater and source water in the United States and in drinking water in 12 northeast and mid-atlantic states, 1993–2002, Scientific Investigations Report 2005–5268. Reston,

Virginia.

Moran, M.J., Zogorski, J.S., Squillace, P.J., 2007. Chlorinated solvents in groundwater of the United States. Environ. Sci. Technol. 41, 74–81. https://doi.org/10.1021/es061553y

Mrema, E.J., Rubino, F.M., Brambilla, G., Moretto, A., Tsatsakis, A.M., Colosio, C., 2013. Persistent organochlorinated pesticides and mechanisms of their toxicity. Toxicology 307, 74–88. https://doi.org/10.1016/j.tox.2012.11.015

Muller, E.E.L., Bringel, F., Vuilleumier, S., 2011. Dichloromethane-degrading bacteria in the genomic age. Res. Microbiol. 162, 869–876. https://doi.org/10.1016/j.resmic.2011.01.008

Muller, J.A., Rosner, B.M., von Abendroth, G., Meshulam-Simon, G., McCarty, P.L., Spormann, A.M., 2004. Molecular identification of the catabolic vinyl chloride reductase from *Dehalococcoides* sp. strain VS and its environmental distribution. Appl. Environ. Microbiol. 70, 4880–4888. https://doi.org/10.1128/AEM.70.8.4880-4888.2004

Mundle, S.O.C., Vandersteen, A.A., Lacrampe-Couloume, G., Kluger, R., Sherwood Lollar, B., 2013. Pressure-monitored headspace analysis combined with compound-specific isotope analysis to measure isotope fractionation in gas-producing reactions. Rapid Commun. Mass Spectrom. 27, 1778–1784. https://doi.org/10.1002/rcm.6625

Myneni, S.C.B., 2002. Formation of stable chlorinated hydrocarbons in weathering plant material. Science (80-.). 295, 1039–1041. https://doi.org/10.1126/science.1067153

N

Naidoo, V., Wolter, K., Cuthbert, R., Duncan, N., 2009. Veterinary diclofenac threatens Africa's endangered vulture species. Regul. Toxicol. Pharmacol. 53, 205–208. https://doi.org/10.1016/j.yrtph.2009.01.010

Nakamura, R., Obata, T., Nojima, R., Hashimoto, Y., Noguchi, K., Ogawa, T., Yohda, M., 2018. Functional expression and characterization of tetrachloroethene dehalogenase from *Geobacter* sp. Front. Microbiol. 9, 1774. https://doi.org/10.3389/fmicb.2018.01774

Nijenhuis, I., Andert, J., Beck, K., Kästner, M., Diekert, G., Richnow, H.H., 2005. Stable isotope fractionation of tetrachloroethene during reductive dechlorination by *Sulfurospirillum multivorans* and *Desulfitobacterium* sp. strain PCE-S and abiotic reactions with cyanocobalamin. Appl. Environ. Microbiol. 71, 3413–3419. https://doi.org/10.1128/AEM.71.7.3413-3419.2005

Nijenhuis, I., Kuntze, K., 2016. Anaerobic microbial dehalogenation of organohalides-state of the art and remediation strategies. Curr. Opin. Biotechnol. 38, 33–38. https://doi.org/10.1016/j.copbio.2015.11.009

Nijenhuis, I., Nikolausz, M., Köth, A., Felföldi, T., Weiss, H., Drangmeister, J., Großmann, J., Kästner, M., Richnow, H.H., 2007. Assessment of the natural attenuation of chlorinated ethenes in an anaerobic contaminated aquifer in the Bitterfeld/Wolfen area using stable isotope techniques, microcosm studies and molecular biomarkers. Chemosphere 67, 300–311. https://doi.org/10.1016/j.chemosphere.2006.09.084

Nikel, P.I., Perez-Pantoja, D., de Lorenzo, V., 2013. Why are chlorinated pollutants so difficult to degrade aerobically? Redox stress limits 1,3-dichloprop-1-ene metabolism by

Pseudomonas pavonaceae. Philos. Trans. R. Soc. B Biol. Sci. 368, 20120377–20120377. https://doi.org/10.1098/rstb.2012.0377

Nikolausz, M., Nijenhuis, I., Ziller, K., Richnow, H.H., Kastner, M., 2006. Stable carbon isotope fractionation during degradation of dichloromethane by methylotrophic bacteria. Environ. Microbiol. 8, 156–164. https://doi.org/10.1111/j.1462-2920.2005.00878.x

O

Öberg, G.M., 2003. The biogeochemistry of chlorine in soil, in: Gribble, G. (Ed) Natural Production of Organohalogen Compounds. Springer, Berlin, Heidelberg, pp. 43–62. https://doi.org/10.1007/b10447

Öberg, G.M., Bastviken, D., 2012. Transformation of chloride to organic chlorine in terrestrial environments: variability, extent, and implications. Crit. Rev. Environ. Sci. Technol. https://doi.org/10.1080/10643389.2011.592753

Odencrantz, J.E., Vogl, R.A., Varljen, M.D., 2003. Natural attenuation rate clarifications: the true picture is in the details. Soil Sediment Contam. An Int. J. 12, 663–672. https://doi.org/10.1080/714037713

Otero, N., Soler, A., Canals, À., 2008. Controls of $\delta^{34}S$ and $\delta^{18}O$ in dissolved sulphate: learning from a detailed survey in the Llobregat River (Spain). Appl. Geochemistry 23, 1166–1185. https://doi.org/10.1016/j.apgeochem.2007.11.009

P

Palau, J., Cretnik, S., Shouakar-Stash, O., Höche, M., Elsner, M., Hunkeler, D., 2014a. C and Cl isotope fractionation of 1,2-dichloroethane displays unique $\delta^{13}C/\delta^{37}Cl$ patterns for pathway identification and reveals surprising C-Cl bond involvement in microbial oxidation. Environ. Sci. Technol. 48, 9430–9437. https://doi.org/10.1021/es5031917

Palau, J., Jamin, P., Badin, A., Vanhecke, N., Haerens, B., Brouyère, S., Hunkeler, D., 2016. Use of dual carbon–chlorine isotope analysis to assess the degradation pathways of 1,1,1-trichloroethane in groundwater. Water Res. 92, 235–243. https://doi.org/10.1016/j.watres.2016.01.057

Palau, J., Marchesi, M., Chambon, J.C.C., Aravena, R., Canals, À., Binning, P.J., Bjerg, P.L., Otero, N., Soler, A., 2014b. Multi-isotope (carbon and chlorine) analysis for fingerprinting and site characterization at a fractured bedrock aquifer contaminated by chlorinated ethenes. Sci. Total Environ. 475, 61–70. https://doi.org/10.1016/j.scitotenv.2013.12.059

Palau, J., Yu, R., Mortan, S.H., Shouakar-Stash, O., Rosell, M., Freedman, D.L., Sbarbati, C., Fiorenza, S., Aravena, R., Marco-Urrea, E., Elsner, M., Soler, A., Hunkeler, D., 2017. Distinct dual C–Cl isotope fractionation patterns during anaerobic biodegradation of 1,2-dichloroethane: potential to characterize microbial degradation in the field. Environ. Sci. Technol. 51, 2685–2694. https://doi.org/10.1021/acs.est.6b04998

Panagos, P., Van Liedekerke, M., Yigini, Y., Montanarella, L., 2013. Contaminated sites in Europe: review of the current situation based on data collected through a european network. J. Environ. Public Health 2013, 1–11. https://doi.org/10.1155/2013/158764

Pandey, J., Chauhan, A., Jain, R.K., 2009. Integrative approaches for assessing the ecological sustainability of in situ bioremediation. FEMS Microbiol. Rev. 33, 324–375. https://doi.org/10.1111/j.1574-6976.2008.00133.x

Payne, K.A.P., Quezada, C.P., Fisher, K., Dunstan, M.S., Collins, F.A., Sjuts, H., Levy, C., Hay, S., Rigby, S.E.J., Leys, D., 2015. Reductive dehalogenase structure suggests a mechanism for B_{12}-dependent dehalogenation. Nature 517, 513–516. https://doi.org/10.1038/nature13901

Penny, C., Vuilleumier, S., Bringel, F., 2010. Microbial degradation of tetrachloromethane: mechanisms and perspectives for bioremediation. FEMS Microbiol. Ecol. 74, 257–275. https://doi.org/10.1111/j.1574-6941.2010.00935.x

Peuke, A.D., Rennenberg, H., 2005. Phytoremediation. EMBO Rep. 6, 497–501.

Pöritz, M., Goris, T., Wubet, T., Tarkka, M.T., Buscot, F., Nijenhuis, I., Lechner, U., Adrian, L., 2013. Genome sequences of two dehalogenation specialists - *Dehalococcoides mccartyi* strains BTF08 and DCMB5 enriched from the highly polluted Bitterfeld region. FEMS Microbiol. Lett. 343, 101–104. https://doi.org/10.1111/1574-6968.12160

Puigdomènech, I., 2010. MEDUSA (Make Equilibrium Diagrams Using Sophisticated Algorithms) Windows interface to the MS-DOS versions of INPUT, SED and PREDOM (FORTRAN programs drawing chemical equilibrium diagrams) Vers. 6 Dec 2010. R. Inst. Technol. Stock. Sweden.

R

Real Decreto 140/2003, de 7 de febrero, por el que se establecen los criterios sanitarios de la calidad del agua de consumo humano. Ministerio de la Presidencia «BOE» núm. 45, de 21 de febrero de 2003. Referencia: BOE-A-2003-3596. Madrid.

Redon, P.O., Jolivet, C., Saby, N.P.A., Abdelouas, A., Thiry, Y., 2013. Occurrence of natural organic chlorine in soils for different land uses. Biogeochemistry 114, 413–419. https://doi.org/10.1007/s10533-012-9771-7

Reineke, W., 1984. Microbial degradation of halogenated aromatic compounds, in: Gibson, D.T. (Ed) Microbial Degradation of Organic Compounds. Marcel Dekker Inc., New York, NY, pp. 319–360.

Renpenning, J., Rapp, I., Nijenhuis, I., 2015. Substrate hydrophobicity and cell composition influence the extent of rate limitation and masking of isotope fractionation during microbial reductive dehalogenation of chlorinated ethenes. Environ. Sci. Technol. 49, 4293–4301. https://doi.org/10.1021/es506108j

Ritalahti, K.M., Amos, B.K., Sung, Y., Wu, Q., Koenigsberg, S.S., Löffler, F.E., 2006. Quantitative PCR targeting 16S rRNA and reductive dehalogenase genes simultaneously monitors multiple *Dehalococcoides* strains. Appl. Environ. Microbiol. 72, 2765–2774. https://doi.org/10.1128/AEM.72.4.2765-2774.2006

Rivett, M.O., Chapman, S.W., Allen-King, R.M., Feenstra, S., Cherry, J.A., 2006. Pump-and-treat remediation of chlorinated solvent contamination at a controlled field-experiment site. Environ. Sci. Technol. 40, 6770–6781. https://doi.org/10.1021/es0602748

Rodríguez-Fernández, D., Torrentó, C., Guivernau, M., Viñas, M., Hunkeler, D., Soler, A.,

Domènech, C., Rosell, M., 2018a. Vitamin B$_{12}$ effects on chlorinated methanes-degrading microcosms: dual isotope and metabolically active microbial populations assessment. Sci. Total Environ. 621, 1615–1625. https://doi.org/10.1016/j.scitotenv.2017.10.067

Rodríguez-Fernández, D., Torrentó, C., Palau, J., Marchesi, M., Soler, A., Hunkeler, D., Domènech, C., Rosell, M., 2018b. Unravelling long-term source removal effects and chlorinated methanes natural attenuation processes by C and Cl stable isotopic patterns at a complex field site. Sci. Total Environ. 645, 286–296. https://doi.org/10.1016/j.scitotenv.2018.07.130

Rosell, M., Finsterbusch, S., Jechalke, S., Hübschmann, T., Vogt, C., Richnow, H.H., 2010. Evaluation of the effects of low oxygen concentration on stable isotope fractionation during aerobic MTBE biodegradation. Environ. Sci. Technol. 44, 309–315. https://doi.org/10.1021/es902491d

Ruder, A.M., 2006. Potential health effects of occupational chlorinated solvent exposure. Ann. N. Y. Acad. Sci. 1076, 207–227. https://doi.org/10.1196/annals.1371.050

S

Sanford, R.A., Chowdhary, J., Löffler, F.E., 2016. Organohalide-respiring *Deltaproteobacteria*, in: L. Adrian and F.E. Löffler (Ed) Organohalide-Respiring Bacteria. Springer Berlin Heidelberg, Berlin, Heidelberg, pp. 235–258. https://doi.org/10.1007/978-3-662-49875-0_11

Seidel, K., Kühnert, J., Adrian, L., 2018. The complexome of *Dehalococcoides mccartyi* reveals its organohalide respiration-complex is modular. Front. Microbiol. 9, 1130. https://doi.org/10.3389/fmicb.2018.01130

Sharak Genthner, B.R., Friedman, S.D., Devereux, R., 1997. Reclassification of *Desulfovibrio desulfuricans* Norway 4 as *Desulfomicrobium norvegicum* comb. nov. and confirmation of *Desulfomicrobium escambiense* (corrig., formerly "*escambium*") as a new species in the genus *Desulfomicrobium*. Int. J. Syst. Bacteriol. 47, 889–892. https://doi.org/10.1099/00207713-47-3-889

Sharak Genthner, B.R., Mundfrom, G., Devereux, R., 1994. Characterization of *Desulfomicrobium escambium* sp. nov. and proposal to assign *Desulfovibrio desulfuricans* strain Norway 4 to the genus *Desulfomicrobium*. Arch. Microbiol. 161, 215–219. https://doi.org/10.1007/BF00248695

Sherwood Lollar, Barbara, Hirschorn, S., Mundle, S.O.C., Grostern, A., Edwards, E.A., Lacrampe-Couloume, G., Sherwood Lollar, B., 2010. Insights into enzyme kinetics of chloroethane biodegradation using compound specific stable isotopes. Environ. Sci. Technol. 44, 7498–7503. https://doi.org/10.1021/es101330r

Sherwood Lollar, Barbara, Hirschorn, S.K., Chartrand, M.M.G., Lacrampe-Couloume, G., Sherwood Lollar, B., 2007. An approach for assessing total instrumental uncertainty in compound-specific carbon isotope analysis: implications for environmental remediation studies. Anal. Chem. 79, 3469–3475. https://doi.org/10.1021/ac062299v

Shouakar-Stash, O., Drimmie, R.J., Zhang, M., Frape, S.K., 2006. Compound-specific chlorine isotope ratios of TCE, PCE and DCE isomers by direct injection using CF-IRMS. Appl. Geochemistry 21, 766–781. https://doi.org/10.1016/j.apgeochem.2006.02.006

References

Shouakar-Stash, O., Frape, S.K., Drimmie, R.J., 2003. Stable hydrogen, carbon and chlorine isotope measurements of selected chlorinated organic solvents. J. Contam. Hydrol. 60, 211–228. https://doi.org/10.1016/S0169-7722(02)00085-2

Sims, J.L., Suflita, J.M., Russell, H.H., 1992. Groundwater Issue: in-situ bioremediation of contaminated groundwater. Washington, D.C. EPA/540/S-92/003.

Slater, G.F., Sherwood Lollar, Barbara, Sleep, B.E., Edwards, E.A., Sherwood Lollar, B., 2001. Variability in carbon isotopic fractionation during biodegradation of chlorinated ethenes: implications for field applications. Environ. Sci. Technol. 35, 901–907. https://doi.org/10.1021/es001583f

Smets, B.F., Pritchard, P., 2003. Elucidating the microbial component of natural attenuation. Curr. Opin. Biotechnol. 14, 283–288. https://doi.org/10.1016/S0958-1669(03)00062-4

Soares, A.A., Albergaria, J.T., Domingues, V.F., Alvim-Ferraz, M. da C.M., Delerue-Matos, C., 2010. Remediation of soils combining soil vapor extraction and bioremediation: Benzene. Chemosphere 80, 823–828. https://doi.org/10.1016/j.chemosphere.2010.06.036

Song, D.L., Conrad, M.E., Sorenson, K.S., Alvarez-Cohen, L., 2002. Stable carbon isotope fractionation during enhanced in situ bioremediation of trichloroethene. Environ. Sci. Technol. 36, 2262–2268. https://doi.org/10.1021/es011162d

Sparling, D.W., 2016. Organochlorine pesticides, in: Sparling, D. W. (Ed) Ecotoxicology Essentials. Elsevier, pp. 69–107. https://doi.org/10.1016/B978-0-12-801947-4.00004-4

Spira, Y., Henstock, J., Nathanail, P., Müller, D., Edwards, D., 2006. A European approach to increase innovative soil and groundwater remediation technology applications. Remediation 16, 81–96. https://doi.org/10.1002/rem.20103

Steffan, R.J., Schaefer, C.E., 2016. Current and future bioremediation applications: bioremediation from a practical and regulatory perspective, in: L. Adrian and F.E. Löffler (Ed) Organohalide-Respiring Bacteria. Springer Berlin Heidelberg, Berlin, Heidelberg, pp. 517–540. https://doi.org/10.1007/978-3-662-49875-0_22

Stelzer, N., Imfeld, G., Thullner, M., Lehmann, J., Poser, A., Richnow, H.H., Nijenhuis, I., 2009. Integrative approach to delineate natural attenuation of chlorinated benzenes in anoxic aquifers. Environ. Pollut. 157, 1800–1806. https://doi.org/10.1016/j.envpol.2009.01.029

Stroo, H.F., Leeson, A., Ward, C.H., Amber, W.R., 2013. Bioaugmentation for groundwater remediation. Springer New York, New York, NY. https://doi.org/10.1007/978-1-4614-4115-1

Stroo, H.F., Ward, C.H., 2010. In situ remediation of chlorinated solvent plumes, 1st ed, SERDP/ESTCP Environmental Remediation Technology. Springer New York, New York, NY. https://doi.org/10.1007/978-1-4419-1401-9

Sung, Y., Fletcher, K.E., Ritalahti, K.M., Apkarian, R.P., Ramos-Hernández, N., Sanford, R.A., Mesbah, N.M., Löffler, F.E., 2006a. *Geobacter lovleyi* sp. nov. strain SZ, a novel metal-reducing and tetrachloroethene-dechlorinating bacterium. Appl. Environ. Microbiol. 72, 2775–2782. https://doi.org/10.1128/AEM.72.4.2775-2782.2006

Sung, Y., Ritalahti, K.M., Apkarian, R.P., Löffler, F.E., 2006b. Quantitative PCR confirms purity of strain GT, a novel trichloroethene-to- ethene-respiring *Dehalococcoides* isolate.

Appl. Environ. Microbiol. 72, 1980–1987. https://doi.org/10.1128/AEM.72.3.1980-1987.2006

Świderek, K., Paneth, P., 2012. Extending limits of chlorine kinetic isotope effects. J. Org. Chem. 77, 5120–5124. https://doi.org/10.1021/jo300682f

T

Tang, S., Edwards, E.A., 2013. Identification of *Dehalobacter* reductive dehalogenases that catalyse dechlorination of chloroform, 1,1,1-trichloroethane and 1,1-dichloroethane. Philos. Trans. R. Soc. B Biol. Sci. 368, 20120318. https://doi.org/10.1098/rstb.2012.0318

Tarnawski, S.-E., Rossi, P., Brennerova, M. V., Stavelova, M., Holliger, C., 2016. Validation of an integrative methodology to assess and monitor reductive dechlorination of chlorinated ethenes in contaminated aquifers. Front. Environ. Sci. 4, 1–16. https://doi.org/10.3389/fenvs.2016.00007

Tegtmeier, D., Riese, C., Geissinger, O., Radek, R., Brune, A., 2016. *Breznakia blatticola* gen. nov. sp. nov. and *Breznakia pachnodae* sp. nov., two fermenting bacteria isolated from insect guts, and emended description of the family *Erysipelotrichaceae*. Syst. Appl. Microbiol. 39, 319–329. https://doi.org/10.1016/j.syapm.2016.05.003

Thullner, M., Kampara, M., Richnow, H.H., Harms, H., Wick, L.Y., 2008. Impact of bioavailability restrictions on microbially induced stable isotope fractionation. 1. Theoretical calculation. Environ. Sci. Technol. 42, 6544–6551. https://doi.org/10.1021/es702782c

Torgonskaya, M.L., Zyakun, A.M., Trotsenko, Y.A., Laurinavichius, K.S., Kümmel, S., Vuilleumier, S., Richnow, H.H., 2019. Individual stages of bacterial dichloromethane degradation mapped by carbon and chlorine stable isotope analysis. J. Environ. Sci. 78, 147–160. https://doi.org/10.1016/j.jes.2018.09.008

Torrentó, C., Palau, J., Rodríguez-Fernández, D., Heckel, B., Meyer, A., Domènech, C., Rosell, M., Soler, A., Elsner, M., Hunkeler, D., 2017. Carbon and chlorine isotope fractionation patterns associated with different engineered chloroform transformation reactions. Environ. Sci. Technol. 51, 6174–6184. https://doi.org/10.1021/acs.est.7b00679

Trueba-Santiso, A., Parladé, E., Rosell, M., Lliros, M., Mortan, S.H., Martínez-Alonso, M., Gaju, N., Martín-González, L., Vicent, T., Marco-Urrea, E., 2017. Molecular and carbon isotopic characterization of an anaerobic stable enrichment culture containing *Dehalobacterium* sp. during dichloromethane fermentation. Sci. Total Environ. 581–582, 640–648. https://doi.org/10.1016/j.scitotenv.2016.12.174

U

USEPA, 2019. National Primary Drinking Water Regulations [WWW Document]. URL https://www.epa.gov/ground-water-and-drinking-water/national-primary-drinking-water-regulations#one (accessed 4.18.19).

USEPA, 2015. Volatile organic compounds: technical overview [WWW Document]. URL https://www.epa.gov/indoor-air-quality-iaq/technical-overview-volatile-organic-

compounds#definition (accessed 7.6.19).

USEPA, 2010. Superfund remedy report, 13th ed. Report no. EPA-542-R-10-004. Washington, D.C. U.S. EPA Office of Solid Waste and Emergency Response.

USEPA, 2002. Elements for effective management of operating pump and treat systems. 542-R-02-009. OSWER 9355.4-27FS-A., USEPA Fact Sheet. Cincinnati, OH.

USEPA, 2000. Engineered approaches to in situ bioremediation of chlorinated solvents: Fundamentals and field applications. U. S. Environ. Prot. Agency 1–144. https://doi.org/EPA 542-R-00-008

USEPA, 1995. How to evaluate alternative cleanup technologies for underground storage tank sites - A guide for corrective action plan reviewers, Chapter 11, Dual-phase extraction. EPA 510-B-17-003.

USEPA, 1989. Record of Decision: Firestone Tire & Rubber Co. (Salinas Plant). EPA/ROD/R09-89/039. Washington, DC.

USEPA, 1983. Record of Decision: Sylvester, OU2, Nashua NH.EPA/ ROD/R01-83/007. Washington, DC.

V

van der Zaan, B., Hannes, F., Hoekstra, N., Rijnaarts, H.H.M., De Vos, W.M., Smidt, H., Gerritse, J., 2010. Correlation of *Dehalococcoides* 16S rRNA and chloroethene-reductive dehalogenase genes with geochemical conditions in chloroethene-contaminated groundwater. Appl. Environ. Microbiol. 76, 843–850. https://doi.org/10.1128/AEM.01482-09

van Warmerdam, E.M.M., Frape, S.K.K., Aravena, R., Drimmie, R.J., Flatt, H., Cherry, J.A. a, 1995. Stable chlorine and carbon isotope measurement of selected chlorinated organic solvents. Appl. Geochem. 10, 547–552. https://doi.org/10.1016/0883-2927(95)00025-9

Vidali, M., 2001. Bioremediation. An overview. Pure Appl. Chem. 73, 1163–1172. https://doi.org/10.1351/pac200173071163

Voudrias, E.A., 2001. Pump-and-treat remediation of groundwater contaminated by hazardous waste: can it really be achieved? Glob. NEST J. 3, 1–10. https://doi.org/10.30955/gnj.000199

W

Wagner, D.D., Hug, L.A., Hatt, J.K., Spitzmiller, M.R., Padilla-Crespo, E., Ritalahti, K.M., Edwards, E.A., Konstantinidis, K.T., Löffler, F.E., 2012. Genomic determinants of organohalide-respiration in *Geobacter lovleyi*, an unusual member of the *Geobacteraceae*. BMC Genomics 13, 200. https://doi.org/10.1186/1471-2164-13-200

Wang, M., Zhang, B., Li, G., Wu, T., Sun, D., 2019. Efficient remediation of crude oil-contaminated soil using a solvent/surfactant system. RSC Adv. 9, 2402–2411. https://doi.org/10.1039/c8ra09964b

Wanner, P., Parker, B.L., Chapman, S.W., Lima, G., Gilmore, A., Mack, E.E., Aravena, R.,

2018. Identification of degradation pathways of chlorohydrocarbons in saturated low-permeability sediments using compound-specific isotope analysis. Environ. Sci. Technol. 52, 7296–7306. https://doi.org/10.1021/acs.est.8b01173

Wartenberg, D., Reyner, D., Scott, C.S., 2000. Trichloroethylene and cancer: epidemiologic evidence. Environ. Health Perspect. 108, 161–176. https://doi.org/10.1289/ehp.00108s2161

Weathers, L.J., Parkin, G.F., 2000. Toxicity of chloroform biotransformation to methanogenic bacteria. Environ. Sci. Technol. 34, 2764–2767. https://doi.org/10.1021/es990948x

Wei, K., Grostern, A., Chan, W.W.M., Richardson, R.E., Edwards, E.A., 2016. Electron acceptor interactions between organohalide-respiring bacteria: cross-feeding, competition, and inhibition, in: L. Adrian and F.E. Löffler (Ed) Organohalide-Respiring Bacteria. Springer Berlin Heidelberg, Berlin, Heidelberg, pp. 283–308. https://doi.org/10.1007/978-3-662-49875-0_13

Wei, N., Finneran, K.T., 2011. Influence of ferric iron on complete dechlorination of trichloroethylene (TCE) to ethene: Fe(III) reduction does not always inhibit complete dechlorination. Environ. Sci. Technol. 45, 7422–7430. https://doi.org/10.1021/es201501a

Wiedemeier, T.H., Swanson, M.A., Moutoux, D.E., Kinzie Gordon, E., Wilson, J.T., Wilson, B.H., Kampbell, D.H., Haas, P.E., Miller, R.N., Hansen, J.E., Chapelle, F.H., 1998. Technical protocol for evaluating natural attenuation of chlorinated solvents in ground water, EPA/600/R-98/128. U.S. EPA, Washington DC 20460.

Wong, Y.K., Holland, S.I., Ertan, H., Manefield, M.J., Lee, M., 2016. Isolation and characterization of *Dehalobacter* sp. strain UNSWDHB capable of chloroform and chlorinated ethane respiration. Environ. Microbiol. 18, 3092–3105. https://doi.org/10.1111/1462-2920.13287

Wu, S., Jeschke, C., Dong, R., Paschke, H., Kuschk, P., Knöller, K., 2011. Sulfur transformations in pilot-scale constructed wetland treating high sulfate-containing contaminated groundwater: a stable isotope assessment. Water Res. 45, 6688–6698. https://doi.org/10.1016/j.watres.2011.10.008

X

Xie, C.H., Yokota, A., 2005. *Pleomorphomonas oryzae* gen. nov., sp. nov., a nitrogen-fixing bacterium isolated from paddy soil of *Oryza sativa*. Int. J. Syst. Evol. Microbiol. 55, 1233–1237. https://doi.org/10.1099/ijs.0.63406-0

Y

Yang, Y., Cápiro, N.L., Marcet, T.F., Yan, J., Pennell, K.D., Löffler, F.E., 2017a. Organohalide respiration with chlorinated ethenes under low pH conditions. Environ. Sci. Technol. 51, 8579–8588. https://doi.org/10.1021/acs.est.7b01510

Yang, Y., Higgins, S.A., Yan, J., Şimşir, B., Chourey, K., Iyer, R., Hettich, R.L., Baldwin, B.R., Ogles, D.M., Löffler, F.E., 2017b. Grape pomace compost harbors organohalide-respiring *Dehalogenimonas* species with novel reductive dehalogenase genes. ISME J. 11,

2767–2780. https://doi.org/10.1038/ismej.2017.127

Yu, R., Andrachek, R.G., Lehmicke, L.G., Freedman, D.L., 2018. Remediation of chlorinated ethenes in fractured sandstone by natural and enhanced biotic and abiotic processes: A crushed rock microcosm study. Sci. Total Environ. 626, 497–506. https://doi.org/10.1016/j.scitotenv.2018.01.064

Z

Zanaroli, G., Negroni, A., Häggblom, M.M., Fava, F., 2015. Microbial dehalogenation of organohalides in marine and estuarine environments. Curr. Opin. Biotechnol. 33, 287–295. https://doi.org/10.1016/j.copbio.2015.03.013

Zinder, S.H., 2016. The genus Dehalococcoides, in: L. Adrian and F.E. Löffler (Ed) Organohalide-Respiring Bacteria. Springer Berlin Heidelberg, Berlin, Heidelberg, pp. 107–136. https://doi.org/10.1007/978-3-662-49875-0_6

Zogorski, J.S., Carter, J.M., Ivahnenko, T., Lapham, W.W., Moran, M.J., Rowe, B.L., Squillace, P.J., Toccalino, P.L., 2006. The quality of our nation's waters: volatile organic compounds in the nation's groundwater and drinking-water supply wells, U.S. Geological Survey Circular 1292. Reston, Virginia.